The Stratigraphy and Environments of Deposition of Early-Mid Pleistocene Sediments of the Pohangina Region, Eastern Wanganui Basin, New Zealand.

A thesis presented in partial fulfilment of the
requirements for the degree of
Master of Science with Honours in
Quaternary Science
at Massey University, Palmerston North, New Zealand.

Hannah Brackley
1999

ABSTRACT

The Pohangina Anticline is one of several growing structures on the northeastern Manawatu Plains. The axis of this asymmetrical anticline lies within the valley of the Pohangina River, with the strata on the western limb dipping gently 2-3° to the west, and those on the eastern limb dipping at up to 70° to the east. The axis of the anticline plunges at 1-2° to the south.

The sediments are 1.3-0.6 Ma in age. Age control is provided by several coarse pumiceous tuffs within the sediments. These time planes for regional correlation have been examined using electron microprobe analysis. The Rewa pumice (1.29 ± 0.12 Ma) lies near the base of the studied sequence. Pumice from the Potaka eruption (1.05 ± 0.05 Ma) is well exposed at several sites. The Kaukatea pumice (0.87 ± 0.05 Ma) is exposed as both tuff and airfall deposits, and the Kupe pumice (0.63 ± 0.08 Ma) appears near the top of the studied sequence. Using these tuffs and the dip of the beds, rates of deformation of 7° per 100 ka have been calculated.

The Castlecliffian/Nukumaruan sediments accumulated in a gradually shallowing marine environment. Conditions were shallow marine until about the time of the Potaka pumice eruption, above the Potaka the sediments are dominantly fluvial including lignites, overbank deposits and channel gravels, all deposited in a lower coastal plain setting.

Sequence stratigraphy and tephrochrononlogy provide correlation of the studied section with age equivalent sections farther west at Castlecliff, Turakina and the Rangitikei River. Cyclothems 33 to 40 are present within the stratigraphy, and are characterised by alternating coarse and fine grained sediments, indicating climatic fluctuations.

ACKNOWLEDGEMENTS

I owe many thanks to my chief supervisor Alan Palmer, who has willingly provided so much time, advice and support throughout the course of this study. Julie Palmer has provided thought-provoking discussions and reviews of my work as co-supervisor, which have been both stimulating and helpful.

A big thank you goes to my whole family, who have had faith in my ability to complete this research, and have been a great source of encouragement. Marilyn also proved to be a very willing and able field assistant, remaining undeterred by swarms of wasps and deep river crossings!

I'd like to thank Joe Whitton for his assistance with the XRD laboratory work, and when computer problems arose, Mike Bretherton's help was much appreciated. Thanks is owed to Leighanne Empson and Bernd Striewski, for their help and advice in using the SediGraph.

I am very grateful to the landowners who allowed me access on to their properties - without their assistance I could not have accessed the key sites in order to complete this study.

Thanks must go to my colleagues within the department, who have provided support and encouragement, as we all follow a path of research.

TABLE OF CONTENTS

List of Figures

Chapter Five

Chapter Six

List of Tables

Chapter Five

Chapter Six

List of Plates

CHAPTER ONE : INTRODUCTION

1.1 Wanganui Basin

Wanganui Basin is a sedimentary basin situated in the south western part of New Zealand's North Island. It is roughly elliptical in shape, with dimensions of about 350km by 150km (Stern *et al.*, 1993). The basin may be subdivided into northern and southern components, with the boundary between the North Wanganui and South Wanganui Basins being defined by the Pipiriki High (Ministry of Commerce, 1993) (Figure 1.1). The structural relationship of the North and South Wanganui Basins is unclear, but there is a marked stratigraphic distinction between the two sub-basins. The sediments of the South Wanganui Basin are dominantly of Pliocene and Pleistocene age, while the North Wanganui Basin contains an Oligocene-Pleistocene sequence.

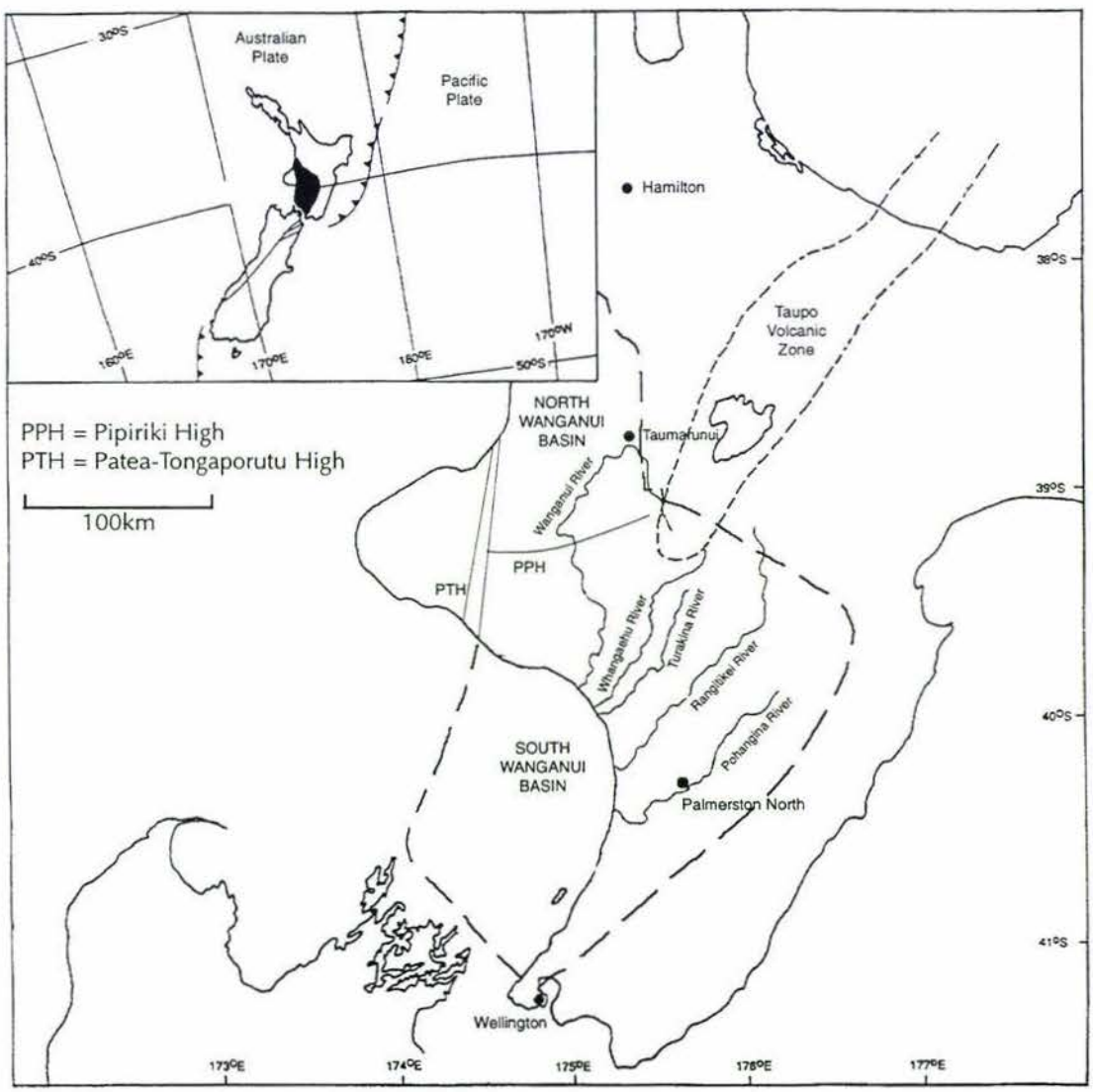

Figure 1.1: Location map of the North and South Wanganui Basins.
(adapted from Pillians (1994))

North Wanganui Basin

The North Wanganui Basin occupies approximately 9,500km^2 of the central, western part of New Zealand's North Island. The basin, mostly onshore, is about 120km long and 60-80km wide. The western margin is represented by a horst, known as the Patea-Tongaporutu High (Figure 1.1) while the eastern margin is immediately to the east of Taumarunui, where an uplifted block of Mesozoic basement is capped by Pliocene andesitic volcanics (Ministry of Commerce, 1993).

The North Wanganui Basin contains a sequence of Oligocene to Pleistocene sediments, up to 2,500m thick. The sediments offlap from the north and plunge gently to the south at up to 5°. A series of normal faults strike north-east, and associated and parallel with these are a number of small anticlines and synclines (Ministry of Commerce, 1993).

South Wanganui Basin

The South Wanganui Basin is located in the south-central part of the North Island and extends over an area of 22,500km^2, about half of which is offshore (Ministry of Commerce, 1993).

The South Wanganui Basin is a back-arc basin (Pillans, 1994) lying within the transition zone between the convergent Tonga-Kermadec subduction system to the north-east and the Alpine Fault continent-continent transform to the south-east. The basin is situated above the subducting Pacific Plate and subduction processes strongly influence the tectonics within the basin. However, unlike the opening back-arc basin of the Taupo Volcanic Zone, the South Wanganui Basin is under compression - it is not the result of extensional thinning of the crust, but has formed by crustal downwarping (Ministry of Commerce, 1993).

The western boundary of the South Wanganui Basin is represented by the Patea-Tongaporutu High, which separates the Wanganui and South Taranaki Basins. It is a north-trending structural high of Triassic-Jurassic basement, clearly defined by gravity and seismic measurements and drilling but with no surface expression (Hunt, 1980). Traditional theories suggest that the eastern boundary of the South Wanganui Basin is the North Island main axial ranges, but two lines of evidence suggest that it may in fact be farther east.

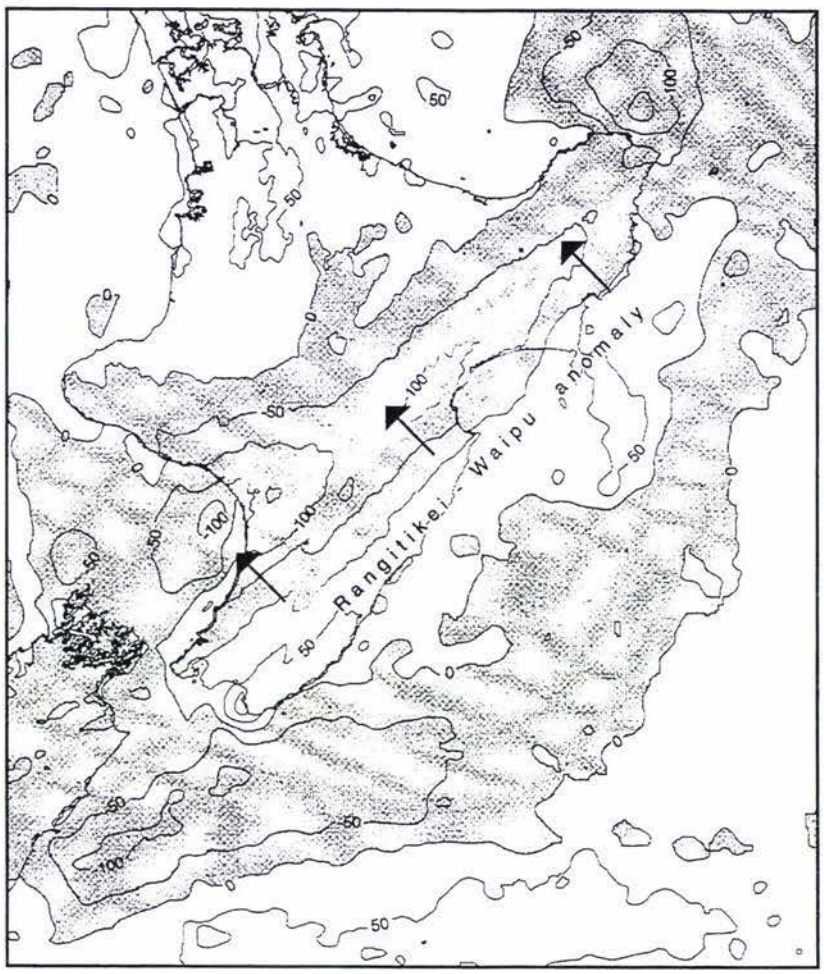

Figure 1.2: Bouger and Free Air gravity anomalies of the lower North Island. Contours are in mgal (from Field *et al.* (1997)).

Firstly there is a strong negative gravity anomaly associated with the Wanganui Basin, termed the Rangitikei-Waiapu anomaly (Figure 1.2). As the map indicates this anomaly extends farther east than the main axial ranges, into the Hawkes Bay low, thereby suggesting that the eastern boundary of the South Wanganui Basin has not always been defined by the ranges. Along the Rangitikei-Waipu anomaly, the axial ranges are associated with slightly less negative gravity anomaly values, reflecting a lack of Tertiary and Quaternary sediment cover.

Secondly, Beu *et al.* (1980) suggest that during the Pliocene there was a shallow seaway linking the Wanganui and Hawkes Bay depressions. Shallow marine sediments were deposited unconformably over older strata including basement rocks that were subsiding. Anderton (1981) also suggests that during the early Pliocene, marine connections existed across the trend of the main axial ranges between the South Wanganui Basin and the Hawkes Bay and Wairarapa Basins to the east. These marine connections became progressively limited as the axial ranges emerged during the Pleistocene and they were eventually cut off in the late Pleistocene. Thus it may be interpreted that the South

Wanganui Basin did originally extend farther east, and that the basement rocks of the axial ranges have more recently developed as a piercement structure.

The South Wanganui Basin contains up to 4km of interfingered shallow marine and terrestrial sediments of Plio-Pleistocene age. During the Plio-Pleistocene, regional tilting involved progressive subsidence and onlap to the south, and as the depocentre migrated to the south, offlap and emergence of the northern part of the South Wanganui Basin occurred. By the early Pleistocene the South Wanganui Basin was confined within the limits of the present basin (Anderton, 1981). Anderton suggests that the southward migration of the South Wanganui Basin depocentre is consistent with the southward propagation of the subduction zone beneath northern New Zealand, proposed by Walcott (1978).

South Wanganui Basin sediments dip gently toward the depocentre, and are cut by NE-NNE trending faults. Gentle anticlines at the margins of the basin are related to deeper block-faulting of basement (Anderton, 1981).

1.2 Terminology

Time Scale

In this work, the terms early, mid and late Pleistocene are defined by the following time periods:

late Pleistocene	0.35 Ma - Present
mid-Pleistocene	1.07 - 0.35 Ma
early Pleistocene	1.81 - 1.07 Ma

0.35 Ma is the boundary of the late Pleistocene, as used by Abbott and Carter (1999). It is marked by the transition between the Castlecliffian and Haweran Stages and therefore places the Rangitawa Tephra in the Late Pleistocene. The boundary at 1.07 Ma is represented by the base of the Jaramillo Subchron (Abbott & Carter, 1999) and 1.81 Ma is commonly recognised as the boundary between the Pliocene and the Pleistocene (Naish *et al.*, 1998).

Tuffs

An attempt has been made in this study to clearly distinguish between tephras and tuffs. All but one of the sampled pumice units consist of reworked ignimbrites, so are referred to as tuffs. The Kaukatea pumice at Beehive Creek is a tephra.

1.3 Previous Work

Many geological studies have investigated various aspects of the Wanganui Basin, helping to develop a history of the basin and its sediments. In 1943 the Superior Oil Company produced a report on the geology of the "Palmerston - Wanganui Basin", based on field work by Feldmeyer, Jones, Firth and Knight. The mapping was based on standard sections in the Rangitikei, Turakina, Mangawhero and Wanganui Rivers. Foraminiferal faunas were obtained and used to establish seven zones. The foraminiferal zones were attributed to the standard New Zealand stages, but no detailed correlation was made with the type sections on the Wanganui coast. The rock units as they are mapped in the Superior report (1943) are tabulated below (Table 1.1).

Stage	Formation	Horizon
Castlecliffian	Castlecliff	Kimbolton Ash Coutts Creek Basal Ash
Nukumaruan	Petane	Waipuru Shellsand Mangamako Shellsand Ohingaiti Sand
	Lower Nukumaruan	Tuha Sand Hautawa Reef Basal Lower Nukumaruan Sand
Waitotaran	Mangaweka Mudstone Utiku Sand Taihape Mudstone Reef-bearing Sand	Mangamahu Concretions Conglomeratic Limestone Mataroa Concretions Taihape Sand No. 1 Reef Undifferentiated Reefs

Table 1.1: Pliocene rock units mapped by Superior Oil Company (NZ) Ltd, 1939 - 1942.

The work of Te Punga (1952) and Fleming (1953) provided a basic understanding of the Wanganui Basin stratigraphy, which has been used by more recent workers as a foundation. Te Punga worked in the Rangitikei Valley, toward the eastern margin of the Wanganui Basin, while Fleming worked from the Turakina valley westwards (Fig 1.1). Molluscs were used to provide paleontological correlations between the two areas.

Te Punga (1952) provided the first stratigraphical description of the Rangitikei valley, and by incorporating the paleontology and tephrochronology, he correlated a number of the beds to other studied areas. In the last two decades, extensive research has been undertaken, and several aspects, such as the tephrochronology and sequence stratigraphy of the basin have become more thoroughly understood.

Fleming (1953) provided the first detailed stratigraphy of the Wanganui Basin sediments, as part of a regional geological study of the Wanganui and Waverley Survey Districts. He made extensive use of the Superior Oil Company report (1943) during the field work, and the mapping of some rock units was also taken from the oil company's map, with minor corrections (Fleming, 1953).

A number of methods have been used to determine the structure of the Wanganui Basin, in order to build up a greater knowledge of the basin and its history. One important study was that of Anderton (1981), in which CRP (common reflection-point) profiles were interpreted in order to determine the structure and evolution of the South Wanganui Basin. Seismic data showed that the South Wanganui Basin is a broad half-graben trending north-northeast, bordered to the south east by a complex zone of block faulting. The western boundary is marked by broad north-south trending basement uplifts, the D'Urville and Patea Highs, which lie en echelon with a narrow graben between.

Anderton also compiled the following outline of the evolution of the South Wanganui Basin:

- The area covered by the present South Wanganui Basin was largely emergent during the Miocene. Basin development occurred during the Plio-Pleistocene with regional tilting involving progressive subsidence to the south and emergence to the north.
- The Southern Wanganui Basin has subsided since the mid Pliocene, allowing the deposition of approximately 4000m of mainly marine sediments. Shallow water conditions were maintained throughout.
- Marine connections to the north west became progressively limited until cut off in the late Pleistocene. During the early Pliocene, marine connections existed across the trend of the axial ranges.
- During the late Pliocene - early Pleistocene, marine connections with the eastern basin continued, but became more restricted.
- By mid Pleistocene the basin was restricted to the north and west, and the Manawatu Strait no longer existed through the area of the present Manawatu Gorge.

• In the late Pleistocene, onlap of Plio-Pleistocene sediments extended sufficiently far south to allow a marine connection to the east, via Cook Strait.

• During glacial episodes of the late Pleistocene, much of the basinal area now lying beneath western Cook Strait was exposed, and then submerged during interglacial episodes.

• The depocentre of the South Wanganui Basin showed a progressive southward shift from early Pliocene to late Pleistocene.

Age Control

A number of methods have been used to provide age control within sedimentary sequences. One of the early developments was made by Fleming (1957) through the use of the macrofossil *Pecten*. *Pecten* is now of global importance as an index fossil and is used widely for correlation. Within New Zealand sediments, *Pecten* is not found in deposits older than the Castlecliffian Stage (mid-Pleistocene). The FAD of *Pecten* is at the Kaikokopu Shell Grit, just above the Bruhnes-Matuyama boundary (see Table 1.3). Fleming (1957) distinguished consistent zones across the Wanganui basin where different subspecies of *Pecten* were found, related to the progressive evolution of the species. Different *Pecten* subspecies are restricted to particular formations and therefore are helpful in the identification and correlation of formations across the Wanganui basin, and the establishment of stratigraphic constraints (Van der Neut, 1996).

Widespread reworked pumice horizons (tuffs) and airfall tephras, that are the distal correlatives of voluminous welded rhyolitic ignimbrite sheets, are commonly found within the sediments of the Wanganui Basin. They were initially mapped by Te Punga (1952) and they have proven to be very useful tools in the dating and correlation of sediments. Fundamental work on the tuffs and tephras of the Wanganui Basin was carried out by Seward (1974), when she identified a number of tuffs in the marine Pleistocene sediments of the Wanganui Basin. Most were identified as occurring in the early Middle Pleistocene, representing the initiation of the major rhyolitic volcanic activity of the central North Island. Seward described the units, their mineral assemblages, and other characteristics, allowing the tuffs and tephras to provide possible intrabasinal and interbasinal correlation.

Seward (1974) correlated a number of tuffs in the Wanganui Basin with North Island ignimbrites and provided fission track ages (Table 1.2).

Age (Ma)	Tephra or Tephra Bearing Horizon	Ignimbrite(s)	Revised Ages (Ma)
0.28	Upper Finnis Road Tephra		
0.32	Lower Finnis Road Tephra	Whakamaru	
0.38	Rangitawa Pumice	Atiamuri	0.34
	Kupe Pumice		0.63
0.45	Waiomio Shell Bed		
0.52	Waitapu Shell Conglomerate	Paeroa Range Group	
0.57	Kaukatea Ash		0.87
0.61	Potaka Pumice	Lower Ahuroa	1.05
0.74	Rewa Pumice		1.29
0.88	Mangapipi Ash	Unknown, Waitearíki, Aongatete	1.60
1.04	Ridge Ash		
1.06	Pakihikura Pumice	Rangitoto	1.63
1.26	Mangahou Ash		
1.50	Ohingaiti Ash	Tridymite Rhyolite	2.20

Table 1.2: Wanganui Basin tuffs, their fission track ages and ignimbrites as correlated by Seward (1974), with their revised ages from Naish *et al.* (1998).

For a number of years, fission track and paleomagnetic dating of ignimbrites and distal tuffs and tephras provided the only method of establishing relative stratigraphic positions between different sites, and were also used to correlate the tuffs and tephras to ignimbrites (Froggatt, 1983). An important new development arose when Froggatt (1983) demonstrated the usefulness of the electron microprobe in the development of a comprehensive volcanic stratigraphy for the upper Quaternary in New Zealand.

It was shown that tuffs and tephras may be identified in a range of environments through the electron microprobe analyses of their glass shards, thus allowing correlation between the distal tuffs or tephras and ignimbrite sheets. Glass identification using the electron microprobe provided a more precise chronology of sedimentation and tectonic events in the Wanganui Basin, as well as allowing the integration of stratigraphic studies on marine and river terraces, loess stratigraphy, palynology, and a detailed paleoclimatic analysis to be made (Froggatt, 1983).

The usefulness of the tuffs and tephras within the Wanganui Basin sediments was further illustrated when Alloway *et al.* (1993) revised the marine chronology of the basin through the use of isothermal plateau fission-track (ITPFT) dating of tephras. The Rangitawa Tephra

yielded ages that were in excellent agreement with previously determined zircon fission-track age estimates of about 0.35 Ma (Kohn *et al.*, 1992), while previously determined ages of the Potaka and Pakihikura pumices, including Seward's dates were found to be considerably underestimated. New ITPFT ages of 1.05 ± 0.05 and 1.63 ± 0.15 Ma for the Potaka pumice and Pakihikura pumice respectively, are consistent with new magnetostratigraphic data, thus placing the Potaka within the Jaramillo Subchron and the Pakihikura within the Matuyama Chron.

In general, the original glass fission track ages of Seward (1976) are now considered to be minimum ages for the Wanganui Basin tephras (Alloway *et al.*, 1993). Pillans (1994) accepted her age for the Rangitawa pumice and the Upper and Lower Finnis Road Tephras, however, this work suggests new identifications for those tuffs found at Finnis Road (see chapter 3).

In the last two decades, the magnetostratigraphy of basin sediments has proved to be a very useful tool, particularly for correlating sequences to the oxygen isotope timescale. Turner and Kamp (1990) described and revised the magnetostratigraphy for the lower part of the Castlecliff section in the Wanganui Basin, and presented the first published data on the occurrence of the Matuyama/Bruhnes boundary on land in New Zealand. This work illustrated that magnetostratigraphy can be used to provide chronologic and stratigraphic controls.

Pillans *et al.* (1994) extended the work of Turner and Kamp (1990), and presented magnetostratigraphic, lithostratigraphic and tephrostratigraphic results from four successions of early to middle Pleistocene age. They reached the following conclusions:

- The Matuyama/Bruhnes geomagnetic polarity transition is closely associated with the Kaikokopu Shell Grit
- The base of the Jaramillo Subchron lies beneath the Potaka Pumice at all sections
- The top of the Jaramillo Subchron appears to lie above the first incoming of Potaka Pumice and below the Kaukatea Ash.

Table 1.3 provides an overview of the Wanganui Basin Quaternary stratigraphy as summarised by Pillans (1994).

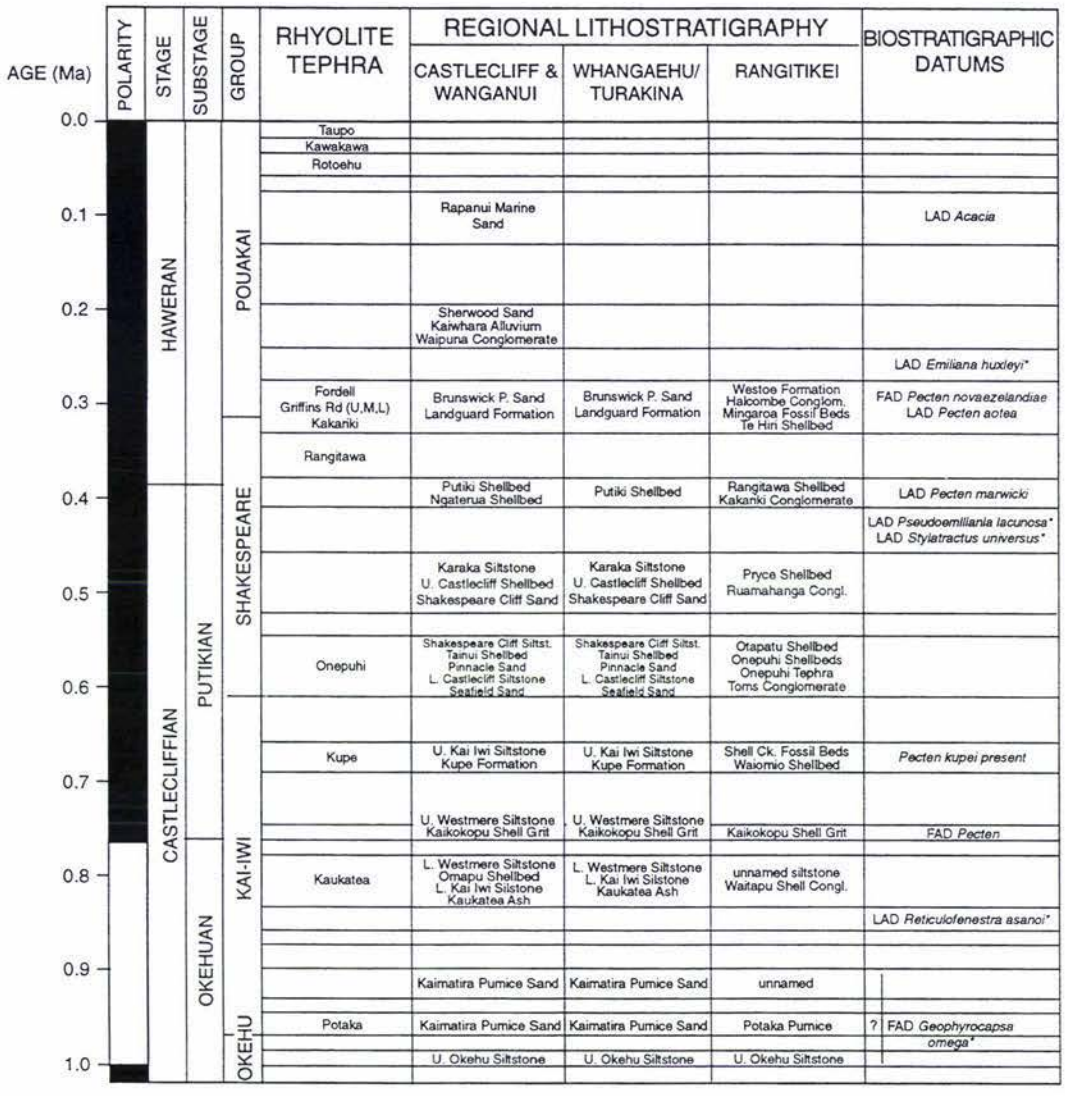

Table 1.3: Summary of the Quaternary stratigraphy in the Wanganui Basin (adapted from Pillans (1994)).

Sequence Stratigraphy

Sequence stratigraphy may be defined as the study of sediment relationships within a chronostratigraphic framework of repetitive, genetically related strata bounded by surfaces of erosion or nondeposition (Boggs, 1995). The concept of sequence stratigraphy was first introduced when the word 'cyclothem' was proposed by Weller in 1932 for "a series of beds deposited during a single sedimentary cycle of the type that prevailed during the Pennsylvanian Period", and they have since been recognised in rocks of many different ages.

Vella (1963) recognised the development of cyclothems in the Wairarapa, Hawke's Bay and Wanganui, considered them to be due to glacio-eustatic sea level fluctuations and was able to correlate between the regions. He identified that cyclothem boundaries in the New Zealand Pleistocene and upper Pliocene coincided with fossil zone boundaries and

therefore stages. Because cyclothems were found to be more widespread they were then considered to be more useful as stratigraphic units than formations.

Since discovering the cyclical nature of the Wanganui basin sediments, a number of geologists have applied the concept of sequence stratigraphy. Basin sediments have been correlated to the glacio-eustatic sea level changes and the oxygen isotope curve. Beu and Edwards (1984) worked for a number of years toward correlating the cycles in New Zealand on-land marine sequences with the "multi-glacial" Pleistocene time scale. They correlated the Castlecliff Section with the numbered oxygen isotope stages of Shackleton and Opdyke (1973) and Gardner (1982). Local correlation was principally by biostratigraphy, but also by lithostratigraphy and fission-track dates on tephras. They assumed that the obvious sedimentary cycles were caused primarily by glacio-eustatic sea level changes, with the shallow marine sediments being deposited during interglacial periods while the unconformities were representative of the basin being exposed above sea level during glacial periods.

Pillans (1991) reviewed and revised the stratigraphic subdivisions of the New Zealand Quaternary. He outlined the varying markers that have previously been used to define the Plio-Pleistocene boundary in New Zealand, and suggested a new date of 2.4 Ma for the boundary, which may be associated with the first faunal evidence of cooling in New Zealand Plio-Pleistocene sequences.

Kamp and Turner (1990) identified eleven complete marine unconformity-bounded sequences in the Castlecliff Section, and based on magnetostratigraphy, the section was correlated with the benthic oxygen isotope curve from DSDP core 552A from the North Atlantic. The correlation provides a geochronologic framework for the assessment of eustatic control in marine sediment sequences, while an approximation of the sea level history may be gained from an oxygen isotope curve, as their patterns tend to mimic each other.

Pillans (1994) also worked on correlations of the Wanganui Basin stratigraphy to the isotopic record. In this case, correlations were made to the isotopic record of Site ODP 677 through the study of three particular aspects of the Wanganui Basin Quaternary stratigraphy: shallow marine sediments, marine terraces and their cover beds, and river terraces and their cover beds.

On the basis of magnetostratigraphy and ITPFT ages, Pillans *et al.* (1994) correlated the cyclothems at Wanganui with oxygen isotope stages 17 - 31. They extended the work of Turner and Kamp (1990) using magnetostratigraphy, lithostratigraphy and tephrostratigraphy to make a definitive correlation across the basin, allowing detailed comparison with oxygen isotope records and the tuned orbital chronology of deep-sea cores. It was also suggested that regional tectonics, probably the initiation of uplift of the main axial ranges, played a major role in changing the character of cyclothems at Wanganui below stage 31.

Abbott and Carter (1994) analysed ten mid-Pleistocene cyclothems from a section exposed at Wanganui. The cyclothems were interpreted as corresponding to fifth (100 ka) and sixth (40 ka) order sequences, equivalent to odd-numbered oxygen isotope stages 11-31. Each cyclothem was subdivided into three parts, corresponding to the transgressive systems tract, mid-cycle condensed shellbed and highstand systems tract of the Exxon sequence stratigraphic model. It was concluded that the sediments were deposited during interglacial conditions, with the glacial periods being represented by surfaces of marine planation and bioerosion at the base of each cyclothem.

Naish and Kamp (1995) recognised twenty cyclothems within an 1100m thick marine cyclothemic succession in the Rangitikei River valley between Mangaweka and Vinegar Hill. Each cycle contains both fine grained and coarse grained units. Each cyclothem is characterised by a similar lithofacies architecture, corresponding to the 41,000 year Milankovitch obliquity frequency, and the twenty cyclothems are correlated with oxygen isotope stages 100-58.

Naish and Kamp (1997) illustrated that each of the cyclothems is represented by an individual depositional sequence comprising transgressive, highstand and regressive systems tracts, with the systems tracts being deposited during phases of known sea level cycles indicated by the contemporary oxygen isotope ice-volume curve. The glacio-eustatic sea level falls during most cycles were of insufficient magnitude to expose the outer shelf because of the high rate of basin subsidence, hence the Rangitikei section provides a good example of regressive strata deposited landward of the contemporary shelf break (Naish & Kamp, 1997). It was illustrated that cyclothems contain the following architectural elements in ascending stratigraphic order: (1) a basal sequence boundary; (2) a thick or thin transgressive systems tract; (3) a sharp downlap surface; (4) a highstand systems tract; and (5) a thick regressive systems tract. Condensed shellbeds, along with

sedimentological and stratal characteristics of the sequences, are also important indicators of stratigraphic architecture (Kamp & Naish, 1998).

Local Studies

Ower (1943) investigated the Pohangina area for The Superior Oil Company Ltd, and identified several "ash beds"*. To the west of the Pohangina Fault, an anticline was interpreted, with steep dips to the south-east and shallow dips to the west.

Kingma (1962) mapped most of the Pohangina Anticline strata as Castlecliffian gravels, sands and silts with or without pumice bands, either in marine sequences or in much dissected high terraces.

Seward (1974) studied the Finnis Road sequence as part of a sedimentological record of the Wanganui Basin sediments. She used fission track dating to age tephras within the sediments (Table 1.2). However her method has since been found to underestimate the ages, and so the ages of the Wanganui Basin tephras have more recently been revised by Alloway *et al.* (1993).

MacPherson (1985) described the stratigraphy and identified tephras in Pleistocene sediments from the Finnis Road area. He concluded that the provenance of the sediments was largely from the Central Volcanic Zone, and that they were deposited in a shallow marine environment 180-420 ka. MacPherson correlated eleven tephra layers on and around Finnis Road with known tephras elsewhere in the North Island. He identified tephras within the study area as being correlatives of the Kawakawa Tephra, Kaingaroa Ignimbrite, Matahina Ignimbrite, Mount Curl Tephra, Omokoroa 9 Tephra, and the Lower Kakariki Tephra.

Pillans (1994) worked with the same Finnis Road sediments, and found radiolarian assemblages lacked *Stylatractus universus*, known to become extinct about 420 ka. He concluded that the Lower Finnis Road tephra was younger than 340 ka, as it also contained what he thought was occasional reworked Rangitawa Pumice glass shards.

* The term ash, applied correctly means airfall tephra less than 2mm in diameter. These deposits are termed tuffs in this study.

Manning (1988) described the stratigraphy and interpreted paleoenvironment of deposition of mid-Quaternary sediments in Culling's Gullies, north east of Finnis Road. He tentatively correlated the upper tuff unit (Tephra A) with the Lower Finnis Road Ash of Seward (1974) and also concluded that the major sediment sources were the main axial greywacke ranges and the central North Island volcanic region. Manning concluded that sands with mainly plane parallel bedding had been deposited in a high energy shallow marine environment, very often influenced by tides, while other sediments showed signs of being deposited in an estuarine environment. Thus he believed the environment of deposition was a wave influenced shallow marine delta, just seaward of an estuary.

Townsend (1993) studied the stratigraphy and paleoenvironment of deposition of the mid-Quaternary sediments in Beehive Creek, 2km north east of Pohangina Township. Her study of the mineralogy and grain characteristics of the sands, and of the tephras, enabled her to determine the source of the sediments and their environment of deposition. The major source areas were thought to be the greywacke axial ranges to the east, and the Central Volcanic Plateau to the north. Large trough cross bedding was thought to be indicative of a fluvial system, while plane parallel sands and cross beds were considered to be distinctly marine, and lignite bands represented an estuarine component. Thus it was concluded that the environment of deposition was a river dominated delta, with a shallow marine component just seaward of an estuary. Deposition was thought to be have been quite rapid, as large amounts of sediment have been deposited and a number of large dewatering structures were present within the stratigraphy. Townsend (1993) sampled and probed four tephras from Beehive Creek. T3 was the only sample which could be correlated to a sample of known age, that being the Rangitawa Pumice.

Jackson *et al.* (1998) examined the drainage systems on the Marton, Feilding, Mt. Stewart-Halcombe and Pohangina anticlines, all of which are thought to be located above buried, west-dipping reverse faults in the basement. Using a 0.3 Ma marine horizon, it was calculated that the anticlines have vertical uplift rates of <1mm per year, and their drainage patterns have evolved in response to the regional tilting (Jackson *et al.*, 1998). It was observed that the four anticlines are asymmetric, with gently sloping western limbs and steeply dipping eastern limbs, which was interpreted as reflecting the westward dip of the underlying reverse faults.

Jackson *et al.* (1998) suggested that all four of the anticlines deform mid-Quaternary sediments that are younger than about 0.5 Ma. The slope of the fold axes were used to

estimate a tilt rate of approximately 4×10^{-8} rad/yr (7×10^{-10} deg/yr) towards the south, averaged over about 300 000 years. The regional tilting is thought to be related to the development and southward migration of the South Wanganui Basin depocentre (Jackson *et al.*, 1998). The revision of previously published ages in this study suggests that sediments being deformed by these anticlines are in fact older than 0.5 Ma.

1.4 Aims and Objectives

Several studies have previously looked at different parts of the Pohangina area, but they have never been tied together or incorporated into an overall knowledge of the geology. The Pohangina Anticline itself is a feature that is again relatively unknown, yet its formation could be indicative of tectonic activity in the Manawatu. Thus a study such as this will tie together and review the previous work, and expand where necessary in order to provide a better overall knowledge of the geology of the Pohangina Anticline.

The overall aim of this study was to tie together existing studies, clarify ages of the sediments, and determine the environments of deposition in the light of sequence stratigraphy.

Specific aims of the study were:

- To integrate current knowledge of the geology of the Pohangina Anticline area, examine new stratigraphic sections and to re-examine ages of tuffs.
- To determine the paleogeography of the area and therefore the environments of deposition for the sediments.
- To calculate the rates of sediment deformation/anticline formation.
- To construct a sequence stratigraphic model for the area from an analysis of sedimentary facies.

1.5 Location of the Study Area

The Pohangina Anticline is situated on the eastern side of the Wanganui Basin, north east of Palmerston North. It is adjacent to the Ruahine Ranges, being the most eastern of several growing anticlines on the north eastern Manawatu plains (Figure 1.3).

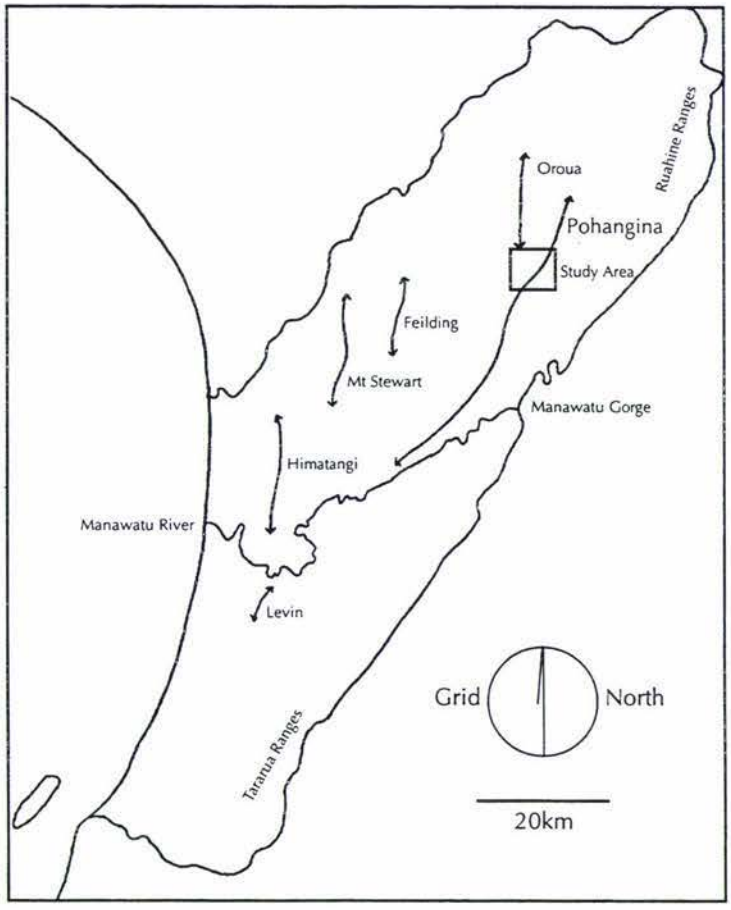

Figure 1.3: Location map of the growing anticlines in the Manawatu region (adapted from Heerdegen, 1972).

The study area covers approximately 133 km^2, lying between the Oroua and Pohangina Rivers (Figure 1.4). It is bounded to the south by Valley Road and to the north by the Te Awa Gullies. This study area encompasses several sites such as Finnis Road, Cullings Gullies and Beehive Creek, where previous studies have been carried out (see Section 1.2).

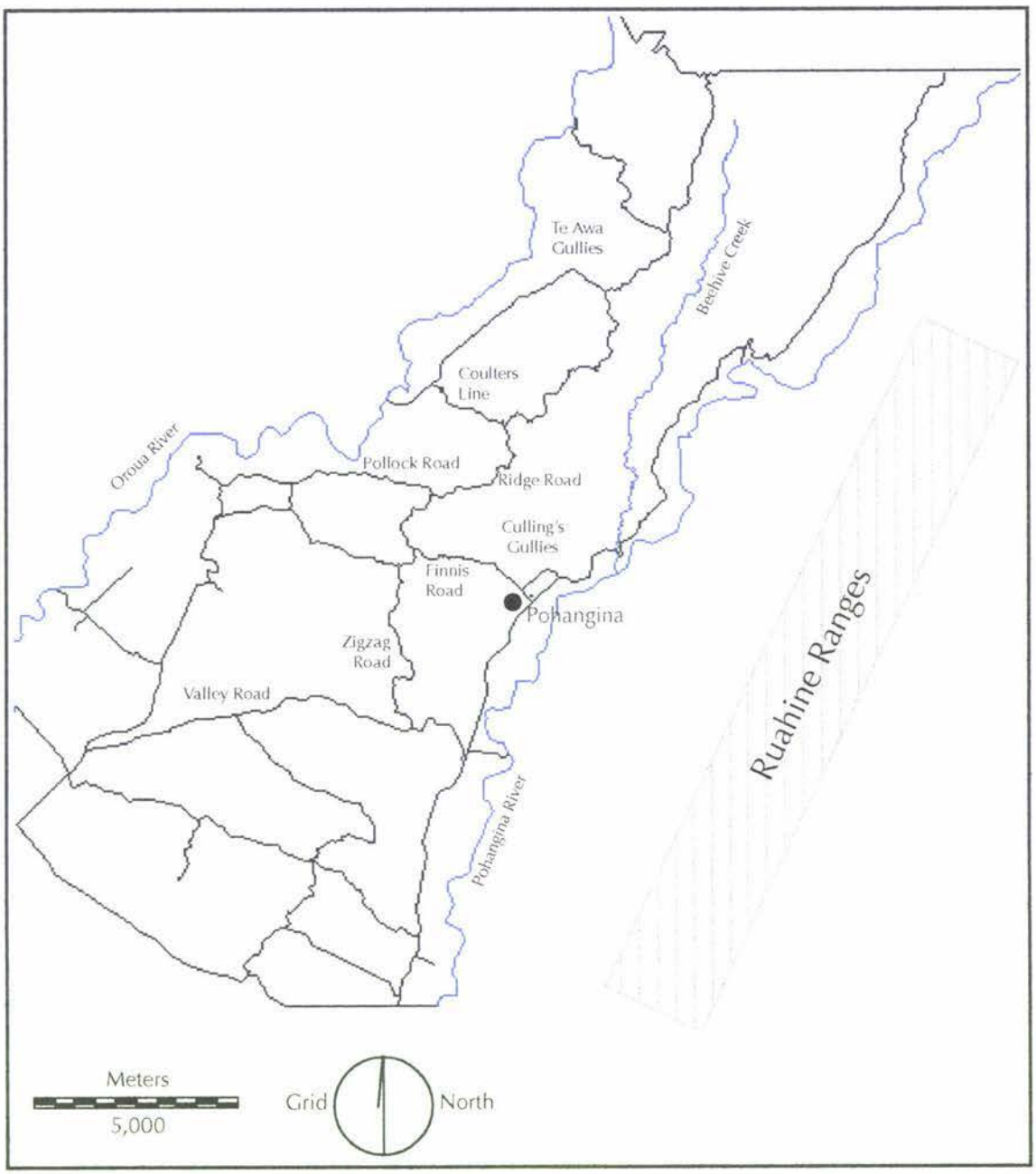

Figure 1.4: Location map of the study area.

The sediments of the Pohangina Anticline are Plio-Pleistocene soft unconsolidated muds and sands, often with a capping of gravels. Many of the sediments are pumice rich, and several tuff layers are well preserved within the stratigraphy.

CHAPTER 2: STRATIGRAPHY

2.1 Introduction

In this chapter the stratigraphy of the study area is outlined and discussed, while more detailed discussions and analyses of some of the sediments are provided in the following chapters. Seven locations were chosen where the stratigraphy was well exposed: Beehive Creek, Finnis Road, Culling's Gullies, Branch Road, Pollock Road, Stewart's Gully and two sites in the Oroua River (Figure 2.1).

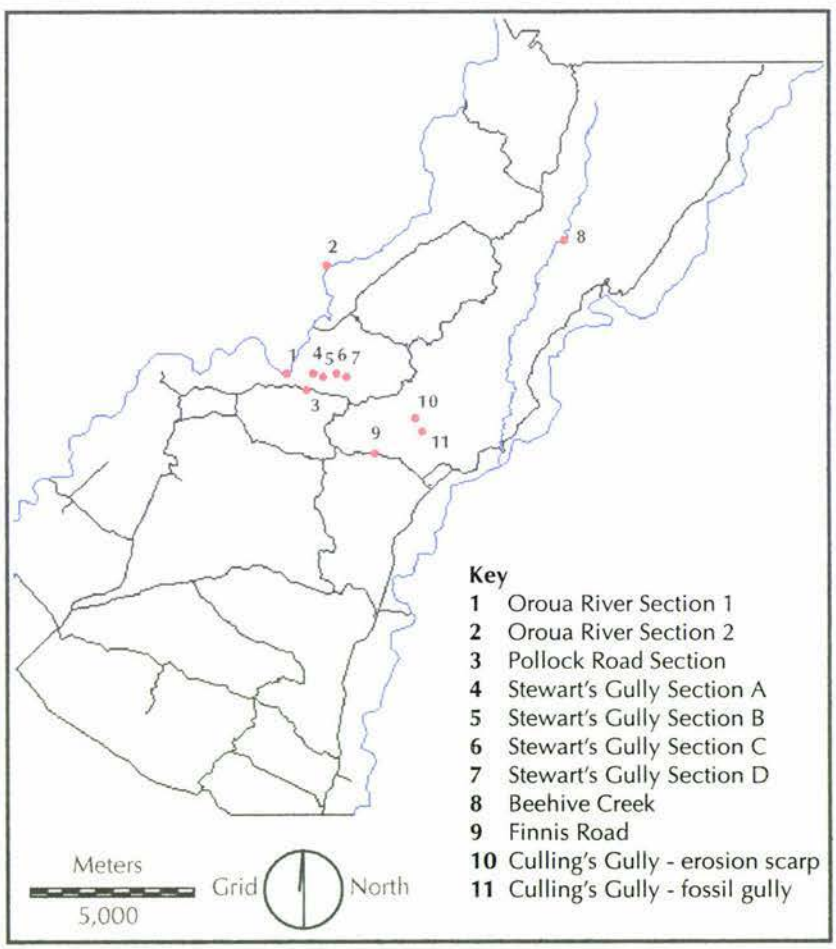

Figure 2.1: Location map indicating the eleven key sites within the study area.

Field work in the study area was carried out predominantly in the first few months of 1998, and consisted largely of logging up a number of stratigraphic columns, some of which had been previously studied by the authors mentioned in section 1.3, and the collection of grain size and tuff samples. Sections were measured using an altimeter for height control, with trig points of known altitude being used regularly to calibrate the altimeter. Each section was described in detail, using description techniques suggested by Andrews (1982). Stratigraphic columns and section descriptions are contained in

Appendix A. In this study, grid references quoted refer to NZMS 260, Sheet T23, entitled Kimbolton (Edition 1, 1982).

Three of the sites have been studied previously, and that work has been re-examined and incorporated into this study. The stratigraphy of the Beehive Creek area has previously been discussed by Townsend (1993), but is reinterpreted in this study. At this location, most of the sediments are dipping steeply (40-70°) to the east, and the creek meanders along the strike of the beds. A thorough and complete interpretation is rather difficult, as it is often unclear whether it is in fact facies changes being observed rather than stratigraphic changes. Thus this study re-evaluates the stratigraphy of Beehive Creek in the light of facies changes along the strike of the beds. The stratigraphy of Finnis Road has previously been discussed by MacPherson (1985), but is reinterpreted in this study, as new correlations are assigned to the tuff units, altering the time period represented by the sediments. Manning (1988) studied the stratigraphy of Culling's Gullies, but that is also reinterpreted in this study, after the revised correlation of tuff units.

2.2 Stratigraphy and Sedimentary Structures

The stratigraphy of the study area is subdivided for convenience into three intervals separated by tuff marker beds. The details of their identification are given in Chapter 3. The Rewa pumice (1.29 $\pm$ 0.12 Ma) lies at the base of the studied sequence, and the first incoming of pumice belonging to the Potaka eruption (1.05 $\pm$ 0.05 Ma) lies about 90m stratigraphically above. The Kaukatea pumice (0.87 $\pm$ 0.05 Ma) is exposed as both tuff and airfall deposits within the study area, approximately 80m above the Potaka pumice. The entire interval between the Potaka and Kaukatea is pumiceous. Another tuff, identified as the Kupe (0.65 $\pm$ 0.08 Ma) appears near the top of the studied sequence.

Interval 1: Rewa pumice to Potaka pumice

The sediments in this part of the sequence are very sand dominated, characteristically with parallel bedding, which is sometimes rippled and burrowed, and occasional flaser beds. This stratigraphic interval is best illustrated by the sediments at Cullings Gullies, where the Rewa Pumice is near the bottom of the sequence (see Chapter 3). The unit of reworked Rewa Pumice is rippled and convoluted. At one location (T23/479127) within the tuff unit there is a channel lag deposit of peat, pumice and silt clasts, above water escape structures (Manning, 1988). A shellbed is present just below the tuff unit, consisting of pebbly coarse sand with silt clasts and occasional pumice lapilli amongst the

broken shells. Pumiceous sands above the tuff unit characteristically contain abundant water escape features. The thick sand units contain some ripples, cross beds, silt flasers and a few burrows. A unit containing common silt layers is found above the pumiceous sands in one gully (T23/472130), while in the other (T23/476126) there is a shellbed. This second shellbed is laterally discontinuous, about 1-1.5m thick and the majority of the shells are broken (Plate 2.1). Manning (1988) identified the species present within the shellbeds, and concluded that they represented accumulations of dead organisms from several different environments. Above the shellbed the sediments are again very sand dominated but slightly more massive than those in the lower part of the sequence, with parallel laminations gradually developing higher in the stratigraphy. At the very top of the sequence but still below the Potaka Pumice, there is a higher proportion of silt within the sediments.

Plate 2.1: Laterally discontinuous shellbed 10m from the top of the Fossil Gully section, within Culling's Gullies (T23/477127). Scale marked at 100mm intervals. (See Appendix A for stratigraphic column and descriptions).

At Beehive Creek a shell bed lies directly beneath pumiceous sands containing the Rewa pumice. The pumiceous sands are cross bedded, and some layers are oversteepened and deformed. A thick unit of interbedded mud and sand overlies the Rewa pumice unit, with some of the mud being quite rich in organic matter. Two 50mm lignite layers are also present within this unit, enclosing an unidentified white tuff layer, about 7m from the

base of the unit. In Beehive Creek, the Potaka pumice unit consists of very pumiceous sand with common pebble sized pumices and fine laminations. About 70m of sediment is present between the Rewa pumice and the first incoming of the Potaka pumice.

At Finnis Road there is at least 75m of sediment between the Rewa and Potaka pumices. The reworked Rewa pumice is present in a unit of parallel bedded pumiceous sand with distinct tabular cross bedding in places (Plate 2.2).

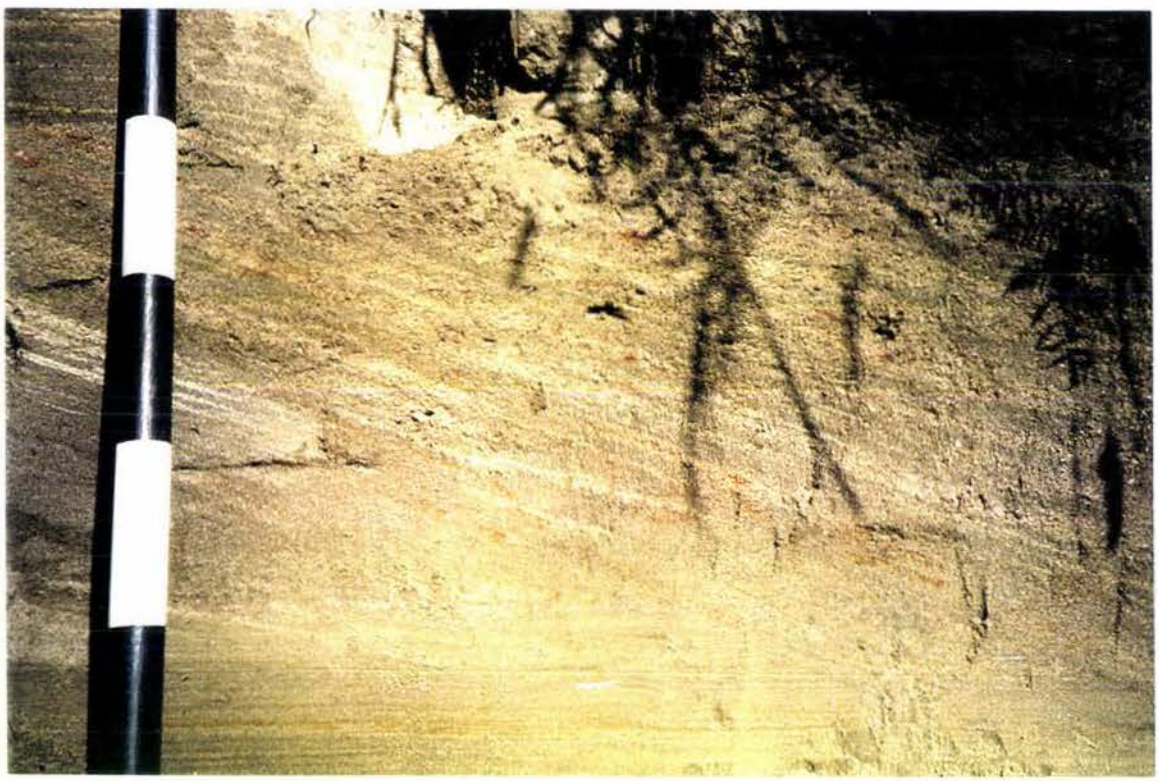

Plate 2.2: Reworked Rewa pumice (pale laminae) within cross bedded sands at Finnis Road (T23/475114). Scale marked at 100mm intervals.
(See Appendix A for stratigraphic column and descriptions).

Above the Rewa pumice unit is a unit of parallel bedded sand, with some discontinuous mud layers. Convolute bedding is present, and some scattered greywacke pebbles are found near the top of the unit. The overlying unit consists of alternating sand and silt with occasional mud layers, and some flaser bedding. Above that is a 0.5m layer of silt rip-up clasts overlain by parallel laminated sands and lenticular bedding. Convolutions and flaser beds increase up the unit, and the sediments then return to alternating sand, silt and mud. 4.5m of orange-yellow parallel bedded sands make up the following unit. The top half of this unit contains small convolutions, ripples, small channels, nodules and lenticular beds. At the top of the unit is a very small pebble layer. Above this at least 3m of well bedded and rippled sands are present with some fine pebble lenses, but the

stratigraphy then becomes obscured. About 48m above the orange-yellow parallel bedded sands is the tuff unit containing the Potaka pumice (Plate 2.3). It is a 4m unit of pumice-rich cross bedded sands with mud rip up clasts, channel trough cross bedding and pumice-filled channels.

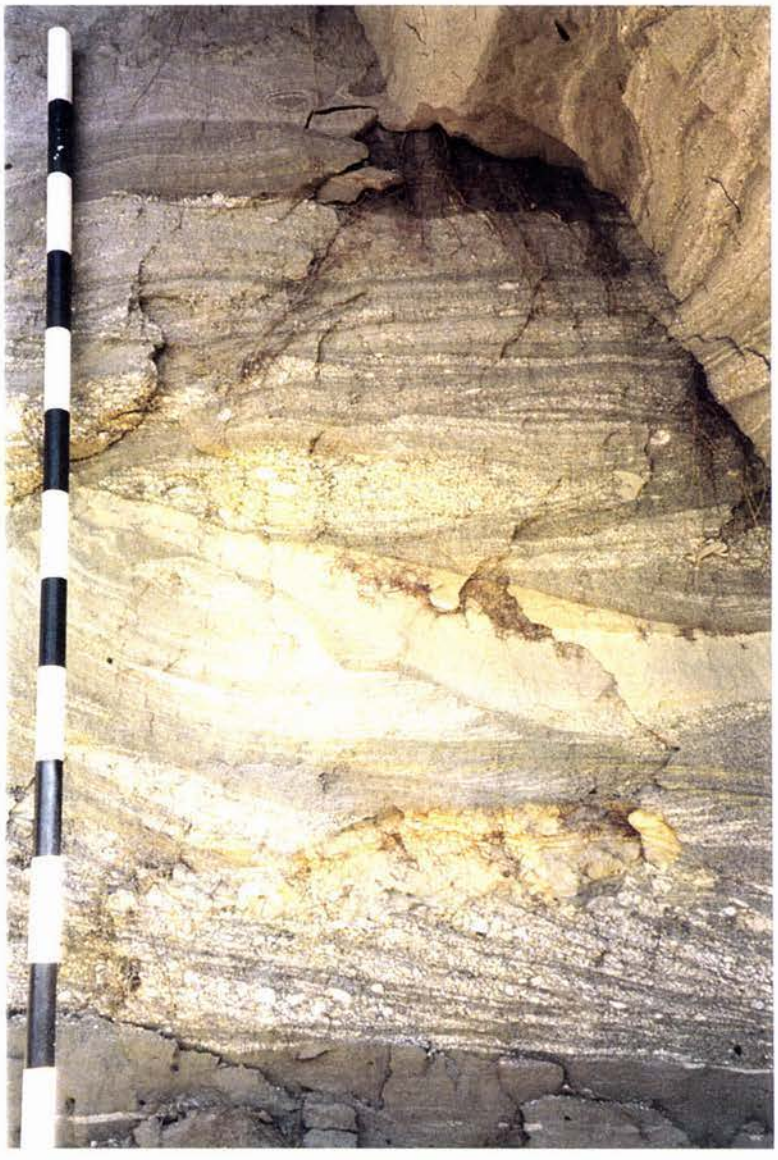

Plate 2.3: Reworked Potaka pumice at Finnis Road (T23/483120) with cross bedding, channels and rip up clasts. Scale marked at 100mm intervals. (See Appendix A for stratigraphic column and descriptions).

Interval 2: Potaka pumice to Kaukatea pumice

The sediments in this interval of the sequence are sand dominated in places, but there is a distinct increase in the proportion of mud and lignite layers, and no shells are present.

The southern Oroua River site (T23/436145) is the best for this stratigraphic interval (Plate 2.4). The first incoming of reworked Potaka pumice dips just below river level at the bottom of the sequence, while the Kaukatea pumice is near the top of the sequence, about

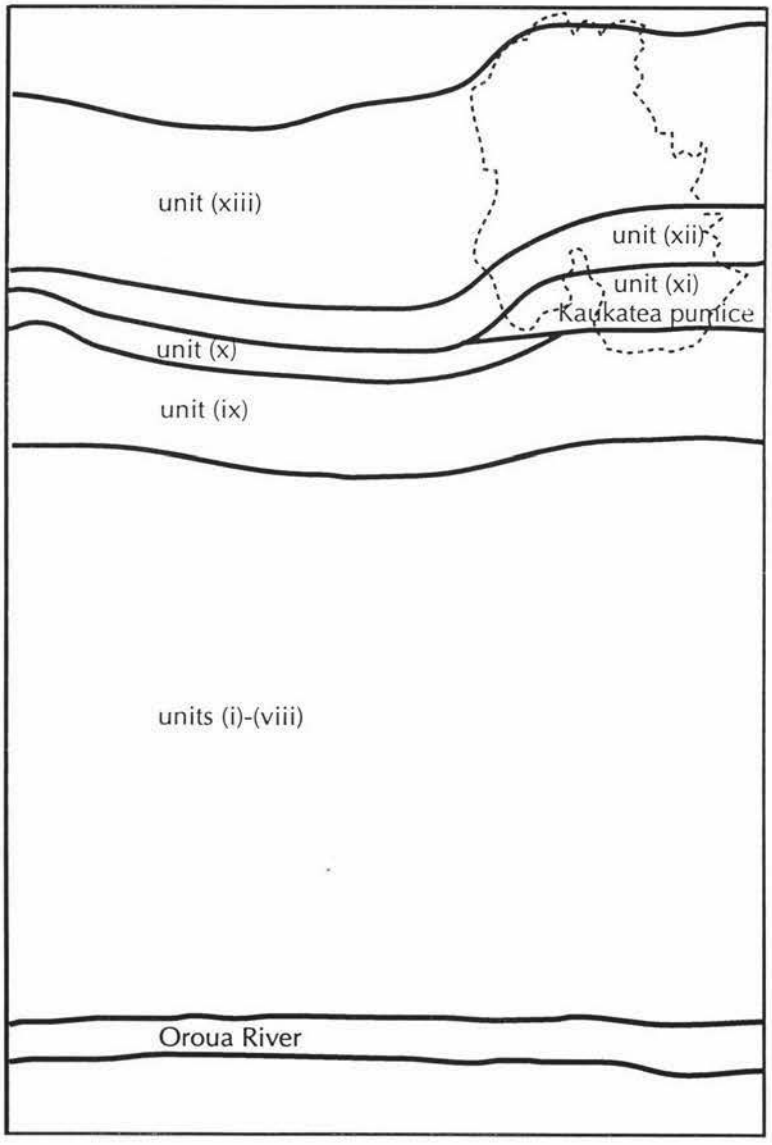

Figure 2.2: Sketch of Oroua River section 1, indicating the stratigraphic units.

70m above the Potaka pumice. The beds at this site are characteristically parallel bedded and dip 1-2° toward the south west. Above the Potaka pumice are several units of interbedded mud and sand (often pumiceous). Pumice-filled channels, mud clasts, flaser beds and ripples are all found in the unit directly above the Potaka pumice. Some of the mud layers are rich in organic matter with some burrowing being present. A 1.5m lignite layer is present about half way between the two tuff units. Above this is burrowed sand followed by more interbedded sand and mud units, displaying dewatering structures. A 2m thick unit of iron stained conglomerate sits directly beneath the 3m unit of Kaukatea pumice. The average pebble size in the conglomerate is about 50mm, and the unit is clast supported, with very little matrix although some sand lenses are present.

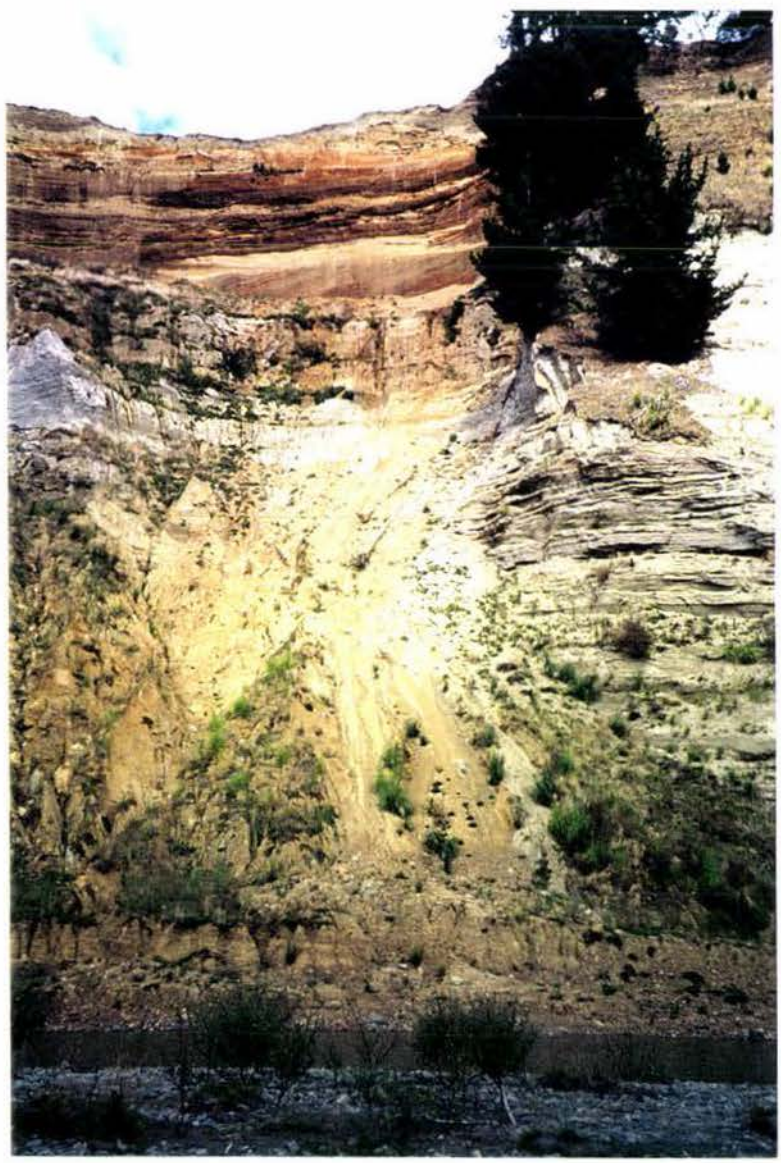

Plate 2.4: Oroua River Section 1 (T23/436145). The Potaka pumice is just below river level, and the Kaukatea pumice is near the top of the sequence (see Figure 2.2 opposite). (See Appendix A for stratigraphic column and descriptions).

At Beehive Creek (T23/503144) the Potaka pumice is a unit of finely laminated pumiceous sands, and is overlain by a unit of parallel bedded sands and silts with burrowing, root channels and ripple cross bedding. A 3m conglomerate lies directly above the parallel bedded sands with silt rip up clasts at the base. The pebbles are iron stained, clast supported and commonly about 20mm in diameter. Another sandy parallel bedded unit overlies the gravel unit, and contains a number of thin (0.2-0.4m) lignite layers interbedded with mud. A 0.3m strongly burrowed layer of airfall Kaukatea tephra is preserved near the base of this unit.

Stewart's Gully exposes sediment that lies above the Potaka pumice, but the Kaukatea pumice is not present. The Potaka pumice (T23/455144) is a thick (>3m)unit of pumice conglomerate. The sediments above the Potaka pumice are dominantly parallel bedded sands which are commonly pumiceous, with some fine mud layers and a gravel layer near the top of the sequence. Dewatering structures are present within some of the more pumiceous sediments (Plate 2.6), but generally there is a lack of sedimentary structures such as ripples and cross beds.

Plate 2.5: Dewatering structures within pumiceous sands at Stewart's Gully (T23/453145) Scale marked at 100mm intervals.
(See Appendix A for stratigraphic column and descriptions).

The Pollock Road site (T23/442140) provides an excellent outcrop of the Kaukatea pumice (Plate 2.6). At the base of the section is a unit of finely laminated blue silts. These are overlain by at least 3m of conglomerate, which is iron stained, predominantly clast supported, and has an average pebble size of about 20mm. A 0.4m sand lens is present near the base of the conglomerate. Above a sharp planar contact on the conglomerate is at least 5m of pure pumice. The grain size of the pumice varies from coarse sand size to fine lapilli, and some dewatering structures and crossbedding can be seen.

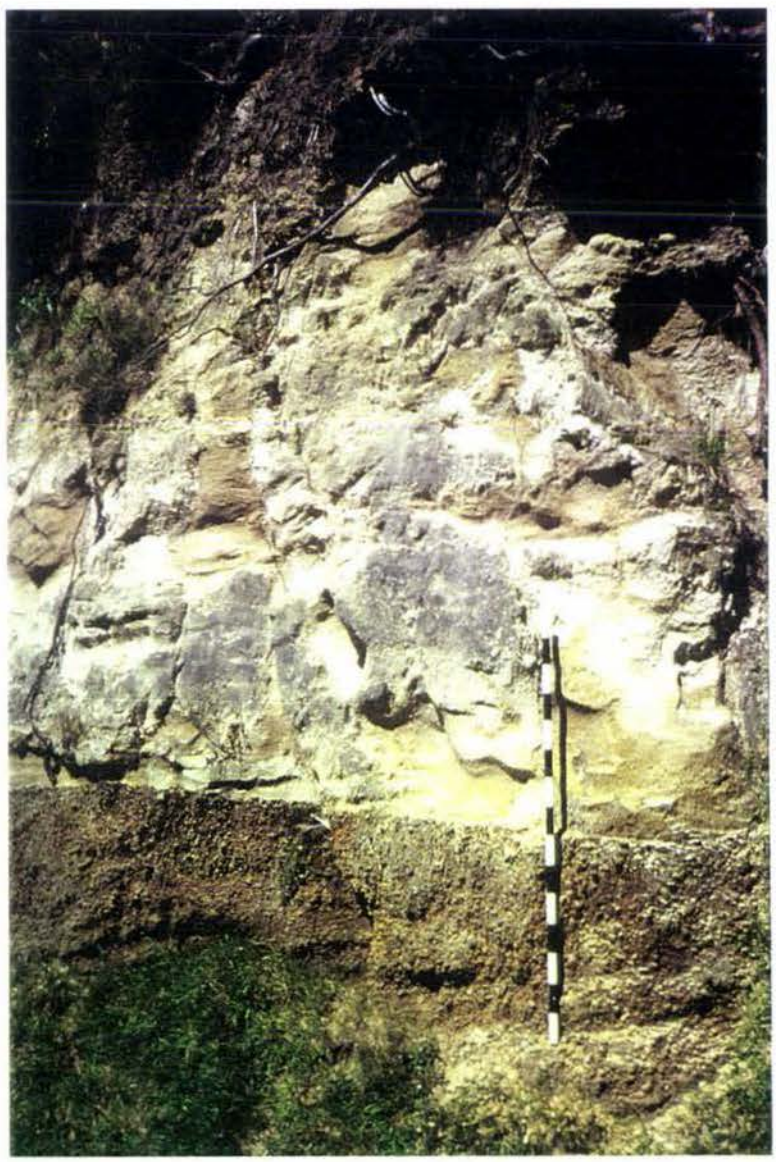

Plate 2.6: The Kaukatea pumice at Pollock Road (T23/442140) where it is sitting directly on a 2m unit of conglomerate. Scale marked at 100mm intervals. (See Appendix A for stratigraphic column and descriptions).

Interval 3: Kaukatea pumice to Kupe pumice

This stratigraphic interval is dominated by several thick conglomerate layers, and is also marked by a lack of pumiceous sediments between the two tuff units. The conglomerate units throughout the study area are all very similar - characteristically iron stained,

either clast supported or lacking matrix, and on average the pebbles are moderately rounded and about 20mm in size (Plate 2.7).

Plate 2.7: Typical conglomerate unit (Oroua River Section 1(T23/436145) unit (xiii)). Pebbles are clast supported, moderately rounded, iron stained and up to 20mm diameter. Scale marked at 100mm intervals.

The Kupe pumice is not preserved at Beehive Creek, but above the Kaukatea pumice there are four thick conglomerates, with sand, mud and lignite between. The contacts between the units are all sharp, and the sediments between the gravels tend to be sand dominated at the base, and fine upwards into mud and lignite layers. The sand units characteristically show a lack of sedimentary structures, with only laminations being obvious. At one site, where the beds are steeply dipping, the weakly bedded sand contains occasional layers of small angular greywacke pebbles (Plate 2.8).

Plate 2.8: Steeply dipping sediments at Beehive Creek (T23/502131).

The mud units are rich in organic matter, commonly have vertical burrows up to 100mm deep and are sometimes bioturbated. The lignite layers found associated with the mud units are about 0.5m thick, and show varying degrees of lignite development, from pale brown organic matter rich mud, to black layers of lignite. They are sometimes burrowed, bioturbated and contain root channels.

The site at which the Kupe pumice is found within the study area is at the top of Finnis Road (T23/449121). The site was described by MacPherson (1985) as part of his study of the area, but the tuff unit was not identified. A 2.8m conglomerate sits at the base of the section, with pebbles up to 40mm diameter, a coarse sand matrix and infrequent mud clasts. Above the gravel is 2.7m of medium sand with several mud lenses, and overlying that is the 1.7m tuff unit. The tuff is coarse sand to grit sized, though a channel within the unit is filled with coarser pumice.

2.3 Discussion

Sedimentary structures are generated by a variety of sedimentary processes, such as fluid flow, sediment gravity flow, soft sediment deformation and biogenic activity, so they reflect the environmental conditions that prevailed when, or soon after, the sediments were deposited (Boggs, 1995). They are therefore very helpful indicators when interpreting previous depositional environments.

Table 2.1 indicates the dominant sedimentary structures that are found in both the sand and mud dominated sediments at five of the sections within the study area, once again using the tuff units to divide the stratigraphy into three depositional periods.

Interval	Section				
	Oroua River 1	**Stewart's Gully**	**Finnis Road**	**Culling's Gullies**	**Beehive Creek**
Kaukatea - Kupe * Sediments are dominantly mud	Not Present	Not Present	Mostly obscured except for near Kupe	Not Present	Muds: interbedded with lignites
Potaka - Kaukatea * Sediments are dominantly sand	Sands: parallel bedding, channels, convolutions Muds: some burrows & flasers	Sands: parallel bedding, some convolutions	Obscured	Not Present	Sands: parallel bedding, ripple cross bedding Muds: burrows, root channels
Rewa - Potaka * Sediments are dominantly sand	Not Present	Not Present	Sands: parallel bedding, convolutions some cross bedding Muds: flasers	Sands: parallel bedding, convolutions Muds: burrows	Sands: parallel bedding, some cross bedding

Table 2.1: The dominant sedimentary structures found in both the sand and mud sediments at the five main sections within the study area

Interval 1: Rewa pumice to Potaka pumice

All sections are dominated by parallel bedded sands (Plate 2.9). Ripples and cross bedding are uncommon structures, but where they are preserved they provide useful paleocurrent data (refer to Chapter 4).

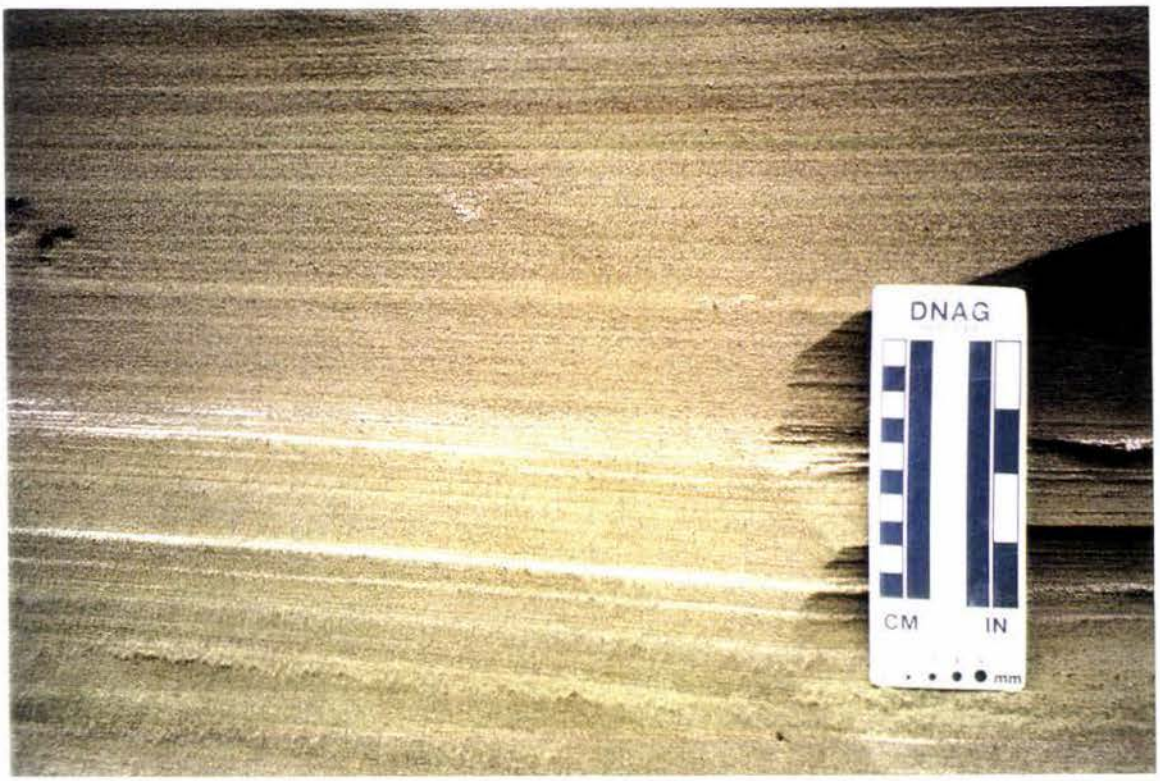

Plate 2.9: Pale pumice layers within parallel bedded sands at Stewart's Gully Section D (T23/454144). (See Appendix A for stratigraphic column and descriptions).

At Culling's Gullies the Rewa to Potaka interval is dominated by thick units of parallel bedded sands. Parallel bedding may be a result of sediment deposition in one of several ways. Three such methods of deposition are suspension, swash and backwash on beaches, and the plane bed phase of upper flow regime of a steady current (Boggs, 1995). The swash and backwash action of waves on a beach is the method thought to be responsible for these parallel bedded sands.

The pumiceous sediments of Culling's Gullies are often convoluted, providing good evidence of rapid sedimentation (Plate 2.10). Convolutions may be produced in more than one way, with liquefaction being the most important factor in their formation. Wunderlich (1967) described convolute bedding as a common feature on the steeper slopes of sand bars in tidal environments. During low tide, subaerial exposure of the sediment surface results in expulsion of water and compaction of the sediment, thus producing local liquefaction and resulting in the development of convolutions.

Plate 2.10: Convoluted pumiceous sand at Culling's Gullies (T23/472131). Darker layers are ferromag and titanomag rich sands. Scale marked at 100mm intervals.

At several locations within Culling's Gullies, some of the finer sediments show signs of burrowing (Plate 2.11). These deep vertical burrows are typical of the *Scolithos* ichnofossil found in tidal or intertidal zones, where they provide shelter from the scouring current action for the invertebrates that inhabit them, and also prevent drying when the sediments are exposed.

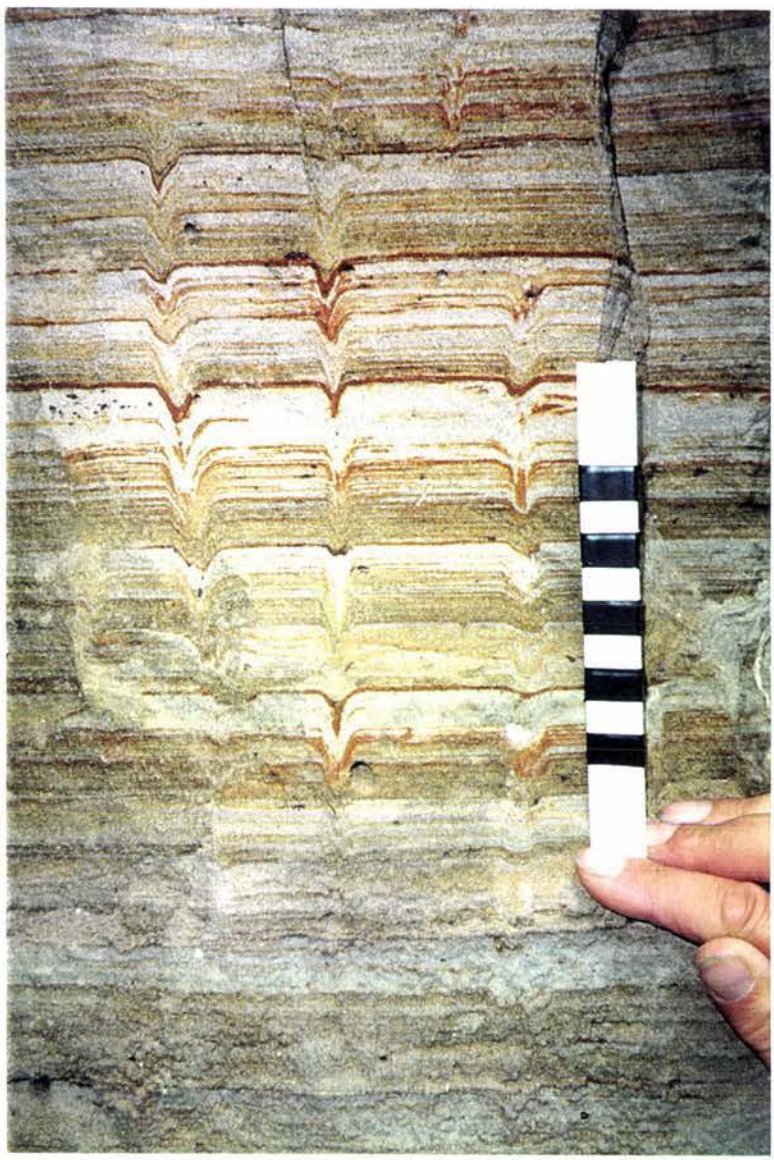

Plate 2.11: Burrows of *Scolithos* ichnofossil at Culling's Gullies (T23/485125).The burrows are typical of tidal or intertidal zones, where they provide shelter and protection from drying for the invertebrate inhabitants. Scale marked at 10mm intervals.

The lignite rip-up clasts at Culling's Gullies (Plate 2.12) were probably transported rapidly in a fluvial system to the coast. The lignite does not occur in place at Culling's Gullies, but does occur close to the Rewa Pumice at both Beehive Creek and Rangitikei Valley.

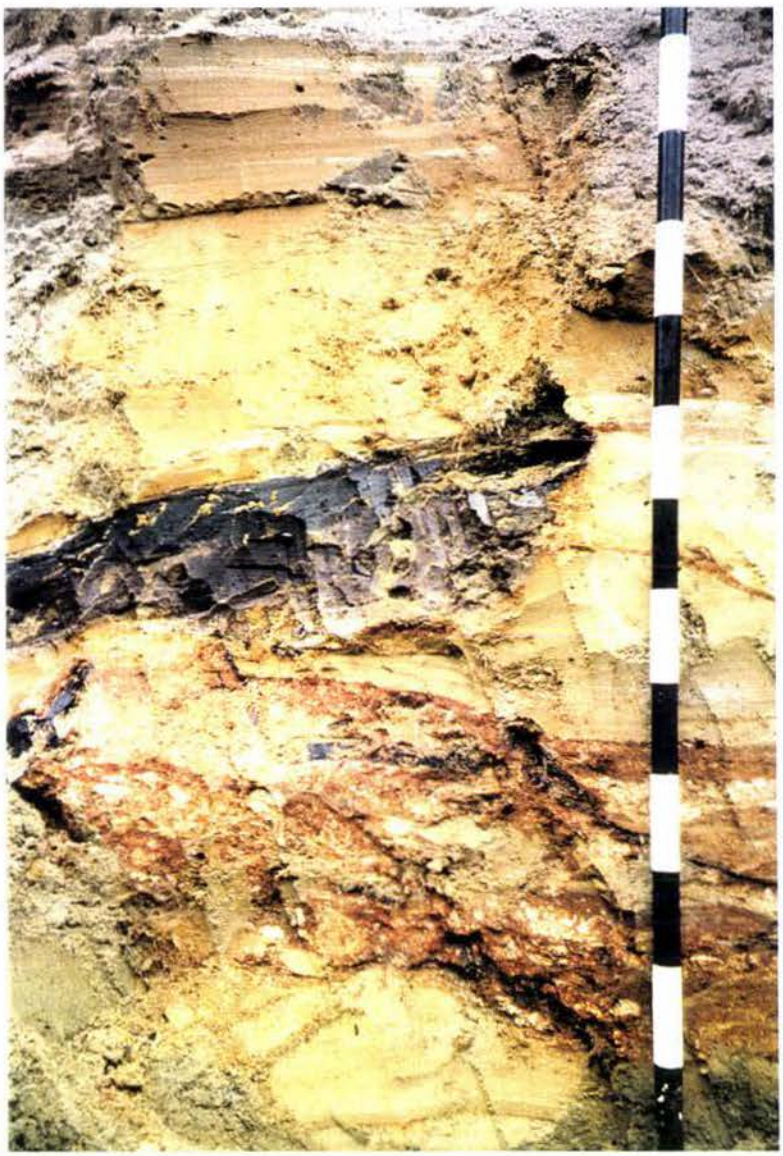

Plate 2.12: Lignite rip up clasts at Culling's Gullies (T23/484127). Scale marked at 100mm intervals. (See Appendix A for stratigraphic column and descriptions).

At Beehive Creek, sand units once again commonly display parallel bedding. East of the axis of the Pohangina Anticline they have been tilted up to 70° toward the east. Some trough cross beds are also present within the sands, formed as a result of ripple migration (Boggs, 1995). Cross bedding may form under different environmental conditions and it can be difficult to differentiate cross bedding formed in fluvial and marine environments, but the presence of a shellbed just below the Rewa pumice and another above (Townsend, 1993) is a reliable indicator of shallow marine conditions during this time interval, assuming the shellbed is not reworked. However, there must also have been brief periods of terrestrial conditions, leading to the formation of lignites and root-bearing muds.

At Finnis Road the sand dominated sediments are again predominantly parallel bedded, but some contain flaser and wavy bedding. The presence of these structures may be attributed to the alternation of current or wave action and quiet water (Reineck & Singh, 1973). Flaser bedding is most commonly found on tidal flats and in subtidal environments where sand deposition from current flow or wave action alternates with the deposition of muds from slack water (Boggs, 1995).

Several units within the Finnis Road stratigraphy show convolutions, particularly recognisable in the pumiceous sediments - similar to Culling's Gullies. Again the occurrence of convolute bedding suggests that sedimentation was at least occasionally rapid, causing liquefaction and deformation of the soft sediments.

Interval 2: Potaka pumice to Kaukatea pumice

This time interval is well represented by the sediments of the Oroua River sequence, and the Potaka pumice marks a change in the characteristics of sediments and the structures seen. The pumiceous sands near the base of the sequence are dominantly parallel bedded, but are sometimes disrupted by channels which are up to 1m wide, 15cm deep and contain mud clasts. Channels are very common in both fluvial and tidal sediments (Boggs, 1995) and are formed by erosive currents as they cut across previously formed beds. The sediments gradually change up the section from being sand dominated to mud dominated, and although there is a general lack of sedimentary structures, some bioturbation is present within the mud dominated layers, indicating the activity of living animals within the sediment or on the sediment surface (Reineck & Singh, 1973). As the mud content increases, there is also an increasing organic matter content, and one lignite layer is present. These changes within the stratigraphy suggest a shallowing environment, and a change from shallow marine to fluvially dominated conditions. The conglomerate directly beneath the Kaukatea pumice is typical of a fluvial system, as it lacks matrix and contains rounded to well rounded dominantly equant pebbles (see Chapter 4).

The sediments at Stewart's Gully are predominantly parallel bedded sands, with some fine mud layers (Plate 2.13). Once again these sediments may be interpreted as representing a shallow marine or tidal flat setting. A nearby fluvial system provided some coarser sediment slugs at times, represented by a couple of outcrops where discontinuous conglomerates and pumice filled channels are preserved. Convolutions present within the pumiceous sediments again indicate liquefaction of the soft sediments, likely to be due to rapid sedimentation.

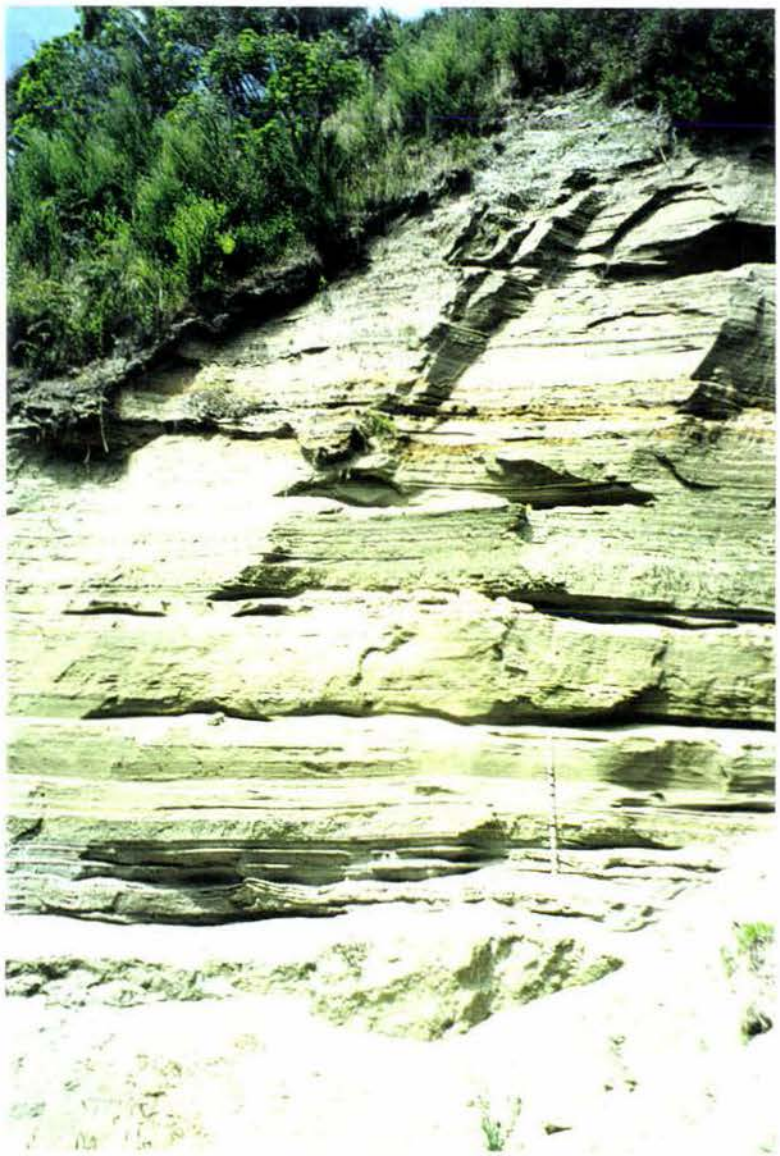

Plate 2.13: Section D at Stewart's Gully (T23/454144) indicating the predominance of parallel bedded sands. Scale marked at 100mm intervals. (See Appendix A for stratigraphic column and descriptions).

At Beehive Creek the sand sediments that were deposited during this time period are also dominantly parallel bedded, once again characteristic of either deposition by swash and backwash in a beach environment or during the plane bed phase of upper flow regime transport (Boggs, 1995). The silts show both indications of burrowing and root channels, or ripples. The asymmetrical ripples are suggestive of a current influence, perhaps due to a fluvial current or tidal flow of water over the sediments. Root channels and vertical burrows indicate that these sediments were deposited in an environment in which plants and invertebrates could inhabit, such as a tidal flat or shallow delta.

The first incoming of the Potaka pumice is represented by thick units of the pumice, with extensive cross bedding and convolutions. It is thought that the Potaka pumice was

fluvially deposited on the coast, with such a large influx causing the coast to prograde, and therefore a change from shallow marine to terrestrial conditions.

Interval 3: Kaukatea pumice to Kupe pumice

This interval is represented by only the stratigraphy of Beehive Creek, and the upper part of the Oroua River section. The most distinctive feature of this time interval is the common occurrence of interbedded lignite and mud layers, between thick conglomerates. The conglomerates are more laterally continuous than the lignite and mud, and again contain rounded equant pebbles and lack a matrix, suggesting a fluvially dominated depositional environment (see Chapter 4). The lignites can only have formed in place, so are representative of the vegetation which was inhabiting distal parts of the fluvial system, while the muds are likely to have been overbank deposits. The sands that appear within this interval lack sedimentary structures and could represent either fluvial levee deposits or marine incursions. Grain size characteristics of these sand samples are discussed in Chapter 4.

2.4 Summary

The dominance of plane parallel bedded sands during the Rewa to Potaka interval, and a lack of many other sedimentary structures, suggest that sand was deposited dominantly in a shallow marine environment, possibly by the swash and backwash of wave action. Sediment supply would seem to have been continuous and changed little, with only small mud layers being present. The presence of shellbeds, burrows and convolute laminations all provide evidence for deposition within a tidal zone. Sediment was also fluvially transported to the coast, including lignite rip up clasts at Culling's Gullies and silt rip up clasts at Finnis Road.

Sediments deposited during the Potaka to Kaukatea interval show a gradual change in environment and sediment supply. On the western side of the anticline, the sediments have an increased mud content, and the development of in place lignites indicates a change from shallow marine conditions to a lower energy environment where plant matter could accumulate and remain undisturbed. The first conglomerate unit within the Oroua River sequence indicates that fluvial conditions dominated that area just before the first incoming of the Kaukatea pumice. Sediments of Stewart's Gully are similar to those in the Oroua River, and again a conglomerate near the top of the unit is suggestive of a fluvial influence. At Beehive Creek, on the eastern side of the anticline, the fine sediments of this

time interval are representative of a tidal flat or delta, as indicated by the burrows and root channels. It would appear that the Beehive Creek area did not experience such dominantly fluvial conditions before the deposition of the Kaukatea pumice. However, the fact that the Kaukatea pumice is preserved as an airfall deposit within the Beehive Creek sediments indicates a change from shallow marine to a more terrestrial environment.

Within the Kauakatea to Kupe interval, there is an obvious influx of fluvially deposited conglomerates, with associated muds and lignites. It is thought that by the time the Kaukatea pumice was deposited, the Pohangina Anticline area was dominantly experiencing deposition within a fluvial system.

CHAPTER 3: AGE CONTROLS

3.1 Introduction

Back-arc volcanism in the Taupo Volcanic Zone (Figure 1.1) to the north-north east of Wanganui Basin has contributed significant quantities of volcanic sediment to the basin (Pillans, 1994). These volcaniclastic sediments consist of rhyolite pumice that originated from large eruptions and was subsequently transported into the basin, to be preserved as tuff units.

The tuff layers provide good age control for the enclosing sediments. A pure tuff layer is more likely to represent the first incoming of new pumice, and hence the age of the eruption closely dates the incoming of sediment. When the pumice is dispersed throughout a thick unit of sediment however, only the maximum age of the sediments can be assessed. In the Pohangina Anticline study area, pumices were commonly spread through many metres of sediment.

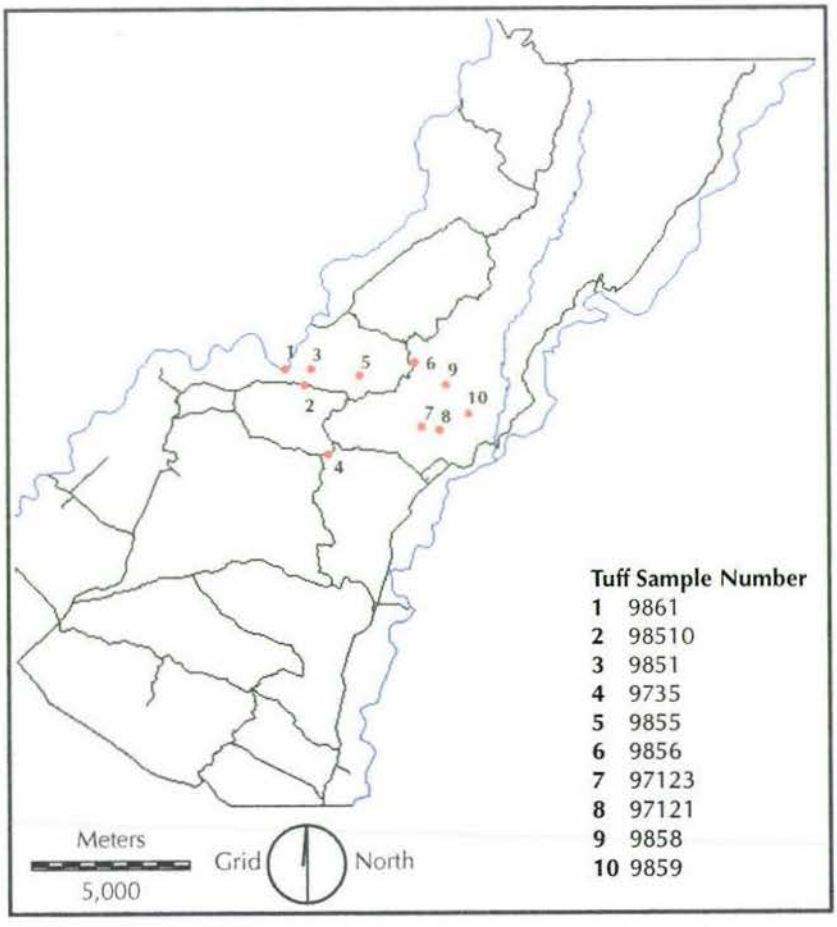

Figure 3.1: Map of the study area, locating the sites where tuff samples were collected.

Many of the tuffs look alike in the field, but chemical identification based on fingerprinting of volcanic glass shards, along with the stratigraphic positions of the tuffs allow most to be readily distinguished. In order to support the identification of the rhyolitic tuffs, or reworked pumice that were present, samples were taken and prepared for glass chemistry analysis by the JEOL 733 Electron Microprobe at Victoria University Analytical Facility, Wellington.

The methodology for the complete process followed a number of steps:

1. The sample was collected from the outcrop, and placed in a drying oven at 35°C for two to three days until thoroughly dry.
2. A small quantity of pure pumice was split from each sample, crushed and glass shards obtained using a 125-250μm seive diameter.
3. Glass from each sample was poured into holes drilled in a plug of epoxy resin then filled and mixed with epoxy. Up to eight samples fit on each plug.
4. The resin plugs were ground to expose the glass grains and then polished with progressively finer grade diamond pastes (6μm, 3μm, 1μm) using the Struers Planopol3. The polishing times were increased between grades.
5. The polished plugs were coated with a carbon film of a standard 25nm thickness. This makes the surface conductive, while preventing the sample from becoming charged and reducing the effective electron energy. The coating is deposited in a high vacuum chamber by electrically heating a narrow carbon rod.
6. The coated sample is connected to the brass sample holder by a combination of metallised tape and a silver based paint.
7. The JEOL 733 Electron Microprobe was used to analyse the chemistry of selected glass shards in each sample.

The electron microprobe is a specialist scanning electron microscope designed to analyse the elements present within the glass shards by measuring the intensities and wavelengths of characteristic x-rays emitted from the point on the sample where the stationary electron beam is focused.

A 10μm beam diameter and 8.5nA beam current were used for all analyses. At least ten glass shards were probed for each sample, with the following constituents being identified: SiO_2, TiO_2, Al_2O_3, FeO, MnO, MgO, CaO, Na_2O, K_2O and Cl.

Each analysis was normalised to 100% on a fluid-free basis for comparison with pub-

lished data. The original and normalised electron microprobe analyses are given in Appendix B. Sample 9858 was found to have two distinct populations within the fifteen glass shards that were analysed, so they were subsequently separated, and referred to as samples 9858(1) and 9858(2).

For this study, the identities of the tuffs have been determined firstly through stratigraphic control and then secondly by using glass chemistry analyses. Good stratigraphic control is provided throughout the study area, so different outcrops of the same tuff can be correlated confidently. Four methods have been used to interpret the glass chemistry data and identify the tuffs:

- bivariate plots
- ternary plots
- similarity coefficients (SC)
- coefficients of variation (CV)

The published data used for glass chemistry comparison was obtained from two sources, both working with Wanganui Basin tuffs. Pillans *et al.* (1994) provided representative analyses for the Rewa, Potaka, Kaukatea and Kupe volcanic events, analysed by electron microprobe using a beam current of 80nA and a 20μm beam diameter. Shane and Froggatt (1991) gave microprobe analyses for glass shards from the Rewa pumice, Potaka pumice and Kaukatea ash, analysed using a 10μm beam diameter. It was decided that both sets of reference data should be used for the calculation of similarity coefficients and coefficients of variation, as Pillans *et al.* (1994) provided representative analyses for all four tuffs thought to be in the study area, while Shane and Froggatt (1991) only provided analyses for three reference pumices, but they were analysed under microprobe conditions more similar to the samples from the study area.

Sodium values have been found to increase markedly as the beam diameter is increased or beam current is lowered (Froggatt, 1983). Thus it is a recognised problem that sodium values may vary with microprobe settings. Samples for this study were all analysed by the Electron Microprobe using an 80nA beam current and a 10μm beam diameter. The smaller beam diameter was used because some of the samples had very small grains or extreme vesiculation. For example, samples 9858(1) and 97123 both had very thin walled vesicular shards, too small to be probed by a 20μm beam.

Using the 10μm beam, the amount of Na_2O in the Pohangina Anticline samples is mark-

edly lower than that in the data from Pillans *et al.* (1994) and even lower than the data from Shane and Froggatt (1991). It would appear that the differences may in fact be due to other changes in Electron Microprobe conditions between the analyses of Froggatt, Pillans and myself rather than the use of different beam diameters. A new operator has taken control of the Electron Microprobe, and it has been reprogrammed and cleaned since the analyses of Shane and Froggatt (1991) and Pillans *et al.* (1994). The new operator believes Na_2O values have probably decreased by 25% (Patterson Pers comm, 1999). Na_2O was never a reliable element to compare to the glass standard, and it was therefore decided to omit Na_2O from the list of elements when computing the similarity coefficients and coefficients of variation.

3.2 Results

Ten key samples were taken:

• Sample 97121 was collected from Culling's Gully (T23/483126), from a 5m unit of very pumiceous sand and pumice lapilli. Relative to the other samples it has a high FeO content (for discussion of probe results see following sections), a low K_2O content, a fairly high CaO content and a slightly lower SiO_2 content.

• Sample 97123 was collected from Culling's Gully (T23/478127), from an 8m unit of very pumiceous fine grey sand, with a similar stratigraphic position to sample 97121. Chemically this sample is very similar to sample 97121.

• Sample 9735 was collected from the top of Finnis Road (T23/449119), from a 1.7m unit of pure coarse sand sized pumice. Relative to the other samples, sample 9735 has a low CaO content and a slightly higher SiO_2 content, while its levels of FeO and K_2O are average.

• Sample 9851 was collected from Section A of Stewart's Gully (T23/444145), from cross bedded pumice rich sediments within a unit of disturbed sand, mud and pumice. This sample has fairly low levels of FeO and SiO_2 with a high K_2O content and an average CaO content.

• Sample 9855 was collected from Stewart's Gully (T23/459143) from a 300mm layer of pure pumice within several metres of pumiceous sand. This sample is chemically very similar to sample 9851, but has a slightly higher SiO_2 content.

• Sample 9856 was collected from the top of the Branch Road walkway (T23/476147) from a 3m unit of sand sized pumice. The chemical characteristics of this sample is that it has low K_2O and SiO_2 levels, while the FeO and CaO content are fairly high.

• Sample 9858 was collected from the Branch Road walkway (T23/485140) from a unit of coarse pure pumice. This sample was found to contain two distinct populations, so is referred to as two subsamples. Subsample 9858(1) has a very low level of FeO, an average CaO content, and quite high levels of K_2O and SiO_2. Subsample 9858(2) has a slightly higher FeO content, and slightly lower SiO_2 and K_2O levels than 9858(1), while its CaO content is very similar.

• Sample 9859 was collected from the Branch Road walkway (T23/492131) from a 2m unit of convoluted pure coarse sand sized pumice. The chemistry of sample 9859 is similar to samples 9851 and 9855 with fairly high levels of K_2O and low FeO and CaO content. The SiO_2 content is slightly higher than sample 9858(2).

• Sample 98510 was collected from the Pollock Road site (T23/442140) from a 5m unit of pure coarse sand to fine lapilli sized pumice sitting directly on a 2m conglomerate unit. This sample has a chemistry that is high in SiO_2, slightly low in CaO and K_2O, and has an average FeO content relative to the other samples.

• Sample 9861 was collected from the bottom of the Oroua River section (T23/436145). It was coarse sand sized pumice within a 150mm deep channel also containing some small mud rip up clasts. Chemically this sample is very similar to sample 9859, with a high SiO_2 content, fairly low levels of CaO and FeO, and a K_2O content slightly higher than others.

Bivariate Plots

Bivariate plots can be useful tools for distinguishing between different tuffs and tephras, due to characteristic variations in their glass chemistries. The bivariate plots used for this study; %FeO v %CaO, %SiO_2 v %K_2O and %SiO_2 v %FeO, are used to chemically compare samples from the study area with four known pumices.

The following three bivariate plots illustrate the average glass compositions of 11 tuff samples from the study area and 4 representative samples from Pillans et al. (1994). Data used for these plots may be found in Appendix C.

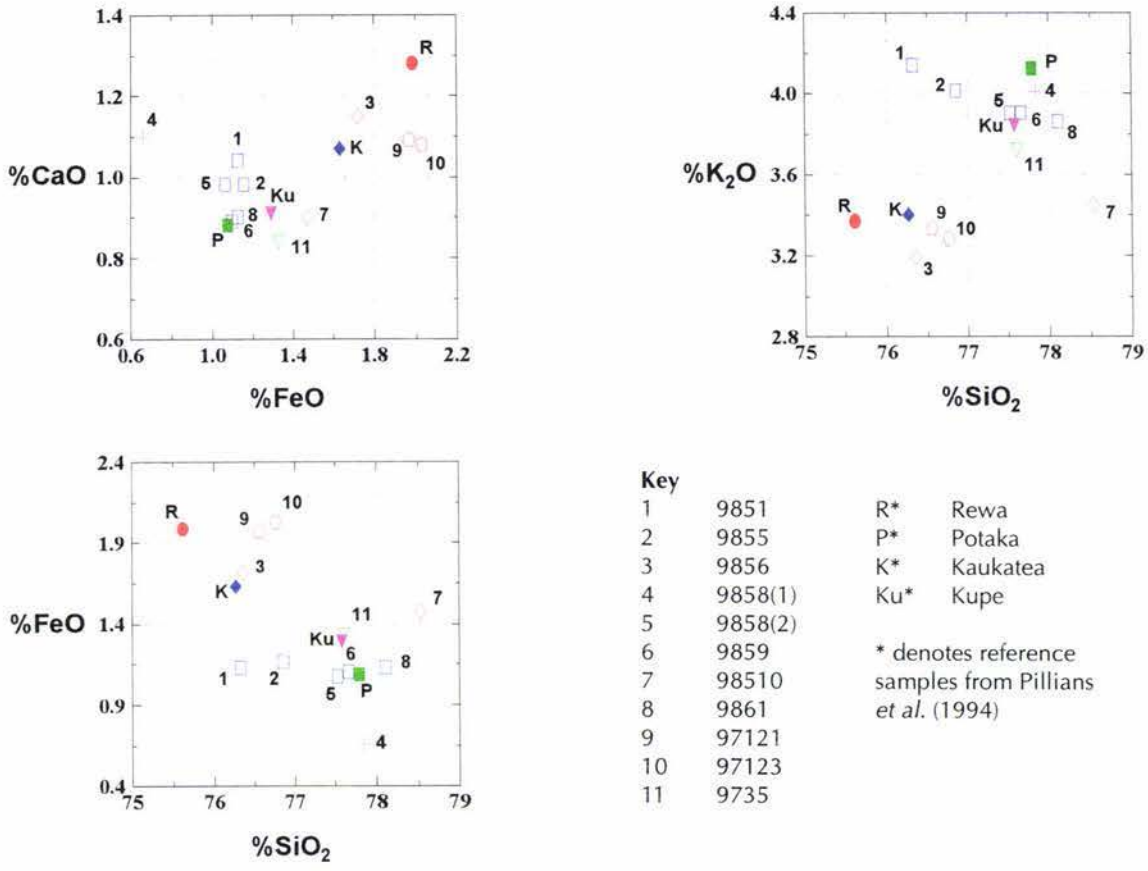

Figure 3.2: Bivariate plots of %CaO v %FeO, %K_2O V %SiO_2 and %FeO v %SiO_2 for the eleven tuff samples from the study area and four reference samples.

The bivariate plot of %CaO v %FeO has separated the samples into four groups, separated by their different percentages of FeO. Within each group, there is some small variation in the percentages of CaO.

The bivariate plot of %K_2O v %SiO_2 has shown the tuff samples as being divided into two groups - those with higher and lower percentages of K_2O. Samples thought to be representative of the Kupe and Potaka pumices, along with their reference samples, have higher %K_2O values than the samples thought to be representative of the Rewa and Kaukatea pumices and their reference samples. Some variation is shown within the SiO_2 percentages for three of the four groups - only the Kupe pumice of Pillans *et al.* (1994) has a %SiO_2 very similar to its correlative sample from the study area.

The bivariate plots of %FeO v %SiO_2 and %CaO v %FeO effectively distinguish the four tuffs due to the different percentages of FeO. Again the variation in SiO_2 percentages is evident within three of the groups. It would seem that the lower Na_2O in the analyses of this study has lead to a concomitant increase in SiO_2 measured

Ternary Plots

The normalised and averaged FeO, CaO and $^1/_3K_2O$ percentages for both the study area samples and the representative data from Pillans *et al.* (1994) are presented in Table 3.1.

	% FeO	% CaO	% $^1/_3$ K_2O
Sample 97121	47.3	26.0	26.7
Sample 97123	48.3	25.7	26.0
Sample 9735	38.7	24.5	36.8
Sample 9851	31.7	29.1	39.2
Sample 9855	33.5	28.0	38.5
Sample 9856	43.8	29.2	27.0
Sample 9858(1)	21.4	35.5	43.1
Sample 9858(2)	31.8	29.3	38.9
Sample 9859	33.4	26.9	39.7
Sample 98510	41.7	25.5	32.8
Sample 9861	34.0	27.0	39.0
Kupe*	37.1	26.1	36.8
Kaukatea*	42.6	27.9	29.5
Potaka*	32.4	26.4	41.2
Rewa*	45.3	29.2	25.5

* reference data from Pillans *et al.* (1994)

Table 3.1: Normalised percentages of CaO, FeO and $^1/_3K_2O$ for the eleven tuff samples and four reference samples.

The eleven tuff samples from the study area are plotted on a ternary diagram (Figure 3.3), to illustrate the chemical similarities to the four reference tuffs from Pillans *et al.* (1994). The ternary diagram illustrates that samples from the study area can be divided into four groups, based on their chemical similarities to the reference tuffs of Pillians *et al.* (1994).

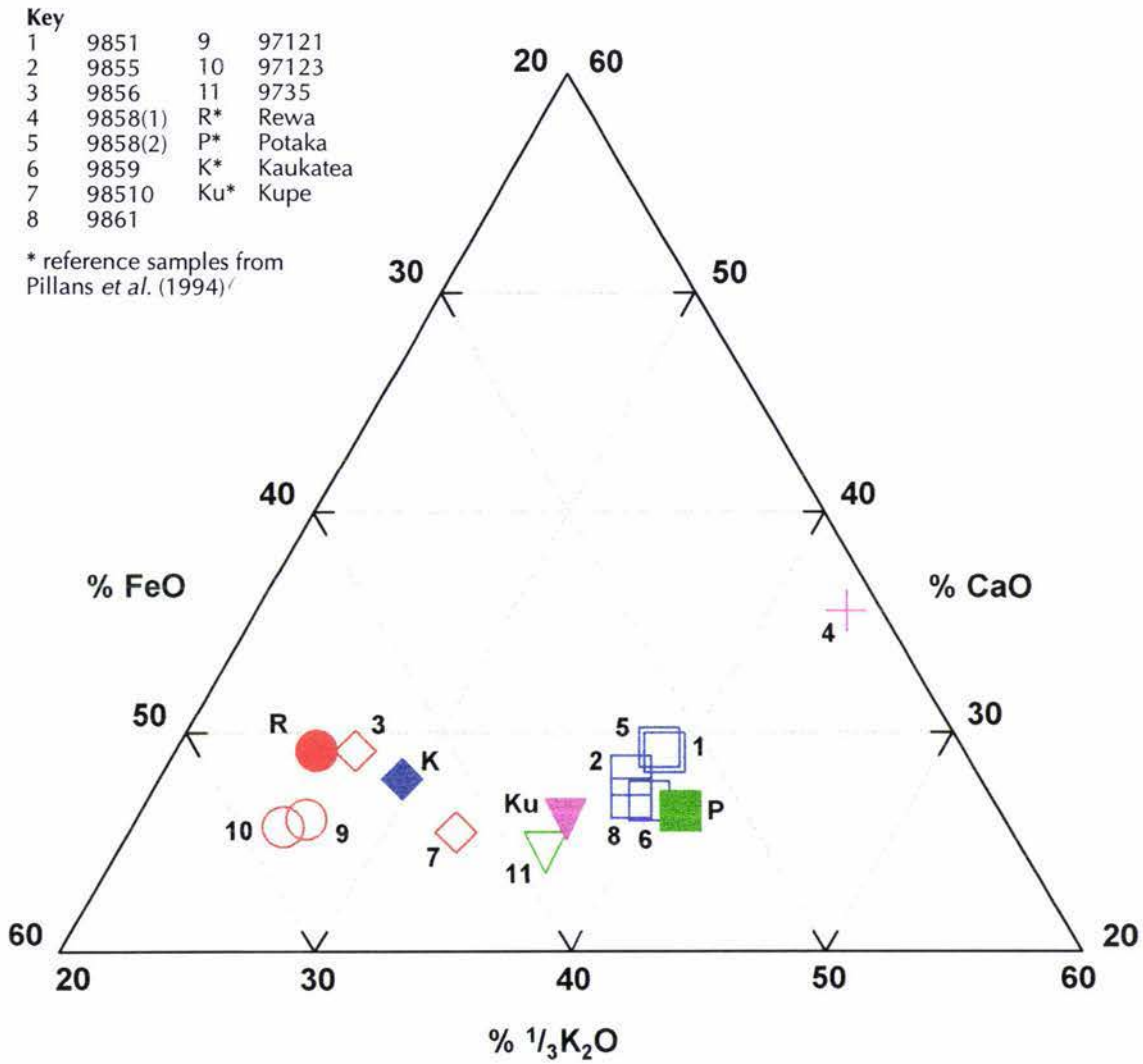

Figure 3.3: Ternary Diagram comparing the Electron Microprobe Analyses for the 11 tuffs from the study area with 4 known tephras from Pillans *et al.*(1994).

Similarity Coefficients and Coefficients of Variation

Similarity coefficients (SC) and coefficients of variation (CV) (Borchardt *et al.* 1971) were calculated by means of statistically comparing the normalised chemical data from the study area tuff samples with published data. The elements used to compare tuffs from the study area with the reference tuffs were SiO_2, TiO_2, Al_2O_3, FeO, MgO, CaO, and K_2O. The decision not to use Na_2O is discussed in section 3.3.

The sampled tuffs are identified as being chemically indistinguishable from the reference tuffs when the volcanic glass similarity coefficient values are ≥ 0.92 and the coefficients of variation are ≤ 12, as defined by Froggatt (1992). Tables 3.2 and 3.3 present the calculated SC and CV values respectively. Where the highest SC or lowest CV values differ to the chosen correlations, blank boxes indicate the best statistical correlation, while shaded boxes indicate the chosen correlations.

Tuff Sample	Pillans *et al.* (1994)				Shane & Froggatt (1991)		
	Rewa	Potaka	Kauk.	Kupe	Rewa	Potaka	Kauk.
97121	0.90	0.75	0.93	0.79	0.91	0.80	0.72
97123	0.91	0.74	0.94	0.81	0.91	0.79	0.72
9735	0.81	0.84	0.84	0.91	0.84	0.90	0.80
9851	0.71	0.74	0.77	0.75	0.74	0.75	0.67
9855	0.75	0.81	0.82	0.85	0.77	0.84	0.72
9856	0.82	0.69	0.86	0.74	0.82	0.73	0.69
9858(1)	0.77	0.87	0.79	0.87	0.81	0.86	0.70
9858(2)	0.78	0.92	0.83	0.96	0.83	0.94	0.75
9859	0.82	0.90	0.86	0.92	0.86	0.93	0.76
98510	0.82	0.82	0.90	0.89	0.84	0.88	0.78
9861	0.79	0.88	0.84	0.92	0.82	0.92	0.75

Table 3.2: SC values for the tuff samples when chemically compared to reference data. Blank boxes indicate the best statistical correlation, while shaded boxes indicate the chosen correlations, where the two differ.

Sample	Pillans *et al.* (1994)				Shane & Froggatt (1991)		
	Rewa	Potaka	Kauk.	Kupe	Rewa	Potaka	Kauk.
97121	11.87	19.35	8.00	14.59	13.51	17.35	28.93
97123	11.35	18.42	6.88	15.34	11.52	16.04	28.28
9735	14.43	12.66	9.80	6.95	11.91	8.99	29.83
9851	23.36	26.89	22.64	23.57	26.37	25.07	28.87
9855	17.03	19.94	15.97	15.99	17.35	18.32	28.01
9856	18.11	19.12	14.33	17.14	18.76	17.80	29.86
9858(1)	19.20	13.76	20.08	15.04	20.27	12.45	28.54
9858(2)	13.69	8.73	14.44	5.72	13.83	3.88	28.29
9859	13.30	14.33	12.69	10.90	12.62	8.41	28.48
98510	12.05	16.17	9.37	10.91	9.98	13.35	30.34
9861	14.24	14.74	10.15	8.52	11.96	10.62	27.89

Table 3.3: CV values for the tuff samples when chemically compared to reference data. Blank boxes indicate the best statistical correlation, while shaded boxes indicate the chosen correlations, where the two differ.

3.3 Discussion

The bivariate plots were used as an aid to distinguish between the tuffs in the study area and provide correlation with reference samples. The two plots most useful for differentiating between the tuffs were those plotting %FeO v %SiO_2 and %CaO v %FeO, due to the different amounts of iron in the Kupe, Kaukatea, Potaka and Rewa tuffs. The third bivariate plot (%K_2O v %SiO_2) effectively distinguishes the Potaka and Kupe samples on the basis of their higher levels of potassium, but the Kaukatea and Rewa tuffs have very similar percentages of K_2O, and their SiO_2 percentages overlap.

It is evident from the %FeO v %SiO_2 and %K_2O v %SiO_2 plots that the five possible Potaka pumice samples (9851, 9855, 9858(2), 9859 and 9861) show a considerable variation in SiO_2 content, while the FeO and K_2O levels are relatively similar. Shane (1994) studied the glass chemistry of the Potaka pumice and observed a chemical zonation within exposures of both ignimbrite and fluvially deposited tuff. Shards from different stratigraphic heights in the exposures formed a linear trend on variation diagrams. This is suggestive of pre-eruptive zonation of the magma chamber, but FeO and CaO levels were found to be high in the base of the unit - the reverse of most zoned eruptives (Shane, 1994).

The individual shards of the five possible Potaka pumice samples from the study area were plotted on a bivariate plot of %CaO v %FeO as used by Shane (1994) in order to determine whether a similar chemical zonation could be identified (Figure 3.4). As the plot indicates, the individual glass shards vary greatly in both FeO and CaO levels, such that no chemical zonation is evident between the five samples. This may be due to extreme mixing of the pumice during its transportation to the study area.

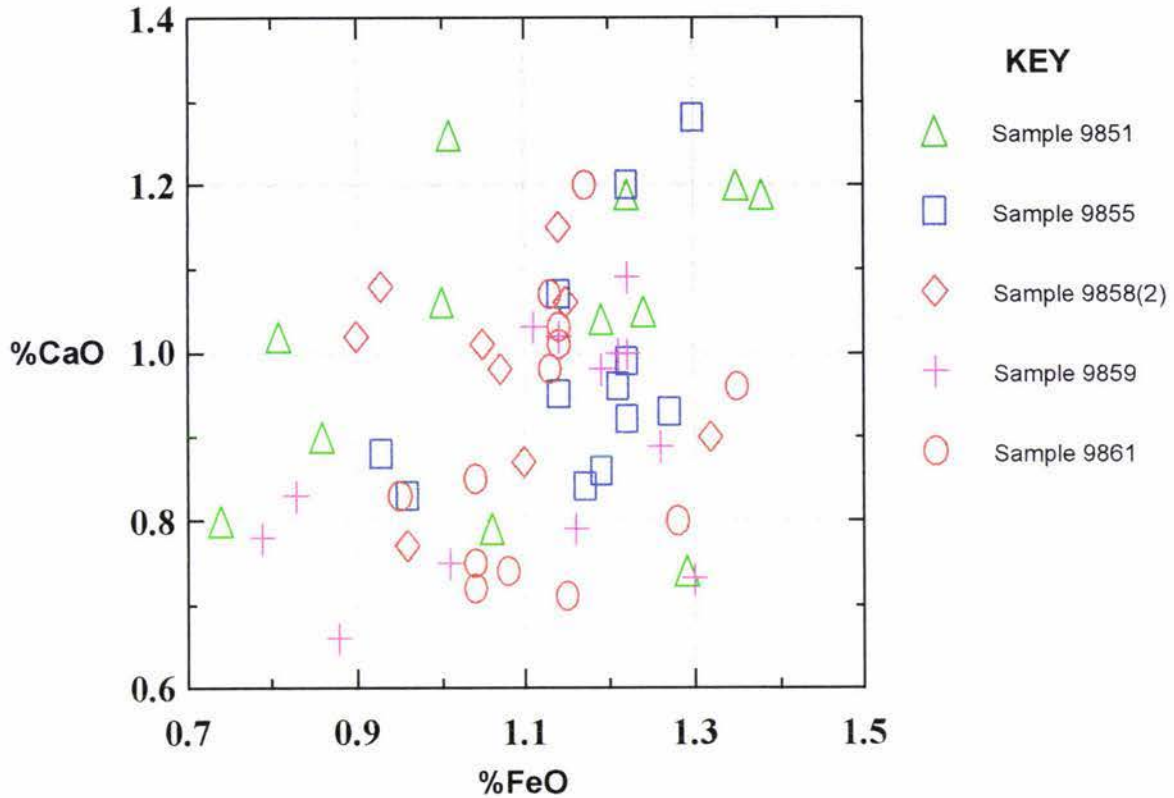

Fig 3.4: %CaO v %FeO for all glass shards of the five possible Potaka pumice samples from the study area.

The ternary diagram has been used as another method to further illustrate that the tuff samples from the study area provide good matches for the Rewa, Potaka, Kaukatea and Kupe pumices, again using reference data from Pillans *et al.* (1994). Ten of the eleven samples from the study area plot in positions on the ternary diagram that are chemically similar to one of the four reference pumices. Sample 9858(1) remains unidentified, with a chemistry distinctly different to other samples and reference tuffs.

Ten tuff samples within the study area have been identified through the use of stratigraphy, bivariate plots and a ternary diagram, and the calculation of similarity coefficients (SC) and coefficients of variation (CV) have proven to be supportive of most of those identifications. Not all correlations reached the SC of $\geq$0.92 or CV of $\leq$12 which was suggested by Froggatt (1983) to show that glass analyses were chemically indistinguishable.

The Rewa pumice is near the base of the stratigraphy, and has an age of 1.29 $\pm$ 0.12Ma (Shane *et al.*, 1996). Samples 97121 and 97123 come from marine sands near the base of Culling's Gullies sediments. When compared to the Rewa pumice of both Pillans *et al.* (1994) and Shane & Froggatt (1991), samples 97121 and 97123 have SC values of 0.90 or above, suggesting they are chemically similar, although the values are slightly below 0.92. The CV values of sample 97123 are below 12 when compared to both Rewa pumice

reference samples, indicating it is chemically indistinguishable, while sample 97121 is slightly less well matched to the Rewa pumice of Shane & Froggatt (1991) with a CV of 13.51.

The Potaka pumice, with an age of 1.05 ± 0.05Ma (Shane, 1994), is well exposed at a number of sites within the study area, and it lies about 130m stratigraphically above the Rewa pumice. With the use of the ternary and binary diagrams, five tuff samples would appear to be good matches for the Potaka pumice. Samples 9851, 9855, 9858(2), 9859 and 9861 all plot close to the reference sample of Pillans *et al.* (1994) on the binary and ternary plots, although some variation in SiO_2 percentages has been noted. Sample 9858(2) may be considered as chemically indistinguishable from the Potaka pumice, as it has SC values of 0.92 and 0.94 when compared to the reference samples of Pillans *et al.* (1994) and Shane and Froggatt (1991) respectively, and CV values of 8.73 and 3.88. Samples 9859 and 9861 are both chemically indistinguishable from the Potaka sample of Shane and Froggatt (1991), with SC values of $\geq$0.92 and CV values of $\leq$12. However, they do not provide quite such good matches with the Potaka pumice of Pillans *et al.* (1994) when calculating the SC and CV values. This slight discrepancy in values may be due to the previously mentioned different conditions under which the two Potaka reference samples were probed. In order to correctly identify these tuffs, it is necessary to consider the stratigraphy as well as the results of chemical comparisons, and when doing so, it would seem that samples 9859 and 9861 are most likely to be representative of the Potaka pumice. Although samples 9851 and 9855 had good stratigraphic control and plotted close to the Potaka pumice of Pillans *et al.* (1994) on the binary and ternary diagrams, the SC and CV values do not provide good matches with either of the Potaka pumice reference samples, as the SC values for both samples are well below 0.92 and the CV values are much higher than 12. It is not known why the chemical correlations were not established, but a couple of suggestions are that it may be a result of chemical zonation within the Potaka pumice, such that the reference samples represent a different stratigraphic section of the pumice, or that the transportation and reworking of those samples within the study area has had a more marked influence on their chemistries.

The Kaukatea pumice has an age of 0.87 ± 0.05Ma (Shane *et al.*, 1996) and is most often found sitting on a gravel conglomerate, about 70m stratigraphically above the Potaka pumice. Sample 9856 seems a reasonable match for the Kaukatea pumice of Pillans *et al.* (1994) when plotted on the binary and ternary diagrams, and stratigraphically it seems the most likely identification. However, the SC and CV values for that sample do not

suggest a good match with either of the Kaukatea pumice reference samples. The highest SC value for sample 9856 is 0.86, resulting from the comparison with the Kaukatea pumice of Pillans *et al.* (1994). Although this does not suggest indistinguishable chemistries, none of the other reference samples provide a better match. Again, these SC and CV results may be misleading, due to the change in probe conditions since the samples of Pillans *et al.* (1994) and Shane and Froggatt (1991) were carried out. Another reason for poor matches is the low number of Kaukatea pumice samples recorded in the literature. Because there have been realatively few chemical studies done, data available for comparison is very limited.

Particularly good stratigraphic control is provided for sample 98510, and on the binary and ternary diagrams it is a reasonable match for the Kaukatea pumice, although it is higher in SiO_2 and lower in CaO than both sample 9856 and the reference sample of Pillans *et al.* (1994). The SC and CV values resulting from the chemical comparison of sample 98510 with the two reference Kaukatea pumices, indicate that it is chemically very similar to that of Pillans *et al.* (1994). A CV value of 9.37 is well below the cut off value of 12, and the SC value is 0.90. Considering all the evidence, it seems most likely that samples 9856 and 98510 both represent the Kaukatea pumice.

Sample 9735 has an SC of 0.91 and CV of 6.95 when compared with the Kupe pumice analysed by Pillans *et al.* (1994). The CV value suggests that the sample is chemically indistinguishable from the reference data, and when considered alongside the results from the ternary and binary diagrams, as well as the stratigraphic control within the study area, sample 9735 may be confidently identified as the Kupe pumice, with an age of 0.63 ± 0.08 Ma (Shane *et al.*, 1996).

Sample 9858(1) remains unidentified within this study. Although it was collected from the same site as sample 9858(2) it does not plot close to other Potaka pumice samples on the binary or ternary diagrams, as it has a markedly lower level of FeO. When the SC and CV were calculated for this sample, they did not indicate a chemistry very similar to any of the reference samples. Of all the values, the best matches were with the Potaka pumice of both Pillans *et al.* (1994) and Shane and Froggatt (1991), with CV values being 13.76 and 12.45 respectively, but the SC values were both well below 0.92.

3.3 Conclusion

With each of the different methods contributing to the correlation of samples from the study area to reference pumices, it can be confidently stated that ten of the tuff samples from the study area have been positively identified as being the Rewa, Potaka, Kaukatea and Kupe pumices (Table 3.4). Stratigraphy provided the initial identification, and it has been supported through the comparison of chemical characteristics using bivariate plots, ternary diagrams, similarity coefficients and coefficients of variation.

Sample	Suggested identification
9735	Kupe pumice (0.65 + 0.08 Ma)
98510	Kaukatea pumice (0.87 + 0.05 Ma)
9861	Kaukatea pumice (0.87 + 0.05 Ma)
9851	Potaka pumice (1.05 + 0.05 Ma)
9855	Potaka pumice (1.05 + 0.05 Ma)
9858(2)	Potaka pumice (1.05 + 0.05 Ma)
9859	Potaka pumice (1.05 + 0.05 Ma)
9861	Potaka pumice (1.05 + 0.05 Ma)
97121	Rewa pumice (1.29 + 0.12 Ma)
97123	Rewa pumice (1.29 + 0.12 Ma)
9858(1)	Unknown

Table 3.4: Suggested identifications for the tuff samples collected from the study area. Ages are from Shane *et al.* (1996), Shane (1994) and Wilson *et al.* (1995).

With good stratigraphic control of the tuff layers assisting the chemical identification of the samples, it is clear that four volcanic events are well represented within the study area. The tuff layers are illustrated in the stratigraphic column of Figure 3.5.

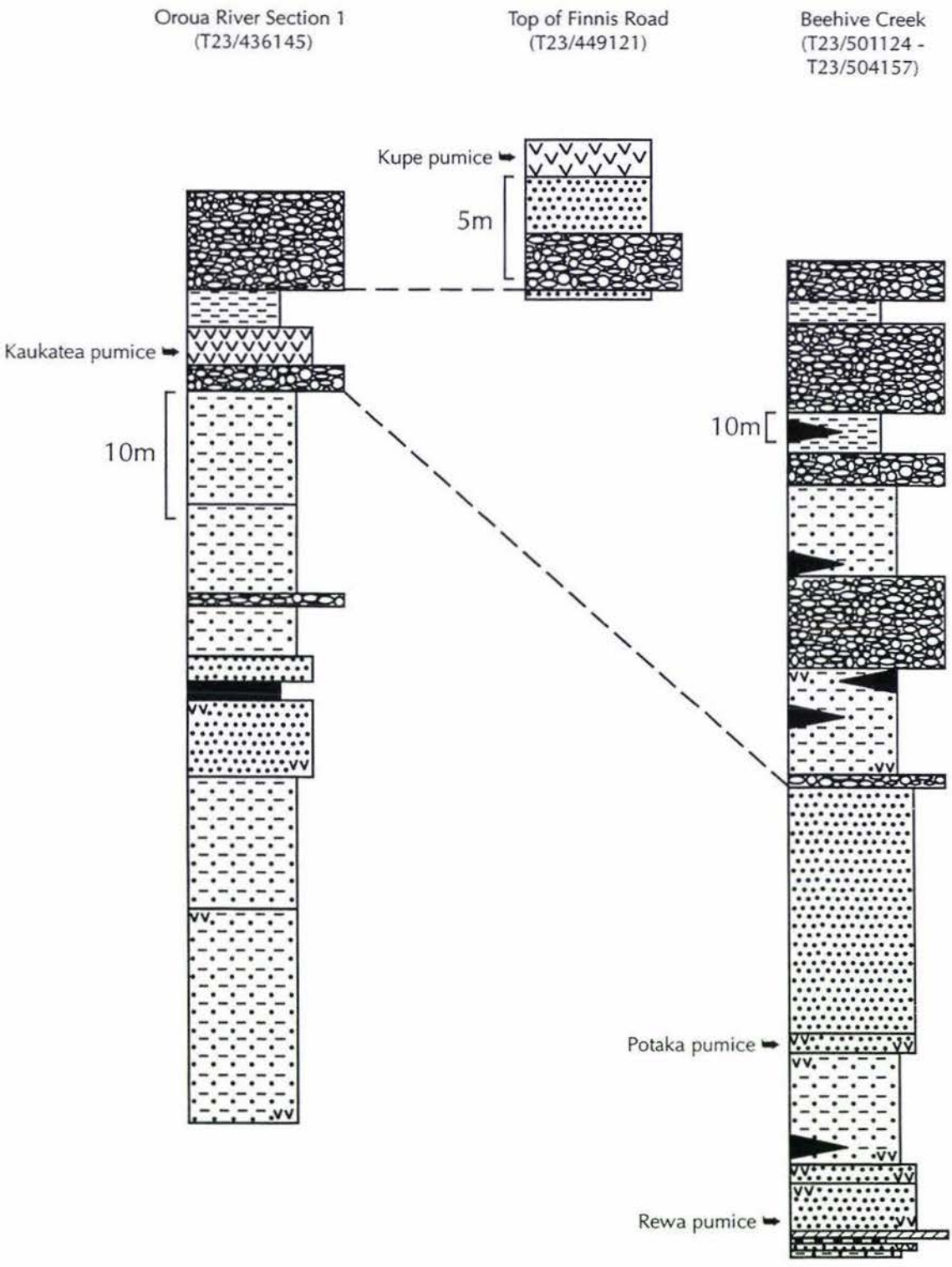

Figure 3.5: Composite stratigraphic column indicating the presence of four tuff units.

CHAPTER 4: GRAVELS AND SANDS

4.1 Introduction

In this chapter the sediment properties of the gravel and sand units within the stratigraphy of the Pohangina Anticline will be discussed. The sediment properties that were studied for both the gravels and sands were grain size and paleocurrent directions. By studying the characteristics of these sediments, some conclusions have been drawn concerning their mode of transport and deposition.

Grain Size

Grain size is a fundamental property of all sediments and sedimentary rocks, making it one of the most important descriptive properties of the rocks (Boggs, 1995). Every sediment sample contains a range of grain size, and in order to compare and interpret samples, we need to be able to characterise the grain sizes statistically. The following discussion introduces grain size parameters and how they may be used to define and compare the characteristics of sediments.

A scale widely adopted for describing the distribution of clastic particles is the Udden-Wentworth scale (Figure 4.1). In this scale, the various grades are separated by factors of two about a grain size centre of 1.0mm (Leeder, 1982). Krumbein introduced a logarithmic transformation of the Udden-Wentworth scale, to develop the well known and often used phi scale. The following equation defines the phi scale:

$$\phi = -\log_2 d \quad \text{where } d \text{ is the diameter in millimetres.}$$

There are three main advantages of using the phi scale. Firstly, the main points on the Udden-Wentworth scale become whole numbers rather than fractions. Secondly, the scale is reversed such that larger sizes become negative and the smaller sizes become positive numbers. Also, the use of the phi scale permits use of arithmetic rather than logarithmic graph paper and simplifies the calculation of both graphic and numerical descriptive statistics.

Millimetres	Phi () Units	Wentworth Size Class
64	-6.00	cobble
16	-4.00	pebble
4	-2.00	
3.36	-1.75	
2.83	-1.50	granule
2.38	-1.25	
2.00	-1.00	
1.68	-0.75	
1.41	-0.50	very coarse sand
1.19	-0.25	
1.00	0.00	
0.84	0.25	
0.71	0.50	coarse sand
0.59	0.75	
0.50	1.00	
0.42	1.25	
0.35	1.50	medium sand
0.30	1.75	
0.25	2.00	
0.210	2.25	
0.177	2.50	fine sand
0.149	2.75	
0.125	3.00	
0.105	3.25	
0.088	3.50	very fine sand
0.074	3.75	
0.0625	4.00	
0.053	4.25	
0.044	4.50	coarse silt
0.037	4.75	
0.031	5.00	
0.0156	6.00	medium silt
0.0078	7.00	fine silt
0.0039	8.00	very fine silt
0.0020	9.00	clay

Figure 4.1: Summary of the Udden-Wentworth size classification for sediment grains (after Pettijohn *et al.* 1972).

There are a number of different ways in which the grain size of a sediment may be determined. The most suitable method depends largely upon the purpose of the study, the range of grain size that can be measured, and the degree of lithification of the sediment. The following table outlines the various grain size fractions analysed for this study, and the different techniques that were used.

Sediment Size	Method of Grain Size Measurement
Gravel	Manual measurement of individual clasts, using callipers
Sand	Dry sieving
Silt and Clay	SediGraph

The measurement techniques are discussed in more detail in later sections, where each sediment type is discussed individually.

Grain Size Parameters

1. Mean Grain Size

The mean size is the arithmetic average of all the particles seen in a sample. In this study the Graphic Mean (M_Z) has been calculated using Folk's formula :

$$M_Z = \frac{(\phi 16 + \phi 50 + \phi 84)}{3}$$

Mean grain size is a function of both the size range of the source material, and the amount of energy imparted to the sediment (Folk, 1974). Once the limitations of the source material have been considered, it is then possible to apply the rule that sediments generally become finer in the direction of transport (Folk, 1974). For sand dominated sediments, this fining is generally attributed to abrasion of the grains, while for gravels the fining may be due to a number of factors, such as sediment supply, selective sorting and abrasion of the grains.

2. Standard Deviation/Sorting

The sorting of a sample has been obtained using Folk's Inclusive Graphic Standard Deviation (σ_I):

$$\sigma_I = \frac{(\phi 84 - \phi 16)}{4} + \frac{(\phi 95 - \phi 5)}{6.6}$$

This standard deviation gives a measure of the spread of the sample. Folk suggested the following verbal classification scale for sorting:

$\sigma_I < 0.35$	very well sorted
0.35 - 0.50	well sorted
0.50 - 0.71	moderately well sorted
0.71 - 1.0	moderately sorted
1.0 - 2.0	poorly sorted
2.0 - 4.0	very poorly sorted
$\sigma_I > 4.0$	extremely poorly sorted

The sorting of a sediment depends on at least four factors:

- the size range of the source material
- the mode of deposition
- the current characteristics
- the rate of sediment supply

Folk (1974) identified two types of deposition - "bean spreading", in which currents work over thin sheets of grains continuously, and "city-dump" deposition, in which sediments are dumped down the front of an advancing series of crossbeds and then rapidly buried by more sediment. Generally the former type of deposition will give a better level of sorting.

In terms of current characteristics, those with relatively constant strength will result in sediments having better sorting than those with fluctuating strengths. Currents of intermediate and constant strength tend to produce the best sorting (Folk, 1974). Very weak or very strong currents do not sort grains well.

The rate of sediment supply influences the sorting of the sediment. For example, a stable coast receiving little sediment will tend to sort the sediments more effectively than a beach where large loads of sediments are brought down by rivers. Catastrophic events such as floods play an important role in sediment supply within a river system. During periods of quiescence the sediment supply may be relatively low, resulting in little change to the river system, then when a large flood occurs, large amounts of sediment are brought into the system, changing the characteristics of the river. Thus river systems tend to have greater fluctuations in sediment supply and transportation than beaches.

3. Kurtosis

Grain size frequency curves can show various degrees of sharpness or peakedness, with the degree of peakedness being called kurtosis. Folk's formula for the Graphic Kurtosis of a sample is:

$$K_G = \frac{\phi 95 - \phi 5}{2.44(\phi 75 - \phi 25)}$$

Kurtosis measures the ratio between the sorting in the "tails" of the curve and the sorting in the central portion (Folk, 1974). An excessively peaked or leptokurtic curve is one in which the central portion is better sorted than the tails, while a flat-peaked or platykurtic curve occurs when the tails are better sorted than the central portion.

Folk (1974) suggested the following verbal limits for kurtosis measurements:

$K_G < 0.67$	very platykurtic
0.67 - 0.90	platykurtic
0.90 - 1.11	mesokurtic
1.11 - 1.50	leptokurtic

1.50 - 3.00	very leptokurtic
$K_G > 3.00$	extremely leptokurtic

4. Skewness

Most natural sediment grain size populations are not symmetrical like the ideal normal distribution, so skewness measures are used to indicate the asymmetry of such a population. In a skewed population, the mode, mean and median are all different (Figure 4.2).

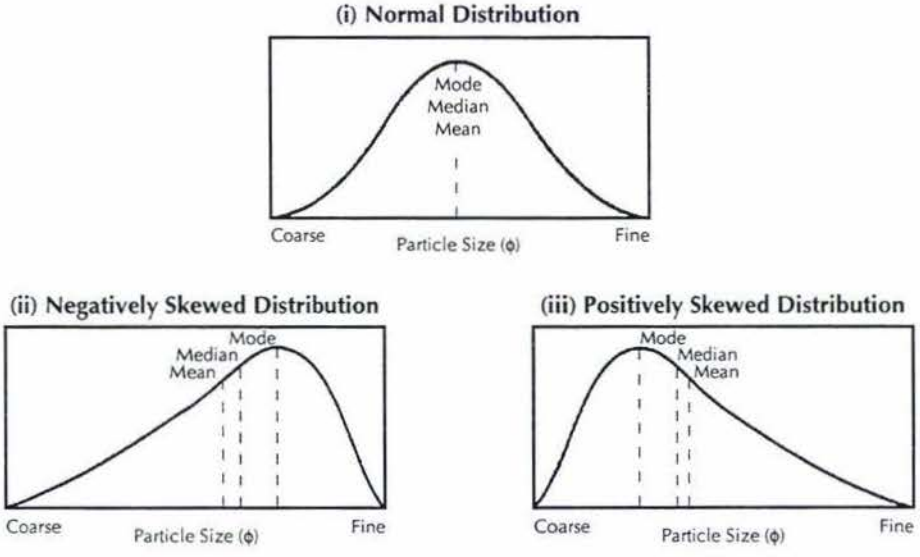

Figure 4.2: Frequency curves illustrating the difference between skewed curves and normal frequency curves.

Skewness measurements reflect the sorting in the "tails" of grain size populations (Boggs,1995). Those with a tail of excess fine particles are termed 'positively skewed', as they are skewed toward positive phi values, while populations with a tail of excess coarse particles are termed 'negatively skewed', indicating a skewness toward negative phi values.

The Inclusive Graphic Skewness (Sk_I) is calculated using Folk's formula:

$$Sk_I = \frac{\phi16 + \phi84 - 2\phi50}{(\phi84 - \phi16)} + \frac{\phi5 + \phi95 - \phi50}{(\phi95 - \phi5)}$$

The following verbal classifications for skewness were proposed by Folk (1974):

$Sk_I > 0.30$	strongly fine skewed
0.30 - 0.10	fine skewed
0.10 - -0.10	near symmetrical
-0.10 - -0.30	coarse skewed
$Sk_I < -0.30$	strongly coarse skewed

Paleocurrents

The orientation of many sedimentary structures and fabrics is related to the currents that formed them (Blatt, Middleton & Murray, 1980). In some cases, the orientation is indicative of the direction of movement, while in other cases it only indicates the line of movement.

Cross beds and imbrication are two types of sedimentary structure that indicate the direction in which the current was flowing when the sediments were deposited. Cross bedding, generally in sandy sediments, is one of the most widely used indicators of paleocurrent direction. The dip and dip direction of the foresets represent the current direction at the time the sediment was deposited.

The fabric of conglomerates represents the orientation of the individual pebbles. In some conglomerate units the pebbles may have a strongly preferred orientation, while in others there may not be any obvious pattern. A commonly occurring fabric is imbrication, formed when the long axes of the pebbles dip in an upstream direction. Well organised fabrics suggest that clasts have been free to move individually and independently above the bed and then selectively incorporated onto the bed when they were deposited in a stable position. Clasts that did not come to rest in the stable, upstream-dipping orientation would most often be re-entrained (Collinson & Thompson, 1982).

Paleocurrent measurements were determined for both sand and gravel units within the study area, and will be discussed in the following sections.

4.2 GRAVELS

4.2.1 Introduction

The upper part of the stratigraphy of the Pohangina Anticline is dominated by a number of thick gravel units. Five sites were chosen within the study area, at which the gravel units could be more closely studied, and measurements taken.

Measurements at four of the sites were made during field work for this research, while data for the fifth site (Beehive Creek) was obtained from 1997 Massey University Earth Science student projects. The procedure for recording the pebble measurements was as follows:

1. At each site, fifty pebbles were randomly selected, within an area of about 1m by 1m.
2. Each pebble was individually removed, to identify the long axis, and it was then replaced in its original position.
3. The dip and dip direction of the long axis was recorded.
4. The pebble was removed in order to measure the lengths of the long, short and intermediate axes, using callipers.
5. At the same time, the lithology and roundness of the pebble was also noted.

The lengths of the pebble axes (D_S, D_I, D_L) are used to calculate the ratios D_I/D_L and D_S/D_I in order to plot the pebbles from each site onto a Zingg diagram. Pebble shapes are classified according to where they plot on a graph using the ratios (Figure 4.3). The four shape fields (oblate, bladed, prolate and equant) may then be used to help determine the mode of transport of the pebbles.

When studying the shape of sediments, it is preferable that comparisons are made only between particles that are comparable in mineral composition, fabric and size grade. Ideally, pebbles should be structurally isotropic (Blatt, Middleton & Murray, 1980). The best approximations to isotropic rocks found in nature are massive crystalline rocks, chert, quartz and massive sandstones. For this study, the gravels that were measured were all greywacke, of a similar size grade, and had comparable fabrics.

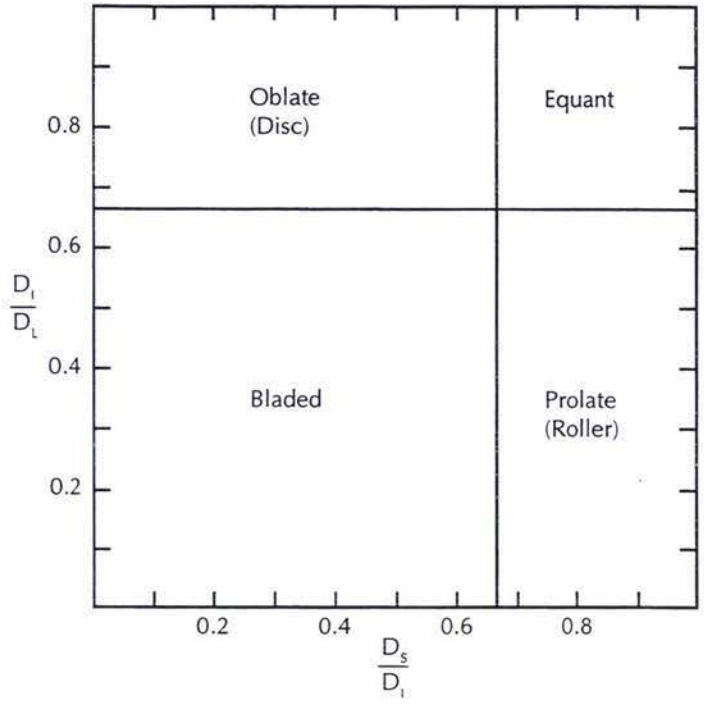

Figure 4.3: Zingg diagram used for the classification of pebble shapes (from Blatt, Middleton & Murray, 1980).

4.2.2 Results

• Pebble Shape and Imbrication

Raw data from the pebble measurements, listing the short, intermediate and long axes length, the orientation and the roundness of the pebbles at each of the five sites are contained in Appendix D.

Table 4.1 contains the average length of the three axes, measured in millimetres, and the average short/intermediate and intermediate/long ratio for each site.

	Short Axis (mm)	**Int. Axis** (mm)	**Long Axis** (mm)	**Short/Int.**	**Int./Long**
Finnis Road*	11.6	18.2	29.8	0.64	0.61
Ridge Road*	17.7	29.4	48.0	0.60	0.61
Pollock Road†	13.0	20.0	37.7	0.65	0.53
Oroua River†	13.8	21.6	37.3	0.64	0.58
Beehive Creek†	22.9	34.3	49.2	0.67	0.70

* Possible correlative gravel units
† Correlative gravel units

Table 4.1: Average lengths (in mm) of pebble axes and the axes ratios for the gravel units within the study area.

Rose diagrams have been constructed for each of the five pebble measurement sites (figure 4.4) to indicate the current directions at the time the gravel units were deposited.

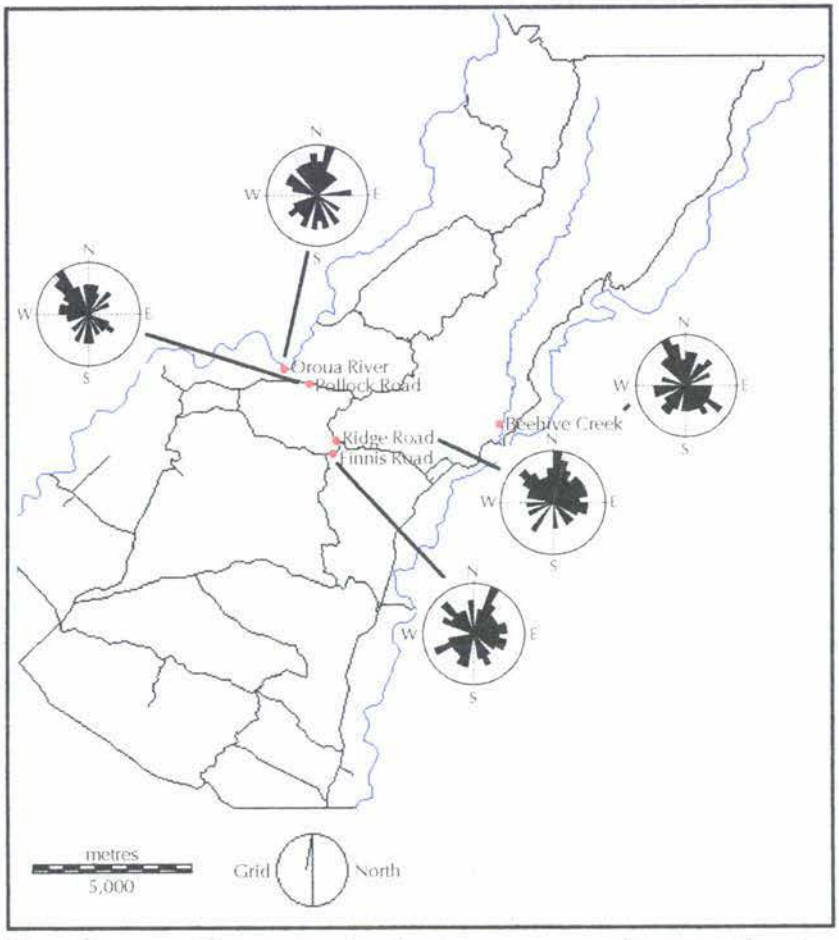

Figure 4.4: Rose diagrams illustrating the dominant current directions for the gravel units, obtained from imbrication measurements at each of the five sites.

Rose diagrams for the conglomerates from Pollock Road, the Oroua River and Beehive Creek have vector means of 317°, 329° and 339° respectively, indicating that they were deposited by a current flowing from the north west. These three conglomerates are likely to be the same stratigraphic unit. The rose diagrams for the Ridge Road and Finnis Road conglomerates have vector means of 15 ° and 44° respectively, suggesting deposition from a north or north east flowing current. It is possible that these two conglomerates are part of the same stratigraphic unit.

• Pebble lithology and roundness

When the pebble imbrication measurements were carried out at the five sites, the lithology and roundness of each pebble was also noted. It was found that all of the pebbles at each site were greywacke, and the roundness of the pebbles varied relatively little, with most pebbles at four of the sites being sub-rounded to well rounded in shape.

The percentages of pebbles at each site that were sub-angular, sub-rounded, rounded and well rounded is presented in Table 4.2. Rounding is greatest at Pollock Road and least at Beehive Creek.

Location	Pebble Shape Percentages			
	Sub-Angular	Sub-Rounded	Rounded	Well Rounded
Finnis Road	0	26	56	18
Ridge Road	2	52	46	0
Pollock Road	0	0	68	32
Oroua River	0	4	66	30
Beehive Creek	14	54	32	0

Table 4.2: Percentages of pebbles in each shape class for the gravel units within the study area.

4.2.3 Discussion

• Pebble Shape

Zingg Diagrams have been constructed (Figure 4.5) to show the pebble shape at each of the five sites. From these diagrams, it is evident that the pebble forms at each of the five sites plots toward the upper right hand corner, near the 'equant' field.

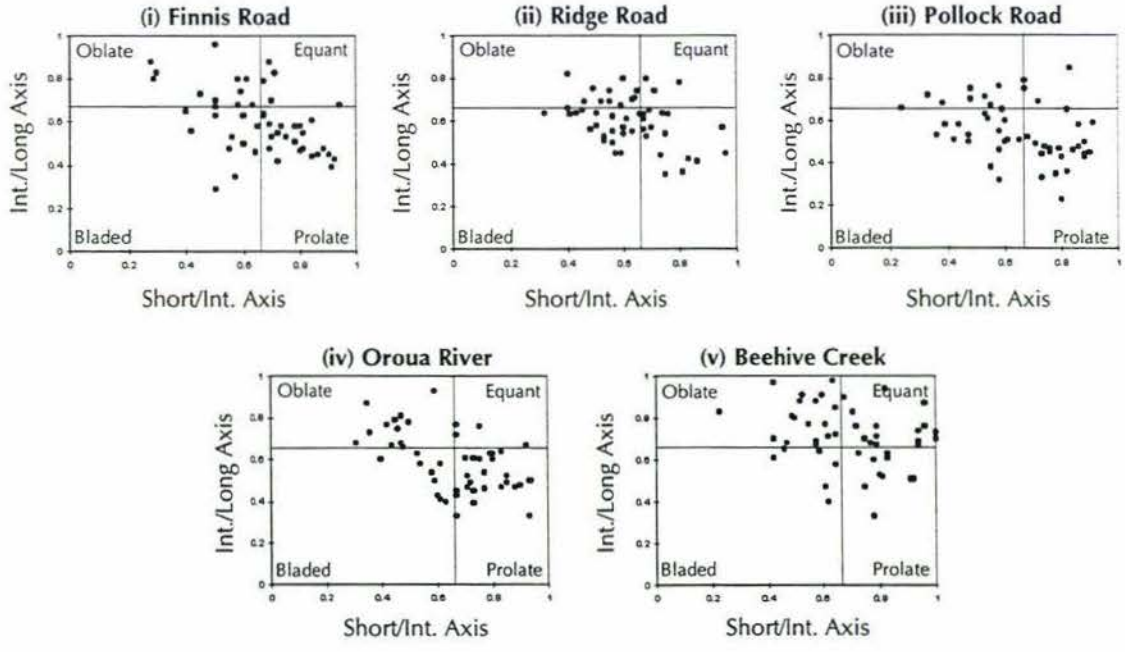

Figure 4.5: Zingg diagrams for the five pebble sites.

All of these Zingg diagrams indicate that deposition of the conglomerates could have ocurred within a fluvial environment. None have clear marine characteristics, and the Beehive Creek conglomerate in particular shows a strong fluvial signature (Figure 4.5(v)).

It has not yet been demonstrated that the form of particles, as expressed by Zingg shape measures, can be used alone as a reliable tool for interpreting depositional environments (Boggs, 1995). In this case, the generally spherical form of the pebbles, the sedimentological characteristics (associated overbank deposit sediments, channel structures and imbrication) along with the pebble roundness are suggestive of a fluvial environment of deposition.

The form of larger particles has an affect on their transportability, when they are moved by traction along the bed (Boggs, 1995). Equant and roller-shaped clasts tend to be more readily transported than blades and discs with the same mass, and this may lead to preferential transportation of pebbles downstream.

The two variables that are important in determining the roundness of transported pebbles are pebble composition and size (Boggs, 1995). Obviously soft pebbles will become rounded more readily than hard pebbles, and large pebbles are often more rounded than smaller pebbles. The presence of well rounded spherical pebbles is generally indicative of fluvial transport. However, roundness is not a direct indicator of fluvial environments - disc and roller shaped pebbles from beach environments may also be rounded, but not spherical.

Braided river systems generally occur in areas of rapid erosion, with sporadic and high discharge and there is often little vegetation to hinder run off (Selley, 1996). For these reasons, braided rivers are generally overloaded with sediment. Soon after a channel is cut it is once again choked with sediment. Thus bars are formed and new channels are diverted. Repeated bar formation and channel branching generates a network of braided channels over the whole depositional area (Selley, 1996).

Braided river channels are generally broader and shallower than those of meandering rivers. Within braided channels the sediment is transported by traction currents in the form of longitudinal and transverse bar systems (Selley, 1996). The gravels commonly show imbrication, may fine upwards, are dominantly horizontally bedded and sometimes cross bedded (Reading, 1978). Sands commonly show tabular sets of cross bedding, with ripple cross lamination sometimes preserved above the sets. Within the braided river system, fine sediments are deposited and preserved in rare abandoned channels which result from channels becoming choked with sediment and switching routes.

Gravel transport is not regular at any point in a braided river system, but occurs as a series of pulses or sediment 'slugs' at different spatial and temporal scales. Variation in the texture and structure of gravel deposited from traction currents reflect the extreme unsteadiness of flow and transport rates in natural gravel-bed rivers (Miall, 1996).

• Pebble Imbrication

Imbrication is commonly preserved in clast supported conglomerates, and develops when the clasts are deposited from traction currents as bed load. Clast supported gravels are thought to be a result of high bed-shear stress conditions, when only the coarsest clasts are deposited, while finer clasts and sand will infiltrate the clast framework at lower flow velocities (Miall, 1996).

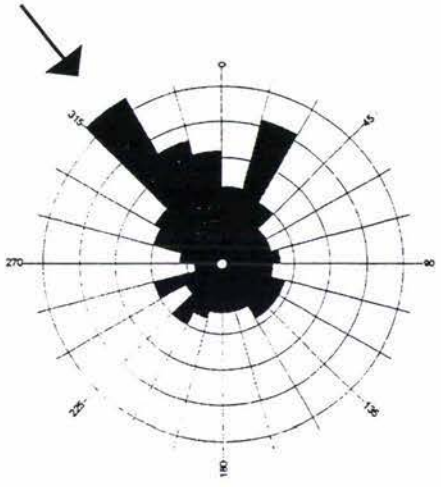

Figure 4.6: Rose Diagram illustrating the dominant current direction at the time the gravel units were deposited in the study area.

A Rose Diagram was constructed by combining the imbrication measurements of the five sites, to give an overall paleocurrent direction for the whole study area (Figure 4.6). It indicates that the dominant flow direction was from the north west when the gravels were deposited.

The Finnis Road and Ridge Road conglomerate units occupy similar stratigraphic positions and are possible correlatives. The vector means of individual pebble imbrication measurements for the sites are 044° and 015° respectively, indicating that the pebbles at both sites were deposited by a current flowing from the north north-east but the imbrication is weak. The conglomerates at the Finnis Road and Ridge Road sites, considered to be stratigraphically and lithologically equivalent, were deposited under similar environmental conditions.

The Pollock Road, Oroua River and Beehive Creek conglomerate units were deposited under similar environmental conditions just before the incoming of the Kaukatea pumice. The pebbles are lithologically similar, and imbrication is stronger than at Finnis Road and Ridge Road. Imbrication vector means of 317°, 329° and 339° clearly indicate a flow from the north west, the direction from which the Kaukatea pumice must have been transported. At Pollock Road and Oroua River, thick alluvially deposited Kaukatea pumice directly overlies the gravels. At Beehive Creek airfall ash rests on 0.8m of fine grained alluvium over gravels.

• Depositional Environment

In the lower North Island there are well preserved river terrace sequences which have formed in response to climatic fluctuations during the Pleistocene. In the Rangitikei River valley for example, terraces formed as the river carried and deposited large amounts of gravel during cool climate episodes, and then cut down through the gravels when supply waned during warmer climatic periods. Due to the high rate of uplift in the region of the Rangitikei River, the terraces have been well preserved.

The gravel units within the stratigraphy of the Pohangina Anticline are most likely to have been deposited during cold climate episodes, but regional subsidence rather than uplift has resulted in terraces being inundated and the gravel units being preserved as layers 2-28m thick within the stratigraphy.

Two distinctly different sets of gravels are observed. Firstly there are several layers of gravels that were deposited before the incoming of the Kupe pumice (0.63 ± 0.05 Ma) and have been measured for this study, and secondly the Porewan, Ratan and Ohakean terrace gravels that have been deposited during cool climate periods within about the last 70 000 years. The two sets of gravels are quite different in appearance - the older gravels are characteristically iron stained, clast supported, weakly cemented, well sorted and the pebbles are about 20mm in size. Contrastingly, the younger terrace gravels are uncemented and more poorly sorted with dominantly larger pebbles.

The finer gravels may be present either because they were deposited in a subsiding basin (lower energy regimes), because the central North Island and Ruahine Ranges are lower (therefore fluvial systems have less energy) or perhaps because they came a greater distance.

The absence of andesite pebbles indicates the Central North Island andesitic volcanoes were not present at the time, or that ignimbrites from which the pumices were derived flowed beyond the Central North Island andesites active at the time, and the headwaters of streams eroding the ignimbrites did not extend as far north as the Central North Island andesites.

4.2.4 Conclusion

The roundness of the pebbles, the presence of imbrication and the clast supported nature of the gravel units are characteristic of sediments fluvially deposited from traction currents during periods of high bed-shear stress. The gravel units are likely to have been deposited during cool climate events, on braided river systems when erosion of the main axial ranges would have been greater and a large amount of coarse clastic sediment was available.

The paleocurrent directions obtained from the imbrication of the gravels suggest that they were deposited by a river entering the area from the north west. This is consistent with the most likely source areas of the pumice tuffs that are interbedded with the gravels. The fact that the sampled gravels were exclusively greywacke suggests that they are likely to have originated from the main axial ranges of the North Island.

4.3 SANDS

4.3.1 Introduction

A number of samples were collected and sieved to study the sedimentary characteristics of the sands within the study area.

The procedure for sieve analyses is summarised as follows:

1. Dry samples were disaggregated thoroughly, while taking care not to crush the grains.
2. Using a sample splitter, a representative sample was collected, generally weighing about 25-35g.
3. An accurate weight of the sample was recorded.
4. A nest of clean sieves ranging from about 0.5ϕ to 4 ϕ, at 0.25ϕ intervals, were stacked in order, with a pan at the bottom.
5. The sample was poured into the top sieve, and the cover added.
6. The sieve nest was secured to the sieve shaker, and shaken for 15 minutes.
7. Each sieve was removed, inverted and cleaned to collect the sediment, with the weight of the sediment fraction on that sieve being recorded. The fraction finer than 4ϕ that remained in the pan was also weighed.

4.3.2 Results

• Grain Size

Raw sieve data for the nine sands that were collected from the Pohangina Anticline study area may be found in Appendix E.

Histograms and cumulative percentage curves were plotted for each of the samples, and the critical percentiles were obtained (5^{th}, 16^{th}, 25^{th}, 50^{th}, 75^{th}, 84^{th} and 95^{th} percentiles). Folk's statistical parameters were then calculated for each sample, and a summary of those parameters is outlined in table 4.3.

	Sample	Graphic Mean (M_z)	Incl. Graphic Std. Dev. (σ_I)	Graphic Kurtosis (K_G)	Incl. Graphic Skewness (Sk_I)
1	Stewart's Gully D1	2.83	0.37	1.18	0.19
2	Stewart's Gully D2	2.72	0.41	1.19	0.12
3	Branch Road Corner A*	1.97	1.47	0.80	-0.43
4	Branch Road Corner B	2.65	0.51	1.14	0.10
5	Oroua River 1 C	2.82	0.33	1.33	0.12
6	Oroua River 1 E	3.48	0.48	0.79	-0.14
7	Beehive Creek 1	2.97	0.47	1.27	0.15
8	Beehive Creek 3	2.87	0.31	1.23	0.29
9	Beehive Creek 6	2.60	0.27	0.97	-0.03

*Very pumiceous sample

Table 4.3: Folk's statistical parameters for the nine sand samples collected from the study area. Sample numbers 1-9 refer to Figures 4.8 & 4.9.

From the statistical grain size parameters, each of the nine samples could be given the following verbal classifications according to Folk (1974):

Sample 1 - Stewart's Gully D1: well sorted, leptokurtic, fine skewed

Sample 2 - Stewart's Gully D2: well sorted, leptokurtic, fine skewed

Sample 3 - Branch Road Corner A: poorly sorted, platykurtic, strongly coarse-skewed

Sample 4 - Branch Road Corner B: moderately well sorted, leptokurtic, near symmetrical

Sample 5 - Oroua River 1C: very well sorted, leptokurtic, fine skewed

Sample 6 - Oroua River 1E: well sorted, platykurtic, coarse skewed

Sample 7 - Beehive Creek 1: well sorted, leptokurtic, fine skewed

Sample 8 - Beehive Creek 3: very well sorted, leptokurtic, fine skewed

Sample 9 - Beehive Creek 6: very well sorted, mesokurtic, near symmetrical

Table 4.4 shows the median and one percentile values for the samples, converted from phi units into microns. These values may be plotted on a C-M diagram, in order to help discriminate between depositional environments (Passega, 1964).

	Sample	Median (μm)	One Percentile (μm)
1	Stewart's Gully D1	143.6	241.5
2	Stewart's Gully D2	153.9	353.6
3	Branch Road Corner A	183.0	nd
4	Branch Road Corner B	164.9	466.5
5	Oroua River 1 C	143.6	366.0
6	Oroua River 1 E	88.4	250.0
7	Beehive Creek 1	134.0	258.8
8	Beehive Creek 3	134.0	225.3
9	Beehive Creek 6	164.9	307.8

Table 4.4: Median and one percentile values for the nine sands from the study area. Sample numbers 1-9 refer to Figure 4.10.

Grain size data has been collated from three other studies within the study area, to assist in the contrasting and comparison of data. Table 4.5 shows the key statistical parameters for grain size data collected by Townsend (1993), Manning (1988) and MacPherson (1985).

	Sample	Median	Mean	Std. dev.	Skewness	Kurtosis
10	TTA	1.2	1.43	0.90	0.41	1.15
11	TTB	1.3	1.43	0.77	0.29	1.91
12	TTC	1.7	1.75	0.58	0.25	1.01
13	TTD	1.7	1.72	0.68	0.15	1.13
14	TTE	2.6	2.63	0.27	0.20	1.95
15	TTG	2.8	2.82	0.42	0.25	0.85
16	TTO	2.4	2.40	0.66	0.00	1.84
17	DMA	2.80	2.82	0.38	0.09	1.32
18	DMB	2.65	2.65	0.29	0.11	1.29
19	DMC	1.50	1.40	0.41	0.39	1.81
20	DMD	2.83	2.90	0.45	-0.17	1.50
21	DME	2.95	2.90	0.35	0.14	1.91
22	DMF	2.73	2.70	0.32	0.14	1.78
23	DMG	3.33	3.40	0.47	-0.25	1.43
24	AM1/1		3.23	0.28	-0.01	1.21
25	AM6/1		3.87	1.57	0.57	8.19
26	AM15/1		2.80	0.37	-0.13	1.10
27	AM22/4		2.68	0.35	-0.04	1.15
28	Finnis Rd 1		2.80	0.38	-0.01	
29	Finnis Rd 2		2.90	0.49	0.24	
30	Finnis Rd 3		2.70	0.53	-0.04	
31	Finnis Rd 4		2.60	0.70	-0.29	
32	Finnis Rd 5		3.80	0.48	-0.73	
33	Finnis Rd 6		2.60	0.86	0.06	

Table 4.5: Statistical parameters for sand samples collected within the study area during previous studies by Townsend(1993) (TTA-TTO), Manning(1988) (DMA - DMG), MacPherson(1985) (AM 1/1, 6/1, 15/1, 22/4), and Massey University Student Projects (1994) (Finnis Rd 1-6). Sample numbers 10-33 refer to Figures 4.8 & 4.9.

As the data indicates, these samples are dominantly fine and medium sands (Udden-Wentworth size classification) with three very fine sands also (DMG, AM1/1, AM6/1). One sample (AM6/1) is poorly sorted, the majority are moderately to well sorted, and four are very well sorted (TTE, DMB, DMF, AM1/1). Most of the samples are near symmetrical to strongly fine skewed, with only three being coarse skewed (DMD, DMG, AM15/1). The kurtosis of most samples ranges from mesokurtic to very leptokurtic, with one extremely leptokurtic sample (AM6/1) and one platykurtic sample (TTG).

• Paleocurrents

Cross beds and ripples were used to obtain paleocurrent measurements for the sand-dominated sediments. Rose diagrams (Figure 4.7) were constructed to illustrate the dominant current directions during the deposition of sediments at the measured sites. When the rose diagram indicates paleocurrent flow dominantly in a single direction, the paleocurrent vector is said to be unimodal. If two principal directions are indicated, it is bimodal, and if three or more flow directions are shown on the rose diagram, the paleocurrent flow is called polymodal (Boggs, 1995).

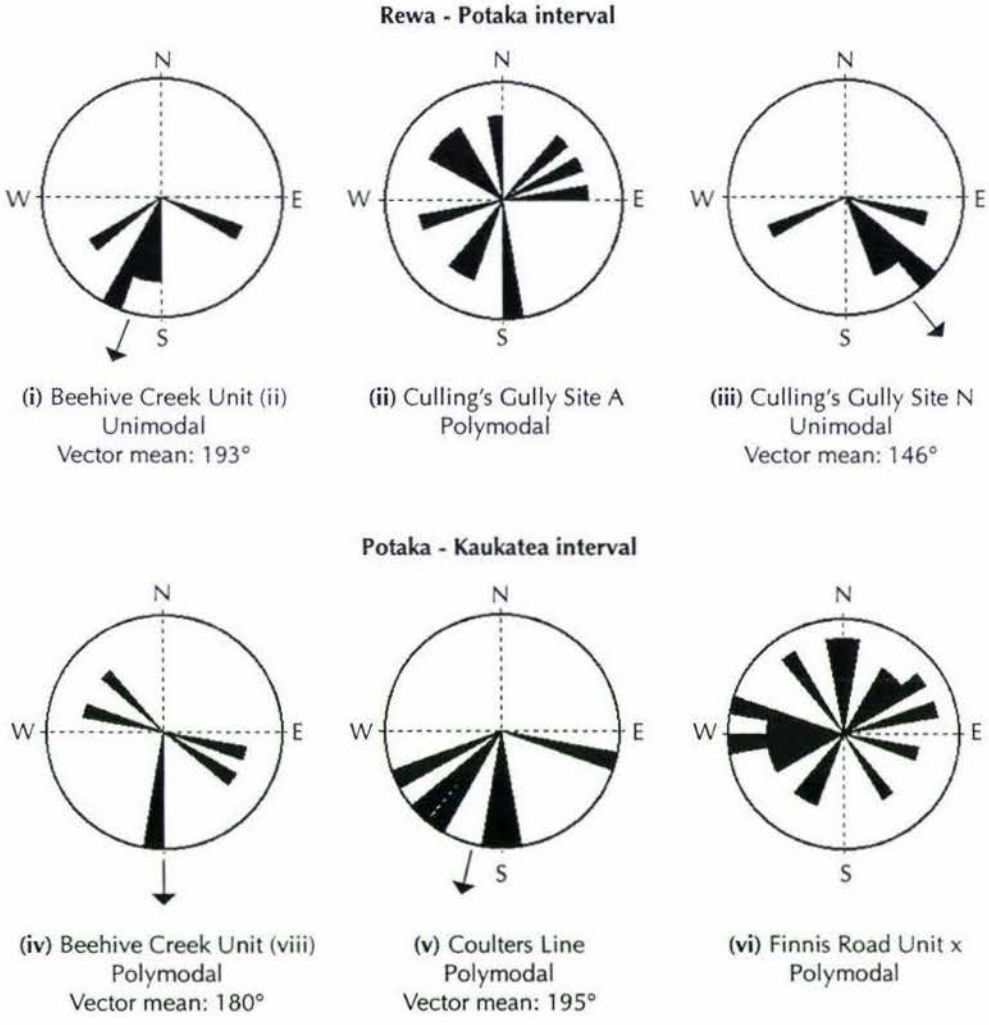

Figure 4.7: Rose diagrams illustrating the dominant sand paleocurrent directions from three sites within each of the Rewa - Potaka and Potaka - Kaukatea intervals. Arrows indicate vector means and therefore current directions.

4.3.3 Discussion

• Grain size

Sediment grain size characteristics can often be helpful in determining the environment of deposition of a sediment. There is a certain correlation of grain size with environments - for example, you don't usually find conglomerates being deposited in swamps or silts accumulating on beaches (Folk, 1974). However, in this study the facies changes did result in finer sediments accumulating on beaches and gravels being deposited in swamps as the climate deteriorated.

A number of attempts have been made to relate grain size characteristics of sediments directly to the depositional environment. Friedman (1961, 1967) sampled sands from both fluvial and marine environments, and found several ways to effectively distinguish them. One way is by plotting a graph of standard deviation (sorting) versus skewness. On this graph, beach sands characteristically have negative skewness and good sorting (low standard deviation), whereas river sands typically have positive skewness and poorer sorting. This comparison is limited to medium and fine sands, because the skewness of coarse river sands tend to be inconclusive as an indicator of the depositional environment (Friedman, 1961).

Another graph Friedman used to help differentiate between beach and river sands was standard deviation versus mean. Again, it is the standard deviation that is environment-sensitive, so the sorting of the samples helps to distinguish the two depositional environments, as beach sands are better sorted than river sands.

The differences between grain size characteristics of beach and river sands may be related to the mode of deposition. The positive skewness of river sands (i.e. the presence of a fine tail) is because river water generally contains a fairly high concentration of suspended clay and silt, which is carried along with the coarser grained sand load. In the beach environment however, the low energy conditions that allow deposition of silt and clay from suspension are not often attained, and the fine sediments are winnowed out by the waves and currents, resulting in a negative skewness and better sorting.

In all depositional environments, sorting is strongly dependent on grain size (Folk, 1974). The best sorted sediments are usually those with a mean grain size of around 2ϕ to 3ϕ, representing the fine sand fraction. As sediments get coarser, their sorting tends to worsen

until those with a mean grain size of 0ϕ to -1ϕ show the poorest sorting. Sorting then tends to improve again in the gravel range of -3ϕ to -5ϕ, with some gravels being as well sorted as the best-sorted sands. At the other end of the size range, sorting tends to worsen in fluvial sediments as they get finer than fine sands, so fine silts with a mean grain size of 6ϕ to 8ϕ often have the poorest sorting values. Sorting then tends to gradually improve, with pure detrital clay sediments (10ϕ) having better sorting.

Friedman's plots differentiate between the beach and river sands by differentiating between the environmental processes that operate in those environments and the availability of fine sediment for transportation and deposition. The modes of sediment transport differ between the two environments - river sands are commonly deposited through rolling, saltation and suspension, while in the beach environment saltation is usually the only important mechanism (Friedman, 1967).

These different modes of sediment transport are illustrated by the cumulative frequency plots. When the probability scale is used, river sands commonly have three differently sloped log-normal distributions resulting from the three modes of transportation, while beach sands are commonly composed of just one log-normal distribution (Friedman, 1967).

The cumulative frequency plots for the nine sand samples collected for this study are presented in Appendix F. They illustrate that eight of the samples are typical of fluvial sediments, having three distinct distributions, while the Branch Road Corner B sample has a cumulative frequency plot that is more typical of a beach sand, with only one real distribution.

Another way to differentiate between depositional environments was suggested by Passega (1964), in which two properties of the grain size distribution are used - the one percentile (C) to measure the coarsest grains in the deposit and the median (M). The different environments may be determined by studying the patterns produced by plotting a number of samples on a C-M diagram. The action of transporting agents causes the separation of sediments by producing gaps in the size distribution and this in turn allows us to analyse the transportation characteristics when suitable grain size parameters are used (Passega, 1964). Ideally about thirty samples of a deposit should be used, with each sample being a deposit of homogeneous sedimentation, representing all textures available.

All available grain size analyses from the study area have been plotted on diagrams developed by Friedman (1961, 1967) and Passega (1964) in order to help determine their environments of deposition within the study area. Some of the data was obtained from previous studies carried out by Townsend (1993), Manning (1988), MacPherson (1985) and class projects from Massey University (1994) as well as grain size data that was collected for this study. Only the nine sand samples collected for this study have been used on the C-M diagram, as the one percentile value was not reported in some previous analyses. Figures 4.8 and 4.9 show the data plotted on diagrams of standard deviation versus skewness and standard deviation versus mean developed by Friedman (1961, 1967) and figure 4.10 shows the data plotted on a C-M diagram, as developed by Passega (1964).

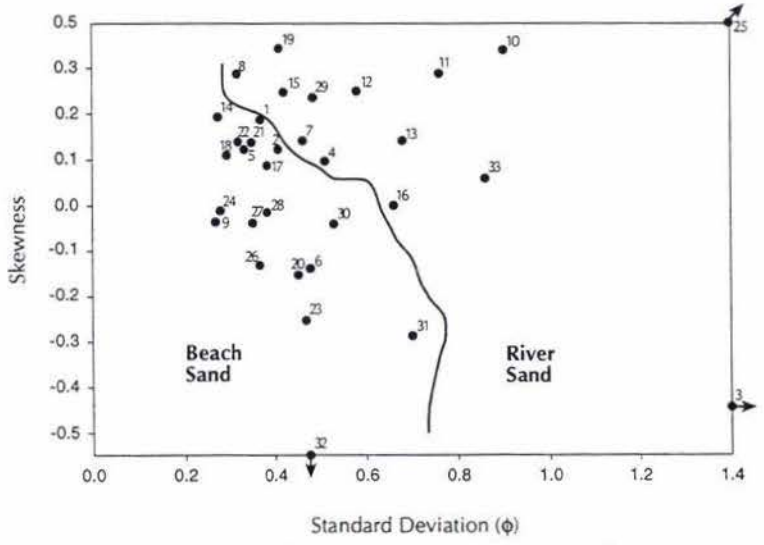

Figure 4.8: Graph of standard deviation (sorting) versus skewness, used to help differentiate between beach and river sands (after Friedman, 1961, 1967). Sample numbers 1-33 refer to Tables 4.3 & 4.5

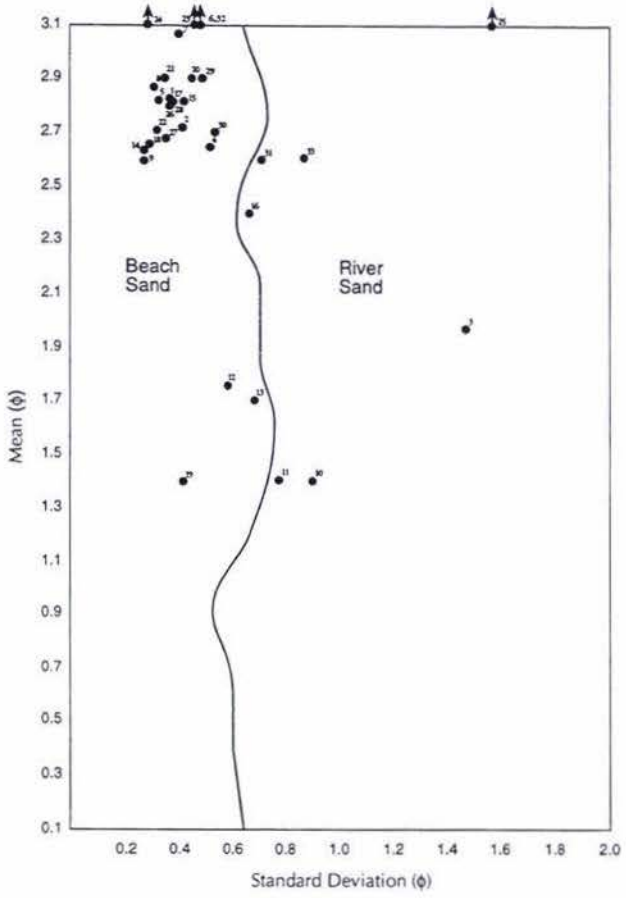

Figure 4.9: Graph of standard deviation (sorting) versus mean, used to help differentiate between beach and river sands (after Friedman, 1961, 1967).
Sample numbers 1-33 refer to Tables 4.3 & 4.5.

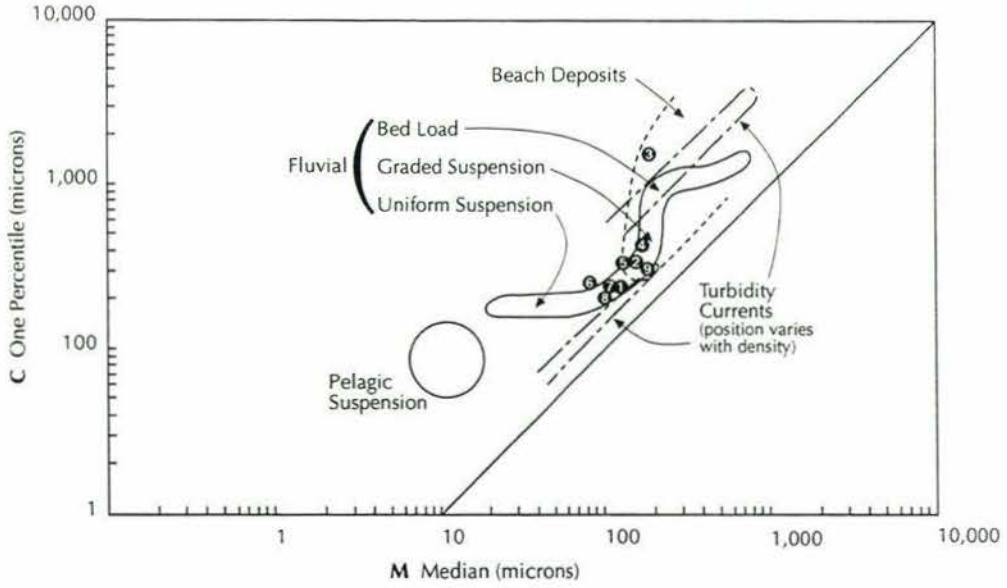

Figure 4.10: C-M pattern for the nine sand samples within the study area, used to help discriminate between different depositional environments (after Passega, 1964).
Sample numbers 1-9 refer to Table 4.4.

On both of Friedman's diagrams there is a reasonable spread of values, with sand samples plotting as both beach and river deposits. In order to find a clearer explanation, the samples have been divided into three stratigraphic intervals, separated by the tuff units. The first interval contains sixteen samples that were collected from sediments between the Rewa and Potaka tuff units (Samples 10-13, 17-23, 26 & 28-31). Of these sediments, nine plot as beach deposits on both of the graphs, two plot as river deposits, and the remaining five samples plotted as beach sands on one graph and river sands on the other. These results are interpreted as suggesting that the sand samples are predominantly from beach deposits, but that other samples may be river sediments. The environment of deposition during this time interval may have been a shallow marine embayment, with a river carrying large amounts of sediment out to the coast. This environment is consistent with the sedimentary structures that were noted for this interval of the stratigraphy (refer to Chapter 2). The lignite clasts at Culling's Gullies and the high sedimentation rates are indicative of fluvial transport, while shallow marine or tidal conditions are confirmed by the presence of shellbeds and burrows.

If the locations of the sand samples are considered alongside the interpretation from Friedman's graphs, a trend does become apparent. The samples that were collected from sites on the western side of the anticline, such as Finnis Road and Culling's Gullies have predominantly plotted as beach sands on both of the graphs, while those collected from Beehive Creek on the eastern side are plotting on the graphs as having a stronger fluvial influence. This is an indication that the coastline during this time period was near to where the axis of the anticline now lies.

The second stratigraphic interval contains eleven samples taken from sediments that lie between the Potaka and Kaukatea tuff units (Samples 1-6, 24-25, 27 & 32-33). When plotted on Friedman's two graphs (Figures 4.8 and 4.9), seven of the samples plot as beach sands on both graphs, three plot as river sands on both graphs and one sample plots as a river deposit on the graph of standard deviation versus skewness but as a beach deposit on the graph of standard deviation versus mean.

These results suggest that the sands have grain size properties that are characteristic of both the marine and fluvial environments. An environment that could result in such sediment characteristics is a shallow coastal setting where there is a high input of fluvial sediment, such as a fluvially dominated delta. In that setting, the sediments being transported by the river will have taken on the characteristic signatures of fluvially deposited

sediments, and are then taken to the coast where they are rapidly redeposited within the beach environment. In such a case, it is unlikely that the sediments will be reworked within the marine environment sufficiently to take on the grain size signatures of marine sands. The fluvial sands will become mixed with beach sands, and the characteristic signatures that can help to differentiate sediments from the two environments may be obscured. The coastal environment suggested by Friedman's graphs is consistent with the sedimentary structures that were observed for the sediments within this second interval of the stratigraphy. On the western side of the anticline a low energy deltaic-type setting was suggested by the increased presence of muds and lignites, while on the eastern side burrows and root channels represent a tidal flat or deltaic environment.

The third stratigraphic interval is above the Kaukatea pumice unit. Within this interval, five samples were analysed (Samples 7-9 & 15-16), with one sample plotting as beach sand on both of Friedman's graphs, one plotting as river sand on both, and three plotting as river sands on the graph of standard deviation versus skewness but as beach sands on the graph of standard deviation versus mean. All of these samples were collected from the Beehive Creek area, so it would seem that by this time interval, the eastern part of the Pohangina Anticline area had a greater fluvial influence. It was possibly a fluvially dominated deltaic environment or a shallow marine setting where large amounts of fluvial sediment were also being deposited. A dominantly fluvial setting for this interval is supported by the influx of conglomerates (as discussed in Chapter 2) with associated muds and lignites.

The C-M diagram developed by Passega (1964) (Figure 4.10) suggests that of the nine sand samples, four were deposited in a fluvial environment (1, 6, 7, 8), another four could have been deposited in either a fluvial or beach environment (2, 4, 5, 9), and the one pumiceous sample is plotting as a beach deposit (3), due to its much higher one percentile value (a result of the hydraulic inequivalence of pumice and quartzo-feldspathic sand). The samples plotted were taken from sediments within two of the stratigraphic intervals: six are from sediments between the Potaka and Kaukatea tuff units (1-6) while three are from sediments younger than the Kaukatea tuff (7-9). Using the C-M plot, it would seem that the sediments that were deposited since the incoming of Potaka Pumice have a strong fluvial influence. The fact that the C-M diagram suggests that four of them could also be beach deposits is consistent with the earlier interpretation that the Pohangina Anticline area was a shallow marine embayment with a large input of fluvial sediments.

• Paleocurrents

Sands within the study area are dominantly parallel bedded on a centimetre scale and there is a general lack of sedimentary structures from which paleocurrent directions might be obtained. Thus measurements were taken from a small number of sites, and the number of measurements at most sites was limited.

Within the Rewa pumice to Potaka pumice interval, paleocurrent measurements were obtained from two sites at Culling's Gully and one site in Beehive Creek. All three sites contained reworked Rewa pumice within sand dominated sediments (See Appendix A for stratigraphic columns and descriptions). Rose diagrams for Beehive Creek Unit (ii) (Figure 4.7 (i)) and Culling's Gully Site N (Figure 4.7 (iii)) both indicate a southward flowing current. The vector mean for the unit at Beehive Creek is 193°, while in Culling's Gully the vector mean for the paleocurrent directions is 146°. These paleocurrents are unimodal and the directions suggest fluvial deposition, as the paleoslope for the area was toward the south. At Site A in Culling's Gully, of a similar stratigraphic height to site N, the rose diagram (Figure 4.7 (ii)) indicates a wide spread of current directions. This suggests either the interaction of fluvial and tidal currents in a delta type setting, or that the directions are unreliable because of intraformational slumping, although this was not obvious at the time the measurements were taken.

Within the Potaka pumice to Kaukatea pumice interval, paleocurrent measurements were obtained from sites at Coulter's Line (T23/453157), Beehive Creek and Finnis Road. The sediments at Coulter's Line (Figure 4.7 (v)) and the Potaka pumice at Beehive Creek (Figure 4.7 (iv)) both indicate a variable but mostly southward flowing paleocurrent, supportive of fluvially dominated deposition as was earlier suggested for this time interval. At Finnis Road, paleocurrent directions for the Potaka pumice unit are very scattered (Figure 4.7 (vi)) suggesting interaction of opposing current directions.

Townsend (1993) also collected some paleocurrent data for the Beehive Creek area, in order to help determine the environment of deposition. Two sites provided paleocurrent data from pumiceous sands containing the Rewa pumice, while a third set of measurements were collected from the Potaka pumice unit. Townsend (1993) suggested that the resulting rose diagrams were representative of a fluvial system (unimodal current) which experienced a sea level rise (bimodal current) and subsequent fall, such that the original fluvial system had returned when the Potaka pumice was deposited.

Paleocurrent data collected for this study has helped to illustrate that the rapid influxes of pumice probably caused rapid aggradation in river systems and progradation of the coastline. Pumice deposited as deltas or in estuaries was reworked by tidal currents. This is particularly evident at the Potaka unit of Finnis Road, where the paleocurrent directions vary greatly. No marked current changes have been noted between the Rewa to Potaka and Potaka to Kaukatea intervals. Paleocurrent directions may vary greatly over different parts of the study area.

4.3.4 Conclusion

Through the use of graphs developed by Friedman (1961, 1967) and Passega (1964) to interpret sediment grain size characteristics, it is evident that sand samples from the Pohangina Anticline indicate changing depositional environments with time, with the environments also varying across the anticline.

In the time period from the Rewa pumice to the Potaka pumice, the characteristics of the sands suggest that they have predominantly been deposited in a beach environment, while they also have a fluvial influence. An environment where such characteristics may be achieved is a shallow marine embayment or delta, with a river carrying sediment out to the coast. During this time period the coastline was positioned between the Oroua River and Beehive Creek areas, indicated by the Beehive Creek sands having a stronger fluvial influence than the Oroua River sands.

Within the second stratigraphic interval (between the Potaka and Kaukatea pumices) the samples have characteristics of both fluvial and marine sands. Their environment of deposition may have been a shallow coastal setting, with a high input of fluvial sediment.

After the deposition of the Kaukatea tuff, sediment characteristics of the samples from the Beehive Creek area suggest they were deposited in an environment similar to those in the second stratigraphic interval, such as a fluvially dominated delta.

Overall the characteristics of the sand samples suggest that within the time period represented by the stratigraphy, a marine embayment has experienced rapid shallowing due to a high rate of fluvial sedimentation. Thus the depositional environments represented by the sediments have changed from a shallow marine setting to a fluvially dominated coastal environment.

CHAPTER 5: MUDS

5.1 Introduction

In this chapter, the characteristics of selected finer grained sediments from the study area are described. Eight samples were collected from various units within the stratigraphy. Their grain size distributions were calculated by sieving (<4ϕ) and the sedigraph (>4ϕ), and their mineralogies were studied through the use of X Ray Diffraction techniques.

• *SediGraph*

The SediGraph method of grain size analysis assumes that the particles are dispersed in a fluid and settle in accordance with Stokes' Law (Coakley & Syvitski, 1991). The SediGraph then monitors the rate at which particles fall below a certain depth in the sedimentation column, in order to give an acurate measure of the cumulative size distribution of the sediment in suspension. The SediGraph uses a collimated beam of x-rays to sense the changing sediment concentration with time. The x-ray beam used in the SediGraph does not disturb or change the suspension, and the sample is maintained at a constant temperature, and isolated from contamination and physical disturbances. Therefore the analytical accuracy of the procedure is increased (Coakley & Syvitski, 1991).

From Stokes' Law, it can be shown that a particle of spherical equivalent diameter D will settle a distance h in time t according to the expression:

$$D = K(h/t)^{0.5}$$

where $K = [18n/(p_s - p_l)g]^{0.5}$, n is the liquid viscosity, p_s and p_l are the densities of the solid and liquid phases respectively and g is the acceleration due to gravity. Consequently, after a given time t_i all particles larger than the corresponding diameter D_i will have fallen below a given distance h from the surface of the suspension.

Due to the small dimensions of the SediGraph's sedimentation cell, only a small sediment sample is required to achieve a suitable concentration level. The following steps were followed when analysing the silt and clay sediments for this study:

1. 3-4g of sample was weighed in a 50ml beaker.
2. 15ml of 0.5% sodium pyrophosphate was added to the sample in the beaker to help deflocculate the clays.
3. The beaker was stirred mechanically for about an hour.
4. The sample was inserted in the SediGraph, and another 15ml of 0.5% sodium pyro-

phosphate was used to rinse all of the sediment from the beaker.

5. The apparatus was rinsed between running each sample, and each sample took approximately one hour to be analysed.

• *X Ray Diffraction*

X Ray Diffraction (XRD) is a method used to identify the various crystalline species present in clays. The basic principle of XRD is that each crystalline substance has a characteristic arrangement of atoms which diffracts x rays in a unique pattern (Whitton and Churchman, 1987). XRD patterns are printed out on chart paper, and the peaks are attributable to the basal spacings of clay minerals. The XRD method is non-destructive and requires only small amounts of sample.

Samples from the study area were analysed by X Ray Diffraction, to determine their clay mineralogy. The samples were prepared by the methods outlined in Whitton and Churchman (1987). The following flow chart summarises the treatments that were carried out on the sediment samples.

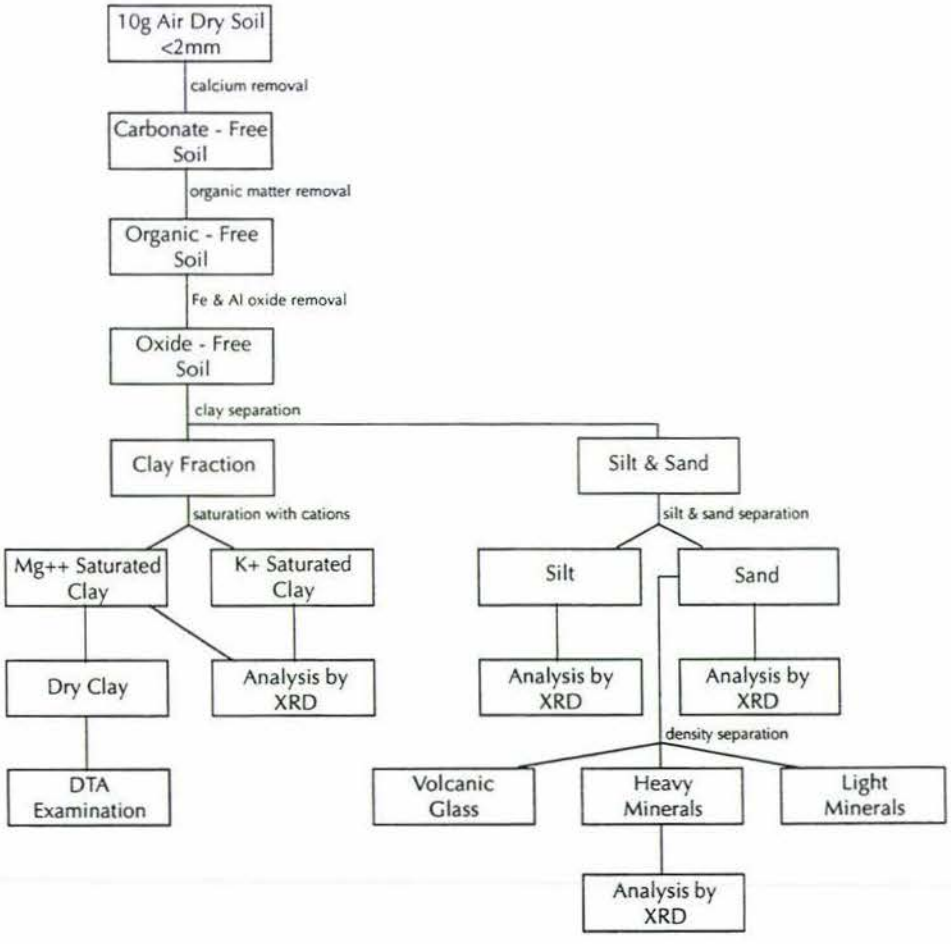

Figure 5.1: Flow chart for the X Ray Diffraction analysis of the fine sediment samples (after Whitton & Churchman, 1987).

Note:

- Calcium was removed from the samples by adding 1:1 hydrochloric acid.
- Organic matter was removed by adding hydrogen peroxide "100 volume" and heating in a water bath.
- Iron and aluminium oxides and oxyhydroxides were removed by adding citrate reagent and sodium bicarbonate and heating in a water bath, then adding sodium dithionite (see Whitton & Churchman (1987) for details).
- The clay fraction was separated by collecting the supernatant after centrifuging (see Table 1 in Whitton & Churchman (1987) for centrifuge settings). The silt and sand fractions that remained were then separated by dispersing with distilled water and using settling times to remove the silt in suspension, until only sand remains in the test tube.
- The sand fraction was separated into light and heavy mineral fractions using varying densities of sodium polytungstate: 2.8gcm^{-3} for separating the heavy minerals, 2.45gcm^{-3} for the volcanic glass, and 2.2gcm^{-3} for the plant opals.
- Some of the clay was saturated with potassium ions by adding potassium chloride (100g of KCl dissolved in 1L of distilled water), and the rest was saturated with magnesium ions by adding magnesium chloride (100g of $MgCl_2$ dissolved in 1L of distilled water) and 1:1 hydrochloric acid.

After the mud samples had all gone through the stages of pre-treatment, the various fractions of each sample were analysed by x ray diffraction, such that nine XRD patterns were obtained for each of the eight samples. The nine fractions that were analysed by XRD are:

Mg^{++} saturated clay in air
Mg^{++} saturated clay in glycerol
K^{+} clay - heated at 550°C for 2 - 3 hours
K^{+} saturated clay in air
Silt
Silt in glycerol
Silt - heated at 550°C for 2 - 3 hours
Sand
Sand - heavy mineral fraction

- *Differential Thermal Analysis*

Differential Thermal Analysis (DTA) measures exothermic and endothermic effects that occur when a sample is either heated or cooled. A thermogram is printed, and a quantita-

tive estimate of gibbsite and kandites may be made.

5.2 Results

Eight mud samples were chosen for analysis. Thier locations, stratigraphic positions and characteristics are presented in Table 5.1.

Sample	Grid Reference	Stratigraphic Position	Brief Sample Description
1	Oroua River T23/436145 (Unit (ix) in stratigraphic columnn)	Approx 6m below the Kaukatea pumice	From a 9m unit of grey fine sand and mud, burrowed and partially bioturbated, with some organic matter.
2	Oroua River T23/436145 (Unit (vi) in stratigraphic column)	Approx 23m below the Kaukatea pumice	From a sandy mud layer within a 4m sequence of pebbly sand and mud layers.
3	Oroua River T23/436145 (Unit (ii) in stratigraphic column)	Approx 35m above the Potaka pumice	From a 5cm thick, normally graded mud layer within a 10.5m unit of organic rich finely bedded mud and fine muddy sand.
4	Beehive Creek T23/502130 (Unit (xi) in stratigraphic column)	Approx 25m above the Kaukatea tephra	From a lignitic mud layer, with vertical burrows up to 10cm filled with muddy sand.
5	Beehive Creek T23/504135 (Unit (xi) in stratigraphic column)	Approx 15m above the Kaukatea tephra	From the middle of a massive mud unit, 2m above a lignite layer.
6	Beehive Creek T23/505138 (Unit (xi) in stratigraphic column)	Approx 1m above the Kaukatea tephra	From the mud dominated top of a 30cm unit of interbedded sand and silt.
7	Beehive Creek T23/505138 (Unit (xi) in stratigraphic column)	Approx 8m above the Kaukatea tephra	From a 3m unit of parallel laminated mud, silt and fine sand. Grey in colour and commonly lignitic.
8	Beehive Creek T23/505140 (Unit (ix) in stratigraphic column)	Approx 3m below the Potaka pumice	Silty, bioturbated mud.

Table 5.1: Locations of the eight samples chosen for XRD analysis, their stratigraphic position, and a brief description of their character (See Appendix A for stratigraphic columns and descriptions).

• *Grain Size*

The sediments were sieved in order to measure the sand fraction (2ϕ - 4ϕ) and then the SediGraph was used to determine the grain size distribution of the silt and clay fraction (>4ϕ). Together, they provide a complete grain size distribution for those sediments. The raw sieve and SediGraph data is presented in Appendix H.

Histograms and cumulative percentage curves were plotted (presented in Appendix I) and the graphical statistics were also calculated for each of the samples, using the RSA computer program (Sampson, 1992). A summary of the critical statistics is outlined in table 5.2.

Sample	Graphic Mean	Incl. Graphic Std. Dev.	Incl. Graphic Kurtosis	Graphic Skewness	Grain size Classification
Sample 1	4.55	0.98	1.28	-0.11	sandy silt
Sample 2	3.22	0.85	1.68	0.28	silty sand
Sample 3	3.83	1.80	2.26	0.19	silty sand
Sample 4	4.07	2.21	0.94	0.21	silty sand
Sample 5	4.16	1.70	1.32	0.26	silty sand
Sample 6	3.65	1.83	1.02	0.45	silty sand
Sample 7	4.20	1.51	1.49	0.31	silty sand
Sample 8	4.91	1.91	1.23	-0.31	sandy silt

Table 5.2: Statistical grain size parameters for the eight samples, as calculated by the RSA computer program. Grain size classifications according to Folk *et al.* (1970).

From the statistical grain size parameters, the eight samples could be given the following verbal classifications according to Folk (1974):

Sample 1: moderately sorted, leptokurtic, coarse skewed
Sample 2: moderately sorted, very leptokurtic, fine skewed
Sample 3: poorly sorted, very leptokurtic, fine skewed
Sample 4: very poorly sorted, mesokurtic, fine skewed
Sample 5: poorly sorted, leptokurtic, fine skewed
Sample 6: poorly sorted, mesokurtic, strongly fine skewed
Sample 7: poorly sorted, leptokurtic, strongly fine skewed
Sample 8: poorly sorted, leptokurtic, strongly coarse skewed

• *Mineralogy*

The following tables summarise the mineralogy of the sand, silt and clay fractions of the mud samples, as determined by X Ray Diffraction and Differential Thermal Analysis. The numbers are expressed as percentages of each sample.

Sand Fraction Mineralogy

Sample	Quartz	Feldspar	Mica	Chlorite	Heavy Minerals	Volcanic Glass
1	48	36	3	4	7	2
2	43	41	5	3	6	1
3	41	40	5	5	8	1
4	52	28	5	8	6	1
5	46	35	5	6	7	1
6	49	33	6	5	6	1
7	49	30	4	8	8	1
8	42	33	6	5	9	5

Table 5.3: Percentages of quartz, feldspar, mica, chlorite, heavy minerals and volcanic glass in the sand fraction of each of the eight samples.

Silt Fraction Mineralogy

Sample	Quartz	Feldspar	Mica	Chlorite	Mica-Chlorite
1	20	22	33	21	4
2	25	17	43	15	0
3	23	17	33	23	4
4	29	21	28	20	2
5	20	23	31	24	2
6	24	21	39	16	0
7	20	22	35	21	2
8	23	24	32	21	0

Table 5.4: Percentages of quartz, feldspar, mica, chlorite and mica-chlorite in the silt fraction of each of the eight samples.

Clay Fraction Mineralogy

Sample	Quartz	Feldspar	Mica	Chlorite	Smectite	Vermiculite	Mica-Vermiculite	Mica-Chlorite	Kandite
1	6	6	51	12	12	0	1	4	8
2	3	3	53	5	12	3	3	5	13
3	6	6	48	10	13	2	0	3	12
4	3	4	63	4	6	6	2	3	9
5	4	4	59	12	6	0	2	4	9
6	4	3	52	5	14	1	0	5	16
7	3	4	53	9	12	1	0	3	15
8	5	6	55	10	10	0	1	2	11

Table 5.5: Percentages of quartz, feldspar, mica, chlorite, smectite, vermiculite, mica-vermiculite, mica-chlorite and kandite in the clay fraction of each of the eight samples.

Heavy Minerals

Sample	Chlorite	Epidote	Hornblende	Mica	Ilmenite	Magnetite
1	23	48	8	16	2	3
2	14	47	11	21	4	3
3	35	34	2	27	2	0
4	25	54	1	11	4	5
5	36	25	5	22	7	5
6	6	70	6	8	7	3
7	18	58	3	15	6	0
8	22	51	2	18	4	3

Table 5.6: Percentages of chlorite, epidote, hornblende, mica, ilmenite and magnetite in the heavy mineral portion of the sand fraction of each of the eight samples.

There follows a description of each sample and its clay, silt and sand mineralogy.

Sample 1 is a sandy silt from the Oroua River section. It has a sand fraction with a slightly lower percentage of mica than that for the other samples, while the percentage of volcanic glass is a little higher. In the silt fraction, there is a low percentage of quartz and one of the highest percentages of mica-chlorite. In the clay fraction, the percentage of mica-chlorite is slightly higher, while the percentage of kandite is the lowest of all of the samples. Of the heavy minerals present in the sand fraction, the percentage of hornblende was slightly higher than that of the other samples, and the percentage of ilmenite was one of the lowest.

Sample 2, a silty sand from lower in the Oroua River section, has the highest percentage of feldspar in the sand fraction, and the percentage of chlorite is slightly lower than that for the other samples. The mineralogy of the silt fraction indicates that it has comparatively low percentages of feldspar and chlorite, and the highest percentage of mica in that fraction. The clay fraction mineralogy is low in quartz, feldspar and chlorite, while the percentages of mica-vermiculite and mica-chlorite are quite high when compared to the other samples.

Sample 3 is a silty sand also collected from the Oroua River section, and has a mineralogy fairly similar to sample 2, particularly in the sand fraction. In the silt fraction, the percentage of mica is lower, while the chlorite and mica-chlorite percentages are higher. In the clay fraction the percentages of quartz and feldspar are both high, as is the chlorite and smectite, while the percentage of mica is the lowest of the eight samples. The heavy mineral fraction of the sand has relatively low percentages of epidote, hornblende and ilmenite, while the values for chlorite and mica are high.

Sample 4 is a silty sand collected from Beehive Creek, and has quite a different mineralogy to the samples from the Oroua River section. Sample 4 has the highest percentage of quartz and chlorite and the lowest percentage of feldspar in the sand fraction mineralogy. The silt fraction also has the highest percentage of quartz but the lowest percentage of mica. This is reversed in the clay fraction, where the percentage of quartz is quite low and yet the percentage of mica is the highest of all samples. Sample 4 also has comparatively low percentages of chlorite and smectite, and a high percentage of vermiculite. The heavy mineral part of the sand fraction indicates that the percentage of hornblende is low and the percentage of magnetite is high.

Sample 5 is a massive silty sand also collected from Beehive Creek, from a similar stratigraphic position to sample 4, yet their mineralogies vary in a number of ways. In the silt fraction there is a comparatively low percentage of quartz and a fairly high percentage of feldspar, and the percentage of chlorite is the highest of all samples. The clay fraction shows fairly high percentages of mica and chlorite , while the percentage of smectite is the lowest of the samples. The heavy mineral part of the sand fraction indicates that it has the highest percentages of chlorite, ilmenite and magnetite, while the percentage of epidote is the lowest of all samples.

Sample 6 is a silty sand collected from 1m above the Kaukatea tephra in Beehive Creek.

The sand fraction of this sample had high values for the percentages of both quartz and mica, but a low amount of volcanic glass considering its proximity to the Kaukatea tuff. The silt fraction has a fairly high percentage of mica, and the percentage of chlorite is quite low. The clay fraction shows higher percentages of smectite, mica-chlorite and kandite. The heavy mineral fraction of this sample has very low percentages of chlorite and mica, a high percentage of ilmenite, and an extremely high percentage of epidote compared to other samples.

The mineralogy of sample 7, a silty sand from Beehive Creek, is not too dissimilar to sample 6 in the sand fraction, though the percentage of chlorite is higher in sample 7. In the silt fraction, there is a comparatively low percentage of quartz, and in the clay fraction the percentage of kandite is slightly higher than for most of the other samples. In the heavy mineral part of the sand fraction the percentage of epidote is fairly high when compared to the other samples.

Sample 8 is a bioturbated sandy silt collected from just below the Potaka pumice in Beehive Creek. The mineralogy of the sand fraction indicates that it has a higher percentage of volcanic glass than any of the other samples. It also has the highest percentages of heavy minerals and mica, but a low percentage of quartz. In the silt fraction, there is a high percentage of feldspar, and in the clay fraction there is a high content of feldspar and chlorite.

There are considerable differences between samples, and the various size grades. For example, sample 6 has the highest percentage of mica in the sand fraction, yet that same sample also has the lowest percentage of mica in the heavy mineral sand fraction. The reason for such variations is the range in density values for the micas. The heavy minerals were separated from the sand fraction using sodium polytungstate with a density of $2.8gcm^{-3}$, yet the density of micas vary - biotite may range from 2.7 to 3.2, and muscovite from 2.8 to 3.1. This means that if a large proportion of the mica that was present in the whole sand fraction was biotite with a density of $2.7gcm^{-3}$, then it would not be included with the heavy mineral fraction, as appears to have happened with sample 6. In hindsight, an optical examination of the sample would have been beneficial to the recognition of the species of mica present.

• *Lignites*

Lignite layers are present in the Oroua River, Beehive Creek and Gulling's Gullies sections. In the Oroua River section (T23/436145) a 1.5m lignite layer (unit (iv)) lies above a 2m unit of highly burrowed sands, and below a 6m unit of parallel bedded pumiceous sand (see Appendix A). The contacts are clearly defined, and the lignite is dark grey in colour with a silty texture.

At Beehive Creek (T23/504157-T23/501124) lignite layers are present within four of the units. Unit (vii) is a 35m thick unit of interbedded mud and fine sand. About 7m from the base of the unit, two black 50mm lignite layers enclose a tuff layer (see Appendix A). Unit (xi) is a 34m thick unit of parallel bedded sand and mud, interbedded with numerous lignite layers. The lignites are up to 0.5m thick, dark brown to black in colour and usually have sharp contacts. The associated muds commonly have burrows and/or root channels. One 0.3m lignite layer in this unit lies directly beneath the Kaukatea tephra. Unit (xiii) is a 30m mud dominated unit, with a number of interbedded dark brown or black lignite layers, up to 0.5m thick. Again the muds often have root channels. Unit (xv) is another mud dominated unit, 12m thick, with lignites present in the middle and at the top of the unit. There are also some logs within the sediments near the top (see Appendix A).

At Culling's Gullies, the lignite is not preserved as layers within the sediment, but is present as rip up clasts within channels (see Appendix A). At Fossil Gully (T23/477127) units (v) and (vi) both contain lignite clasts, which are dark brown/black in colour, and generally elongated in shape, up to 0.5m long (see Plate 2.12).

The lignites found in the Oroua River and Beehive Creek sections have formed in place, and represent the vegetation that inhabited distal parts of a dominantly fluvial environment. The lignite rip up clasts of Culling's Gullies are most likely to have been rapidly transported to the coastal environment by a fluvial system (see Section 2.2).

5.3 Discussion

Several characteristics of these fine grained sediments are helpful when trying to determine the environments in which they were deposited.

The muds from the Beehive Creek area are closely associated with a number of lignite layers, suggesting that deposition was occurring in a dominantly non-marine environment. Organic matter will only accumulate in a very low energy, saturated and anaerobic environment, where the plant matter can grow, remain undisturbed, and later be buried. Such conditions are most often found in estaurine or river flood plain settings.

A number of gravel units are also present at Beehive Creek from about the time of the Kaukatea tephra, suggesting that sedimentation was occurring in a dominantly fluvial environment by this time period, as discussed in Chapter 4. Thus the muds and lignites that are associated with the gravel units are likely to be overbank flood deposits in a dominantly fluvial setting.

The fine sediment samples from The Oroua River section contain some organic matter, but lignite layers are thinner, finer and uncommon compared to Beehive Creek. The stratigraphy of the Oroua River section indicates an increasing proportion of mud within the sediments passing up through the sequence from the Potaka pumice to the Kaukatea pumice. Sedimentation occurred in a shallowing marine environment. The mud samples are likely to have been deposited in a deltaic type environment. Some detrital organic matter is present, but the conditions have not been stagnant or vegetatively productive enough to allow large amounts of plant matter to accumulate and form lignite.

A greywacke terrain is a likely source for these fine sediments, though the degree to which other lithologies have contributed is not obvious. Epidote is a mineral that is generally derived from greywacke or schist terrains (J Whitton, pers comm.) so its presence in the heavy mineral fraction of all of the samples provides evidence for a source from the greywacke terrains of the lower and central North Island, and this is further supported by the uniformly greywacke lithology of the gravel units discussed in Chapter Four.

The reasonably high percentage of mica (up to 63% in the clay fraction) is likely to be a signature of the greywacke and argillite source rocks from which the fine sediments have been sourced. Soils that have formed on mudstone parent materials, such as the

Turakina Steepland soil, often have up to 75% mica in the clay fraction, at a depth close to the parent material (Rijkse, 1977). Soils developed on mudstone characteristically have higher percentages of mica than those formed on greywacke. Thus those samples with a higher percentage of mica in the clay fraction may have a dominantly mudstone source.

Reed (1957) studied the petrology of greywackes in the Wellington region. When determining the provenance for these rocks, he suggested that the dominant mineral assemblage of quartz, alkali feldspar and biotite provide evidence that the greywackes have been derived mainly from a plutonic terrain of granite, gneiss and metamorphic rocks. Such a plutonic terrain would provide higher percentages of mica, which is reflected in the mineralogy of the fine grained sediments from the Pohangina Anticline area. Reed (1957) also suggested that the plutonic terrain was a northward extension of the granite, gneiss and schist now cropping out on the western side of the South Island. This terrain may also have been a significant source for the mudstones of the Wanganui Basin prior to the uplift of the Ruahine and Kaimanawa Ranges.

Grain Size Sources of Error

The range of particle sizes in the eight samples has necessitated the use of two techniques in order to determine the full set of grain size data. Seiving has been used for grains between 2ϕ and 4ϕ and the SediGraph has been used to analyse grains finer than 4ϕ. The combination of the two methods has produced a bimodal grain size distribution (Figure 5.2) although it is probably not real.

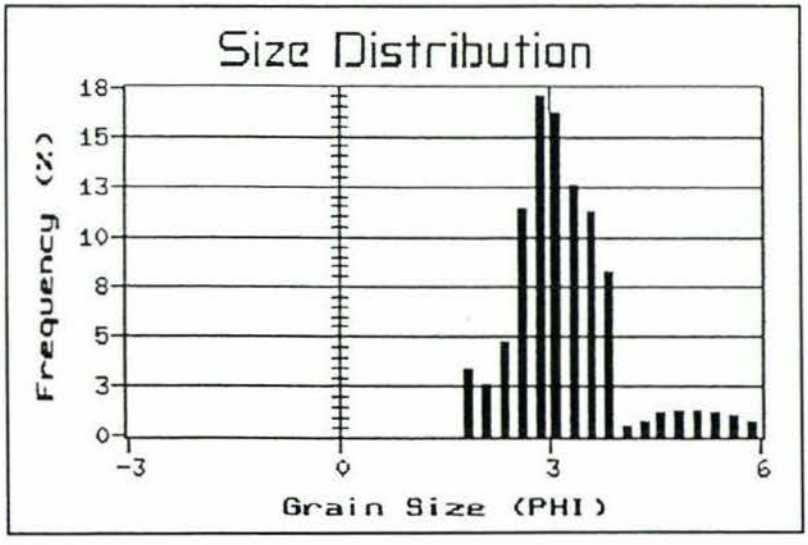

Figure 5.2: Grain size distribution diagram for mud sample 2, illustrating the problem of combining data obtained from two different measuring methods.

If all of the particles had been spherical, then there would not be such a difference at the junction between the two methods and the size distribution graph would not be affected. However for non-spherical particles, methods record the 'size' of a particle as the diameter of an 'equivalent' sphere, and the definition of 'equivalence' varies with methods (Fieller & Flenley, 1990).

In this study, the sieving and SediGraph have different definitions of 'size', hence the two sets of data do not match well for many of the samples. Sieving does not provide a 'pure' grain size measurement, but some compound of size and shape (Blatt, Middleton & Murray, 1980) with a suitable approximation being the intermediate axis diameter or some measure of the cross-sectional area of the particle. The SediGraph measurement method does not measure the actual size of the grains either - it assumes that the particles are dispersed in a fluid and settle according to Stokes' Law, which is used to provide an approximation of the grain size, assuming a uniform density for all grains.

An alternative method that may have been used to avoid the problem when using these two different methods of grain size measurement, would have been to sieve the sediments to 5ϕ or 6ϕ and then run the remaining fine grains through the SediGraph. This is likely to have lessened the problem of bimodal distributions and provided a truer grain size distribution for the samples, however this method was not used for this study, due to the unavailability of 5ϕ and 6ϕ sieves.

Two sets of measurements on the same set of particles obtained by different techniques can be married together by converting the measurements of one geometric size property to that of the other. This conversion requires a knowledge or estimation of the particle shape. Fieller, Flenley and Olbricht (1992) proposed the log skew Laplace distribution for handling mixtures of particle sizes and the marrying of measurements of different aspects of size. For more detailed work on individual beds within the sequence, it would be necessary to come to terms with the marrying procedure.

5.4 Conclusion

The eight fine sediment samples collected for this study showed some variation in their mineralogies when studied using X Ray Diffraction techniques. These sediments appear to have been largely derived from the greywacke terrains of the lower and central North Island. The samples with higher percentages of mica are thought to have had a dominantly mudstone source.

On the western side of thePohangina anticline there are few lignite layers associated with the fine sediments. The proportion of fine sediments increases from the Potaka pumice to the Kaukatea pumice, and they are thought to have been deposited in a deltaic environment.

On the eastern side of the anticline the muds are closely associated with a number of lignite layers, and are likely to have formed in an estaurine or river flood plain setting. From the time of the Kaukatea pumice, there is a large influx of conglomerates within the stratigraphy, indicating a fluvially-dominated environment. Thus the associated muds and lignites are considered to be over bank flood deposits.

CHAPTER 6: INTERPRETATION

6.1 Environments of Deposition and Facies Analysis

The older sediments of the Pohangina area were deposited in a shallow embayment setting, where large volumes of sediment were brought to the coast by fluvial systems. These rivers transported large amounts of sediments out onto the shelf, including huge amounts of pumice, causing rapid progradation of the coastline. The progradation may have been so great that even during sea level highstands, the shoreline was unable to return to its original position. This progradation sees stratigraphically younger sediments displaying stronger fluvial characteristics than those lower in the sequence.

Eventually shallow marine and coastal sedimentation gave way to terrestrial conditions, as evidenced by lignites. At Beehive Creek on the eastern limb of the Pohangina Anticline, there are lignite layers near the Rewa tuff, yet significant lignites occur only above the Potaka tuff on the western limb. Thus it would seem that a terrestrial environment may have dominated on the eastern side of the study area by about 1.29 Ma, whereas on the western side the sedimentation was predominantly shallow marine until after about 1 Ma when it became more fluvially dominated. In this chapter, evidence collected in previous chapters is used to elucidate the environment of deposition or facies, and to place the sediments into the context of climate cycles that influenced sedimentation during the period.

The term 'facies' may be used in different senses, as illustrated by Reading (1978). It can be used to describe a rock product, e.g. 'sandstone facies', or it can genetically describe the products of a process by which a rock is thought to have formed, e.g. 'turbidite facies'. Thirdly it can be used to describe the environment in which a rock or a suite of rocks is thought to have formed, e.g. 'fluvial facies'. Finally it can infer a tectonic process, e.g. 'post-orogenic facies'.

For the purposes of this study, facies describe the environment within which the sequence accumulated. They are determined by identifying the sediment characteristics due to the depositional environment. In this way, the sediments of the Pohangina Anticline have been classified into five facies:

• Fluvial Facies

Fluvial deposits can be divided into three major groups (Reineck & Singh, 1973):

(i) Channel Deposits

Formed mainly from the activity of river channels, the conglomerate units within the Pohangina Anticline stratigraphy are thought to be representative of the channels of a braided river, as discussed in Chapter 4. The conditions of initiation necessary to form braided channels are flows of water carrying copious sediment (King, 1991) as was the case for this eastern margin of the Wanganui Basin.

The conglomerate units at sites such as Beehive Creek, Pollock Road and Oroua River section 1 are dominantly clast supported and show some pebble imbrication. Most of the units exhibit weak horizontal stratification, with only a few isolated cases of cross bedding being evident, such as at the top of Oroua River section 1. They are thought to be typical of braided river systems, as gravels deposited by a braided river system commonly show both plane bedding and cross bedding (King, 1991). The sediment most commonly deposited by braided river systems are horizontally bedded, imbricated gravels, which may appear massive if the bedding is thick, with a uniform texture (Rust & Koster, 1984). Clast supported conglomerates with horizontal stratification and clast imbrication suggest deposition on near-horizontal surfaces, such as the tops of braid bars or as lags on channel floors (Reading, 1978).

The conglomerate units of the Pohangina area were deposited during cold climatic events, when rapid erosion of the main axial ranges occurred and the rivers carried large amounts of coarse sediment. River gravel aggradation occurred during these cool climatic periods, and as such they help to indicate the climatic fluctuations during the time period represented by the Pohangina Anticline sequence.

(ii) Bank Deposits

These sediments include levees, formed by deposition of sediment when flood waters overtop the river banks (Reineck & Singh, 1973). The highest part of a levee is at or near the edge of the channel, and it slopes away from the channel into the flood basin. During a flood, the flow velocity is reduced as the banks are overtopped, thus the coarsest sediment is deposited near the channel, building up the levee. The grain size and rate of deposition both decrease away from the channel (Reineck & Singh, 1973).

In the study area, the levees are generally made up of sand, with some interbedded silt.

With increasing distance from the active channel, the levee sands give way to lignitic muds of the flood basin.

(iii) Overbank Deposits

These are generally fine grained sediments, resulting from heavy floods, when river water flows over the levees and into the flood basin (Reineck & Singh, 1973). The occurrence of interlaminated mud, silt and very fine grained sand is common in overbank fluvial environments, and represents deposition from suspension and from weak traction currents (Miall, 1996).

The fine grained sediments at Beehive Creek are closely associated with a number of lignite layers, indicating deposition in a non-marine environment. Organic matter only accumulates where the plant matter can grow, remain undisturbed and later be buried, such as in very low energy areas of the river flood plain, where sediment supply is very low.

The intercalation of fine grained sediments and lignite layers with the conglomerate units within the sequence at Beehive Creek is another key indicator of deposition within an overbank fluvial environment. The cool climatic periods of river gravel aggradation alternated with periods of warmer climatic conditions, when vegetation was more abundant and finer sediments were deposited.

• Estuarine Facies

An estuary is "a semi-enclosed coastal body of water which has a free connection with the open sea, and within which sea water is measurably diluted with fresh water derived from land drainage" (Reading, 1978). As such the estuary is a low energy environment, commonly characterised by the deposition of fine grained sediments, which are also influenced by the tidal regime.

Tidal flats often occur within estuaries, and are generally made up of almost featureless plains dissected by a network of tidal channels (Reading, 1978). During high tide, waters enter and overtop the channel banks, inundating the adjacent flats, then after a still-stand period, the tidal waters drain via the channels, once again exposing the flats.

The fauna of a tidal flat may contain a large number of individuals, belonging to only a limited number of species (Reineck & Singh, 1973). Therefore sediments of the tidal flat

are often highly burrowed by benthonic organisms. Bioturbation is generally strongest in mud flats, weaker in mixed flats, and weakest in sand flats (Reineck & Singh, 1973). Sediments that have been deposited rapidly tend to have negligible bioturbation.

Sediments of the tidal flats are dominated by interlaminated clays, silts and sands with prolific flaser, wavy and lenticular bedding (Reading, 1978). These characteristics reflect the constantly fluctuating but relatively low energy conditions. Periods of current activity allow traction transport and the deposition of rippled sands, and alternate with periods of quiescence, when the deposition of mud occurs (Boggs, 1996). A fairly high rate of sediment supply is necessary for the preservation of flaser, wavy and lenticular bedding, as they are easily eroded if they are not buried soon after formation and are exposed to stronger currents. Channels of the tidal flats often have relatively coarse sand, shell debris and abundant mud clasts accumulate at the base, forming a basal lag to the channel sequence.

In the Finnis Road sequence, unit (vi) (about 46m from base of section - see Appendix A) contains abundant flaser bedding within the parallel bedded sands, and also contains coarse sand with shell fragments, small pebbles and mud rip up clasts. This unit would thus seem to be fairly typical of an estuarine deposit, with the flasers indicating a fluctuating tidal current, while the coarser sediments are representative of the basal lag of a channel sequence in a tidal flat/estuarine setting.

Unit (vii) at Finnis Road (see Appendix A) contains further evidence of an estuarine environment, with rippled and flaser bedded sands and muds, and some burrowing too. Mud clasts at the base of this unit are again likely to be part of a basal channel lag.

Some of the sediments within the Beehive Creek section also show indications of having been deposited within an estuarine environment. Unit (ix) contains sand and mud layers with some burrowing and bioturbation. This suggests a low energy setting, such as an estuary, where burrowing organisms inhabit the brackish waters. Here these estuarine sediments are overlain by fluvial gravels. This association indicates a fall in sea level, due to the onset of a cool climate event.

Similar features are seen at Oroua River section 1, in unit (ix) about 50m from the base of the section (see Appendix A). This unit contains interbedded mud and silty mud, which are burrowed and bioturbated. These estuarine sediments are also overlain by fluvial

gravels, again interpreted as indicating a drop in sea level.

• Deltaic Facies

Deltas form when fluvially transported sediments enter the relatively still, deeper water of the sea, where the sediments are still influenced by river currents as well as the waves and tides of the sea. The current velocity decreases radially as sediment-laden waters enter the sea, resulting in a radial decrease in grain size from the river mouth.

In an ideal model, three main morphological units appear within a delta:
(i) The delta platform, which is the subhorizontal surface nearest the river mouth. It is composed primarily of sand and is traversed by the distributary channel and its flanking levees. Sediments of the delta platform are mainly made up of marsh deposits and delta front silts and sands (Reineck & Singh, 1973). River channel deposits are also present, along with natural levee deposits. In places this upper part of the delta is influenced by wave action. Parallel laminations are common within sediments deposited within this zone, occurring due to the plane bed sediment transport during swash and backwash flow.

(ii) The delta platform grades away from the source into the delta slope, on which finer sediments come to rest. The delta slope contains sediments that are made up of silt and clay deposits formed off the major deltaic distributaries (Reineck & Singh, 1973). Within the sediments of the delta slope, parallel and lenticular laminations are common. Occasionally ripple bedding, current ripples and small scale graded bedding are common in more silty layers (Reineck & Singh, 1973).

(iii) The delta slope in turn passes down into the pro-delta, where the sediments are characteristically fine grained muddy sediments, i.e. clay and silty clay (Reineck & Singh, 1973) which have settled out of suspension. Seaward of the pro-delta, fine grained material is deposited at a slow rate. Sediments include homogeneous clay, silty clay, shelly clay and shell layers.

Sediments that are saturated with water tend to liquify and lose their internal strength when subjected to a sudden vibration (Miall, 1996). Thus deltaic sediments may commonly exhibit soft sediment deformation (convolutions) as a result of the rapid deposition of saturated sediments. When clay beds are interbedded with sand or silt, the coarser sediments have a higher density when liquified and they tend to founder under gravity,

which may result in the disruption of the sand units (Miall, 1996). In a deltaic environment, the sediment is saturated and therefore has little cohesive strength. If the delta slope becomes oversteepened, shock-induced failure will result in the slumping of material which will then slide downslope (Miall, 1996). As a result, masses of sediment will become deformed due to the development of internal shear or glide surfaces. This is one way in which convolute bedding may develop in deltaic sediments.

Convolutions within the sediments at sites such as Culling's Gullies and Finnis Road may indicate deposition within a deltaic setting. They may form due to slumping on the delta slope, as explained, or be the result of subaerial exposure of the sediment surface during low tide, which causes expulsion of water and compaction of the sediment, thus producing local liquefaction and resulting in the development of convolutions. Convolutions are also an indication of rapid sedimentation, such that the overburden pressure disrupts the sediment and causes dewatering.

Within the Pohangina Anticline sediments, such convolutions are most commonly associated with the highly pumiceous sands. The thickness of the tuff units indicates that the pumice entered the area in large volumes, transported to the coast via a river system. The rapid influx of sediment would have resulted in overloading and the formation of convolutions. The huge volume of sediment entering would have caused progradation of the coastline, thereby resulting in the shallowing or termination of marginal facies such as a delta.

At Stewart's Gully the pumiceous sediments are commonly convoluted (see Chapter 2, Plate 2.5), and at this site the section is overlain by fluvial conglomerates, as a result of a drop in sea level and cold climate aggradation. Here the convoluted deltaic facies have become inundated by the huge volume of sediment, and eventual progradation of the shoreline resulted in a change from a deltaic to a fluvially dominated environment.

• Beach Facies

Sediments deposited within a beach environment can vary greatly depending on the sediment source, the intensity of wave action and tidal currents, and also sea level fluctuations. In the Pohangina area, sediments assigned to the beach facies are typically sand dominated. The sands are well sorted, due to the winnowing effect of the swash and backwash on the shore, and this degree of sorting has been used to differentiate between sands deposited in beach and fluvial environments (see Chapter 4).

Beach sands often exhibit parallel bedding, or may contain symmetrical ripples with crests parallel to the crest of the waves (King, 1991). Ripples were not commonly observed within the Pohangina Anticline sediments. At Culling's Gullies, some ripples were seen, but they showed signs of erosion after their formation - the tops of the ripples had been planed off, perhaps due to stronger currents causing erosion after their formation.

Parallel bedded sands are very common within the Pohangina Anticline sequence. They are best preserved at Stewart's Gully, Culling's Gullies and the bottom of Oroua River section 1. The occurrence of parallel laminations gives important information about the flow regime at the time the sediments were deposited. A Froude number of 1 separates two flow regimes, with each flow regime generating specific bed forms and sedimentary structures. The lower flow regime generates cross laminated and cross bedded sand from ripples and dunes, while antidunes form in response to the upper flow regime. Between the two regimes, when the Froude number is about 1, dunes are smoothed out and horizontal beds are formed as the sand is transported and deposited (Selley, 1988). Thus plane beds may form as a result of an increasing current velocity causing a change from lower to upper flow regimes, and they may also form when current velocity decreases and the sequence of bed forms is reversed.

It is likely that the parallel bedded sands of Culling's Gullies, Stewart's Gully and the bottom of Oroua River section 1 were deposited within a shallowing offshore environment. Sand samples collected from these three sites were interpreted as being dominantly marine sands, due to their grain size characteristics (see Chapter 4). At Stewart's Gully and the Oroua River section 1, sediments of a dominantly terrestrial environment stratigraphically overlie the parallel laminated sands. This is indicative of marine regression, such that the shallowing has led to a change from marine to terrestrial depositional environments.

• Channel Facies

Channels have either U-shaped or V-shaped cross sectional profiles that cut across pre-existing bedding and laminations. They are generally formed by current erosion, and are filled with sediment of a different texture to the beds they truncate. Channels are very common in tidal and fluvial sediments (Boggs, 1995).

Within the the Pohangina area stratigraphy, there are two particular sections where channels have cut into the sediment. Within the Erosion Scarp sequence at Culling's Gullies

(T23/473131), there is a channel about 9m from the base of the section. It has some pebbles at the base and has a sandy matrix, but it dominantly contains large peat clasts. These clasts would have originated from a terrestrial source, where lignite units are more abundant. It is presumed that an erosive current has cut a channel through underlying sediments as it transported the lignite clasts from a terrestrial setting out to the coast. In a coastal location in a subsiding basin, as this was, this can only happen during sea level regression or low stand.

Near the top of the Fossil Gully sequence within Culling's Gullies (T23/477127) a shellbed is contained within another large channel. The shells are broken and are within in a matrix of pebbly sand, also with some mud rip up clasts (see Appendix A). This channel may represent a distributary channel on a delta front, or it may have formed within a beach environment, where an erosive current such as a rip channel has cut through the sands, and shells and coarser sediments have accumulated. No lignite layers or clearly fluvial overbank deposits are found in the Culling's Gullies exposures.

At Finnis Road there are several channels, containing a sandy matrix and large mud rip up clasts. These channels once again indicate an erosive current which has passed through a large mud unit, thus transporting the mud rip up clasts as it cuts a channel through the underlying sediments. No such mud units are seen in the Finnis Road section.

Some of the sites show changing facies within the stratigraphic sequences. One such example is Finnis Road, where parallel bedded sands near the base of the sequence (see Plate 2.2 & Appendix A) are thought to be shallow marine sands, exhibiting some cross bedding and containing the Rewa pumice. These sands then pass up into interbedded sands and muds typical of the estuarine facies, containing abundant flasers beds. Near the top of the sequence, the sediments are more typical of a fluvial facies, with the Potaka pumice representing rapid fluvial deposition. Such a sequence of facies changes is possibly due to a lowering of sea level and progradation of the shoreline, such that within the stratigraphy each facies is terminated by sediments of a progressively more terrestrial facies.

6.2 Age and Development of the Anticline

The geomorphology of the Pohangina Anticline and outlying areas is useful for gaining an overall picture of the structure of the area. The anticline is asymmetrical, with the western limb sloping gently to the west at 2-3°, and the eastern limb has a slope of up to 70°. A NE-SW trending ridge (approximately following Ridge Road) is a dominant feature associated with the anticline, and has sometimes been interpreted as the axis of the anticline (as in Jackson *et al.*, 1998). Steep sided gullies have formed on either side of the ridge, where the capping layers of gravel have been removed, and erosion has proceeded rapidly. Examples of such are Stewart's Gully and the Te Awa Gullies on the western limb, and Culling's Gullies and Beehive Creek on the eastern limb. However, the axis of the anticline is in fact farther east, within the valley of the Pohangina River (Figure 6.1).

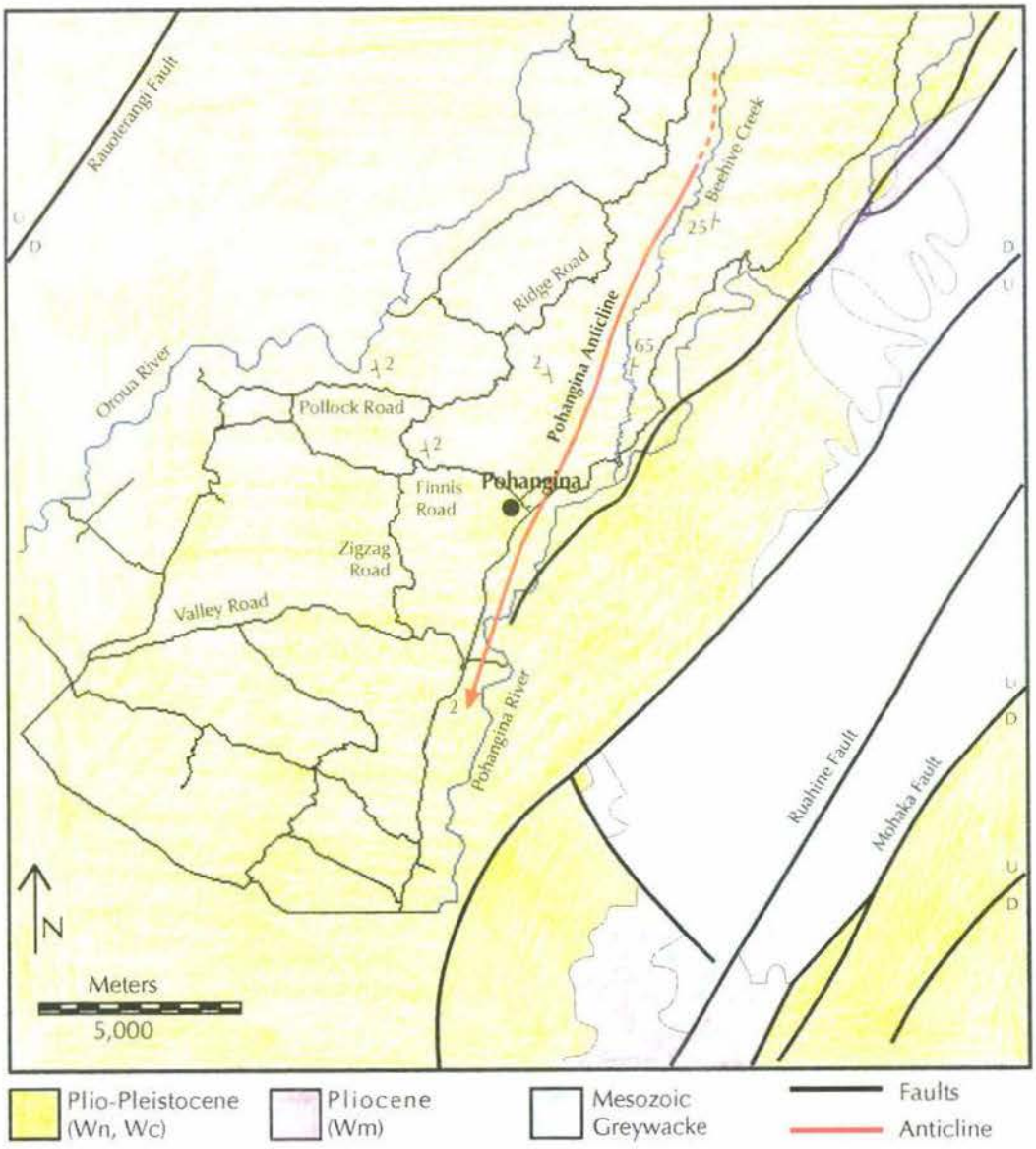

Figure 6.1: Map of the study area, locating the position of the Pohangina Anticline. Geology after Kingma (1962).

South of the study area, the topography is much gentler, where terrace remnant surfaces remain preserved and undisturbed. These surfaces are estimated to be up to 400 ka in age, as they contain the Rangitawa and Griffins Road tuffs (A Palmer, pers comm.).

Sedimentation and deformation rates have been calculated for the Pohangina Anticline area using the tuff units within the study area for time constraints. The average thickness of sediments between the Rewa tuff (1.29 $\pm$ 0.12 Ma) and the Potaka tuff (1.05 $\pm$ 0.05 Ma) throughout the Pohangina Anticline area is approximately 90m. The sedimentation rate for this interval of the sequence is therefore calculated as 0.4m/1000 years. The average thickness of sediments between the Potaka and Kaukatea tuffs (0.87 $\pm$ 0.05 Ma) throughout the Pohangina Anticline area is approximately 80m. The sedimentation rate for this interval of the sequence is therefore calculated as 0.6m/1000 years. The overall estimated sedimentation rate for the study area is therefore approximately 0.5m/1000 years. Sedimentation has been fairly continuous throughout this time period, as no major unconformities or erosion surfaces are seen. Thus the sediment source is likely to have been consistent throughout.

Formation of the anticline itself appears to have occurred since the deposition of the Kaukatea tuff (0.87 $\pm$ 0.05 Ma) or possibly even the Kupe tuff. This is supported by the fact that the Kaukatea tephra and all older tuff units are dipping quite steeply on the eastern limb of the anticline, and also by the paleocurrent directions of the sediments (see Chapter 4) which indicate sediment was largely transported into the area from the north west, i.e. across the present day anticline. The rate of deformation is calculated as being at least 7°/100,000 years, and possibly as much as 10°/100,000 years if the deformation has in fact occurred since the deposition of the Kupe tuff.

The uplift of the Pohangina Anticline has been greater at the northern end, such that it has a gentle southerly plunge. Jackson *et al.* (1998) calculated this southerly plunge as developing at a rate of around 4×10^{-8} rad/year (4×10^{-3} rad/100 ka), or 7×10^{-5} deg/100 ka, averaged over the last 300 ka.

The young age of the anticline and its high deformation rates suggest that the north eastern Manawatu area has seen large earth movements in relatively recent times. This raises concerns regarding future movements and geological hazards.

6.3 Sequence Stratigraphy

Sequence stratigraphy, a widely used explanation for the cyclic nature of sediments, is understood to be driven by variations in the earth's orbital parameters, explained by the Milankovitch theory. The Milankovitch theory predicts that global ice volume, and hence sea level changes, were controlled by seemingly long term periodic variations in the earth's orbital parameters of obliquity, precession and eccentricity (Pillans *et al.*, 1998).

Much work has been done in the Wanganui Basin to characterise the sediments in terms of sequence stratigraphy. A model has been developed for the western Wanganui Basin, where sedimentation evidently kept pace with subsidence throughout much of the basin history (Carter & Naish, 1998) such that sedimentation occurred in a shelf environment, with a maximum water depth of about 75m. Sedimentation during low sea levels characteristically occurred in terrestrial, beach or shoreline environments, while sedimentation during high sea levels occurred on the mid to outer shelf. A complete basin cyclostratigraphy for the last 3.6 Ma has been compiled by Carter *et al.* (1997, 1998) and Saul *et al.* (1998).

Sequence stratigraphic characteristics for the central and eastern Wanganui Basin are not as well known, and have not been widely studied. An aim of this study is to develop a greater knowledge of the sediments of the eastern Wanganui Basin.

The Exxon sequence stratigraphic model summarises the idealised stratigraphic architecture of sediment deposited during a single sea level cycle. In a complete depositional sequence, the sediments belong to one of three main, geometrically separate bodies of sediment termed "systems tracts", representing a sea level rise and subsequent fall.

The Lowstand systems tract (LST) comprises sediment deposited during a lowering sea level. Generally it would be composed of subaerial deposits, but in the western Wanganui Basin sequences, the lowstand systems tract is not represented due to erosion by the following transgression. This results in the formation of a wave-planed surface, characteristically bored by *Barnea similis*, and represents a significant unconformity, forming the sequence boundary at the base of each cycle.

The Transgressive systems tract (TST) forms during the rising part of a sea level cycle, when rapid shoreline transgression occurs. Rapid sea level rise floods the shelf and pre-

vents rivers from incising, such that little fluvial sediment is delivered to the shelf, and marine sediments build in a landward direction (Boggs, 1995). TST sediments of the western Wanganui Basin typically overlie an erosional unconformity and mainly encompass sediments deposited in the intertidal-subtidal shoreface and the muddy nearshore shelf. The sequences are mostly between 0.3m and 8m, suggesting a high rate of sea level rise relative to sediment supply, while sedimentary features are consistent with deposition from rapidly alternating currents (Abbott & Carter, 1994). Van der Neut (1996) recognised that the TST of the depositional sequences in Turakina Valley are thicker than those at the Castlecliff section. This was attributed to a greater supply of sediment toward the east of the basin, probably due to the closer proximity to the main axial ranges and the Taupo Volcanic Zone.

Highstand systems tract (HST) sediments are deposited during and shortly after the sea level maximum. Such conditions allow progradation of the shoreline and the latter part of the HST may be characterised by fluvial sediments (Boggs, 1995). Within the western Wanganui basin sediments the HST is dominantly comprised of shelf siltstone facies up to about 28m thick (Abbott & Carter, 1994).

Abbott and Carter (1999) showed that the coastal Castlecliff section comprised ten disconformity-bound sequences, each typically comprising three parts:

(i) The TST, represented by a basal suite of shoreface and inner shelf sediments with intertidal and shallow subtidal molluscan faunas, and cross bedded, pebbly shell gravels (type A shellbeds).
(ii) The MCS, marking a period of sediment starvation. It contains *in situ* offshore molluscs in a matrix of muddy fine sandstone or fine sandy siltstone (type B shellbed).
(iii) The HST, a unit of terrigenous siltstone, either bedded and unfossiliferous or bioturbated and with a sparsely scattered *in situ* fauna similar to that of the subjacent shellbed (Abbott & Carter, 1999).

Carter and Naish (1998) noted that each Wanganui Basin marine cyclothem contains, in ascending stratigraphic order, some combination of the following sedimentary elements:
- A basal sequence boundary corresponding to an unconformity, on which the ravinement surface (RS) is superposed, as it was cut by the transgressing post-glacial shoreline.
- A transgressive systems tract (TST).
- A local flooding surface (LFS), across which rapid deepening occurs.

• A downlap surface (DLS).

• A highstand systems tract (HST) comprising an aggradational interval of shelf siltstone.

• A regressive systems tract (RST), commencing with a gradational inner shelf to shoreface facies transition, and passing up into strongly progradational shoreline facies.

It must be noted that individual elements may be truncated or superposed on one another, along one of the key surfaces.

The western Wanganui Basin displays a very clear and full record of Pleistocene cyclicty, with sediments having been deposited during a period of known sea level fluctuation driven by Milankovitch orbital controls (Carter *et al.*, 1994, Pillans *et al.*, 1998). The majority of Pliocene-Pleistocene Wanganui Basin sediments are considered to comprise sands, silts and shellbeds deposited in shoreface and shelf environments, while the nonmarine facies are generally thought to be subordinate (Saul *et al.*,1999). In this study of the Pohangina Anticline in the eastern part of the basin, nonmarine facies dominate the equivalent stratigraphy, and the cyclothems do not so clearly contain the sedimentary elements suggested by Carter & Naish (1998).

The pre-terrace late Pliocene-Pleistocene fill of the Wanganui basin comprises 43 superposed cyclothems or sequences (Saul *et al.*, 1999). From the Turakina River section in the axis of the basin, strata thin westward and cycles 23-32 are missing at an unconformity in the Wanganui Coast section. An integrated cyclostratigraphy for the basin has been developed through the presence of eleven major silicic tephra horizons and an established paleomagnetic stratigraphy. Important paleomagnetic boundaries occurring in the basin are the Bruhnes-Matuyama, top and base of Jaramillo and Olduvai, and the Gauss-Matuyama.

Carter *et al.* (1997) and Saul *et al.* (1999) summarised the stratigraphy of the Wanganui Basin, recognising seven major sequence motifs (Figure 6.2) which occur as variations of the stacked cyclothems. Six motifs represent deposition in shelf locations between the highstand and lowstand shorelines (Hawera, Maxwell, Turakina, Seafield, Castlecliff and Rangitikei motifs), while the seventh (Nukumaru motif) includes coquina limestone and represents deposition in shoreface and very shallow water marine environments (Carter & Naish, 1998). Individual sections within the basin are generally dominated by one persistent cyclothem motif, or intervals characterised by a change from one motif to another (Saul *et al.*, 1999).

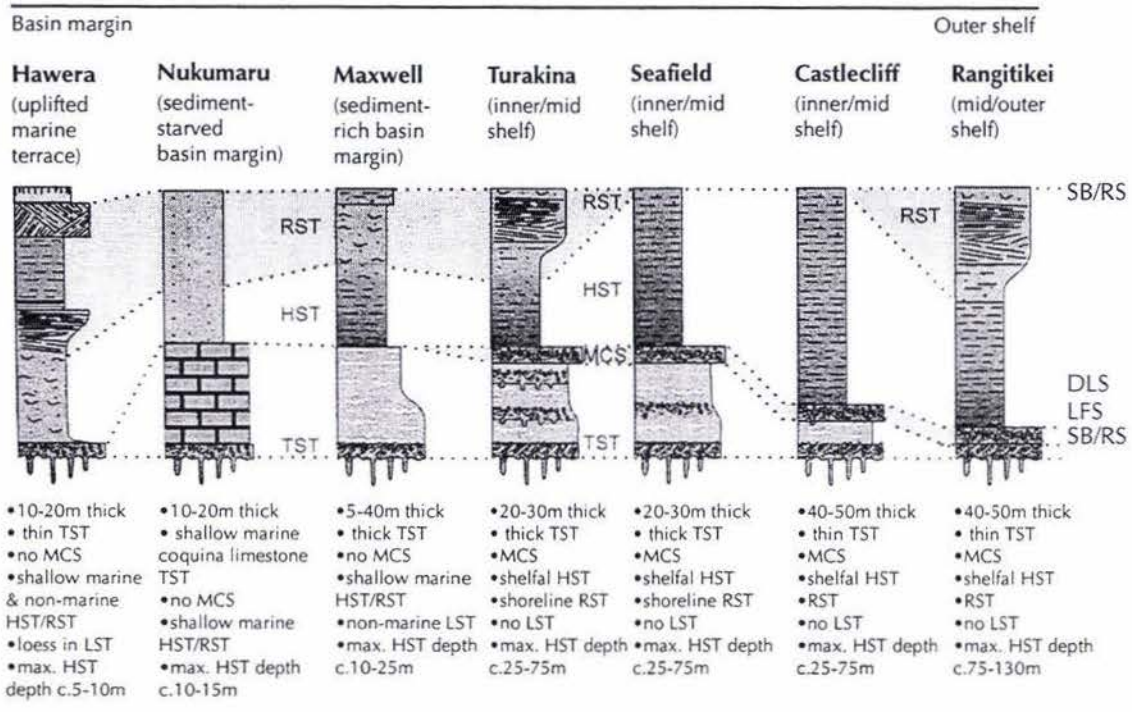

Figure 6.2: The seven major cyclothem motifs recognised within the Wanganui Basin. (From Carter & Naish, 1998).

Faunal, sedimentological and stratigraphic evidence indicates that the motifs represent successively more off-shore locations (from left to right in Figure 6.2) on the paleoshelves that equate with each sequence (Saul *et al.*, 1999). Accordingly, the Hawera motif cycles occur mainly in the tread of uplifted coastal terraces (Pillans, 1990), while the fluvial, lacustrine, lignitic, and shallow marine facies within the Hawera and Birdgrove motifs correspond to the coastal plain and innermost shelf depositional environments. The Nukumaru motif also represents a shallow water environment, starved of highstand terrigenous sediment on the western flank of the basin. The Turakina, Castlecliff and occasional Seafield motif sequences accumulated farther offshore, on the middle shelf, and Rangitikei motif sequences were deposited farthest offshore, toward the basin axis.

N.B. There appears to be a slight discrepancy with the positioning of the Potaka pumice at different sections. In the Castlecliff and Rangitikei sections it is included in cyclothem 35, while in the Wanganui, Whangaehu and Turakina sections it is within cyclothem 36 (Saul *et al.*, 1999). For this study it has been decided to assign cyclothem 35 to the Potaka pumice, due to the geographic proximity to the Rangitikei River sequence.

Pohangina Anticline sequence

On the eastern side of the Wanganui Basin, the higher sedimentation rates appear to have kept up with or exceeded basinal subsidence, such that continuous sedimentation occurred without a marked change in basinal depth. It is also apparent that accomodation was always sufficient to allow deposition of the large quantities of sediment. During periods of high sea level, the sediments aggraded, and when the shoreline receded during low sea level stands, sedimentation resulted in progradation of the shoreline. This unlimited accomodation is well illustrated by the presence of at least 80m of continuous sedimentation between the Potaka pumice (1.05 Ma) and the Kaukatea pumice (0.87 Ma).

Unlike the Castlecliff section, the Pohangina sequence does not contain marine-dominated sediments, and instead lignites and conglomerates are seen within the stratigraphy. The conglomerates represent fluvial aggradation during cold climate episodes, and are analogous to more recently deposited terrace gravels. The lignites and associated muds represent coastal progradation during warmer climates. The occurrence of pumices within the stratigraphy shows the connection of the Pohangina area to the Central North Island.

An attempt has been made to interpret facies of the Pohangina Region on the eastern margin of the basin into the overall sequence stratigraphic framework of the Wanganui Basin (Figure 6.3). Four key tuffs enable correlation to the sections at Castlecliff and Turakina. The Rewa, Potaka, Kaukatea and Kupe pumices are present within cyclothems 32, 35, 37 and 39 respectively. Thus in the time period represented at Pohangina, eight cyclothems occurred. The Pohangina sequence represents the time period when Milankovitch cycles were changing from 0.04 Ma (obliquity) to 0.1 Ma (eccentricity) cycles. During the deposition of the Wanganui Basin sediments, sea level fluctuations were occurring with a magnitude of approximately 50-100m (Carter & Naish, 1998) but due to the changing Milankovitch cycles, sea level fluctuations are not so clearly defined during this period, as approximated by the Oxygen Isotope record.

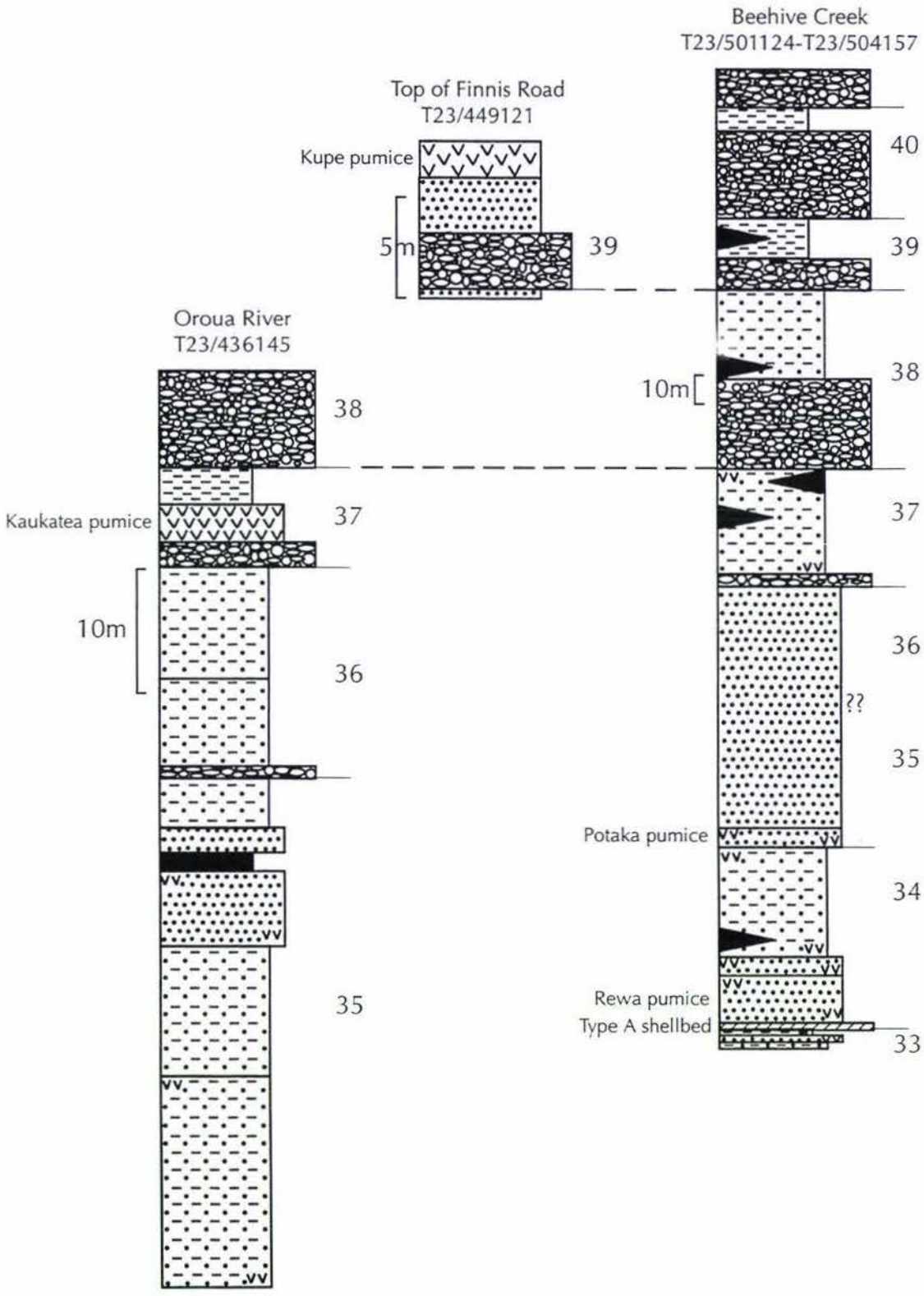

Figure 6.3: Composite stratigraphic column for the Pohangina Anticline sequence, showing the stratigraphic positions of cyclothems, tuff units and shellbed.

Due to the different nature of the sediments of the Pohangina area, it has been decided to use the varying facies to determine the cyclicity of the sequence, and where possible, combine this with the sequence stratigraphic nomenclature used in the western Wanganui Basin (LST, TST, HST etc.). The following discussion outlines the proposed sequence stratigraphic boundaries and intervals within the sediments of the Pohangina area. Figure 6.4 illustrates the cyclothem motif recognised within the sediments of the Pohangina Anticline.

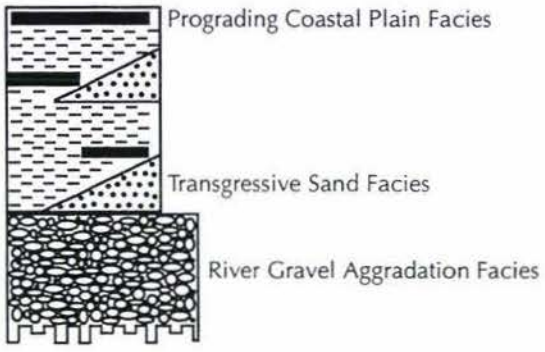

The Pohangina motif:

- up to 60m thick
- conglomeratic RGAF
- shallow marine TSF
- fine grained & lignitic PCPF
- no MCS
- no RST

Figure 6.4: Proposed cyclothem motif for the Pohangina Anticline sequence.

Typically a conglomerate unit overlies the sequence boundary, representing the sediments deposited during cold climatic periods, and equivalent to the LST sediments of the western Wanganui Basin. These conglomerates are referred to as the River Gravel Aggradation Facies (RGAF). Sediments overlying the RGAF are commonly interbedded units of sand and mud, with some lignites, rootlets and burrows. It is proposed that the finer sediments and associated lignites are representative of a prograding coastal plain, and are therefore termed the Prograding Coastal Plain Facies (PCPF) (Figure 6.4). During periods of rapid transgression, marine incursion resulted in the deposition of sand units in places, such that they are interfingered with the terrestrial PCPF sediments. The sands resulting from the marine incursion are referred to as the Transgressive Sand Facies (TSF). Together the PCPF and TSF represent the TST and HST sediments of the sequence stratigraphic model for the western Wanganui Basin.

At Beehive Creek, a Type A shellbed near the base of the sequence represents a sequence boundary, within sediments containing reworked Rewa pumice. The first incoming of the Rewa pumice is not exposed within the study area, and must be lower in the sequence. Thus this sequence boundary is considered to represent that between cyclothems 33 and 34. No gravels are present, but 20m of pumiceous sand overlies the boundary, with trough cross bedding and deformed beds in the top 5m. This suggests rapid infilling

after the LST, with the deposition of marine sands as coastal progradation occurred. Above the sand is 35m of interbedded fine sand and mud, with two thin lignite layers, representing the terrestrial environments that occurred due to the coastal progradation.

The boundary between cyclothems 34 and 35 is not easily defined at Beehive Creek. Townsend (1993) described a 0.5m zone of fragmented shells below the Potaka pumice, which is no longer visible, but may represent a Type A shellbed at the sequence boundary. Sands containing the Potaka pumice represent cyclothem 35 within the Beehive Creek sequence. They are likely to have been deposited in dominantly shallow marine conditions, as part of the Transgressive Sand Facies. In the Oroua River section 1 the base of cyclothem 35 is not defined (Figure 6.3). It is likely to be lower in the sequence, with a large proportion of the sediments at this site representing the TST and HST. The lower half of the section is dominated by sands of the TSF - sands with a shallow marine signature (see Chapter 4), deposited as the coast prograded. Near the top of the cycle the sediments are mud dominated and a 1.5m lignite layer is present, representing the terrestrial sediments of the PCPF.

At Culling's Gullies the shellbed between the Rewa and Potaka pumices is likely to represent the sequence boundary between cyclothems 34 and 35. At this site the sediments are dominantly TSF type sands, deposited within a shallow marine environment.

On the western side of the Pohangina Anticline, a shellbed near the base of the Oroua River section 2 lies just above the Potaka pumice, and is likely to be a Type A shellbed and mark the boundary between sequences 35 and 36 (Plate 6.1). The shellbed is overlain by TSF sediments, and above them are mud-dominated sediments of the PCPF. At the top of the same sequence is a conglomerate, likely to represent the boundary between sequences 36 and 37.

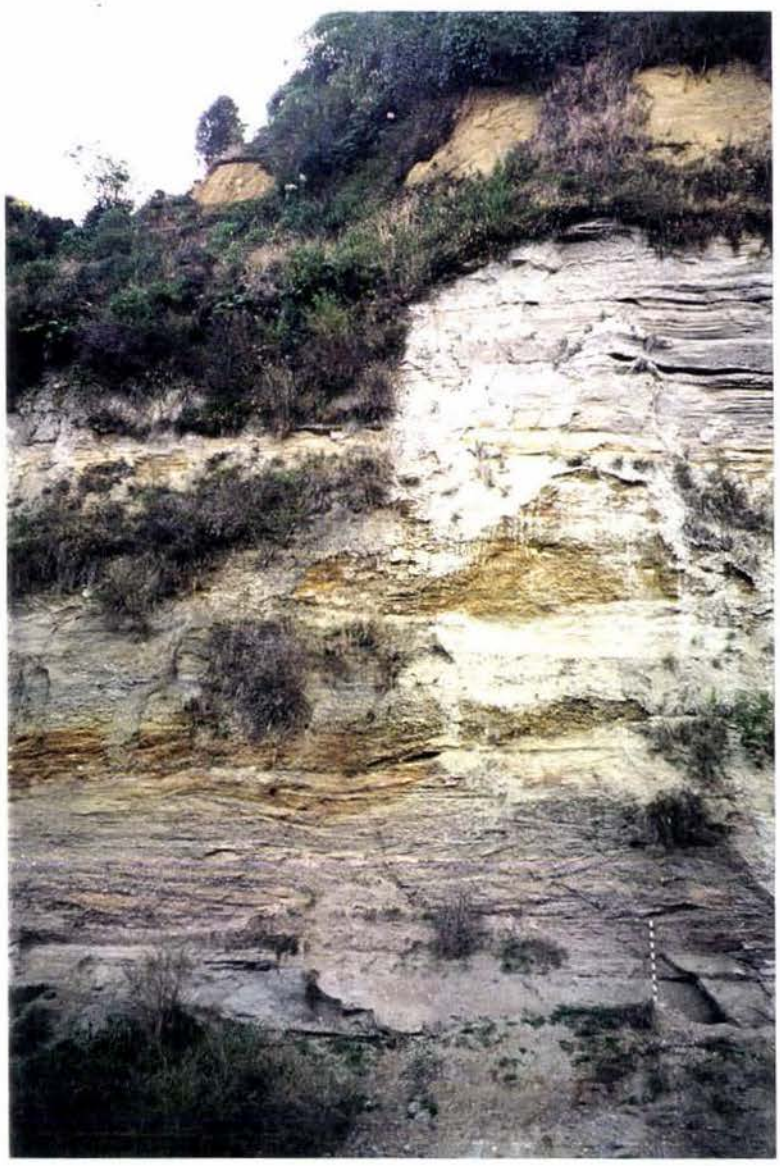

Plate 6.1: Oroua River 2 section (T23/448178) where a Type A shellbed marks the boundary between sequences 35 and 36.
(see Appendix A for stratigraphic column and description).

The boundary between cyclothems 35 and 36 is unclear at Beehive Creek, with only a large unit of sand dominated sediments being present in the interval where the boundary would be expected. In the Oroua River section the boundary has been defined, with a 0.8m thick conglomerate marking the RGAF of cyclothem 36. A 16m unit containing fine sand and mud with burrows, bioturbation and some organic matter near the top of the unit marks the PCPF, as they have been deposited in a dominantly terrestrial or estuarine environment as coastal progradation occurred.

The first conglomerate within the Beehive Creek stratigraphy represents the lowstand systems tract of sequence 37, deposited when fluvial aggradation occurred during a cool climate episode when sea level was low. Above the conglomerate is the TST of cyclothem

37, consisting of sands near the base, overlain by finer grained sediments with associated lignite layers. Sand sample 6 was collected from near the base of the TST (see Chapter 4) and was characterised by Friedman's plots as being a beach deposit. These sands represent the TSF, deposited during a marine incursion when sea level rise exceeded the sediment supply and fluvial progradation. The finer grained sediments and lignites represent flood plain deposits of the PCPF. The Kaukatea pumice is contained within the TST sediments of cyclothem 37. In Rangitikei Valley Kaukatea pumice is found in the Waitapu Shell Conglomerate (Pillans, 1994) which is also most likely a Type A shellbed TST deposit.

In the Oroua River section, cyclothem 37 is well defined with a 2m conglomerate unit marking the RGAF which is directly overlain by the Kaukatea pumice. Above the pumice is a 3m unit of mud, representing sediments of the PCPF, with no indication of marine incursion by this time. The overlying 8m conglomerate marks the cool climate RGAF of cyclothem 38, but the rest of the cyclothem is not revealed.

The base of Gravel Unit 4 in Beehive Creek marks the sequence boundary between cyclothems 37 and 38. The LST of cyclothem 38 is a 29m thick conglomerate, overlain by a TST that is sand dominated near the base, and grades up into fine sand, mud and lignite layers. The presence of lignites indicate that these sediments are representative of warmer climatic conditions. Sand samples 1 and 3 were collected from this unit, and again studied for their depositional environment (see Chapter 4). Both samples plotted as beach deposits on Friedman's graph of Standard Deviation v Mean, and as fluvial deposits on the graph of Standard Deviation v Skewness. Although the characteristics of these sediments are not specific to one environment, it is possible that they indicate a period of marine incursion during the warm climate period of cyclothem 38, therefore indicating the TSF of the cycle. Within this cyclothem, the PCPF is represented by the muds and lignites which accumulated within a terrestrial environment after coastal progradation.

Cyclothem 39 is represented at Beehive Creek by a 10m unit of conglomerate overlain by a 12m unit of fine sediments and lignite. It is apparent that by this time, marine incursions were no longer influencing the sedimentation of the area, and sedimentation is dominantly terrestrial sediments of the RGAF and PCPF.

Sediments representing cyclothem 39 are also present at the top of Finnis Road, where the Kupe pumice has been identified (Chapter 3). A conglomerate unit marks the RGAF,

and is overlain by sands of the PCPF and the Kupe pumice.

Within the Pohangina area, cyclothem 40 is only evident at Beehive Creek. Again it is represented by the cool climate RGAF, overlain by fine muddy sediments of the PCPF. Cyclothem 40 is the youngest identifiable cyclothem within the Pohangina Anticline stratigraphy.

Conclusion

Sediments of the Pohangina Anticline study area have been deposited near the eastern margin of the Wanganui Basin, with high rates of sedimentation and dominantly terrestrial depositional environments. Climatic fluctuations are well represented within the stratigraphy, with cool and warm episodes characterised by RGAF conglomerates alternating with TSF and/or PCPF sediments.

Cyclothems 33 to 40 are represented within the stratigraphy, though the boundary for cyclothem 34/35 is unclear. Sequence boundaries are most often marked by the contact between a unit of fine sediment and an overlying conglomerate. The conglomerate units have been recognised as representing the lowstand systems tract of the cyclothem, deposited during periods of river gravel aggradation, and are overlain by the TST/HST sediments, containing sands of the TSF and/or finer grained, dominantly terrestrial sediments of the PCPF.

6.4 Wanganui Basin correlations

Throughout the Wanganui Basin, widespread tuff units provide excellent age control for the sediments, and are very helpful when correlating sequences across the basin. One of the aims of this study was to correlate the Pohangina Anticline sequence on the eastern margin of the Wanganui Basin, with the much studied western Wanganui Basin section at Castlecliff. Now that a sequence stratigraphic framework has been approximated for the study area, it is possible to correlate between the two sections for cyclothems 33 to 40, thus comparing the depositional environments throughout about 0.5 Ma from 1.29-0.7 million years.

The following table outlines the sequence stratigraphic elements contained within cyclothems 34-40 for the eastern Wanganui Basin (after Abbott & Carter, 1999), and correlates them to the Pohangina Anticline sequence.

Notes for Table 6.1 (following page):

This unit represents shoaling toward the top of the HST

* This unit is typical of the shell-rich facies which accumulate at the feather edge of any shore-connected sediment body and at depths within the reach of wave and tidal currents.

Cyclothem	CASTLECLIFF			POHANGINA	
	Sequence Stratigraphic Element	**Unit**	**Interpreted Environment**	**Sequence Strat. Element**	**Interpreted Environment**
40	HST	Upper Kai-Iwi Siltstone	Shoreface-shelf transition & inner to middle shelf	PCPF	Lower coastal plain
	MC shellbed	Upper Kai-Iwi Shellbed	Innermost shelf & starved inner shelf	RGAF	Fluvial
	TST	Kupe Formation	Tide/storm dominated muddy innermost shelf		
39	HST	Upper Westmere Siltstone	Inner shelf	PCPF	Lower coastal plain
	Type B & MC shellbed	Upper Westmere Shellbed	Shoreface-shelf transition starved inner shelf	RGAF	Fluvial
	TST	Kaikokopu Formation	Tide/storm dominated muddy innermost shelf		
38	HST	Lower Westmere Siltstone	Inner shelf	PCPF	Lower coastal plain
	Type B & MC shellbed	Lower Westmere Shellbed	Inner shelf & starved inner shelf	TSF	Shallow marine
	TST	Ophiomorpha Sand	Lower shoreface	RGAF	Fluvial
37		Omapu Shellbed*	Shoreface-shelf transition	PCPF	Lower coastal plain
	HST	Lower Kai-Iwi Siltstone	Inner to middle shelf	TSF	Shallow marine
	Type B & MC shellbed	Lower Kai-Iwi Shellbed	Starved inner shelf	RGAF	Fluvial
	TST	Kaimatira Pumice Sand	Tide/storm dominated muddy innermost shelf		
36	HST	Upper Okehu Siltstone	Inner shelf	PCPF	Lower coastal plain
	Type B shellbed	Tiostrea-Dosina Bed	*	TSF	Shallow marine
	Type A shellbed &TST	Okehu Shell Grit	Tide/storm dominated muddy innermost shelf	Type A shellbed	Nearshore
35	HST	Lower Okehu Siltstone	Inner shelf	PCPF	Lower coastal plain
	MC Condensed Interval	Rolled Concretion Conglomerate	Starved inner shelf	TSF	Shallow marine
	Type A shellbed & TST	Mowhanau Formation	Tide/storm dominated muddy innermost shelf	Type A shellbed	Nearshore
34	TST	Ototoka Siltstone	Tide/storm dominated muddy innermost shelf	PCPF	Lower coastal plain
	Type A shellbed & lower TST	Butlers Shell Conglomerate	Tide/storm dominated muddy innermost shelf	TSF	Shallow marine
				Type A shellbed	Nearshore

Table 6.1: Correlation of the sedimentary elements contained within cyclothems 34-40 for Castlecliff, western Wanganui Basin (after Abbott & Carter, 1999) and the Pohangina area.
PCPF - Prograding Coastal Plain Facies, TSF - Transgressive Sand Facies, RGAF - River Gravel Aggradation Facies.

Within the western Wanganui Basin sequence, the cyclothems are dominantly represented by the Castlecliff motif. Cyclothems 35 and 36 are both Seafield motifs, while the remaining five cyclothems are all Castlecliff motifs (Carter & Naish, 1998).

The Castlecliff sequence was deposited dominantly within the inner to mid shelf environment (Table 6.1) while within each sequence a deepening is evident from the TST to the HST. The sediments of cyclothems 34 to 36 would all have been deposited within the wave base, near to the shore. The midcycle condensed interval of cyclothem 35 is an indication of rapid sea level rise during that period, causing a starvation of sediment. Within cyclothems 37 to 40, a transition can be seen from a tide/storm dominated innermost shelf or lower shoreface setting when the TST was deposited, to an inner to middle shelf setting when the HST was deposited, indicating a deepening within each cyclothem due to sea level rise.

Within the Pohangina Anticline sequence, an obvious change in depositional environment can be seen from cyclothems 34 to 40, due to shallowing. Cyclothems 34 to 36 contain dominantly marine LST and TST sediments, with the sequence boundaries being marked by shellbeds. During this time, a high rate of sediment supply allowed coastal progradation to occur during deposition of the TST, such that the upper part of each cyclothem is represented by sediments of the prograding coastal plain, including lignites and fluvial muds.

Sediments in cyclothems 37 to 40 have all been deposited within dominantly terrestrial environments, as indicated by their fluvial aggradation gravels of the LST. The Transgressive Sand Facies of cyclothem 37 is thought to represent a marine incursion, but otherwise the cyclothems contain only terrestrial sediments.

Thus it can be seen that the sea level fluctuations represented within each cyclothem of the Castlecliff sequence are not so clearly evident within the sequence on the eastern margin of the Wanganui Basin. Sequences of the western Wanganui Basin had a much lower rate of sediment supply (approximately 0.2m/1000yr, calculated from Abbott & Carter, 1999) than those on the eastern side. The more rapid sedimentation in the east allowed greater progradation of the coast, and sedimentation therefore occurred in a shallower and eventually terrestrial environment on the eastern side of the basin, while the western side was still experiencing shallow marine conditions.

REFERENCES

Abbott, S.T. & Carter, R.M. 1994: The sequence architecture of mid-Pleistocene (c. 1.1-0.4 Ma) cyclothems from New Zealand: facies development during a period of orbital control on sea-level cyclicity. *International Association of Sedimentologists Special Publication* 19, 367-394.

Abbott, S.T. & Carter, R.M. 1999: Stratigraphy of the Castlecliffian type section: 10 mid-Pleistocene sequences from the Wanganui coast, New Zealand. *New Zealand Journal of Geology and Geophysics* 42, 91-111.

Alloway, B.V, Pillans, B.J, Sandhu, A.S. & Westgate, J, A. 1993: Revision of Marine Chronology in the Wanganui Basin, New Zealand, based on the isothermal plateau fission-track dating of tephra horizons. *Sedimentary Geology* 82, 299-310.

Anderton, P.W. 1981: Structure and evolution of the South Wanganui Basin, New Zealand. *New Zealand Journal of Geology and Geophysics* 24, 39-63.

Andrews, P.B. 1982: Revised guide to recording field observations in sedimentary sequences. Report NZGS 102, New Zealand Geological Survey. 74p.

Beu, A.G. & Edwards, A.R. 1984: New Zealand Pleistocene and late Pliocene glacio-eustatic cycles. *Palaeogeography, Palaeoclimatology, Palaeoecology* 46, 119-142.

Blatt, H, Middleton, G.V. & Murray, R.C. 1980: Origin of sedimentary rocks. Prentice Hall. 782p.

Boggs, S. (Jr) 1995: Principles of Sedimentology and Stratigraphy. Prentice Hall. 774p.

Borchardt, G.A, Harvard, M.E. & Schmitt, R.A. 1971: Correlation of volcanic ash deposits by activation analysis of glass separates. *Quaternary Research* 1, 247-260.

Carter, R.M. & Naish, T.R. 1998: A review of Wanganui Basin, New Zealand: global reference section for shallow marine, Plio-Pleistocene (2.5-0 Ma) cyclostratigraphy. *Sedimentary Geology* 122, 37-52.

Carter, R.M, Abbott, S.T, Naish, T. & Saul, G. 1997: High resolution Plio-Pleistocene (2.5-0 Ma) chronocyclostratigraphy and section correlations, Wanganui Basin, New Zealand. Poster 2, School of Earth Sciences, James Cook University, Townsville.

Carter, R.M, Abbott, S.T, Gammon, P, Pillans, B. & Saul, G.R.S. 1994: Sequence analysis of Plio-Pleistocene cyclothems North Island, New Zealand. Handbook and Field Guide, Department of Earth Sciences, James Cook University of North Queensland.

Coakley, J.P. & Syvitski, J.P.M. 1991: SediGraph Technique. In: Principles, methods and application of particle size analysis. Edited by J.P.M Syvitski. Cambridge University Press. 368p.

Collinson, J.D. & Thompson, D.B. 1982: Sedimentary structures. George Allen & Unwin. 194p.

Davis, R.A. (Jr) 1937: Depositional systems - an introduction to sedimentology and stratigraphy. Prentice Hall. 604p.

Dyer, K.R. 1986: Coastal and estaurine sediment dynamics. John Wiley & Sons. 342p.

Field, B.D, Uruski, C.I. and others. 1997: Cretaceous-Cenozoic geology and petroleum systems of the East Coast region, New Zealand. Institute of Geological and Nuclear Sciences Monograph 19. 301p and 7 enclosures.

Fieller, N.R.J. & Flenley, E.C. 1990: The combination of particle size data from a variety of measurement methods.

Fieller, N.R.J, Flenley, E.C. & Olbricht, W. 1992: Statistics of particle size data. *Applied Statistics* 41 No. 1, 127-146.

Fleming, C.A. 1953: The geology of the Wanganui Subdivision. New Zealand Geological Survey Bulletin 52.

Fleming, C.A. 1957: The Genus Pecten in New Zealand. New Zealand Geological Survey Paleontological Bulletin 26.

Folk, R.L. 1974: Petrology of sedimentary rocks. Hemphill Publishing 182p.

Folk, R.L, Andrews, P.B. & Lewis, D.W. 1970: Detrital sedimentary rock classification and nomenclature for use in New Zealand. *New Zealand Journal of Geology and Geophysics* 13, 937-968.

Friedman, G.M. 1961: Distinction between dune, beach, and river sands from their textural characteristics. *Journal of Sedimentary Petrology* 31, 514-529.

Friedman, G.M. 1967: Dynamic processes and statistical parameters compared for size frequency distribution of beach and river sands. *Journal of Sedimentary Petrology* 37, 327-354.

Froggatt, P.C. 1983: Toward a comprehensive upper Quaternary tephra and ignimbrite stratigraphy in New Zealand using Electron Microprobe analysis of glass shards. *Quaternary Research* 19, 188-200.

Froggatt, P.C. 1992: Standardization of the chemical analysis of tephra deposits. Report of the ICCT Working Group. *Quaternary International* 13/14, 93-96.

Froggatt, P.C. & Lowe, D.J. 1990: A review of late Quaternary silicic and some other tephra formations from New Zealand: their stratigraphy, nomenclature, distribution, volume, and age. *New Zealand Journal of Geology and Geophysics* 33 No. 1, 89-109.

Gardner, J.V. 1982: High-resolution carbonate and organic-carbon stratigraphies for the late Neogene and Quaternary from the western Caribbean and eastern equatorial Pacific. In: Prell *et al* (Editors) Initial Report for the Deep Sea Drilling Project. 68, 347-364.

Hatherton, T. 1969: Gravity, seismicity, and tectonics of the North Island, New Zealand. *New Zealand Journal of Geology and Geophysics* 13, 126-144.

Heerdegen, R.G. 1972: Landforms of the Manawatu. Miscellaneous Papers No. 2, Department of Geography, Massey University.

Hunt, T.M. 1980: Basement structure of the Wanganui Basin, onshore, interpreted from gravity data. *New Zealand Journal of Geology and Geophysics* 23 No. 1, 1-16.

Institute of Geological and Nuclear Sciences. 1997: Cretaceous-Cenozoic Geology and Petroleum Systems of the East Coast Region, New Zealand. IGNS Monograph 19.

Jackson, J, Van Dissen, R, Berryman, K. 1998: Tilting of active folds and faults in the Manawatu region, New Zealand: evidence from surface drainage patterns. *New Zealand Journal of Geology and Geophysics* 41, 377-385.

Kamp, P.J. & Turner, G.M. 1990: Pleistocene unconformity-bounded shelf sequences (Wanganui Basin, New Zealand) correlated with global isotope record. *Sedimentary Geology* 68, 155-161.

Kamp, P.J. & Naish, T.R. 1998: Forward modelling of the sequence stratigraphic architecture of shelf cyclothems: application to Late Pliocene sequences, Wanganui Basin (New Zealand). *Sedimentary Geology* 116, 57-80

King, C. 1991: The depositional environments. Longman. 116p.

Kingma, J.T. 1958: Possible origin of piercement structures, local unconformities, and secondary basins in the eastern geosyncline, New Zealand. *New Zealand Journal of Geology and Geophysics* 1, 269-274.

Kingma, J.T. 1962: Geological Map of New Zealand. Sheet 11 Dannevirke. Scale 1:250,000. New Zealand Geological Survey, DSIR.

Kohn, B.P, Pillans, B.J. & McGlone, M.S. 1992: Zircon fission track age for middle Pleistocene Rangitawa Tephra, New Zealand: stratigraphic and paleoclimatic significance. *Palaeogeography, Palaeoclimatology, Palaeoecology* 95, 73-94.

Leeder, M.R. 1982: Sedimentology - process and product. Harper Collins. 344p.

Lewis, D.W. & McConchie, D.M. 1994: Analytical sedimentology. Chapman & Hall. 197p.

MacPherson, A.T. 1985: Stratigraphy and tephra correlations of Pleistocene sediments from the Finnis Road area, Pohangina, Manawatu. Unpublished BSc (Hons) thesis, Victoria University.

Manning, D.A. 1988: Stratigraphy and paleoenvironment of deposition of mid-Quaternary sediments in Culling's Gullies, Pohangina Valley, Manawatu, New Zealand. Unpublished BSc (Hons) thesis, Massey University.

Miall, A.D. 1996: The geology of fluvial deposits: sedimentary facies, basin analysis, and petroleum geology. Springer. 582p.

Ministry of Commerce 1993: An introduction to the Petroleum Geology of New Zealand. New Zealand Petroleum Prospectus.

Naish, T.R. & Kamp, P.J.J. 1995: Pliocene- Pleistocene marine cyclothems, Wanganui Basin, New Zealand: a lithostratigraphic framework. *New Zealand Journal of Geology and Geophysics* 38, 223-243.

Naish, T.R. & Kamp, P.J.J. 1997: Sequence stratigraphy of sixth-order (41 ky) Pliocene-Pleistocene cyclothems, Wanganui basin, New Zealand: a case for the regressive systems tract. *Geological Society of America Bulletin* 109 No. 8, 978-999.

Naish, T.R, Abbott, S.T, Alloway, B.V, Beu, A.G, Carter, R.M, Edwards, A.R, Journeaux, T.D, Kamp, P.J.J, Pillans, B.J, Saul,G. & Woolfe, K.J. 1998: Astronomical calibration of a Southern Hemisphere Plio-Pleistocene reference section, Wanganui Basin, New Zealand. *Quaternary Science Reviews* 17, 695-710.

Naish, T.R, Kamp, P.J.J, Alloway, B.V, Pillans, B.J, Wilson, G.S. & Westgate, J.A. 1996: Integrated tephrochronology and magnetostratigraphy for cyclothemic marine strata, Wanganui Basin: implications for the Pliocene-Pleistocene boundary in New Zealand. *Quaternary International* 34-36, 29-48.

Ower, J.R. 1943: The geology of the Manawatu Saddle and the adjacent fronts of the Ruahine Range, North Island, New Zealand. The Superior Oil Company (NZ) Ltd. 12p.

Passega, R. 1964: Grain size representation by CM patterns as a geological tool. *Journal of Sedimentary Petrology* 34, 830-847.

Pettijohn, F.J, Potter, P.E. & Siever, R. 1972: Sand and Sandstone. Springer. 618p.

Pillans, B.J. 1991: New Zealand Quaternary stratigraphy: an overview. *Quaternary Science Reviews* 10, 405-418.

Pillans, B.J. 1994: Direct marine-terrestrial correlations, Wanganui Basin, New Zealand: the last 1 million years. *Quaternary Science Reviews* 13, 189-200.

Pillans, B.J, Roberts, A.P, Wilson, G.S, Abbott, S.T. & Alloway, B.V. 1994: Magnetostratigraphic, lithostratigraphic and tephrostratigraphic constraints on Lower and Middle Pleistocene sea-level changes, Wanganui Basin, New Zealand. *Earth and Planetary Science Letters* 121, 81-98.

Pillans, B, Chappell, J. & Naish, T.R. 1998: A review of the Milankovitch climatic beat: template for Plio-Pleistocene sea-level changes and sequence stratigraphy. *Sedimentary Geology* 122, 5-21.

Rait, G, Chanier, F. & Waters, D.W. 1991: Landward- and seaward-directed thrusting accompanying the onset of subduction beneath New Zealand. *Geology* 19, 230-233.

Reading, H.G. 1978: Sedimentary environments and facies. Blackwell Scientific Publications. 557p.

Reed, J. J. 1957: Petrology of the Lower Mesozoic rocks of the Wellington District. New Zealand Geological Survey Bulletin n.s 57. 60p.

Reineck, H.E. & Singh, I.B. 1973: Depositional sedimentary environments. Springer-Verlag. 439p.

Rijkse, W.C. 1977: Soils of the Pohangina County. Soil Bureau Bulletin 42 70p.

Robertson, E.I. & Reilly, W.I. 1958: Bouger anomaly map of New Zealand. *New Zealand Journal of Geology and Geophysics* 1, 560-564.

Rust, B.R & Koster, E.H. 1984: Coarse alluvial deposits. In: Facies Models. Edited by Walker, R.G. Geoscience Canada Reprint Series 1. 317p.

Sampson, T. 1992: Rapid sediment analyser program. (Sediment grain size analysis computer program). Geography Department, University of Auckland.

Saul, G, Naish, T.R, Abbott, S.T. & Carter, R.M. 1999: Sedimentary cyclicity in the marine Pliocene-Pleistocene of the Wanganui basin (New Zealand): Sequence stratigraphic motifs characteristic of the past 2.5 m.y. *Geological Society of America Bulletin* 111 No. 4, 524-537.

Selley, R.C. 1988: Applied sedimentology. Academic Press. 446p.

Selley, R.C. 1996: Ancient sedimentary environments and their sub-surface diagnosis. Chapman & Hall. 300p.

Seward, D. 1974: Age of New Zealand Pleistocene substages by fission-track dating of glass shards from tephra horizons. *Earth and Planetary Science Letters* 24, 242-248.

Seward, D. 1976: Tephrostratigraphy of the marine sediments in the Wanganui Basin, New Zealand. *New Zealand Journal of Geology and Geophysics* 19, 9-20.

Shackleton, N.J. & Opdyke, N.D. 1973: Oxygen isotope and paleomagnetic stratigraphy of equatorial Pacific core V 28-238: oxygen isotope temperatures and ice volumes in a 105 and 106 year scale. *Quaternary Research* 3, 39-55.

Shane, P.A.R. 1991: Remobilised silicic tuffs in middle Pleistocene fluvial sediments, southern North Island, New Zealand. *New Zealand Journal of Geology and Geophysics* 34, 489-499.

Shane, P.A.R. 1994: A widespread, early Pleistocene tephra (Potaka tephra, 1Ma) in New Zealand: character, distribution, and implications. *New Zealand Journal of Geology and Geophysics* 37, 25-35.

Shane, P.A.R. & Froggatt, P.C. 1991: Glass chemistry, paleomagnetism, and correlation of middle Pleistocene tuffs in southern North Island, New Zealand and Western Pacific. *New Zealand Journal of Geology and Geophysics* 34, 203-211.

Shane, P.A.R, Black, T.M, Alloway, B.V. & Westgate, J.A. 1996: Early to middle Pleistocene tephrochronology of North Island, New Zealand: Implications for volcanism, tectonism, and paleoenvironments. *Geological Society of America Bulletin* 108 No. 8, 915-925.

Stern, T.A, Quinlan, G.M & Holt, W.E 1993: Crustal dynamics associated with the formation of Wanganui Basin, New Zealand. In: South Pacific sedimentary basins. Sedimentary basins of the world 2. Edited by P.F. Ballance. Elsevier Science Publishers. 413p.

Te Punga, M.T. 1952: The Geology of the Rangitikei Valley. New Zealand Geological Survey Memoir 8.

Townsend, T.D. 1993: Beehive Creek, Pohangina Valley, Manawatu, New Zealand - Stratigraphy and paleoenvironment of deposition of mid-Quaternary sediments. Unpublished BSc (Hons) thesis, Massey University.

Turner, G.M. & Kamp, P.J.J. 1990: Paleomagnetic location of the Jaramillo Subchron and the Matuyama-Brunhes transition in the Castlecliffian stratotype section, Wanganui Basin, New Zealand. *Earth and Planetary Science Letters* 100, 42-50.

Van der Neut, M. 1996: Sequence stratigraphy of Plio-Pleistocene sediments in lower Turakina valley, Wanganui Basin, New Zealand. Unpublished MSc thesis, Massey University.

Vella, P. 1963: Plio-Pleistocene Cyclothems, Wairarapa, New Zealand. Transactions of the Royal Society of New Zealand, *Geology* 2, 15-50.

Walcott, R.I. 1978: Present tectonics and Late Cenozoic evolution of New Zealand. *Geophysics Journal of the Royal Astronomical Society* 52, 137-164.

Walcott, R.I. 1984: Reconstructions of the New Zealand region for the Neogene. *Palaeogeography, Palaeoclimatology, Palaeoecology* 46, 217-231.

Whitton, J.S. & Churchman, G.J. 1987: Standard Methods for mineral analysis of soil survey samples for characterisation and classification in NZ Soil Bureau. NZ Soil Bureau Report 79. 27p.

APPENDIX A

• Stratigraphic Columns and Descriptions for key sites within the study area.

All section descriptions are numbered from the bottom, such that (i) is the base unit of the section.

Oroua River Section 1

Grid Reference: T23/436145

Altitude at base of section: 207m

(i) 17m. Parallel bedded fine sand, mud and pumice (pumice is coarse sand size). Beds cm scale. Some pumice-filled channels, also containing small mud clasts. Mud flasers and some rippled beds.

➢ Tuff sample 9861 taken from a pumice-filled channel (0.17m deep, 0.7m wide).

(ii) 10.5m. Organic rich finely bedded (10-50mm) mud and fine muddy sand. Some burrows.

➢ Sediment sample D taken from a 50mm thick, normally graded unit.

(iii) 6m. Parallel bedded pumiceous sands with occasional muds. Large shallow-angled crossbeds. Directions: 18°@105/10°@188, 15°@105/6°@170

(iv) 1.5m. Lignite layer - dark grey silt, very carbonaceous.

(v) 2m. Highly burrowed medium sands. Burrows up to 10mm across, 50-100mm deep, with limonite rims.

(vi) 4m. Interbedded sands and muds, cm-bedded. Dewatering structures up to 0.3m in size. Ocassional logs 50-100mm. Muds are quite organic-rich.

(vii) 0.8m. Layer of iron stained pebbles, mostly less than 20mm in size. Very little matrix, with mud clasts at the base. Unit thickness is variable.

(viii) 7m. Finely laminated fine sand and mud. Some dewatering features.

(ix) 9m. Interbedded mud and silty mud (cm bedding). Burrowed and partially bioturbated. Some organic matter.

(x) 2m. Iron stained gravels, with average pebble size about 50mm. Very little matrix. Some sand lenses.

(xi) 3m. White pumice sand.

(xii) 3m. Grey mud, no apparent bedding.

(xiii) 8m. Iron stained gravels, with average pebble size about 50mm. Very little matrix. Some sand lenses.

Oroua River Section 1

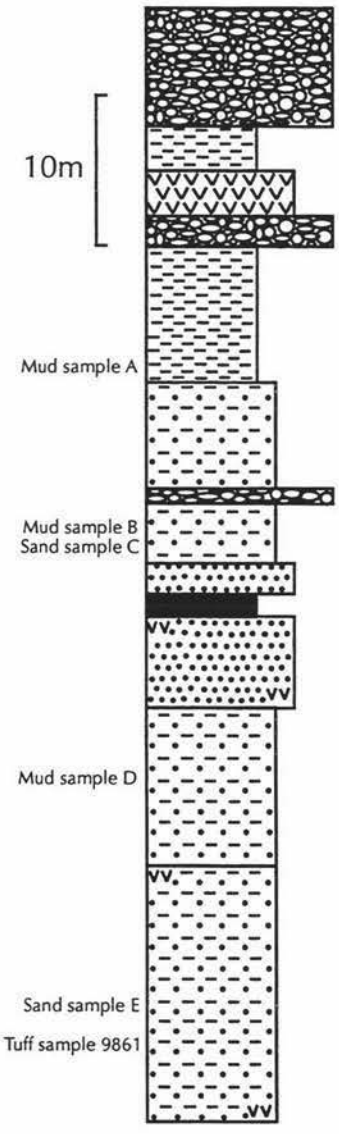

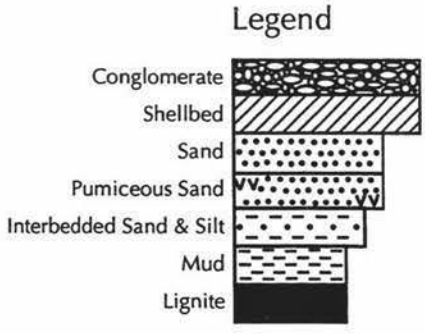

Oroua River Section 2

Grid Reference: T23/448178

Altitude at base of section: 207m

(i) 1m. Fine brown sand. Few mud lenses.

(ii) 0.12m. Coarse sand-granule size pumice, small pebbles and sand.

(iii) 1.1m Massive hardened grey mud.

(iv) 0.5m. Interbedded mud and medium pumiceous sand. Mud 90%, sand 10%. Horizontal bedding.

(v) 3m. Shellbed. Shells whole and broken, with pebbles, coarse sand and pumice pebbles. Cross bedding. Pumice-filled channels. Mud lenses. Some iron staining.

(vi) 7m. Iron stained gravels. Average pebble size 20-30mm. Coarse sand matrix. Sand lense. Faint horizontal bedding.

(vii) 3m. Fine iron stained sand. Few thin pumice streaks. Mud lenses. Horizontal bedding.

(viii) 1m. Medium grey sand. Faint horizontal bedding.

(ix) 0.4m. Grey/brown mud. Rich in organic matter.

(x) 8m. Grey mud. Faint horizontal laminations. 100mm lignite layer 1.5m from base.

(xi) 9m. Fine iron stained sand.

(xii) 1.5m. Grey mud. Faint horizontal laminations.

(xiii) 4m. Fine iron stained sand.

(xiv) 4m. Iron stained gravels.

Oroua River Section 2

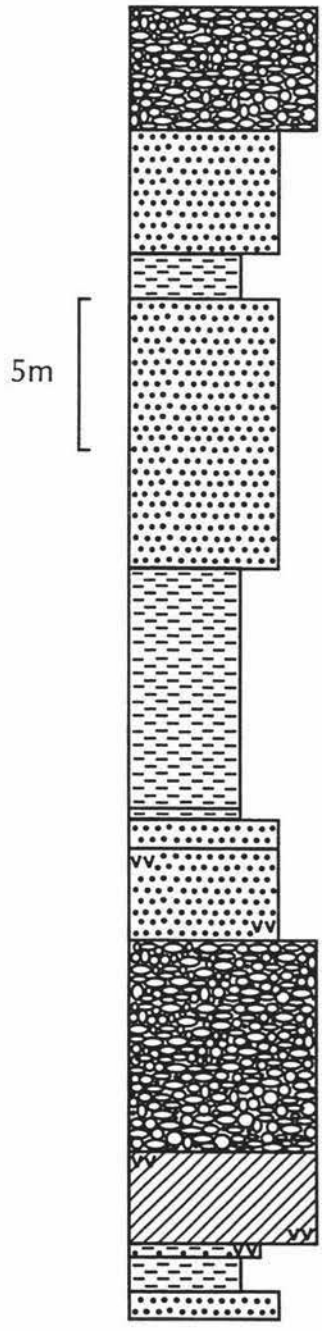

Legend

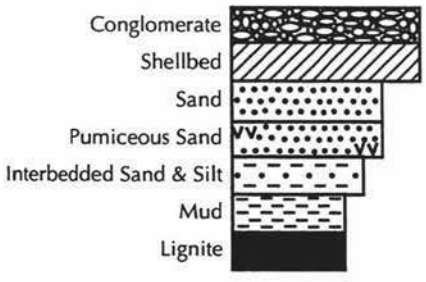

Pollock Road Section

Grid Reference: T23/442140

Altitude at base of section: 278m

(i) 1m. Blue silty sands with extremely fine laminations.

(ii) 2m. Iron stained gravels. Mostly clast supported. Average pebble size about 20mm.

(iii) 5m. Pure pumice. Coarse sand size to fine lapilli. Some dewatering structures and cross bedding.

➢ Tuff sample 98510.

Pollock Road Site

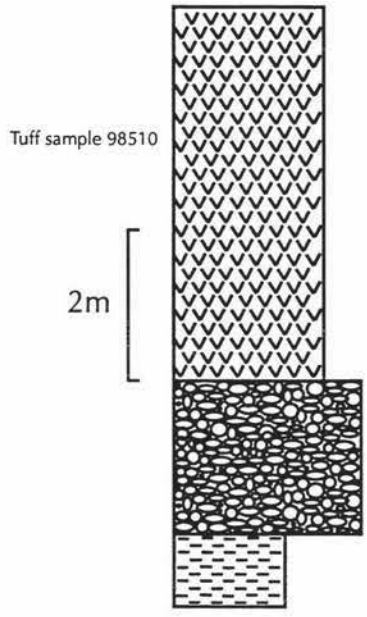

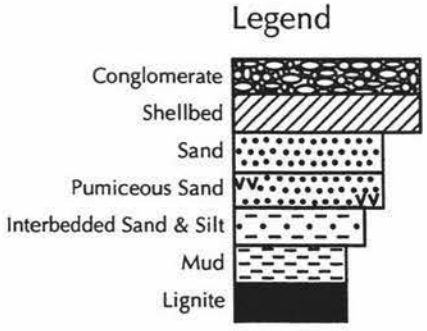

Stewart's Gully Section A

Grid Reference: T23/444145

Altitude at base of section: 197.5m

(i) 0.2m. Fine grey sand, no apparent bedding.

(ii) 0.3m. Fine conglomerate-type mixture. Very poorly sorted coarse iron stained sand, rounded grey/brown mud clasts up to 50mm, pumice and greywacke pebbles up to 30mm. Mud clasts largest and densest in lower 0.2m. Pumice and coarse sand show some near-horizontal bedding. Wavy contacts.

➢ Tuff sample 9851 taken from cross bedded pumice-rich sediments.

(iii) 0.7m. Fine-medium grey/brown pumiceous sand. Some mud clasts. Pumice layers disturbed, with some convolute bedding. Distinct but wavy boundaries.

Tephra sample 9851 from dipping pumice-rich beds, 1.2m from base of section.

(iv) 0.2m. Fine through to coarse grey/brown pumiceous sand with pumice pebbles up to 20mm in size. Very distinct horizontal laminations. Sand and pumice fine upward. Some flattened mud rip-up clasts, up to 20mm in size in lower 50mm of unit. Thickness of unit varies.

(v) 0.5m. Disturbed mixture of fine grey/brown sand, fine-medium grey/brown pumiceous sand and a few greywacke pebbles up to 25mm. Many convolutions. Boundaries distinct but very wavy.

(vi) 0.3m. Fine grey/brown sand with pumice pebbles up to 20mm. Some iron staining. Pumice concentrated into horizontal layers 10mm thick. Some mud clasts in the lower part of unit.

(vii) 0.5m. Grey through to orange/brown fine-medium sand. Well bedded (cm scale). Pebbles up to 15mm and mud clasts up to 70mm in the lower 90mm. Some cross bedding. Directions: 24°@285/14°@192. Unit thickness varies.

(viii) 1.5m. Iron stained conglomerate. Quite well sorted - coarse sand through to 20mm pebbles (average pebble size 5mm). Mud clast layers in lower 0.5m. Some cross bedding, but in opposite direction to unit below.

(ix) 1m. Grey pumiceous sand with horizontal laminations.

(x) 3m. Red/brown conglomerate, average pebble size 20mm. Pebbles fairly well rounded. Very little matrix. No apparent fining or coarsening upward.

Stewart's Gully Section A

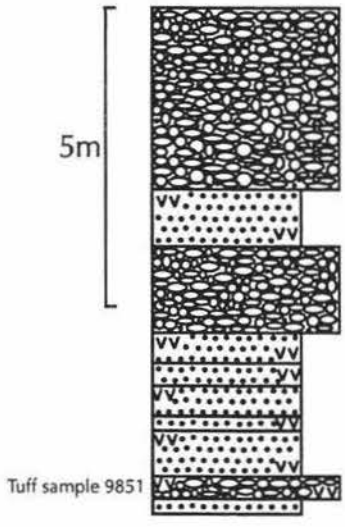

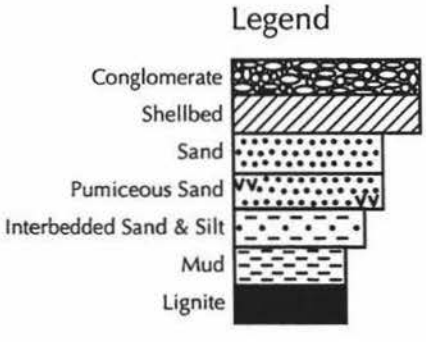

Stewart's Gully Section B

Grid Reference: T23/447144

Altitude at base of section: 200m

(i) 0.5m. Interbedded sands. Orange/brown medium sand, 20-40mm layers and grey medium sand, 5-20mm layers, fining up. Sharp boundaries between all layers. Iron concentrations at the boundaries.

(ii) 1m. Medium sand with cm-bedding. Some iron staining. Mud lenses up to 50mm thick. Sharp boundaries.

(iii) 2.2m. Orange/brown pumiceous sand with mud lenses up to 50mm thick. Parallel laminations, mineral segregation. Some iron staining in the sand. Some cross bedded pumice in top 1m of unit. Also a few channels containing coarser pumice.

(iv) 1m. Interbedded orange/brown and grey fine to medium sands and fine pumice. Ocassional mud flasers and a few pumice pebbles, up to a few cm in size. Some wavy pumice layers, but mainly horizontal parallel bedding. Top of unit defined by distinct iron concentration.

(v) 1m. Interbedded fine to medium sand and grey silty mud. Sand layers up to 0.5m thick, finely laminated with mineral segregation. Silty mud is massive and quite competent, with a low level of organic matter. 0.2m layer of coarser sand, fine pebbles and pumice in middle of the unit.

(vi) 0.7m. Very iron stained coarse sand and fine pebbles. Pebbles up to 40mm, finer at top. More pumice-rich in top 0.2m. Boundaries distinct but wavy.

(vii) 0.4m. Grey silty mud mixed with orange/brown coarse sand and some pumice.

(viii) 0.8m. Pumice-rich sand. Some mud rip-up clasts. Pumice content greatest and coarsest in lower 0.3m. Fining upward, with grey sand at top. Horizontal laminations.

(ix) 2.5m. Fine-medium grey/brown sands. Some wavy laminations. Some pumice layers.

(x) 0.5m. Iron stained gravels, containing large mud rip-up clasts and pumice. Wavy boundaries. Pebbles are well rounded and polished.

(xi) 1m. Fine-medium grey/brown sands. Horizontal laminations.

(xii) 2m. Iron stained gravels with a coarse sand matrix. Faint horizontal imbrication.

Stewart's Gully Section B

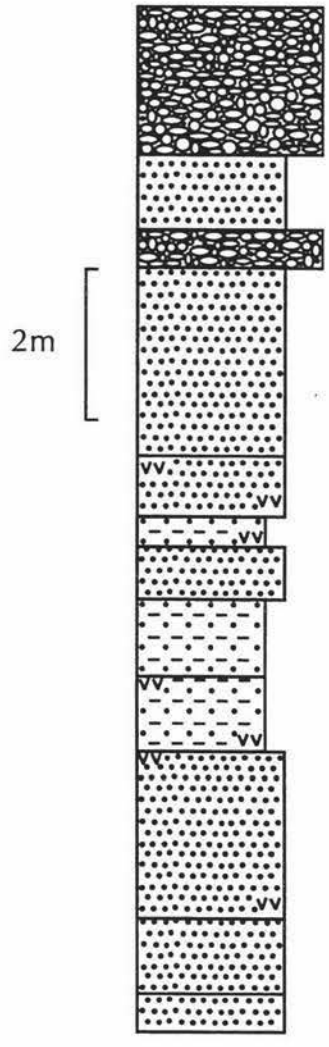

Legend

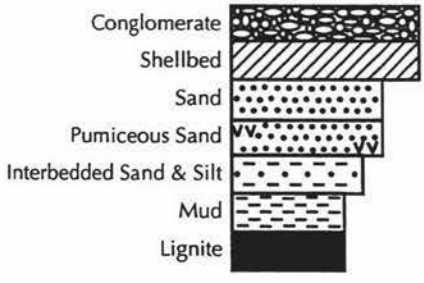

Stewart's Gully Section C

Grid Reference: T23/451145

Altitude at base of section: 207m

(i) 0.81m. Fine to medium parallel bedded sand, with some pumiceous layers. Some iron staining.

(ii) 0.67m. Medium grey sand with coarser pumice pebbles, up to 5mm in size. Pumice in layers parallel to bedding.

(iii) 0.89m. Medium sand with layers of mud (up to 30mm thick), some layers discontinuous. Some small mud rip-up clasts and some iron staining.

(iv) 1.47m. Fine to medium pumiceous sand with some mud layers up to 5mm thick.

(v) 0.92m. Interbedded fine to medium sand layers (up to 0.2m thick) and mud layers (up to 20mm thick). Distinct boundaries. Some iron staining.

Stewart's Gully Section C

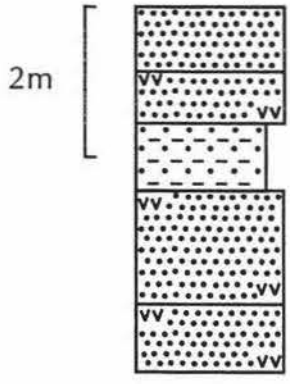

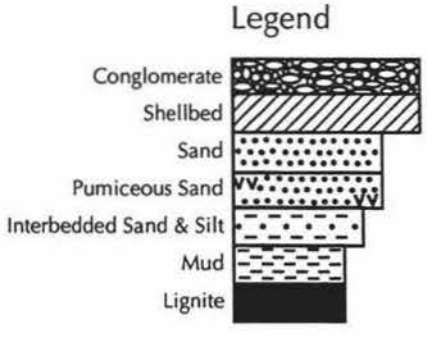

Stewart's Gully Section D

Grid Reference: T23/454144

Altitude at base of section: 213.5m

(i) 0.87m. Grey silty mud. No apparent bedding. Some iron staining. Some root channels and bioturbation.

(ii) 1.15m. Fine to medium laminated sand with some pumiceous layers. Few mud layers and some iron staining.

(iii) 1.05m. Interbedded grey/brown fine sand and fine pumice layers. Horizontal laminations. Some cross bedded pumice in lower 100mm. A few pumice filled channels, 20mm deep and 50mm wide.

(iv) 1.34m. Fine-medium sand with horizontal laminations and some pumiceous layers. Few wavy mud layers up to 20mm thick. Some iron staining.

(v) 2.33m. Silty mud with faint horizontal laminations. Layers of fine cream/orange pumice about 5mm thick. Pumice-filled channel (0.5m wide) with horizontal bedding. Channel of fine grey pumiceous sand 1.5m wide and 0.5m deep, with flattened mud rip-up clasts in lower 0.2m. Top 30mm of unit consists of a cross bedded pumice layer with isolated pumice pebbles up to 15mm in size. Cross bedding direction: 5°@038 (opposite to dominant trend).

(vi) 1.79m. Medium pumiceous sand with distinct horizontal laminations. Several mud layers, up to 10mm thick, some discontinuous.

(vii) 1.31m. Fine to medium pumiceous sand with horizontal laminations. Distinct boundaries, some iron staining.

Stewart's Gully Section D

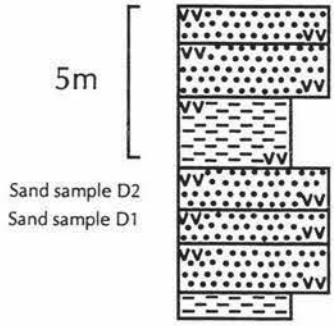

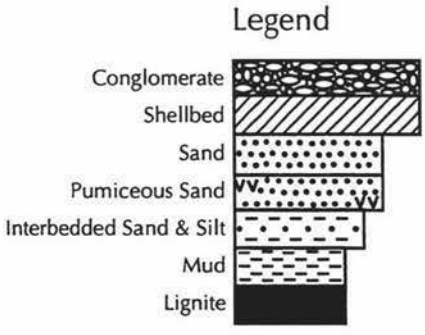

Beehive Creek

Grid Reference at base: T23/504157

Grid Reference at top: T23/501124

(i) 0.7m. Parallel bedded mud and fine sand, mm-cm bedding.

(ii) 2m. Cross bedded coarse pumiceous sand with some iron sand. Shell fragments and mud clasts. Discontinuous mud layers. Paleocurrent directions from the cross beds: 23°@220/6°@120, 20°@235/21°@143, 26°@220/24°@268, 25°@220/14°@278, 17°@230/14°@154, 24°@113/19°@075

(iii) 0.5m. Mud layer. Fairly massive, burrowed on top. Possibly a wave cut surface on top.

(iv) 1m. Shellbed - coarse sandy matrix with many shell fragments and whole shells. Pebbles up to 50mm. Mud rip up clasts.

(v) 15m. Finer parallel bedded sand. Some pumice lenses.

(vi) 5m. Tephric Sand 2. Trough cross bedded pumiceous sand, with beds oversteepened and deformed. Contains Rewa Pumice. Apparent dip of beds: 12°@095.

(vii) 35m Mud-sand unit. Interbedded mud and fine sand, mm-cm bedding. Some mud quite rich in organic matter. Contains a 0.5m massive white mud layer. Near top is parallel bedded sand with fine pumiceous layers, with slightly wavy bedding. Also two 50mm lignite layers enclose a white tuff layer, about 7m from base of unit.

(viii) 6m. Tephric Sand 1. (Potaka) Finely laminated pumiceous sands. Some pumice layers up to 8cm thick. Some mud lenses also.

(ix) 78m. Sands D. Parallel bedded sands and silts, with mm-dm bedding. Occasional silt units up to 150mm thick. Some mud layers. At least 5m of intensely burrowed muddy sand and sandy mud - appears massive, but actually mm-cm bedded. Near the top there are occasional layers of mud, up to 150mm thick. Sandier beds contain pumice and show ripple cross bedding, muddier beds appear to have root channels. Apparent dip: 58°@098

➢ Sediment sample BC8 - silty bioturbated mud, taken from about 3m from top of unit.

(x) 3m. Gravel unit 5. Erosional contact between gravels and Mud/sand unit C, with rip up clasts at the base of the gravel unit.

(xi) 34m. Mud/sand unit C. 0.3m layer of strongly burrowed pale grey airfall pumice near the base. Parallel bedded sands, mm-cm scale. Sand unit contains at least 7m of occasionally pebbly sand, weakly bedded with small reverse faults of 50-100mm throw, perpendicular to dip. Also 2m of finely bedded lignitic bioturbated but interbedded sandy mud and muddy sand. Occasional flasers filled with silt, common thin lenses of pumice. Numerous lignite bands interbedded with mud layers. Thick massive to weakly bedded muds, often bioturbated. Sharp, erosional contact with Gravel unit 4.
➢ Sediment samples BC2-BC7 taken from this unit

(xii) 29m. Gravel unit 4. Gravel sitting on a sharp undulating contact. Contains angular mud rip up clasts within a sandy matrix. Logs also present with the rip up clasts. Some gravels up to 10cm, average of 10-20mm. Clast supported, sieved in some places

(xiii) 30m. Mud/sand unit B. Lignite layers up to 0.5m thick, separated by mud. Mud has many vertical root channels. Occasional sandy mud, dominantly massive and hardened. Layers of sand up to 0.5m thick, containing interbedded sand and silty muddy sand and silt. Some heavy bioturbation. Muddier units have very good burrows (0.1m deep, 20mm wide) with internal herringbone structure. Apparent dips: 50°@100 and 48°@105, 60°@104
➢ Sediment sample BC1 taken from sandy part of unit.

(xiv) 10m. Gravel unit 3. Gravel unit steeply dipping toward the south east. 0.3m thick mud layer about 3m from base of unit.

(xv) 12m. Mud + Lignites A. Mud containing some logs. Sandier section contains less organic matter. Blue-grey sandy mud at base. Lignitic in the middle of the unit, and at the top, where some stumps are found.

(xvi) 28m. Gravel unit 2. Fairly massive gravel unit, most pebbles 10-20mm. No apparent dip.

(xvii) 8m. Graded mud unit. Fine muddy sediments, possibly oxbow lake type.

(xviii) 12m. Gravel unit 1. Flat lying massive gravel unit, with some channel bedding. Channel several metres wide, with axis @145. Gravels up to 100mm in size, but mostly 10-20mm.

Beehive Creek

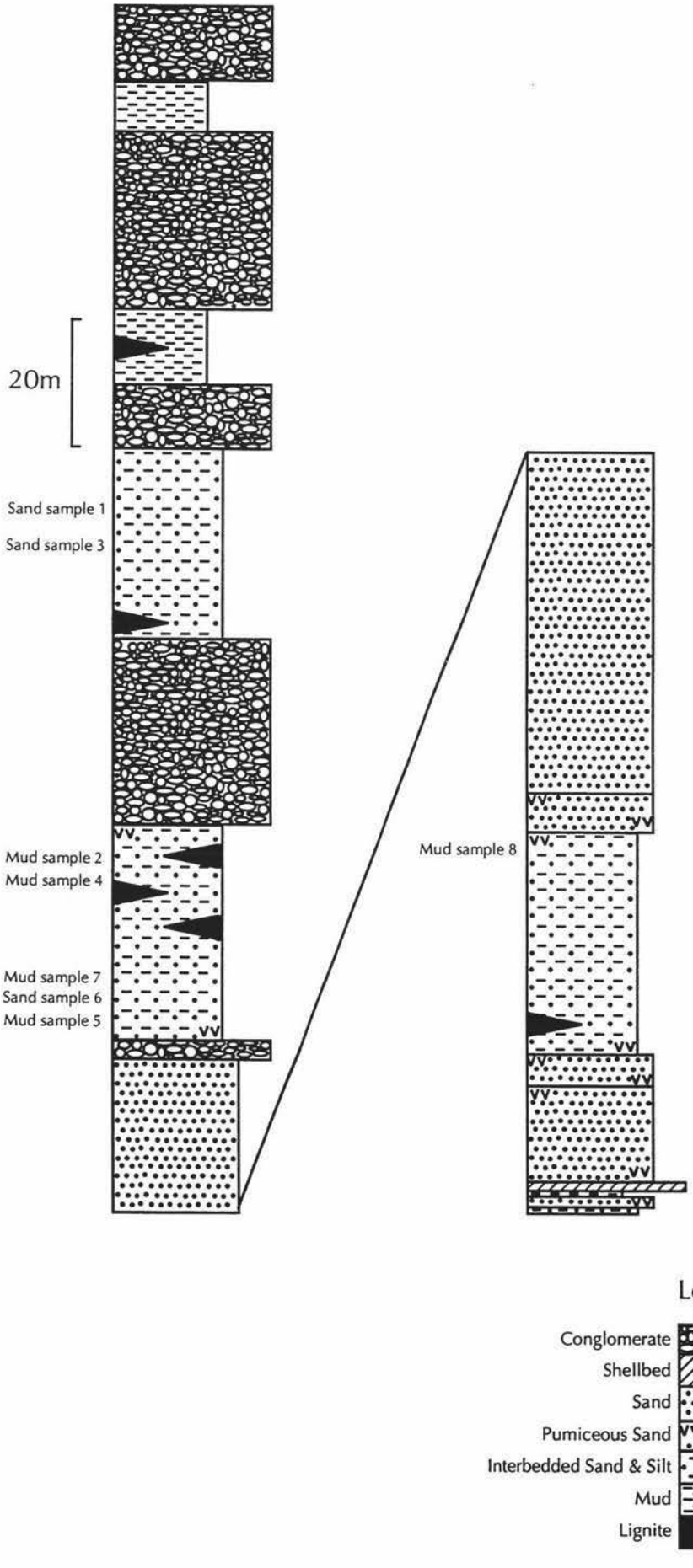

Finnis Road

Grid Reference at Top: T23/465120

Grid Reference at Base: T23/475115

(i) 8m. Fine - medium pumiceous sand with horizontal laminations, some cross bedding, silt clasts, mud lenses and discontinuous mud layers. One layer of convolute bedding at 1.4m. Some ripples. Several pebble layers about 50mm thick, with pebbles up to 20mm in diameter. One coarse pumice-filled channel, 150mm deep, >1m wide.

(ii) 16.5m. Interbedded fine - medium pumiceous sand with some discontinuous mud layers. Two layers of convoluted bedding, up to 1.2m thick. Some scattered greywacke pebbles near top of unit.

(iii) 10m. Alternating sand and silt with occasional mud layers. No pumice present. One silt rip up clast, 200x25mm. Some flaser bedding. Layer of pebbles at 26m - pebbles up to 10mm in diameter.

(iv) 7m. Bottom of unit is 0.5m layer of brecciated silt rip up clasts, overlain by 3m of parallel laminated fine sand and thick lenticular beds. Im of convolute bedding and 0.5m of flaser bedding. 2m of alternating sand, silt and mud at top of the unit.

(v) 4.5m. Dominantly orange coloured sand. 2m of parallel laminated sand and indurated silt at base of the unit, overlain by 2m of the same sediment with ripples, small channels, small convolutions, nodules and lenticular bedding. One 5mm thick pebble layer at 45.5m.

(vi) 8m. Flaser sands. Parallel bedded sands, beds 10-50cm thick. 20cm convoluted and truncated bed in middle of unit. Flaser bedding increases up the unit. Coarse sands contain shell fragments, very small pebbles, mud rip up clasts and pumice (all 1-6mm size).

(vii) 8.5m. Organic muddy sands. Convoluted sands at base, followed by bed of tightly packed mud clasts. Rippled and flaser bedded muds and sands above. At top are thinly bedded rippled and burrowed silts, muds and sands containing organic matter. Iron staining around burrows, filled with coarse sand and organic matter. Small convoluted beds.

(viii) 4.5m. Fe/Mn Nodule sand. Orange-yellow parallel bedded sands, beds about 10mm

thick. Mud lenses and a small fraction of pumice. Lack of grading in sands, small truncated convolutions about 40mm high. Lineations of Fe-Mn nodules in massive sands, infrequent pebbles.

(ix) 6m. Obscured sands. Beds of truncated rippled iron-rich sands, about 20mm thick. Some fine pebbles in lenses. Outcrop becomes obscured.

(x) 4m. Tuff (Potaka). Pumice rich cross bedded sands, with 50-100mm mud rip up clasts. Channel trough cross bedding, flasers, pumice-filled channels.

NB Approximately 42m of stratigraphy is obscured between units (ix) and (x).

Top of Finnis Road

Grid reference: T23/449121

Altitude at base of section: 303m.

(i) 0.4m. Grey medium sand, fairly massive.

(ii) 2.8m. Iron stained gravel. Pebbles up to 40mm. Infrequent mud clasts 100mm. Coarse sand matrix, sand lense.

(iii) 2.7m. Medium brown sand with several mud lenses.

(iv) 1.75m. Grey pumice - coarse sand/grit size. Some bedding. Channel 280mm wide, filled with coarser pumice.

➢ Tuff sample 9735.

Finnis Road

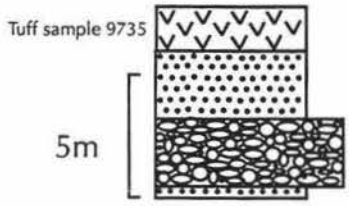
Tuff sample 9735
5m

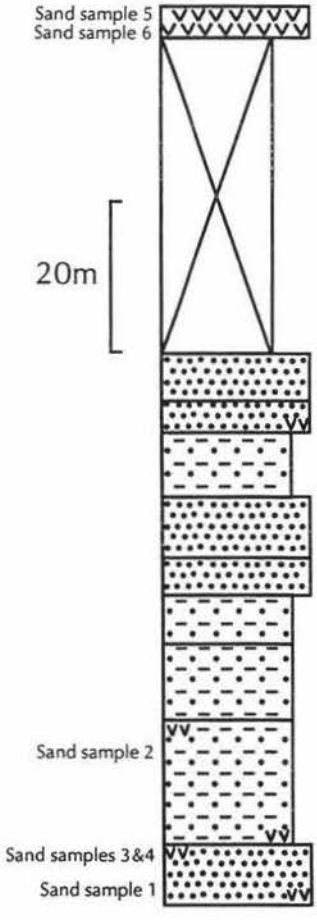
Sand sample 5
Sand sample 6
20m
Sand sample 2
Sand samples 3&4
Sand sample 1

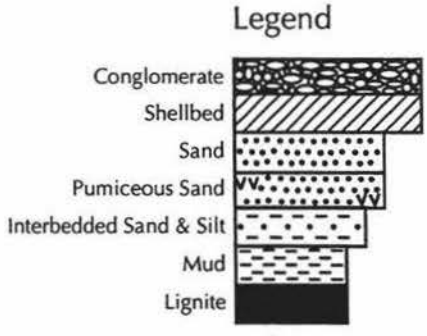
Legend
Conglomerate
Shellbed
Sand
Pumiceous Sand
Interbedded Sand & Silt
Mud
Lignite

Culling's Gullies

• Fossil Gully (from Maning (1988))

Grid reference: T23/477127

(i) 1.1m. Sand with a layer of silt clasts near the base of the unit and some convolute bedding.

(ii) 1.1m. Very pumiceous sand. Some convolute bedding and cross bedding.

➢ Tuff sample 97121 taken from this unit.

(iii) 1.1m. Interbedded sand and silt with horizontal bedding.

(iv) 11.9m. Parallel bedded fine grey sands with occasional pumice layers and some silt layers. Some symmetrical ripples near the base of the unit.

(v) 11.6m. Pumiceous sand with some silt. Pumice content increases up the unit. Some cross bedding. Line of peat clasts over iron stained pebbles, near middle of unit. Discontinuous lense of coarse sand and pebbles with silt clasts and fossil shells.

➢ Tuff sample 97123 taken from this unit.

(vi) 4.1m. Pumiceous sand with horizontal cm-bedding. Line of silt clasts and some convolute bedding. Some peat clasts.

(vii) 4.1m. Horizontally bedded sand and silt.

(viii) 1.1m. Pumiceous sand with several silt layers. Some convolute bedding.

(ix) 14.5m. Horizontally bedded pumiceous sand with some silt layers.

(x) 2.6m. Interbedded sand and silt with a layer of silt clasts and a layer of small pebbles.

(xi) 7m. Sand with layers of silt clasts and small pebble layers. Shellbed near top of unit - abundant angular broken shells and many silt clasts. Discontinuous shellbed, about 1.5m thick.

(xii) 7.3m. Horizontally bedded fine sand.

(xiii) 1.1m. Interbedded coarse grey silt and fine grey sand.

• Erosion Scarp (from Maning (1988))

Grid reference: T23/473131

(i) 3.7m. Pumiceous sand with cross bedding.

(ii) 5.2m. Pumiceous fine grey sand with horizontal bedding.

(iii) 9.2m. Channel at base of unit, containing iron stained pebbles and lignite clasts. Cross bedded fine to coarse pumice lapilli interbedded with cross bedded fine sand and pumiceous fine sand. Occasional lines of silt clasts. Large water escape structures near top of unit (about 0.75m high).

(iv) 11.5m. Horizontally bedded light brown pumiceous fine sand with mm bedding. Contains layer of silt clasts and occasional thin silt layers and lenses. Thin pebble layer near top of unit.

(v) 4.6m. Horizontally bedded light brown fine sand with occasional thin layers of light brown silt. Symmetrical ripples within a thin silt layer.

(vi) 1.5m. Interbedded (cm bedded) layers of fine sand and coarse silt. Silt is harder than sand.

(vii) 3.5m. Fine sand and silt layers (mm bedded). Layer of silt clasts near top of unit with some ripples too.

(viii) 2.9m. Coarse silt, laterally discontinuous with fine sand interbedded with coarse silt. No obvious bedding.

(ix) 23.7m. Massive fine sand. Some faint parallel bedding nearer top of unit. Some iron concretions. Some thin silt layers near top of unit.

(x) 2.3m. Horizontally bedded (mm bedding) fine sand. Several layers of rounded silt clasts, some ripples and cross bedding.

(xi) 3m. Massive grey silt, irregular thickness.

Culling's Gullies

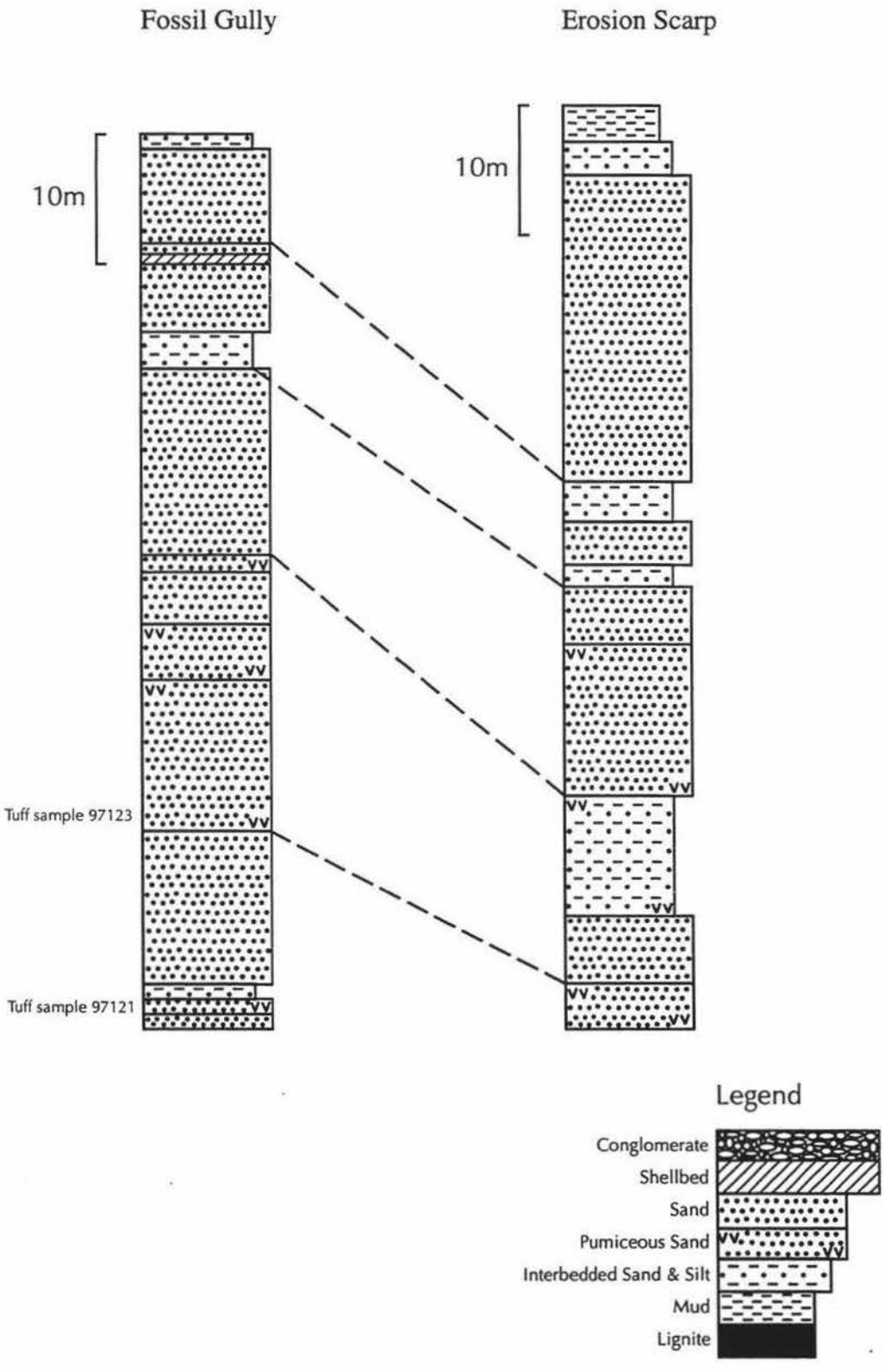

Composite Stratigraphic Column

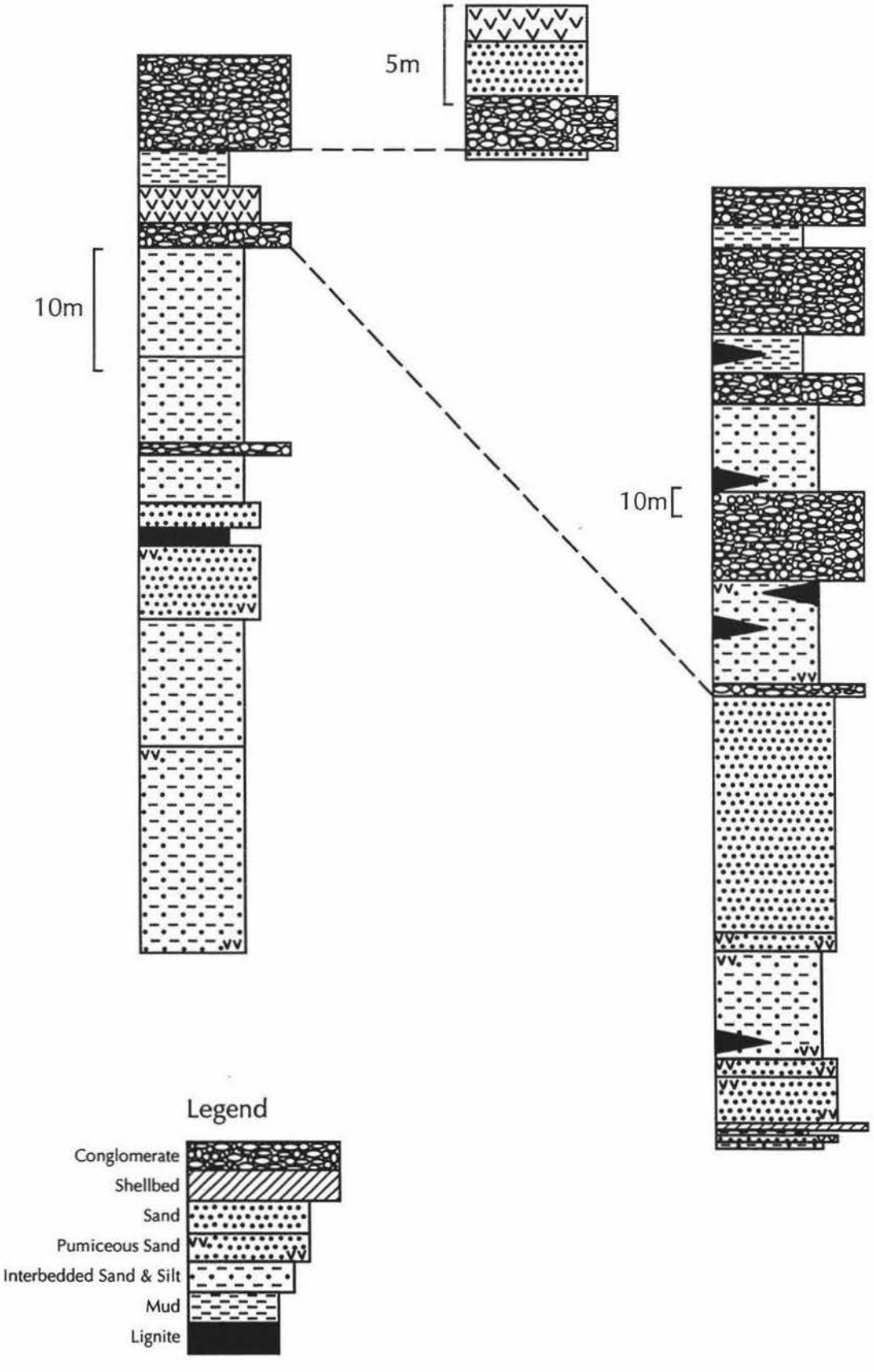

APPENDIX B

- Electron Microprobe Data for the eleven Tuff Samples

Sample 9851	I	II	III	IV	V	VI	VII	VIII	IX	X	XI	XII	XIII	Averages
Raw Data														
SiO_2	75.572	74.003	75.287	75.202	76.144	73.196	73.253	74.421	74.674	73.448	73.672	72.087	72.981	74.15
Al_2O_3	12.233	12.263	12.571	12.133	12.274	12.096	12.252	12.608	12.480	12.334	12.654	12.334	12.516	12.37
TiO_2	0.155	0.172	0.230	0.180	0.420	0.945	2.164	0.277	0.276	0.317	0.217	0.437	0.229	0.46
FeO	0.974	1.254	0.985	0.721	1.057	0.849	0.809	1.187	1.537	1.143	1.190	1.276	1.311	1.10
MnO	0.108	0.033	0.053	0.146	0.109	0.138	0.000	0.202	0.141	0.067	0.086	0.083	0.000	0.09
MgO	0.170	0.209	0.173	0.080	0.118	0.116	0.135	0.146	0.112	0.107	0.101	0.190	0.150	0.14
CaO	1.033	0.720	1.227	0.781	0.784	0.895	1.015	1.151	1.231	0.992	1.007	1.140	1.131	1.01
Na_2O	2.829	3.302	3.191	3.331	3.290	3.198	3.077	3.233	3.135	3.152	2.767	3.464	2.970	3.15
K_2O	3.911	4.074	3.662	4.038	3.795	5.923	5.634	3.405	3.530	3.778	3.649	3.480	3.561	4.03
Cl	0.489	1.150	0.251	0.432	1.322	1.890	1.134	0.298	0.303	0.333	0.382	0.327	0.239	0.66
Total	97.475	97.181	97.63	97.043	99.314	99.245	99.473	96.929	97.420	95.670	95.725	94.817	95.087	
Normalised Data														
SiO_2	77.53	76.15	77.11	77.49	76.67	73.75	73.64	76.78	76.65	76.77	76.96	76.03	76.75	76.33
Al_2O_3	12.55	12.62	12.88	12.50	12.36	12.19	12.32	13.01	12.81	12.89	13.22	13.01	13.16	12.73
TiO_2	0.16	0.18	0.24	0.19	0.42	0.95	2.18	0.29	0.28	0.33	0.23	0.46	0.24	0.47
FeO	1.00	1.29	1.01	0.74	1.06	0.86	0.81	1.22	1.58	1.19	1.24	1.35	1.38	1.13
MnO	0.11	0.03	0.05	0.15	0.11	0.14	0.00	0.21	0.14	0.07	0.09	0.09	0.00	0.09
MgO	0.17	0.21	0.18	0.08	0.12	0.12	0.14	0.15	0.11	0.11	0.11	0.20	0.16	0.14
CaO	1.06	0.74	1.26	0.80	0.79	0.90	1.02	1.19	1.26	1.04	1.05	1.20	1.19	1.04
Na_2O	2.90	3.40	3.27	3.43	3.31	3.22	3.09	3.34	3.22	3.29	2.89	3.65	3.12	3.24
K_2O	4.01	4.19	3.75	4.16	3.82	5.97	5.66	3.51	3.62	3.95	3.81	3.67	3.74	4.14
Cl	0.50	1.18	0.26	0.45	1.33	1.90	1.14	0.31	0.31	0.35	0.40	0.34	0.25	0.67
Total	99.99	99.99	100.01	99.99	99.99	100.00	100.00	100.01	99.98	99.99	100.00	100.00	99.99	
% FeO	29.4	37.6	28.7	25.2	33.7	22.9	21.7	33.8	39.1	33.7	34.5	36.0	36.1	31.7
% CaO	31.2	21.6	35.8	27.2	25.1	23.9	27.3	33.0	31.2	29.5	29.3	32.0	31.2	29.1
% $^1/_3K_2O$	39.4	40.8	35.5	47.6	41.3	53.2	50.9	33.2	29.7	36.8	36.2	32.0	32.7	39.2

Sample 9855	I	II	III	IV	V	VI	VII	VIII	IX	X	XI	XII	Averages
Raw Data													
SiO_2	70.004	72.903	74.202	74.562	74.566	74.577	74.816	74.818	73.412	74.485	73.747	74.512	73.88
Al_2O_3	12.069	12.134	12.061	12.092	12.368	12.348	12.439	12.203	12.303	12.371	12.147	12.11	12.22
TiO_2	0.111	0.177	0.203	0.239	0.230	0.171	0.288	0.380	0.164	0.194	0.296	0.271	0.23
FeO	1.128	1.135	1.248	0.912	1.103	1.137	1.110	0.931	1.155	1.225	1.162	1.176	1.12
MnO	0.019	0.107	0.041	0.224	0.000	0.287	0.135	0.024	0.028	0.140	0.132	0.000	0.09
MgO	0.027	0.174	0.087	0.107	0.148	0.092	0.088	0.038	0.139	0.128	0.168	0.088	0.11
CaO	1.106	0.815	1.228	0.863	1.040	0.812	0.929	0.806	0.917	0.898	0.882	0.955	0.94
Na_2O	3.633	3.289	3.219	3.371	3.252	3.280	3.347	3.358	3.310	2.850	3.275	3.133	3.28
K_2O	3.623	4.016	3.621	3.827	3.825	3.976	4.247	4.280	3.707	3.806	3.434	3.884	3.85
Cl	0.362	0.331	0.390	1.498	0.325	0.489	0.349	0.233	0.336	0.323	0.245	0.000	0.41
Total	92.082	95.079	96.302	97.695	96.857	97.169	97.747	97.071	95.471	96.420	95.489	96.129	
Normalised Data													
SiO_2	76.02	76.68	77.05	76.32	76.99	76.75	76.54	77.08	76.89	77.25	77.23	77.51	76.86
Al_2O_3	13.11	12.76	12.52	12.38	12.77	12.71	12.73	12.57	12.89	12.83	12.72	12.6	12.72
TiO_2	0.12	0.19	0.21	0.24	0.24	0.18	0.29	0.39	0.17	0.20	0.31	0.28	0.240
FeO	1.22	1.19	1.30	0.93	1.14	1.17	1.14	0.96	1.21	1.27	1.22	1.22	1.16
MnO	0.02	0.11	0.04	0.23	0.00	0.30	0.14	0.02	0.03	0.15	0.14	0.00	0.10
MgO	0.03	0.18	0.09	0.11	0.15	0.09	0.09	0.04	0.15	0.13	0.18	0.09	0.11
CaO	1.20	0.86	1.28	0.88	1.07	0.84	0.95	0.83	0.96	0.93	0.92	0.99	0.98
Na_2O	3.95	3.46	3.34	3.45	3.36	3.38	3.42	3.46	3.47	2.96	3.43	3.26	3.41
K_2O	3.93	4.22	3.76	3.92	3.95	4.09	4.34	4.41	3.88	3.95	3.60	4.04	4.01
Cl	0.39	0.35	0.40	1.53	0.34	0.50	0.36	0.24	0.35	0.33	0.26	0.00	0.42
Total	99.99	100.00	99.99	99.99	100.01	100.01	100.00	100.00	100.00	100.00	100.01	99.99	
% FeO	32.7	34.4	33.9	29.8	32.3	34.7	32.2	29.5	35.0	36.1	36.5	34.3	33.5
% CaO	32.2	24.9	33.4	28.2	30.3	24.9	26.8	25.5	27.7	26.4	27.5	27.8	28.0
% $^1/_3K_2O$	35.1	40.7	32.7	42.0	37.4	40.4	41.0	45.0	37.3	37.5	36.0	37.9	38.5

Sample 9856	I	II	III	IV	V	VI	VII	VIII	IX	X	XI	XII
Raw Data												
SiO2	73.687	69.572	69.040	70.491	70.043	70.689	71.08	69.821	70.539	70.725	69.466	72.118
Al2O3	12.566	12.083	12.318	12.52	12.499	12.505	12.498	12.52	12.321	12.263	12.273	12.444
TiO2	0.456	0.309	0.497	0.339	0.357	0.485	0.348	0.191	0.281	0.238	0.441	0.434
FeO	1.562	1.558	1.438	1.456	1.822	1.514	1.494	1.760	1.484	1.540	1.465	1.523
MnO	0.253	0.254	0.103	0.209	0.112	0.153	0.214	0.093	0.079	0.130	0.213	0.149
MgO	0.158	0.114	0.201	0.12	0.209	0.163	0.212	0.182	0.213	0.142	0.127	0.195
CaO	1.105	0.992	0.927	1.258	1.127	0.992	1.090	1.095	1.048	1.189	1.147	1.075
Na2O	2.986	2.433	2.545	2.935	2.646	2.881	2.962	3.077	2.822	2.861	2.478	3.084
K2O	3.072	2.809	3.163	2.896	2.682	2.705	2.949	3.233	3.110	2.793	2.713	2.908
Cl	0.210	0.236	0.268	0.194	0.326	0.370	0.262	0.282	0.393	0.267	0.295	0.300
Total	96.056	90.361	90.501	92.418	91.823	92.457	93.110	92.254	92.288	92.147	90.620	94.231
Normalised Data												
SiO2	76.71	76.99	76.29	76.27	76.28	76.45	76.34	75.68	76.43	76.75	76.66	76.53
Al2O3	13.08	13.37	13.61	13.55	13.61	13.53	13.42	13.57	13.35	13.31	13.54	13.21
TiO2	0.47	0.34	0.55	0.37	0.39	0.52	0.37	0.21	0.30	0.26	0.49	0.46
FeO	1.63	1.72	1.59	1.58	1.98	1.64	1.60	1.91	1.61	1.67	1.62	1.62
MnO	0.26	0.28	0.11	0.23	0.12	0.17	0.23	0.10	0.09	0.14	0.24	0.16
MgO	0.16	0.13	0.22	0.13	0.23	0.18	0.23	0.20	0.23	0.15	0.14	0.21
CaO	1.15	1.10	1.02	1.36	1.23	1.07	1.17	1.19	1.14	1.29	1.27	1.14
Na2O	3.11	2.69	2.81	3.18	2.88	3.12	3.18	3.34	3.06	3.10	2.73	3.27
K2O	3.20	3.11	3.49	3.13	2.92	2.93	3.17	3.50	3.37	3.03	2.99	3.09
Cl	0.22	0.26	0.30	0.21	0.36	0.40	0.28	0.31	0.43	0.29	0.33	0.32
Total	99.99	99.99	99.99	100.01	100.00	100.01	99.99	100.01	100.01	99.99	100.01	100.01
% FeO	42.3	44.6	42.2	39.7	47.4	44.4	41.8	44.7	41.6	42.1	41.7	42.7
% CaO	29.9	28.5	27.1	34.2	29.4	29.0	30.5	27.9	29.5	32.5	32.6	30.1
% 1/3K2O	27.8	26.9	30.7	26.1	23.2	26.6	27.7	27.4	28.9	25.4	25.7	27.2

Sample 9856 Cont'	XIII	XIV	XV	Averages
Raw Data				
SiO_2	71.623	71.069	70.60	70.70
Al_2O_3	12.716	12.768	12.469	12.45
TiO_2	0.100	0.412	0.472	0.36
FeO	1.711	1.726	1.862	1.59
MnO	0.927	0.139	0.112	0.21
MgO	0.119	0.186	0.178	0.17
CaO	0.829	0.960	1.082	1.06
Na_2O	3.030	2.838	2.526	2.81
K_2O	3.023	2.845	3.395	2.95
Cl	0.161	0.283	0.521	0.29
Total	94.238	93.226	93.217	
Normalised Data				
SiO_2	76.00	76.23	75.74	76.36
Al_2O_3	13.49	13.7	13.38	13.45
TiO_2	0.10	0.44	0.51	0.39
FeO	1.82	1.85	2.00	1.72
MnO	0.98	0.15	0.12	0.23
MgO	0.13	0.20	0.19	0.18
CaO	0.88	1.03	1.16	1.15
Na_2O	3.22	3.04	2.71	3.03
K_2O	3.21	3.05	3.64	3.19
Cl	0.17	0.30	0.56	0.32
Total	100.01	99.99	100.01	
%FeO	48.3	47.4	45.8	43.8
%CaO	23.3	26.4	26.5	29.2
$\%^1/_3K_2O$	28.4	26.2	27.7	27.0

Sample 9858(1)	I	II	III	IV	V	VI	VII	Averages
Raw Data								
SiO_2	73.609	74.276	75.312	73.886	73.369	74.06	73.748	74.04
Al_2O_3	11.481	11.834	12.123	12.083	11.941	11.954	12.136	11.94
TiO_2	0.103	0.167	0.114	0.212	0.117	0.100	0.131	0.13
FeO	0.629	0.672	0.723	0.462	0.632	0.751	0.541	0.63
MnO	0.062	0.026	0.135	0.062	0.049	0.087	0.017	0.06
MgO	0.075	0.099	0.072	0.076	0.111	0.096	0.121	0.09
CaO	1.055	1.032	0.982	1.029	1.004	1.101	1.127	1.05
Na_2O	2.913	3.210	3.194	3.101	3.046	3.056	3.142	3.09
K_2O	3.894	3.701	4.054	3.710	3.578	3.726	4.078	3.82
Cl	0.162	0.206	0.162	0.175	0.199	0.185	0.208	0.19
Total	94.484	95.224	96.872	94.796	94.045	95.116	95.249	
Normalised Data								
SiO_2	77.91	78.00	77.74	77.94	78.01	77.86	77.43	77.84
Al_2O_3	12.68	12.43	12.51	12.75	12.70	12.57	12.74	12.63
TiO_2	0.11	0.18	0.12	0.22	0.12	0.11	0.14	0.14
FeO	0.67	0.71	0.75	0.49	0.67	0.79	0.57	0.66
MnO	0.07	0.03	0.14	0.07	0.05	0.09	0.02	0.07
MgO	0.08	0.10	0.07	0.08	0.12	0.10	0.13	0.1
CaO	1.12	1.08	1.01	1.09	1.07	1.16	1.18	1.1
Na_2O	3.08	3.37	3.30	3.27	3.24	3.21	3.30	3.25
K_2O	4.12	3.89	4.18	3.91	3.80	3.92	4.28	4.01
Cl	0.17	0.22	0.17	0.18	0.21	0.19	0.22	0.19
Total	100.01	100.01	99.99	100.00	99.99	100.00	100.01	
% FeO	21.2	23.0	23.8	17.1	22.3	24.2	17.9	21.4
% CaO	35.4	35.0	32.1	37.8	35.5	35.6	37.1	35.5
% $^1/_3K_2O$	43.4	42.0	44.1	45.1	42.2	40.2	45.0	43.1

Sample 9858(2)	I	II	III	IV	V	VI	VII	VIII	Averages
Raw Data									
SiO_2	72.285	72.739	75.186	74.186	74.75	73.327	74.995	74.42	73.99
$Al2O_3$	11.868	12.123	12.093	12.018	11.97	11.931	12.411	12.217	12.08
TiO_2	0.114	0.159	0.115	0.143	0.157	0.132	0.099	0.128	0.13
FeO	0.839	1.039	1.112	1.262	1.008	1.078	0.925	0.888	1.02
MnO	0.083	0.025	0.151	0.055	0.080	0.000	0.211	0.008	0.08
MgO	0.093	0.107	0.095	0.100	0.121	0.127	0.003	0.136	0.10
CaO	0.952	0.819	1.028	0.860	0.975	1.092	0.741	1.035	0.94
Na_2O	3.322	3.207	3.145	2.949	3.184	3.094	3.275	3.115	3.16
K_2O	3.930	3.775	3.341	3.789	3.626	3.719	3.924	3.634	3.72
Cl	0.232	0.166	0.272	0.214	0.252	0.245	0.175	0.199	0.22
Total	93.717	94.161	96.537	95.576	96.125	94.745	96.759	95.78	
Normalised Data									
SiO_2	77.13	77.25	77.88	77.62	77.76	77.39	77.51	77.7	77.53
Al_2O_3	12.66	12.87	12.53	12.57	12.46	12.59	12.83	12.76	12.66
TiO_2	0.12	0.17	0.12	0.15	0.16	0.14	0.10	0.13	0.14
FeO	0.90	1.10	1.15	1.32	1.05	1.14	0.96	0.93	1.07
MnO	0.09	0.03	0.16	0.06	0.08	0.00	0.22	0.01	0.08
MgO	0.10	0.11	0.10	0.10	0.13	0.13	0.00	0.14	0.10
CaO	1.02	0.87	1.06	0.90	1.01	1.15	0.77	1.08	0.98
Na_2O	3.54	3.41	3.26	3.09	3.31	3.27	3.38	3.25	3.31
K_2O	4.19	4.01	3.46	3.96	3.77	3.93	4.06	3.79	3.90
Cl	0.25	0.18	0.28	0.22	0.26	0.26	0.18	0.21	0.23
Total	100.00	100.00	100.00	99.99	99.99	100.00	100.01	100.00	
% FeO	27.1	33.2	34.2	37.3	31.6	31.7	31.2	28.4	31.8
% CaO	30.7	26.3	31.5	25.4	30.4	31.9	25.0	33.1	29.3
% $^1/_3K_2O$	42.2	40.5	34.3	37.3	38.0	36.4	43.8	38.5	38.9

Sample 9859	I	II	III	IV	V	VI	VII	VIII	IX	X	XI	XII	XIII	Averages
Raw Data														
SiO_2	73.286	73.870	74.707	73.573	73.145	75.173	73.907	73.849	73.277	74.479	73.913	71.963	72.451	73.66
Al_2O_3	12.008	11.950	12.287	12.044	11.961	12.113	12.079	12.182	12.184	11.950	12.069	11.879	11.889	12.05
TiO_2	0.130	0.058	0.165	0.052	0.194	0.136	0.063	0.128	0.206	0.077	0.219	0.046	0.219	0.13
FeO	1.074	1.137	1.067	0.959	1.137	0.760	1.163	1.116	0.827	1.250	1.212	0.761	1.137	1.05
MnO	0.044	0.000	0.211	0.049	0.059	0.037	0.046	0.106	0.035	0.053	0.095	0.115	0.191	0.08
MgO	0.154	0.093	0.129	0.052	0.112	0.174	0.165	0.161	0.114	0.199	0.067	0.210	0.173	0.14
CaO	0.961	0.932	0.989	0.707	0.940	0.853	0.958	0.759	0.625	0.701	0.858	0.760	1.013	0.85
Na_2O	2.998	3.230	3.047	3.066	2.759	3.111	3.145	3.259	3.008	3.341	3.549	2.521	2.596	3.05
K_2O	3.703	3.625	3.343	4.017	3.377	4.089	3.715	4.137	3.973	3.650	3.702	3.543	3.200	3.70
Cl	0.212	0.254	0.226	0.199	0.216	0.243	0.150	0.228	0.167	0.196	0.209	0.215	0.203	0.21
Total	94.57	95.148	96.172	94.717	93.901	96.589	95.392	95.925	94.415	95.896	95.893	92.013	93.073	
Normalised Data														
SiO_2	77.49	77.64	77.68	77.68	77.9	77.83	77.48	76.99	77.61	77.67	77.08	78.21	77.84	77.67
Al_2O_3	12.70	12.56	12.78	12.72	12.74	12.50	12.66	12.70	12.90	12.46	12.59	12.91	12.77	12.69
TiO_2	0.14	0.06	0.17	0.05	0.21	0.14	0.07	0.13	0.22	0.08	0.23	0.05	0.24	0.14
FeO	1.14	1.19	1.11	1.01	1.21	0.79	1.22	1.16	0.88	1.30	1.26	0.83	1.22	1.10
MnO	0.05	0.00	0.22	0.05	0.06	0.04	0.05	0.11	0.04	0.06	0.10	0.12	0.21	0.09
MgO	0.16	0.10	0.13	0.05	0.12	0.18	0.17	0.17	0.12	0.21	0.07	0.23	0.19	0.15
CaO	1.02	0.98	1.03	0.75	1.00	0.78	1.00	0.79	0.66	0.73	0.89	0.83	1.09	0.89
Na_2O	3.17	3.39	3.17	3.24	2.94	3.22	3.30	3.40	3.19	.48	3.7	2.74	2.79	3.21
K_2O	3.92	3.81	3.48	4.24	3.60	4.23	3.89	4.31	4.21	3.81	3.86	3.85	3.44	3.90
Cl	0.22	0.27	0.23	0.21	0.23	0.25	0.16	0.24	0.18	0.20	0.22	0.23	0.22	0.22
Total	100.01	100.00	100.00	100.00	100.01	100.01	100.00	100.00	100.01	100.00	100.00	100.00	100.01	
% FeO	32.9	34.6	33.6	31.9	35.5	26.5	34.7	34.2	29.9	39.4	36.6	28.3	35.3	33.4
% CaO	29.3	28.5	31.2	23.7	29.3	26.2	28.4	23.3	22.4	22.2	25.9	28.2	31.5	26.9
% $^1/_3K_2O$	37.8	36.9	35.2	44.4	35.2	47.3	36.9	42.5	47.6	38.4	37.5	43.5	33.2	39.7

Sample 98510	I	II	III	IV	V	VI	VII	VIII	IX	X	XI	Averages
Raw Data												
SiO_2	72.841	73.294	75.091	75.416	75.126	73.297	73.636	75.253	75.158	73.745	76.158	74.46
Al_2O_3	11.63	11.502	11.897	12.051	12.368	11.568	11.664	11.346	12.043	11.525	11.708	11.75
TiO_2	0.476	0.128	0.220	0.204	0.132	0.089	0.216	0.180	0.270	0.250	0.160	0.21
FeO	1.221	1.245	1.382	1.509	1.532	1.304	1.510	1.280	1.576	1.354	1.361	1.39
MnO	0.185	0.051	0.047	0.138	0.075	0.056	0.034	0.018	0.061	0.128	0.066	0.08
MgO	0.167	0.101	0.094	0.121	0.138	0.109	0.133	0.083	0.103	0.070	0.112	0.11
CaO	0.784	0.813	0.900	0.922	0.945	0.820	0.813	0.840	0.926	0.860	0.757	0.85
Na2O	1.738	2.399	2.584	2.641	2.349	2.376	2.254	2.380	2.935	2.177	2.698	2.41
K_2O	3.359	3.297	3.132	3.451	3.457	3.237	3.003	3.311	3.215	3.237	3.293	3.27
Cl	0.273	0.367	0.243	0.209	0.287	0.298	0.232	0.260	0.274	0.250	0.203	0.26
Total	92.683	93.197	95.590	96.661	96.426	93.155	93.494	94.951	96.562	93.596	96.577	
Normalised Data												
SiO_2	78.59	78.64	78.55	78.02	77.91	78.68	78.76	79.25	77.83	78.79	78.86	78.53
Al_2O_3	12.56	12.34	12.45	12.47	12.83	12.42	12.48	11.95	12.47	12.31	12.12	12.4
TiO_2	0.51	0.14	0.23	0.21	0.14	0.10	0.23	0.19	0.28	0.27	0.17	0.22
FeO	1.32	1.36	1.45	1.56	1.59	1.40	1.62	1.35	1.63	1.45	1.41	1.47
MnO	0.20	0.05	0.05	0.14	0.08	0.06	0.04	0.02	0.06	0.14	0.07	0.08
MgO	0.18	0.11	0.10	0.13	0.14	0.12	0.14	0.09	0.11	0.07	0.12	0.12
CaO	0.85	0.87	0.94	0.95	0.98	0.88	0.87	0.88	0.96	0.92	0.78	0.90
Na_2O	1.88	2.57	2.70	2.73	2.44	2.55	2.41	2.51	3.04	2.33	2.79	2.54
K_2O	3.62	3.54	3.28	3.57	3.58	3.47	3.21	3.49	3.33	3.46	3.41	3.45
Cl	0.29	0.39	0.25	0.22	0.30	0.32	0.25	0.27	0.28	0.27	0.27	0.28
Total	100.00	100.01	100.00	100.00	99.99	100.00	100.01	100.00	99.99	100.01	100.00	
% FeO	39.1	39.9	41.7	42.2	42.3	40.7	45.5	39.8	44.1	41.2	42.3	41.7
% CaO	25.1	25.5	27.0	25.7	26.1	25.6	24.4	26.0	25.9	26.1	23.5	25.5
% $^1/_3K_2O$	35.8	34.6	31.3	32.1	31.6	33.7	30.1	34.2	30.0	32.7	34.2	32.8

Sample 9861	I	II	III	IV	V	VI	VII	VIII	IX	X	XI	XII	XIII	Averages
Raw Data														
SiO_2	74.643	76.071	77.869	75.406	76.989	74.516	72.675	73.416	76.305	74.656	77.152	77.749	76.703	75.70
Al_2O_3	11.989	11.892	12.110	11.866	12.451	12.15	11.985	12.039	11.585	11.968	12.376	12.067	11.958	12.03
TiO2	0.152	0.098	0.148	0.205	0.232	0.178	0.098	0.233	0.202	0.187	0.201	0.178	0.188	0.18
FeO	1.083	1.109	1.147	1.093	0.940	1.001	1.009	1.217	1.309	1.121	1.027	1.124	1.012	1.09
MnO	0.000	0.133	0.081	0.084	0.159	0.125	0.079	0.063	0.157	0.034	0.072	0.093	0.023	0.08
MgO	0.188	0.073	0.131	0.136	0.079	0.067	0.111	0.091	0.077	0.071	0.136	0.109	0.136	0.11
CaO	1.028	1.002	0.704	0.976	0.821	0.816	0.692	0.758	0.933	1.143	0.706	0.969	0.735	0.87
Na_2O	3.059	3.092	2.951	2.876	2.861	2.95	2.661	2.747	2.785	2.816	2.743	2.898	2.716	2.86
K_2O	3.424	3.561	4.168	3.287	3.926	3.878	4.101	3.961	3.501	3.407	4.002	3.634	3.726	3.74
Cl	0.188	0.230	0.230	0.269	0.290	0.325	0.213	0.371	0.199	0.199	0.229	0.230	0.239	0.25
Total	95.753	97.27	99.539	96.198	98.748	96.005	93.622	94.897	97.054	95.602	98.642	99.053	97.437	
Normalised Data														
SiO_2	77.95	78.21	78.23	78.39	77.97	77.62	77.62	77.36	78.62	78.09	78.21	78.49	78.72	78.11
Al_2O_3	12.52	12.23	12.17	12.33	12.61	12.66	12.8	12.69	11.94	12.52	12.55	12.18	12.27	12.42
TiO_2	0.16	0.10	0.15	0.21	0.23	0.19	0.10	0.25	0.21	0.20	0.20	0.18	0.19	0.18
FeO	1.13	1.14	1.15	1.14	0.95	1.04	1.08	1.28	1.35	1.17	1.04	1.13	1.04	1.13
MnO	0.00	0.14	0.08	0.09	0.16	0.13	0.80	0.07	0.16	0.04	0.07	0.09	0.02	0.14
MgO	0.20	0.08	0.13	0.14	0.08	0.07	0.12	0.10	0.08	0.07	0.14	0.11	0.14	0.13
CaO	1.07	1.03	0.71	1.01	0.83	0.85	0.74	0.80	0.96	1.20	0.72	0.98	0.75	0.90
Na_2O	3.19	3.18	2.96	2.99	2.90	3.07	2.84	2.89	2.87	2.95	2.78	2.93	2.79	2.95
K_2O	3.58	3.67	4.19	3.42	3.98	4.04	4.38	4.17	3.61	3.56	4.06	3.67	3.82	3.86
Cl	0.20	0.24	0.23	0.28	0.29	0.34	0.23	0.39	0.21	0.21	0.23	0.23	0.25	0.24
Total	100.00	100.02	100.00	100.00	100.00	100.01	99.99	100.00	100.01	100.01	100	99.99	99.99	
% FeO	33.3	33.6	35.3	34.7	30.6	32.1	32.9	36.8	38.4	32.9	33.4	33.9	34.0	34.0
% CaO	31.6	30.4	21.8	30.6	26.7	26.2	22.6	23.1	27.4	33.7	23.2	29.4	24.5	27.0
% $^1/_3K_2O$	35.1	35.0	42.9	34.7	42.7	41.7	44.5	40.1	34.2	33.4	43.4	37.0	41.5	39.0

Sample 97121	I	II	III	IV	V	VI	VII	VIII	IX	X	XI	Averages
Raw Data												
SiO_2	75.165	76.224	71.211	73.568	72.041	73.309	72.268	73.732	73.729	72.524	72.777	73.32
Al_2O3	12.801	12.435	12.926	12.885	12.126	12.629	12.525	12.781	12.399	12.670	12.841	12.64
TiO_2	0.465	0.214	0.261	0.296	0.202	0.256	0.252	0.205	0.477	0.207	0.189	0.27
FeO	1.802	1.723	2.000	2.216	1.696	1.810	1.933	1.807	2.017	1.951	1.822	1.89
MnO	0.125	0.186	0.173	0.090	0.252	0.092	0.075	0.123	0.102	0.121	0.194	0.14
MgO	0.071	0.121	0.204	0.158	0.092	0.118	0.115	0.128	0.115	0.109	0.142	0.12
CaO	0.996	1.067	1.262	0.985	1.014	1.040	0.930	1.026	1.043	1.052	1.005	1.04
Na_2O	2.610	3.305	2.631	3.028	2.423	3.104	2.479	3.227	2.960	3.130	3.357	2.93
K2O	3.022	3.503	2.830	3.190	3.299	3.111	2.845	3.740	3.188	3.237	3.123	3.19
Cl	0.160	0.286	0.194	0.114	0.182	0.260	0.212	0.179	0.222	0.197	0.248	0.20
Total	97.216	99.064	93.693	96.540	93.328	95.731	93.633	96.947	96.251	95.198	95.698	
Normalised Data												
SiO_2	77.32	76.94	76.0	76.2	77.19	76.58	77.18	76.05	76.6	76.18	76.05	76.57
Al_2O_3	13.17	12.55	13.8	13.35	12.99	13.19	13.38	13.18	12.88	13.31	13.42	13.20
TiO2	0.48	0.22	0.28	0.31	0.22	0.27	0.27	0.21	0.50	0.22	0.20	0.29
FeO	1.85	1.74	2.13	2.30	1.82	1.89	2.06	1.86	2.10	2.05	1.90	1.97
MnO	0.13	0.19	0.18	0.09	0.27	0.10	0.08	0.13	0.11	0.13	0.20	0.15
MgO	0.07	0.12	0.22	0.16	0.10	0.12	0.12	0.13	0.12	0.11	0.15	0.13
CaO	1.02	1.08	1.35	1.02	1.09	1.09	0.99	1.06	1.08	1.11	1.05	1.09
Na_2O	2.68	3.34	2.81	3.14	2.60	3.24	2.65	3.33	3.08	3.29	3.51	3.06
K_2O	3.11	3.54	3.02	3.30	3.53	3.25	3.04	3.86	3.31	3.40	3.26	3.33
Cl	0.16	0.29	0.21	0.12	0.20	0.27	0.23	0.18	0.23	0.21	0.26	0.21
Total	99.99	100.01	100.00	99.99	100.01	100.00	100.00	99.99	100.01	100.01	100.00	
% FeO	47.3	43.5	47.4	52.0	44.5	46.6	50.7	44.2	49.1	47.8	47.0	47.3
% CaO	26.1	27.0	30.1	23.1	26.7	26.8	24.4	25.2	25.2	25.9	26.0	26.0
% $^1/_3K_2O$	26.6	29.5	22.5	24.9	28.8	26.6	24.9	30.6	25.7	26.3	27.0	26.7

Sample 97123	I	II	III	IV	V	VI	VII	VIII	IX	X	XI	XII	Averages
Raw Data													
SiO_2	74.944	74.510	75.503	74.078	76.548	75.820	73.935	74.536	75.037	74.666	75.656	74.699	75.00
Al_2O_3	12.593	12.694	12.400	12.544	12.662	13.209	12.283	12.720	12.452	12.594	12.790	12.839	12.65
TiO_2	0.281	0.225	0.176	0.187	0.146	0.230	0.230	0.235	0.209	0.315	0.221	0.257	0.23
FeO	1.915	1.908	1.762	1.907	2.098	1.858	2.209	1.938	2.218	1.908	2.004	2.139	1.99
MnO	0.114	0.002	0.347	0.105	0.117	0.137	0.180	0.143	0.282	0.156	0.226	0.109	0.16
MgO	0.130	0.185	0.192	0.146	0.103	0.161	0.139	0.164	0.318	0.159	0.138	0.141	0.16
CaO	0.787	1.311	0.960	1.033	1.097	1.151	1.283	0.987	0.990	1.054	0.890	1.143	1.06
Na_2O	2.945	2.654	3.192	2.353	2.891	3.126	2.703	3.398	3.339	2.622	2.993	2.961	2.93
K2O	3.199	2.929	3.127	3.058	3.394	3.341	2.840	3.318	3.385	2.876	3.876	3.123	3.21
Cl	0.195	0.215	0.245	0.260	0.348	0.295	0.164	0.204	0.266	0.193	0.196	0.219	0.23
Total	97.103	96.634	97.904	95.672	99.355	99.328	96.965	97.642	98.496	96.542	98.989	97.631	
Normalised Data													
SiO_2	77.18	77.11	77.12	77.43	77.04	76.33	76.25	76.34	76.18	77.34	76.43	76.51	76.77
Al_2O_3	12.97	13.14	12.67	13.11	12.74	13.30	12.67	13.03	12.64	13.05	12.92	13.15	12.95
TiO_2	0.29	0.23	0.18	0.20	0.15	0.23	0.24	0.24	0.21	0.33	0.22	0.26	0.23
FeO	1.97	1.97	1.80	1.99	2.11	1.87	2.28	1.98	2.25	1.98	2.02	2.19	2.03
MnO	0.12	0.00	0.35	0.11	0.12	0.14	0.19	0.15	0.29	0.16	0.23	0.11	0.16
MgO	0.13	0.19	0.20	0.15	0.10	0.16	0.14	0.17	0.32	0.16	0.14	0.14	0.17
CaO	0.81	1.36	0.98	1.08	1.10	1.16	1.32	1.05	1.01	1.09	0.90	1.17	1.08
Na_2O	3.03	2.75	3.26	2.46	2.91	3.15	2.79	3.43	3.39	2.72	3.02	3.03	3.00
K_2O	3.29	3.03	3.19	3.20	3.37	3.36	2.93	3.40	3.44	2.98	3.92	3.20	3.28
Cl	0.20	0.22	0.25	0.27	0.35	0.30	0.17	0.21	0.27	0.20	0.20	0.23	0.24
Total	99.99	100.00	100.00	100.00	99.99	100.00	99.98	100.00	100.00	100.01	100.00	99.99	
% FeO	50.7	45.4	46.9	48.1	48.7	45.0	49.8	48.1	51.0	48.8	47.8	49.4	48.3
% CaO	20.9	31.3	25.5	26.1	25.4	28.0	28.8	24.5	22.9	26.8	21.3	26.4	25.7
% $^1/_3K_2O$	28.4	23.3	27.6	25.8	25.9	27.0	21.4	27.4	26.1	24.4	30.9	24.2	26.0

Sample 9735	I	II	III	IV	V	VI	VII	VIII	IX	X	XI	XII	XIII	XIV
Raw Data														
SiO_2	73.666	75.755	74.220	74.169	72.134	74.503	73.579	74.857	74.060	73.363	74.871	73.691	74.03	74.015
Al_2O_3	12.228	12.116	12.092	12.113	12.204	11.671	12.269	11.968	12.246	12.057	11.949	12.385	12.365	12.596
TiO_2	0.117	0.156	0.188	0.177	0.204	0.224	0.203	0.130	0.104	0.097	0.140	0.196	0.111	0.130
FeO	1.261	1.134	1.339	1.290	1.467	1.066	1.272	1.159	1.457	1.258	1.301	1.369	1.333	1.339
MgO	0.133	0.041	0.115	0.134	0.107	0.131	0.117	0.076	0.099	0.112	0.098	0.136	0.198	0.146
CaO	0.756	0.730	0.832	0.785	0.990	0.817	0.836	0.711	0.939	0.803	0.722	0.821	0.884	0.837
Na_2O	3.146	3.166	3.065	3.211	2.633	2.757	2.627	3.077	2.845	3.451	3.057	3.315	2.916	3.297
K_2O	3.492	3.900	3.567	3.652	3.306	3.393	3.350	3.747	3.261	3.701	3.668	3.638	3.357	3.543
Cl	0.291	0.382	0.234	0.339	0.293	0.282	0.198	0.308	0.379	0.241	0.238	0.255	0.242	0.290
Total	95.090	97.380	95.652	95.870	93.338	94.844	94.451	96.033	95.390	95.083	96.044	95.806	95.436	96.193
Normalised Data														
SiO_2	77.47	77.79	77.61	77.36	77.28	78.55	77.90	77.95	77.64	77.16	77.96	76.92	77.57	76.94
Al_2O_3	12.86	12.44	12.64	12.63	13.08	12.31	12.99	12.46	12.84	12.68	12.44	12.93	12.96	13.09
TiO_2	0.12	0.16	0.18	0.18	0.22	0.24	0.21	0.14	0.11	0.10	0.15	0.20	0.12	0.14
FeO	1.33	1.16	1.40	1.35	1.57	1.12	1.35	1.21	1.53	1.32	1.35	1.43	1.40	1.39
MgO	0.14	0.04	0.12	0.14	0.11	0.14	0.12	0.08	0.10	0.12	0.10	0.14	0.21	0.15
CaO	0.80	0.75	0.87	0.82	1.06	0.86	0.89	0.74	0.98	0.84	0.75	0.86	0.93	0.87
Na_2O	3.31	3.25	3.20	3.35	2.82	2.91	2.78	3.20	2.98	3.63	3.18	3.46	3.06	3.43
K_2O	3.67	4.00	3.73	3.81	3.54	3.58	3.55	3.90	3.42	3.89	3.82	3.80	3.52	3.68
Cl	0.31	0.39	0.24	0.35	0.31	0.30	0.21	0.32	0.40	0.25	0.25	0.27	0.25	0.30
Total	100.01	99.98	99.99	99.99	99.99	100.01	100.00	100.00	100.00	99.99	100.00	100.01	100.02	99.99
% FeO	39.7	35.8	39.9	39.2	41.2	35.3	39.5	37.2	38.4	38.2	40.0	40.2	40.0	39.8
% CaO	23.9	23.1	24.8	23.8	27.8	27.1	26.0	22.8	24.6	24.3	22.3	24.2	26.6	24.9
% $^1/_3K_2O$	36.4	41.1	35.3	36.9	31.0	37.5	34.5	40.0	37.0	37.6	37.7	35.7	33.4	35.2

Sample 9735 cont'	XV	XVI	XVII	XVIII	XIX	Averages
Raw Data						
SiO_2	74.427	73.283	73.003	72.352	74.022	73.89
Al_2O_3	12.108	11.907	11.963	11.770	12.111	12.11
TiO_2	0.113	0.252	0.176	0.161	0.140	0.16
FeO	1.287	1.102	1.212	1.158	1.160	1.26
MgO	0.118	0.133	0.082	0.062	0.091	0.11
CaO	0.767	0.661	0.731	0.810	0.726	0.80
Na_2O	3.190	3.264	3.224	2.687	3.152	3.06
K_2O	3.666	3.516	3.702	3.208	3.724	3.55
Cl	0.251	0.280	0.200	0.326	0.265	0.28
Total	95.927	94.398	94.293	92.534	95.391	
Normalised Data						
SiO_2	77.59	77.63	77.42	78.19	77.60	77.61
Al_2O_3	12.62	12.61	12.69	12.72	12.70	12.72
TiO_2	0.12	0.27	0.19	0.17	0.15	0.17
FeO	1.34	1.17	1.29	1.25	1.22	1.33
MgO	0.12	0.14	0.09	0.07	0.10	0.12
CaO	0.80	0.70	0.78	0.88	0.76	0.84
Na_2O	3.33	3.46	3.42	2.90	3.30	3.21
K_2O	3.82	3.72	3.93	3.47	3.90	3.72
Cl	0.26	0.30	0.21	0.35	0.28	0.29
Total	100.00	100.00	100.02	100.00	100.01	
%FeO	39.3	37.6	38.2	38.0	37.2	38.7
%CaO	23.5	22.5	23.1	26.7	23.2	24.5
$\%^1/_3K_2O$	37.2	39.9	38.8	35.3	39.6	36.8

APPENDIX C

- Percentages of SiO_2, K_2O, CaO and FeO used for the Bivariate Plots.

	%SiO_2	%K_2O	%CaO	%FeO
9851	76.33	4.14	1.04	1.13
9855	76.86	4.01	0.98	1.16
9856	76.36	3.19	1.15	1.72
9858(1)	77.84	4.01	1.10	0.66
9858(2)	77.53	3.90	0.98	1.07
9859	77.67	3.90	0.89	1.10
98510	78.53	3.45	0.90	1.47
9861	78.11	3.86	0.90	1.13
97121	76.57	3.33	1.09	1.97
97123	76.77	3.28	1.08	2.03
9735	77.61	3.72	0.84	1.33
Rewa#	75.63	3.37	1.28	1.99
Potaka#	77.80	4.12	0.88	1.08
Kaukatea#	76.27	3.40	1.07	1.63
Kupe#	77.58	3.84	0.91	1.29

Reference data obtained from Pillans et al. (1994)

APPENDIX D

• Pebble data for the five sites within the study area.

1. **Finnis Road Site**

Grid Reference: T23/450120

Pebble	Short Axis	Int. Axis	Long Axis	Dip & Dip Direction	Roundness	Short/ Long	Int./ Long
1	0.6	1.2	1.8	19°@240	r	0.50	0.67
2	1.6	2.3	4.3	4°@295	r	0.70	0.53
3	0.9	1.6	3.0	25°@025	r	0.56	0.53
4	1.2	2.4	2.5	24°@020	sr	0.50	0.96
5	0.9	1.0	2.2	2°@040	wr	0.90	0.45
6	0.9	1.5	3.0	41°@025	wr	0.60	0.50
7	0.6	1.0	1.6	10°@295	wr	0.60	0.63
8	0.5	1.0	3.5	21°@115	wr	0.50	0.29
9	1.0	1.1	2.8	17°@025	wr	0.91	0.39
10	1.6	1.7	2.5	9°@120	r	0.94	0.68
11	1.1	1.6	3.3	22°@355	sr	0.69	0.48
12	0.8	1.4	4.0	2°@150	r	0.57	0.35
13	1.4	1.8	3.5	11°@330	sr	0.78	0.51
14	1.3	1.8	4.3	3°@095	r	0.72	0.42
15	1.1	1.9	2.8	15°@080	sr	0.58	0.68
16	1.4	1.6	3.3	24°@320	r	0.88	0.48
17	1.0	2.0	3.2	6°@350	r	0.50	0.63
18	1.3	1.6	3.3	4°@160	wr	0.81	0.48
19	1.4	2.4	3.0	13°@240	sr	0.58	0.80
20	1.2	1.6	3.0	11°@245	r	0.75	0.53
21	1.6	1.9	4.3	19°@100	sr	0.84	0.44
22	1.5	2.3	4.0	15°@315	sr	0.65	0.58
23	1.3	1.8	3.3	27°@200	r	0.72	0.55
24	1.0	1.7	2.3	7°@015	r	0.59	0.74
25	1.2	1.8	2.8	12°@215	r	0.67	0.64
26	1.0	1.5	2.4	19°@080	r	0.67	0.63
27	1.1	1.5	2.6	22°@155	r	0.73	0.58
28	1.0	1.5	1.9	9°@315	sr	0.67	0.79
29	1.7	2.1	3.8	4°@250	wr	0.81	0.55
30	1.7	2.8	3.5	21°@110	sr	0.61	0.80
31	1.2	1.9	2.8	11°@315	sr	0.63	0.68
32	1.4	1.8	3.1	2°@305	r	0.78	0.58
33	2.1	2.5	4.1	31°@220	r	0.84	0.61
34	1.1	1.2	2.8	24°@030	sr	0.92	0.43
35	0.6	2.0	2.4	9°@235	r	0.30	0.83
36	0.5	2.2	2.5	11°@105	wr	0.28	0.88
37	1.2	1.5	3.2	12°@140	wr	0.80	0.47
38	2.0	2.9	3.3	3°@070	r	0.69	0.88
39	1.2	1.5	2.6	29°@085	r	0.80	0.58
40	1.2	1.4	3.1	19°@195	r	0.86	0.45
41	0.9	1.3	2.2	31°@050	r	0.69	0.59
42	1.0	2.2	3.0	8°@030	sr	0.45	0.73
43	1.4	3.3	5.9	7°@060	r	0.42	0.56
44	0.7	1.1	2.4	15°@245	r	0.64	0.46
45	0.8	2.8	3.5	18°@315	r	0.29	0.80
46	1.2	2.2	4.6	22°@205	r	0.55	0.48
47	0.6	1.5	2.3	5°@070	r	0.40	0.65
48	0.7	1.4	2.0	19°@190	r	0.50	0.70
49	1.6	2.3	3.3	7°@020	r	0.70	0.70
50	1.7	2.4	2.9	15°@115	sr	0.71	0.83
Totals	58.0	90.8	148.8				
Av.	1.16	1.82	2.98			0.64	0.61

2. **Ridge Road Site**

Grid Reference: T23/449124

Pebble	Short Axis	Int. Axis	Long Axis	Dip & Dip Direction	Roundness	Short/ Long	Int./ Long
1	2.6	4.9	9.3	11°@260	sr	0.53	0.53
2	3.9	5.1	8.1	13°@055	sr	0.76	0.63
3	1.9	4.1	5.9	65°@005	sr	0.46	0.69
4	1.2	2.1	4.7	2°@100	r	0.57	0.45
5	1.6	2.4	3.8	26°@005	r	0.67	0.63
6	2.1	4.3	5.7	36°@045	sr	0.49	0.75
7	1.3	1.9	3.6	20°@020	r	0.68	0.53
8	2.0	2.7	4.2	39°@015	sr	0.74	0.64
9	1.6	3.0	5.9	15°@315	sr	0.53	0.51
10	1.6	2.2	5.0	36°@315	r	0.73	0.44
11	2.0	3.2	5.8	32°@030	sr	0.63	0.55
12	0.9	1.6	2.9	2°@050	r	0.56	0.55
13	1.3	1.6	4.5	11°@095	r	0.81	0.36
14	1.2	2.0	3.7	6°@130	sr	0.60	0.54
15	1.6	2.7	6.0	31°@210	sr	0.59	0.45
16	1.9	2.3	5.5	24°@310	sr	0.83	0.42
17	1.6	2.9	4.2	25°@325	r	0.55	0.69
18	2.3	5.1	7.9	16°@015	sr	0.45	0.65
19	1.3	2.2	3.3	16°@090	sr	0.59	0.67
20	1.9	2.9	4.6	12°@175	r	0.66	0.63
21	1.5	3.0	4.7	15°@355	r	0.50	0.64
22	1.5	2.0	3.7	29°@335	sr	0.75	0.54
23	1.5	3.1	5.5	24°@340	r	0.48	0.56
24	2.1	3.5	4.4	7°@245	sr	0.60	0.80
25	1.5	4.7	7.3	16°@095	r	0.32	0.64
26	1.9	3.0	4.3	8°@080	r	0.63	0.70
27	1.0	1.8	2.9	12°@075	sr	0.56	0.62
28	1.5	2.3	3.1	24°@060	r	0.65	0.74
29	1.9	2.8	3.5	9°@020	sr	0.68	0.80
30	1.7	3.1	4.2	28°@115	r	0.55	0.74
31	0.6	0.8	2.3	34°@355	r	0.75	0.35
32	1.4	2.3	3.8	24°@355	r	0.61	0.61
33	1.2	2.0	3.5	12°@105	r	0.60	0.57
34	1.4	2.5	5.0	39°@300	r	0.56	0.5
35	1.2	1.4	3.4	13°@065	r	0.86	0.41
36	1.6	2.5	3.5	28°@315	r	0.64	0.71
37	2.5	3.6	5.5	33°@215	sr	0.69	0.65
38	1.6	4.0	6.1	4°@140	sr	0.40	0.66
39	0.9	1.8	3.1	23°@005	r	0.50	0.58
40	1.0	1.5	2.7	21°@015	r	0.67	0.56
41	1.6	4.0	4.9	28°@040	sr	0.40	0.82
42	1.4	2.7	3.9	21°@320	sr	0.52	0.69
43	1.4	2.0	3.5	31°@215	sr	0.70	0.57
44	1.2	2.8	4.4	14°@075	r	0.43	0.64
45	6.0	7.5	9.6	47°@295	sr	0.80	0.78
46	2.4	3.6	5.9	24°@005	sr	0.67	0.61
47	2.2	2.3	5.1	19°@015	sa	0.96	0.45
48	3.6	5.1	6.9	26°@360	sr	0.71	0.74
49	2.0	2.1	3.7	21°@280	sr	0.95	0.57
50	1.3	3.2	5.1	12°@305	sr	0.41	0.63
Totals	88.4	146.2	240.1				
Averages	1.77	2.94	4.80			0.60	0.61

3. **Pollock Road Site**

Grid Reference: T23/442140

Pebble	Short Axis	Int. Axis	Long Axis	Dip & Dip Direction	Roundness	Short/ Long	Int./ Long
1	1.9	4.0	5.3	30°@120	wr	0.48	0.75
2	2.4	2.8	4.8	25°@315	r	0.86	0.58
3	1.4	1.8	5.1	39°@325	r	0.78	0.35
4	1.4	1.7	4.7	12°@180	r	0.82	0.36
5	1.8	2.5	3.6	9°@150	r	0.72	0.69
6	1.6	2.9	4.3	6°@015	r	0.55	0.67
7	1.4	1.6	3.7	36°@315	r	0.88	0.43
8	1.4	2.1	2.8	41°@285	wr	0.67	0.75
9	0.8	1.1	3.3	3°@275	wr	0.73	0.33
10	2.9	3.2	5.4	16°@320	wr	0.91	0.59
11	2.0	3.0	3.8	11°@360	r	0.67	0.79
12	0.9	1.5	3.0	10°@330	wr	0.6	0.5
13	1.1	1.9	4.1	23°@320	wr	0.58	0.46
14	1.0	1.9	3.0	36°@110	wr	0.53	0.63
15	1.1	1.5	3.4	1°@355	r	0.73	0.44
16	1.6	1.9	4.1	14°@335	r	0.84	0.46
17	1.6	2.1	4.7	8°@260	wr	0.76	0.45
18	1.5	1.7	3.9	12°@205	r	0.88	0.44
19	0.9	2.5	4.7	32°@285	wr	0.36	0.53
20	0.7	2.9	4.4	2°@045	wr	0.24	0.66
21	1.8	2.1	4.4	12°@040	r	0.86	0.48
22	1.6	2.1	4.5	26°@270	r	0.76	0.47
23	0.7	1.2	3.8	43°@335	wr	0.58	0.32
24	1.3	2.0	3.9	21°@320	wr	0.65	0.51
25	1.0	1.7	2.6	13°@175	wr	0.59	0.65
26	1.1	2.3	3.3	12°@280	r	0.48	0.70
27	1.8	2.2	3.4	21°@360	wr	0.82	0.65
28	1.5	2.3	4.4	21°@315	r	0.68	0.52
29	0.8	1.7	3.4	9°@135	r	0.47	0.50
30	1.6	2.0	4.6	3°@125	r	0.80	0.43
31	1.7	2.3	4.8	23°@300	r	0.74	0.48
32	0.8	1.9	3.7	5°@180	r	0.42	0.51
33	0.8	1.0	4.3	4°@170	r	0.8	0.23
34	1.9	2.3	2.7	24°@020	r	0.83	0.85
35	1.2	2.2	3.6	19°@310	r	0.54	0.61
36	0.5	1.3	1.9	18°@205	wr	0.38	0.68
37	2.9	3.3	6.6	8°@015	r	0.88	0.50
38	1.2	1.7	3.5	20°@355	r	0.71	0.49
39	0.9	1.5	2.9	32°@060	r	0.60	0.60
40	1.1	1.9	2.5	18°@295	r	0.58	0.76
41	1.1	1.4	3.0	27°@310	r	0.79	0.47
42	0.9	2.3	4.0	19°@305	r	0.39	0.58
43	0.6	1.1	2.9	8°@010	r	0.55	0.38
44	0.9	1.7	2.4	11°@325	r	0.53	0.71
45	1.1	1.8	3.5	19°@320	r	0.61	0.51
46	0.7	2.1	2.9	18°@250	wr	0.33	0.72
47	0.8	1.8	3.1	10°@040	r	0.44	0.58
48	0.7	1.2	2.2	9°@275	r	0.58	0.55
49	1.8	2.0	4.4	19°@325	r	0.90	0.45
50	0.8	1.7	3.2	9°@225	r	0.47	0.53
Totals	65.0	100.7	188.5				
Averages	1.30	2.00	3.77			0.65	0.53

4. Oroua River Site

Grid Reference: T23/437145

Pebble	Short Axis	Int. Axis	Long Axis	Dip & Dip Direction	Roundness	Short/ Long	Int./ Long
1	1.5	1.8	3.8	11°@350	wr	0.83	0.47
2	0.9	2.6	3.0	27°@320	wr	0.35	0.87
3	1.2	1.8	4.2	20°@185	r	0.67	0.43
4	1.3	2.2	4.4	20°@180	wr	0.59	0.50
5	0.8	2.2	3.0	9°@200	wr	0.36	0.73
6	1.7	2.0	4.1	6°@360	r	0.85	0.49
7	1.2	1.8	2.5	19°@025	wr	0.67	0.72
8	1.5	1.9	3.0	6°@320	r	0.79	0.63
9	2.4	2.6	3.9	35°@030	r	0.92	0.67
10	1.1	1.8	4.4	8°@350	r	0.61	0.41
11	1.3	1.4	2.8	28°@085	wr	0.93	0.50
12	1.7	2.2	4.8	15°@220	sr	0.77	0.46
13	1.1	1.5	3.3	20°@015	wr	0.73	0.45
14	2.1	4.0	6.4	7°@240	wr	0.53	0.63
15	3.0	3.6	5.6	19°@200	r	0.83	0.64
16	1.6	2.2	3.6	10°@230	wr	0.73	0.61
17	0.6	1.5	2.5	14°@285	r	0.40	0.60
18	1.0	2.4	3.1	9°@210	r	0.42	0.77
19	1.6	2.0	3.2	3°@320	r	0.80	0.63
20	1.8	2.4	4.0	30°@360	r	0.75	0.60
21	1.1	1.3	2.5	21°@330	sr	0.85	0.52
22	1.4	2.3	4.0	12°@160	r	0.61	0.58
23	1.7	2.4	4.6	10°@165	r	0.71	0.52
24	1.5	1.6	3.2	25°@145	r	0.94	0.50
25	1.5	3.1	4.7	9°@140	r	0.48	0.66
26	2.1	3.0	4.9	9°@145	r	0.70	0.61
27	1.4	2.4	4.4	10°@305	r	0.58	0.54
28	1.5	1.7	3.6	35°@345	r	0.88	0.47
29	1.3	1.8	3.7	7°@185	r	0.72	0.49
30	1.0	2.2	2.8	7°@165	r	0.45	0.79
31	1.1	2.4	3.2	8°@010	r	0.46	0.75
32	1.1	3.6	5.3	6°@340	wr	0.31	0.68
33	1.3	1.4	4.2	14°@290	wr	0.93	0.33
34	0.8	1.2	3.6	20°@295	r	0.67	0.33
35	1.0	1.5	3.3	4°@290	r	0.67	0.45
36	1.6	2.7	2.9	11°@305	r	0.59	0.93
37	1.4	3.0	3.7	11°@045	r	0.47	0.81
38	1.2	1.5	2.5	37°@355	r	0.80	0.60
39	0.6	1.0	2.3	42°@345	r	0.60	0.43
40	1.1	1.5	3.8	12°@335	wr	0.73	0.39
41	1.0	1.4	3.0	19°@235	r	0.71	0.47
42	1.0	1.3	2.4	20°@010	r	0.77	0.54
43	1.2	1.9	4.7	7°@170	r	0.63	0.40
44	1.4	2.6	4.5	24°@080	wr	0.54	0.58
45	1.6	3.2	4.1	34°@015	wr	0.50	0.78
46	1.2	1.6	2.1	29°@015	r	0.75	0.76
47	2.6	2.9	6.0	22°@015	r	0.90	0.48
48	0.8	1.7	2.5	44°@355	r	0.47	0.68
49	1.4	3.2	4.8	11°@125	wr	0.44	0.67
50	1.8	2.7	3.5	11°@330	r	0.67	0.77
Totals	69.1	108.0	186.4				
Averages	1.38	2.16	3.73			0.64	0.58

5. **Beehive Creek Site**

Grid Reference: T23/501123

Pebble	Short Axis	Int. Axis	Long Axis	Dip & Dip Direction	Roundness	Short/ Long	Int./ Long
1	4.2	7.6	9.9	20°@005	sa	0.55	0.77
2	1.8	2.3	7.0	14°@158	sr	0.78	0.33
3	1.6	3.7	3.8	6°@162	sr	0.42	0.97
4	1.7	2.8	6.9	42°@120	sr	0.62	0.40
5	1.6	2.2	3.5	7°@180	sr	0.73	0.63
6	2.0	2.4	3.8	8°@315	sr	0.83	0.63
7	1.9	4.5	6.4	8°@120	r	0.42	0.70
8	2.2	4.2	4.8	30°@358	sr	0.52	0.88
9	2.3	3.7	7.8	0°@046	sr	0.61	0.47
10	4.1	6.3	7.4	3°@342	sr	0.65	0.85
11	3.4	4.1	6.7	26°@266	sr	0.83	0.61
12	3.1	6.8	10.4	29°@035	sr	0.46	0.65
13	2.8	5.6	7.0	28°@264	sr	0.50	0.80
14	4.5	6.6	7.3	26°@011	sr	0.68	0.90
15	3.9	5.5	6.6	15°@250	sa	0.71	0.83
16	2.6	3.2	6.1	25°@342	sa	0.81	0.52
17	2.6	4.5	5.1	4°@215	r	0.58	0.88
18	3.0	3.8	5.0	21°@177	r	0.79	0.76
19	2.0	2.5	4.7	8°@225	sa	0.80	0.53
20	1.4	3.0	4.4	7°@015	sr	0.47	0.68
21	2.5	3.2	5.3	14°@200	sr	0.78	0.6
22	1.9	2.4	3.6	15°@135	sa	0.79	0.67
23	3.2	3.4	4.6	10°@128	r	0.94	0.74
24	3.3	3.5	5.1	60°@220	r	0.94	0.69
25	2.6	4.5	6.7	10°@215	sr	0.58	0.67
26	2.9	4.5	4.6	13°@125	sr	0.64	0.98
27	2.9	3.1	4.6	19°@000	sr	0.94	0.67
28	2.4	4.0	4.4	25°@230	sr	0.60	0.91
29	1.6	3.0	3.3	7°@336	sr	0.53	0.91
30	2.4	2.6	5.1	11°@282	r	0.92	0.51
31	1.8	2.9	4.1	13°@310	sr	0.62	0.71
32	2.5	2.6	3.0	19°@096	r	0.96	0.87
33	2.9	3.2	6.3	21°@335	sr	0.91	0.51
34	1.4	2.3	3.0	5°@013	r	0.61	0.77
35	2.1	3.6	5.2	15°@253	sa	0.58	0.69
36	2.0	2.6	3.8	4°@320	r	0.77	0.68
37	1.2	1.6	3.4	16°@337	r	0.75	0.47
38	1.6	2.7	4.2	31°@347	r	0.59	0.64
39	2.4	2.5	3.3	24°@144	r	0.96	0.76
40	2.1	2.1	3.0	7°@339	r	1.00	0.70
41	2.8	3.4	3.6	14°@320	sr	0.82	0.94
42	1.7	3.5	4.3	15°@117	r	0.49	0.81
43	1.6	1.6	2.2	19°@142	r	1.00	0.73
44	1.7	2.6	4.5	22°@063	sr	0.65	0.58
45	2.3	2.9	4.1	26°@347	sa	0.79	0.71
46	1.8	2.5	3.3	1°@327	sr	0.72	0.76
47	1.5	2.3	3.2	3°@043	sr	0.65	0.72
48	0.8	3.5	4.2	42°@336	sr	0.23	0.83
49	0.8	1.9	3.1	10°@106	r	0.42	0.61
50	1.2	1.6	2.3	22°@337	sr	0.75	0.70
Totals	114.6	171.4	246.0				
Averages	2.29	3.43	4.92			0.67	0.70

- All measurements are recorded in cm
- Roundness symbols: sa - subangular, sr - subrounded, r - rounded, wr - well rounded

APPENDIX E

• Raw sieve data for the nine sand samples.

1. **Stewart's Gully D1** Original weight = 29.86g

% of sample lost = 4.25%

Sieve Diam. (ø)	Weight (g)	Percentage	Cumulative Percentage
0.50	0.01	0.03	0.03
1.00	0.03	0.10	0.13
1.50	0.04	0.14	0.27
2.00	0.18	0.63	0.90
2.25	0.91	3.18	4.08
2.50	3.76	13.15	17.23
2.75	7.32	25.60	42.83
3.00	8.35	29.21	72.04
3.25	4.08	14.27	86.31
3.50	2.01	7.03	93.34
3.75	1.12	3.92	97.26
4.00	0.45	1.57	98.83
>4.00	0.33	1.15	99.98

2. **Stewart's Gully D2** Original weight = 24.70g

% of sample gained = 2.15%

Sieve Diam. (ø)	Weight (g)	Percentage	Cumulative Percentage
0.50	0.03	0.12	0.12
1.00	0.06	0.24	0.36
1.50	0.19	0.75	1.11
2.00	0.64	2.54	3.65
2.25	1.59	6.30	9.95
2.50	4.69	18.59	28.54
2.75	6.50	25.76	54.30
3.00	6.30	24.97	79.27
3.25	2.74	10.86	90.13
3.50	1.13	4.48	94.61
3.75	0.61	2.42	97.03
4.00	0.27	1.07	98.10
>4.00	0.48	1.90	100.00

3. **Branch Road Corner A** Original weight = 28.66g

% of sample gained = 0.45

NB: This was a very pumiceous sample.

Sieve Diam. (ø)	Weight (g)	Percentage	Cumulative Percentage
-1.00	1.12	3.89	3.89
-0.50	1.01	3.51	7.40
0.00	1.46	5.07	12.47
0.50	1.91	6.63	19.10
1.00	1.79	6.22	25.32
1.50	1.95	6.77	32.09
2.00	2.31	8.02	40.11
2.25	1.63	5.66	45.77
2.50	1.85	6.43	52.20
2.75	2.68	9.31	61.51
3.00	3.74	12.99	74.50
3.25	2.65	9.20	83.70
3.50	1.56	5.42	89.12
3.75	1.11	3.86	92.98
4.00	0.80	2.78	95.76
>4.00	1.22	4.24	100.00

4. **Branch Road Corner B** Original weight = 34.20g

% of sample gained = 0.26%

Sieve Diam. (ø)	Weight (g)	Percentage	Cumulative Percentage
0.50	0.02	0.06	0.06
1.00	0.20	0.58	0.64
1.50	0.94	2.74	3.38
2.00	2.94	8.57	11.95
2.25	4.25	12.39	24.34
2.50	6.13	17.88	42.22
2.75	6.48	18.90	61.12
3.00	6.00	17.50	78.62
3.25	3.59	10.47	89.09
3.50	1.71	4.99	94.08
3.75	0.97	2.83	96.91
4.00	0.46	1.34	98.25
>4.00	0.40	1.17	99.42

5. **Oroua River 1C** Original weight = 32.49g

% of sample lost = 0.43%

Sieve Diam. (ø)	Weight (g)	Percentage	Cumulative Percentage
0.50	0.09	0.28	0.28
1.00	0.10	0.31	0.59
1.50	0.17	0.53	1.12
2.00	0.43	1.33	2.45
2.25	0.82	2.53	4.98
2.50	3.01	9.30	14.28
2.75	8.28	25.60	39.88
3.00	10.72	33.14	73.02
3.25	4.90	15.15	88.17
3.50	2.07	6.40	94.57
3.75	1.00	3.09	97.66
4.00	0.43	1.33	98.99
>4.00	0.33	1.02	100.01

6. **Oroua River 1E** Original weight = 35.73g

% of sample lost = 0.73%

Sieve Diam. (ø)	Weight (g)	Percentage	Cumulative Percentage
0.50	0.01	0.02	0.02
1.00	0.01	0.02	0.04
1.50	0.08	0.22	0.26
2.00	0.28	0.79	1.05
2.25	0.42	1.18	2.23
2.50	0.66	1.86	4.09
2.75	1.18	3.33	7.42
3.00	3.70	10.43	17.85
3.25	5.64	15.90	33.75
3.50	6.47	18.24	51.99
3.75	6.29	17.73	69.72
4.00	5.33	15.03	84.75
>4.00	5.58	15.73	100.48

7. **Beehive Creek 1** Original weight = 35.78g

% of sample lost = 1.03%

Sieve Diam. (ø)	Weight (g)	Percentage	Cumulative Percentage
1.00	0.08	0.23	0.23
1.50	0.09	0.25	0.48
2.00	0.23	0.65	1.13
2.25	0.80	2.26	3.39
2.50	3.22	9.09	12.48
2.75	6.22	17.57	30.05
3.00	9.98	28.18	58.23
3.25	6.39	18.05	76.28
3.50	3.74	10.56	86.84
3.75	2.23	6.30	93.14
4.00	1.16	3.28	96.42
>4.00	1.27	3.59	100.01

8. **Beehive Creek 3** Original weight = 33.00g

% of sample lost = 0.39%

Sieve Diam. (ø)	Weight (g)	Percentage	Cumulative Percentage
1.00	0.02	0.06	0.06
1.50	0.04	0.12	0.18
2.00	0.11	0.33	0.51
2.25	0.56	1.70	2.21
2.50	2.84	8.64	10.85
2.75	7.47	22.73	33.58
3.00	11.98	36.45	70.03
3.25	6.02	18.31	88.34
3.50	2.41	7.33	95.67
3.75	0.85	2.59	98.26
4.00	0.33	1.00	99.26
>4.00	0.24	0.73	99.99

9. **Beehive Creek 6** Original weight = 35.08g

% of sample gained = 0.03%

Sieve Diam. (ø)	Weight (g)	Percentage	Cumulative Percentage
1.00	0.12	0.34	0.34
1.50	0.16	0.46	0.80
2.00	0.56	1.60	2.40
2.25	2.68	7.64	10.04
2.50	10.17	28.98	39.02
2.75	11.97	34.11	73.13
3.00	6.76	19.26	92.39
3.25	1.92	5.47	97.86
3.50	0.37	1.05	98.91
3.75	0.18	0.51	99.42
4.00	0.09	0.26	99.68
>4.00	0.11	0.31	99.99

- Summary Table of sieving statistics for the 9 sands:

Sample	M_z	σ	K_G	Sk_I	Ø1	M_d
1	2.83	0.37	1.18	0.19	2.05	2.80
2	2.72	0.41	1.19	0.12	1.50	2.70
3	1.97	1.47	0.80	-0.43	nd	2.45
4	2.65	0.51	1.14	0.10	1.10	2.60
5	2.82	0.33	1.33	0.12	1.45	2.80
6	3.48	0.48	0.79	-0.14	2.00	3.50
7	2.97	0.47	1.27	0.15	1.95	2.90
8	2.87	0.31	1.23	0.29	2.15	2.90
9	2.60	0.27	0.97	-0.03	1.70	2.60

APPENDIX F

- Cumulative frequency plots for the nine sand samples.

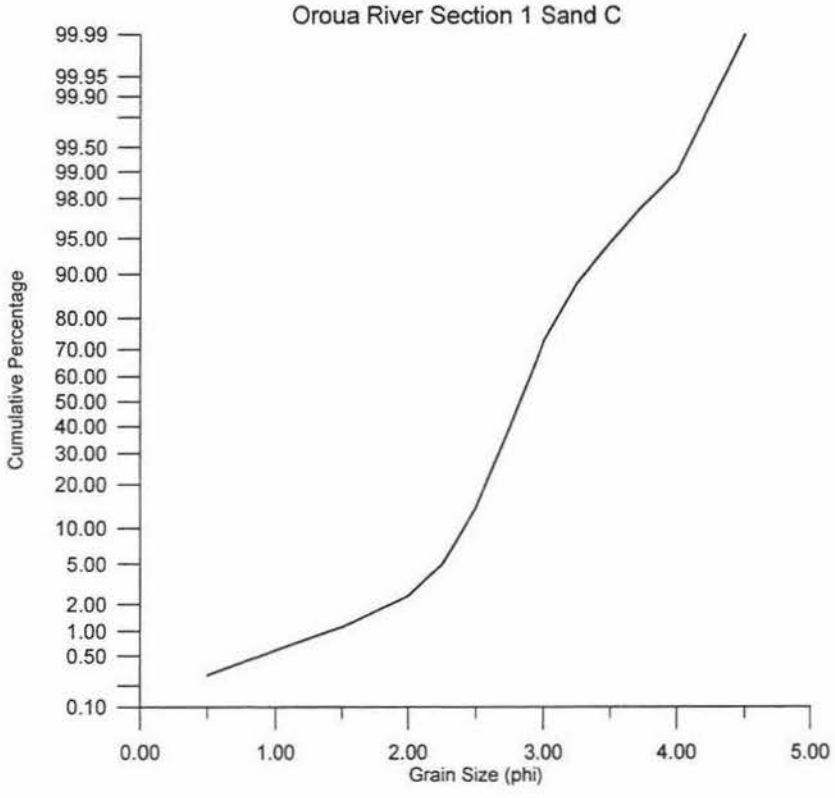

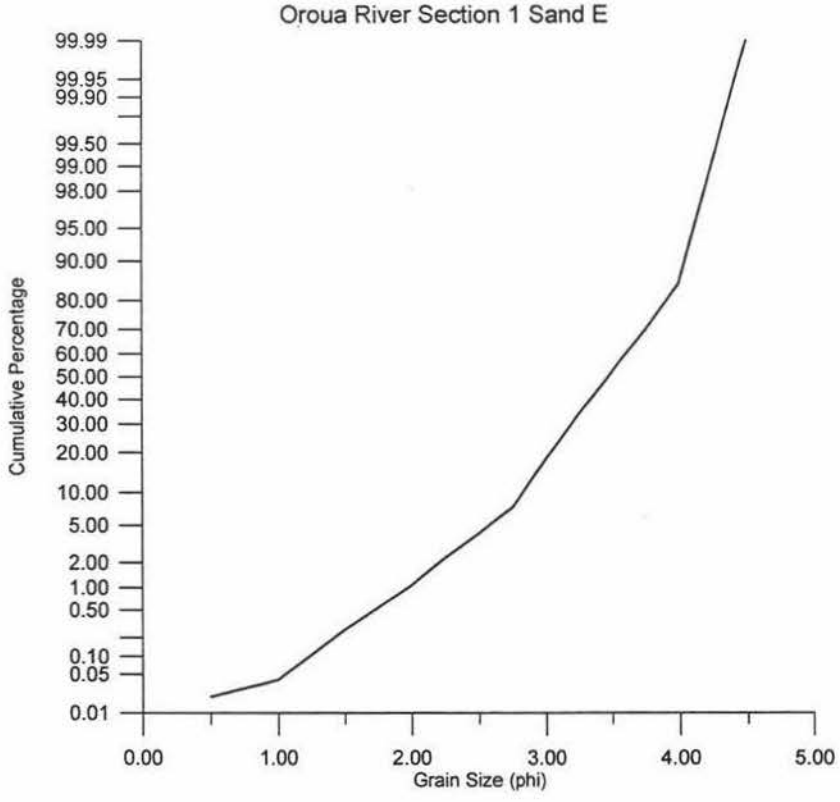

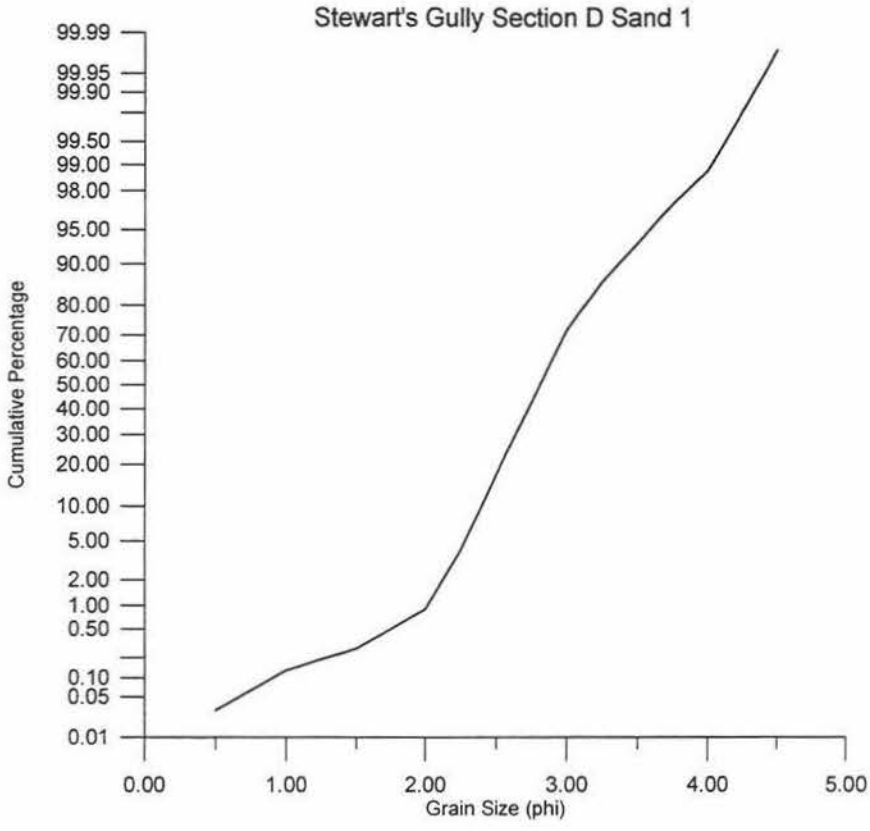
Stewart's Gully Section D Sand 1
Cumulative Percentage
99.99
99.95
99.90
99.50
99.00
98.00
95.00
90.00
80.00
70.00
60.00
50.00
40.00
30.00
20.00
10.00
5.00
2.00
1.00
0.50
0.10
0.05
0.01
0.00
1.00
2.00
3.00
4.00
5.00
Grain Size (phi)

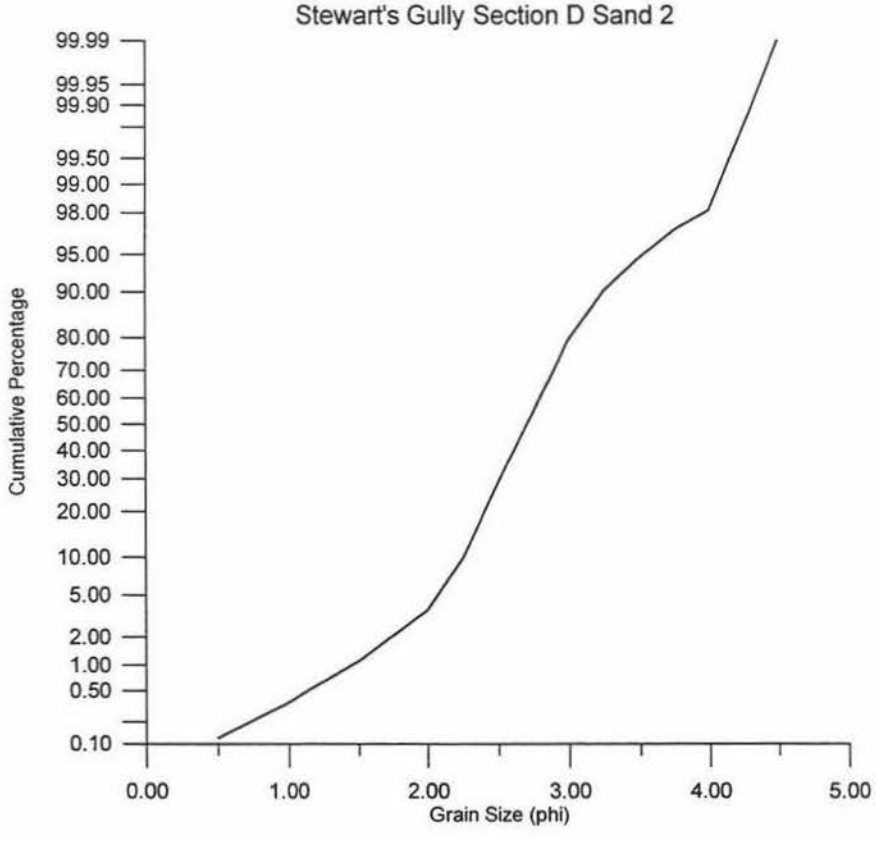
Stewart's Gully Section D Sand 2
Cumulative Percentage
99.99
99.95
99.90
99.50
99.00
98.00
95.00
90.00
80.00
70.00
60.00
50.00
40.00
30.00
20.00
10.00
5.00
2.00
1.00
0.50
0.10
0.00
1.00
2.00
3.00
4.00
5.00
Grain Size (phi)

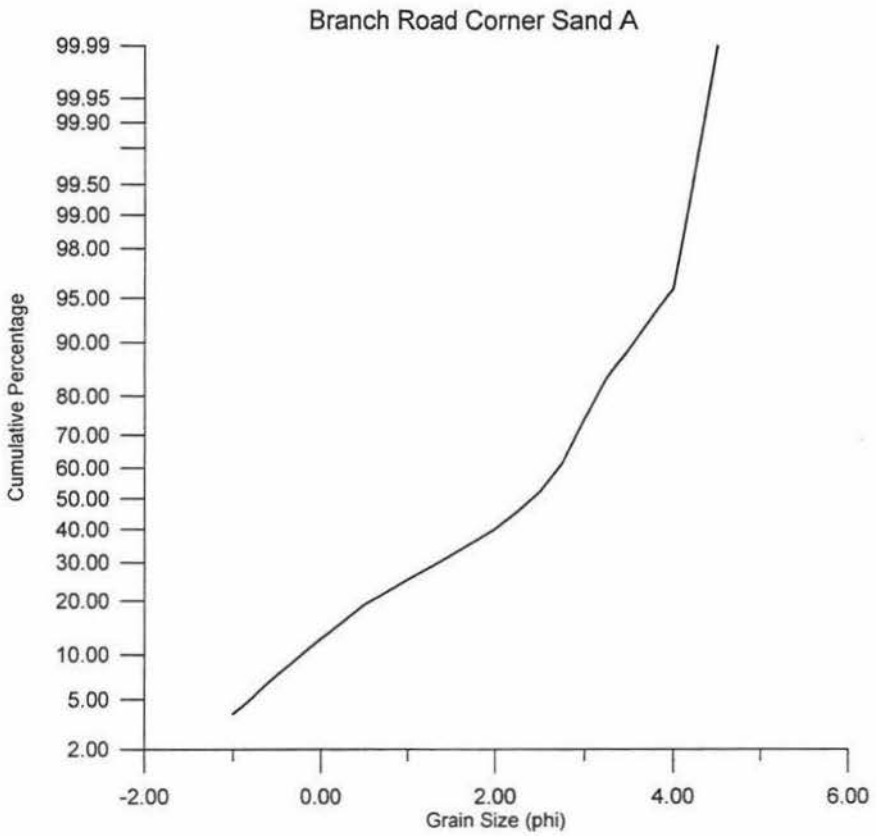
Branch Road Corner Sand A
Cumulative Percentage
99.99
99.95
99.90
99.50
99.00
98.00
95.00
90.00
80.00
70.00
60.00
50.00
40.00
30.00
20.00
10.00
5.00
2.00
-2.00
0.00
2.00
4.00
6.00
Grain Size (phi)

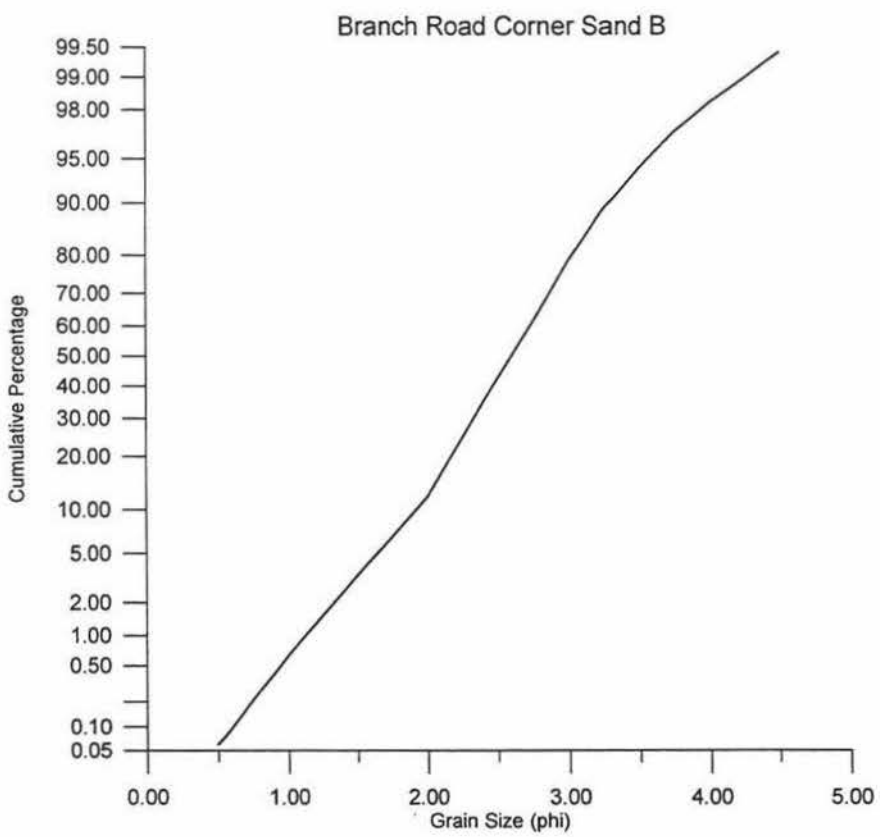
Branch Road Corner Sand B
Cumulative Percentage
99.50
99.00
98.00
95.00
90.00
80.00
70.00
60.00
50.00
40.00
30.00
20.00
10.00
5.00
2.00
1.00
0.50
0.10
0.05
0.00
1.00
2.00
3.00
4.00
5.00
Grain Size (phi)

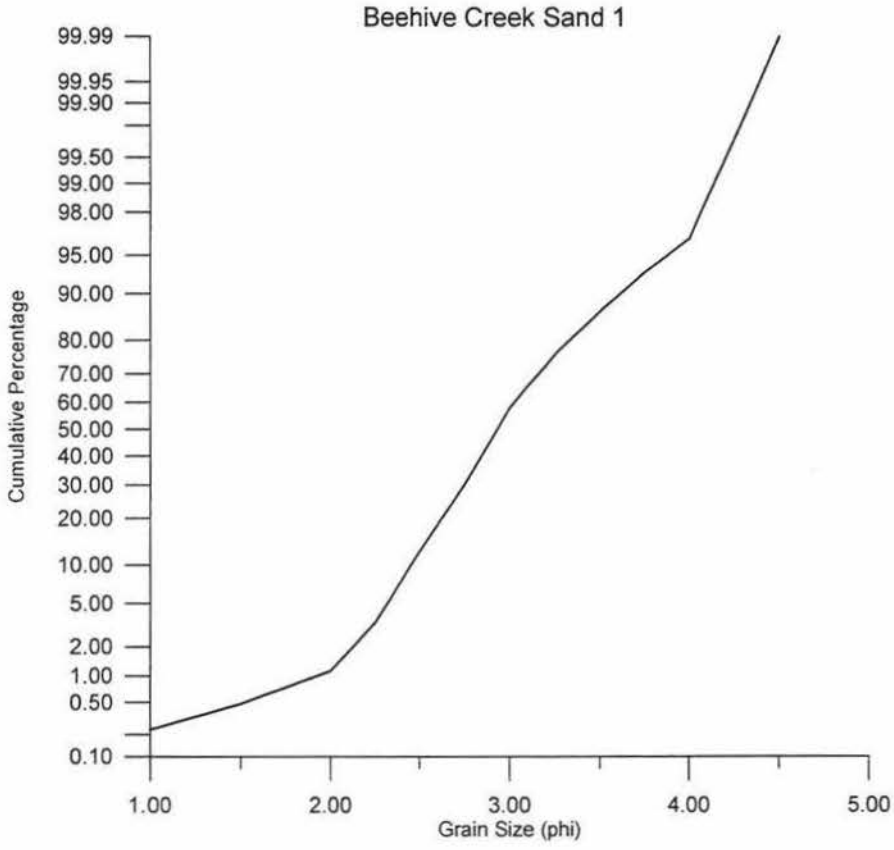
Beehive Creek Sand 1
Cumulative Percentage
99.99
99.95
99.90
99.50
99.00
98.00
95.00
90.00
80.00
70.00
60.00
50.00
40.00
30.00
20.00
10.00
5.00
2.00
1.00
0.50
0.10
1.00
2.00
3.00
4.00
5.00
Grain Size (phi)

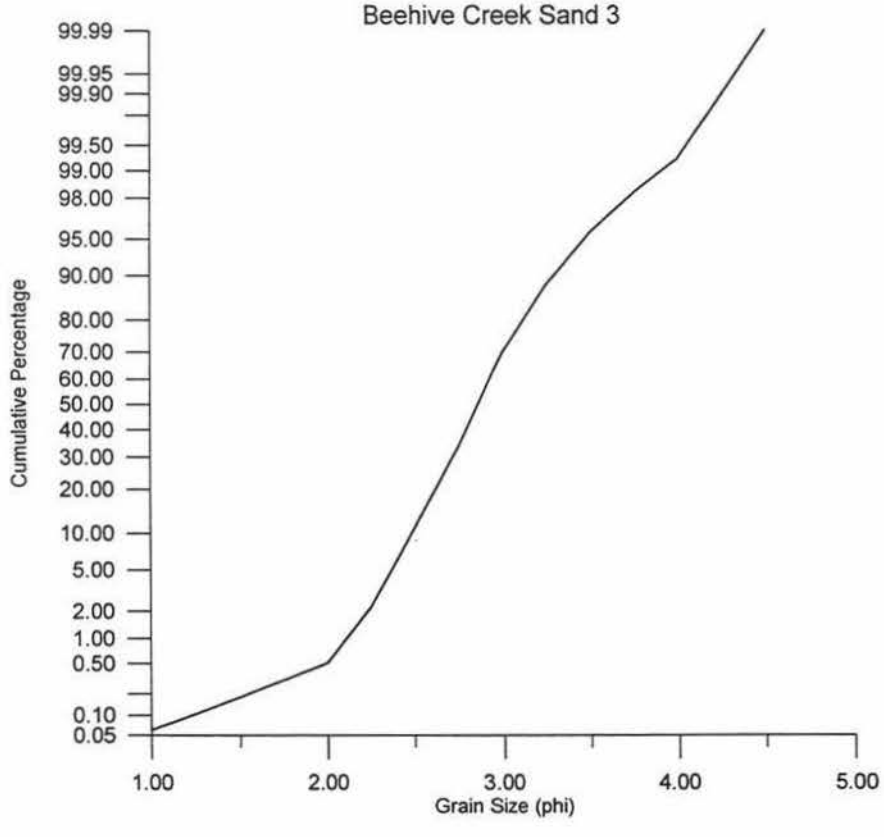
Beehive Creek Sand 3
Cumulative Percentage
99.99
99.95
99.90
99.50
99.00
98.00
95.00
90.00
80.00
70.00
60.00
50.00
40.00
30.00
20.00
10.00
5.00
2.00
1.00
0.50
0.10
0.05
1.00
2.00
3.00
4.00
5.00
Grain Size (phi)

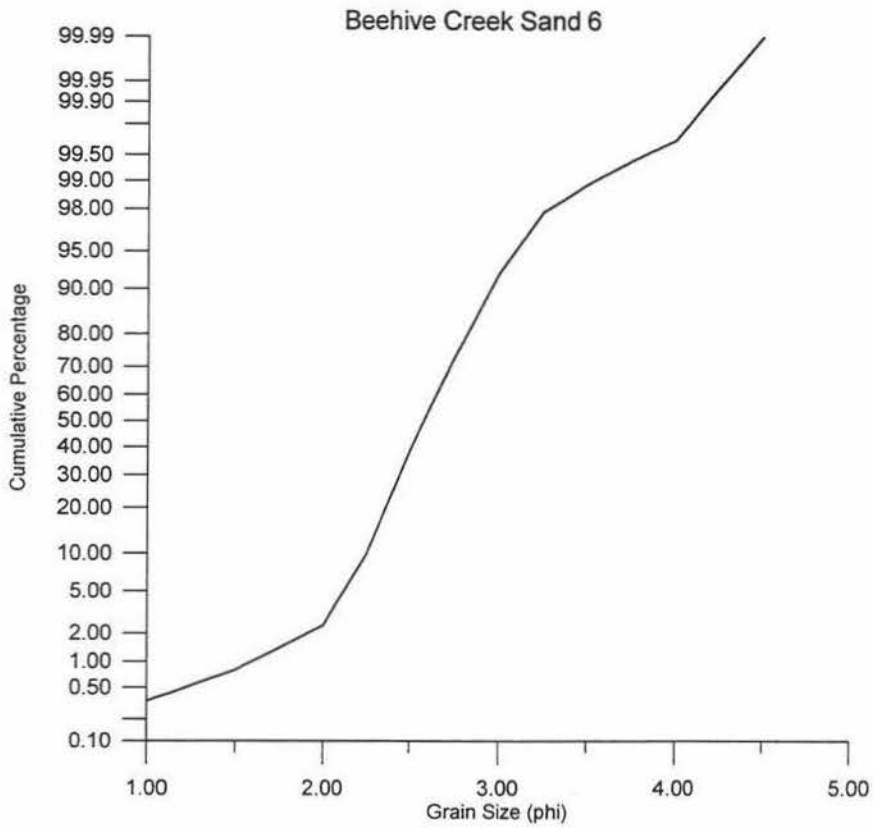
Beehive Creek Sand 6
Cumulative Percentage
99.99
99.95
99.90
99.50
99.00
98.00
95.00
90.00
80.00
70.00
60.00
50.00
40.00
30.00
20.00
10.00
5.00
2.00
1.00
0.50
0.10
1.00
2.00
3.00
4.00
5.00
Grain Size (phi)

APPENDIX G

• Paleocurrent measurements from sand units.

Site	*Apparent Directions*	*True Direction*
Stewart's Gully Section A		
Unit (vii)	24°@285 / 14°@192	25°@248
Oroua River		
Unit (iii)	18°@105 / 10°@188	19°@126
	15°@105 / 6°@170	15°@105
Beehive Creek		
Unit (ii)	23°@220 / 6°@120	25°@195
	20°@235 / 21°@143	28°@187
	26°@220 / 24°@268	27°@239
	25°@220 / 14°@278	25°@206
	17°@230 / 14°@154	20°@200
	24°@113 / 19°@075	22°@118
Unit (vi)	Dip of unit to be subtracted: 18°@090	
	21°@170 / 31°@092	69°@307
	25°@100 / 10°@160	83°@270
	8°@115 / 1°@024	80°@082
	24°@065 / 17°@140	82°@269
	14°@092 / 16°@034	86°@160
Unit (vii)	Dip of unit to be subtracted: 60°@070	
	22°@160 / 26°@062	31°@036
	30°@066 / 3°@075	39°@149
	33°@066 / 3°@175	26°@048
	11°@350 / 9°@078	50°@080
	3°@036 / 30°@078	35°@025
Unit (viii)	(Dip of unit to be subtracted: 60°@070)	

	50°@092 / 25°@127	3°@318
	49°@076 / 45°@130	13°@189
	53°@232 / 37°@120	3°@302
	53°@050 / 37°@120	10°@289
	48°@050 / 15°@186	3°@344
	66°@220 / 45°@275	32°@283

Coulters Line (T23/451147) 3.2m interbedded pumiceous sands. Horizontal bedding, few mud lenses, pumice-filled channels, cross bedding.

	28°@235 / 18°@280	28°@228
	30°@240 / 10°@170	31°@244
	25°@210 / 29°@160	30°@175
	4°@225 / 10°@150	10°@180
	7°@145 / 14°@245	17°@211
	12°@140 / 6°@040	14°@103

Finnis Road

1.2m Tabular Cross Bedding	12°@135/4@035	13°@108
	6°@305/4@255	6°@307
	4°@305/4@075	10°@012
	13°@310/0@230	14°@322
5m Pumiceous Ripples	17°@245/11@320	18°@267
	20°@305/12@215	23°@276
	11°@235/12@135	15°@171
5.6m Pumiceous Cross Beds	11°@310/17@090	38°@026
Unit (x)	13°@029 / 20°@284	27°@328
	14°@194 / 35°@291	38°@265
	16°@326 / 15°@201	31°@264
	6°@180 / 2°@278	7°@205
	12°@332 / 5°@070	13°@003
	24°@102 / 7°@154	26°@078
	1°@325 / 5°@095	8°@046
	1°@195 / 31°@320	37°@286

	5°@352 / 15°@280	25°@285
	13°@028 / 23°@294	27°@328
	2°@007 / 31°@296	32°@280
	14°@086 / 7°@006	9°@050
	9°@212 / 11°@295	13°@260
	7°@291 / 26°@246	30°@212
	4°@070 / 3°@020	4°@070
	6°@014 / 3°@290	7°@353
	4°@210 / 5°@275	6°@254
	20°@330 / 6°@080	23°@008
	6°@015 / 5°@095	7°@059
	10°@340 / 12°@065	15°@032
	17°@315 / 3°@355	22°@274
	8°@270 / 9°@220	9°@243
	3°@230 / 20°@090	31°@144
	1°@275 / 8°@040	12°@357
	16°@065 / 3°@25	11°@108

Culling's Gully

Site N	Dip of bed to be subtracted: 9°@092	
	3°@245 (true)	3°@245
	5°@248 / 18°@022	63°@139
	8°@254 / 23°@350	65°@132
	6°@283 / 16°@022	80°@153
	4°@250 / 22°@008	24°@140
	7°@247 / 4°@006	19°@106
Site A	18°@250 (true)	18°@250
	18°@318 (true)	18°@318
	18°@193 / 11°@126	18°@178
	8°@012 / 12°@077	13°@064
	16°@012 / 21°@292	24°@325
	14°@018 / 11°@296	20°@355
	20°@114 / 4°@007	22°@088
	21°@187 / 20°@252	24°@218
	26°@187 / 20°@254	27°@206

13°@055 / 10°@357	13°@040
18°@124 / 27°@188	17°@176
17°@286 / 15°@330	18°@303

APPENDIX H

- Grain Size Data for the eight mud samples.

Phi	Samples							
	1	2	3	4	5	6	7	8
2.00	0.800	0.690	1.620	2.170	2.050	1.890	1.410	1.660
2.25	0.400	0.550	0.840	1.080	1.180	1.570	0.770	0.760
2.50	0.230	0.960	0.610	0.750	0.950	2.060	0.620	0.510
2.75	0.220	2.330	0.670	0.790	0.920	2.420	0.640	0.550
3.00	0.220	3.490	0.450	0.690	0.940	1.990	0.480	0.380
3.25	0.210	3.330	1.510	0.840	1.220	0.950	0.780	0.460
3.50	0.320	2.570	1.310	0.660	1.680	0.630	0.870	0.420
3.75	1.420	2.310	2.350	0.800	3.790	1.080	3.370	0.600
4.00	4.600	1.690	2.550	1.980	6.560	1.540	6.380	1.190
4.25	1.205	0.108	0.048	0.060	0.352	0.077	0.432	0.053
4.50	1.840	0.166	0.071	0.091	0.528	0.154	0.632	0.178
4.75	2.660	0.237	0.119	0.163	0.907	0.309	0.959	0.480
5.00	3.028	0.281	0.182	0.272	1.340	0.512	1.244	1.031
5.25	2.593	0.281	0.253	0.399	1.544	0.674	1.265	1.706
5.50	1.723	0.250	0.321	0.483	1.462	0.730	1.075	2.257
5.75	0.954	0.208	0.364	0.507	1.205	0.674	0.822	3.399
6.00	0.502	0.168	0.372	0.489	0.921	0.548	0.611	2.097
6.25	0.268	0.137	0.345	0.453	0.704	0.428	0.485	1.582
6.50	0.151	0.113	0.293	0.411	0.555	0.323	0.390	1.084
6.75	0.117	0.097	0.238	0.362	0.474	0.246	0.327	0.729
7.00	0.100	0.082	0.186	0.314	0.420	0.197	0.285	0.515
7.25	0.067	0.066	0.150	0.266	0.352	0.168	0.242	0.355
7.50	0.033	0.050	0.123	0.217	0.284	0.140	0.200	0.267
7.75	0.033	0.039	0.095	0.181	0.244	0.112	0.169	0.213
8.00	0.084	0.034	0.083	0.157	0.230	0.112	0.158	0.195
8.25	0.100	0.032	0.075	0.139	0.217	0.098	0.148	0.178
8.50	0.067	0.026	0.063	0.115	0.190	0.077	0.126	0.142
8.75	0.033	0.021	0.055	0.091	0.149	0.070	0.105	0.124
9.00	0.017	0.016	0.048	0.072	0.122	0.070	0.095	0.107
9.25	0.017	0.013	0.040	0.066	0.108	0.070	0.074	0.089
9.50	0.033	0.010	0.036	0.066	0.108	0.070	0.074	0.089
9.75	0.050	0.010	0.036	0.066	0.095	0.070	0.084	0.089
10.00	0.050	0.013	0.036	0.060	0.095	0.063	0.074	0.107
10.25	0.050	0.013	0.032	0.060	0.095	0.063	0.063	0.107
10.50	0.033	0.008	0.028	0.048	0.095	0.063	0.053	0.089
10.75	0.017	0.008	0.024	0.042	0.068	0.063	0.030	0.071

Numbers are weight (in grams) for each phi interval.

Grain size data was obtained through the use of sieves and a SediGraph.

APPENDIX I

• Size distribution, cumulative frequency plots and statistical data for the eight mud samples.

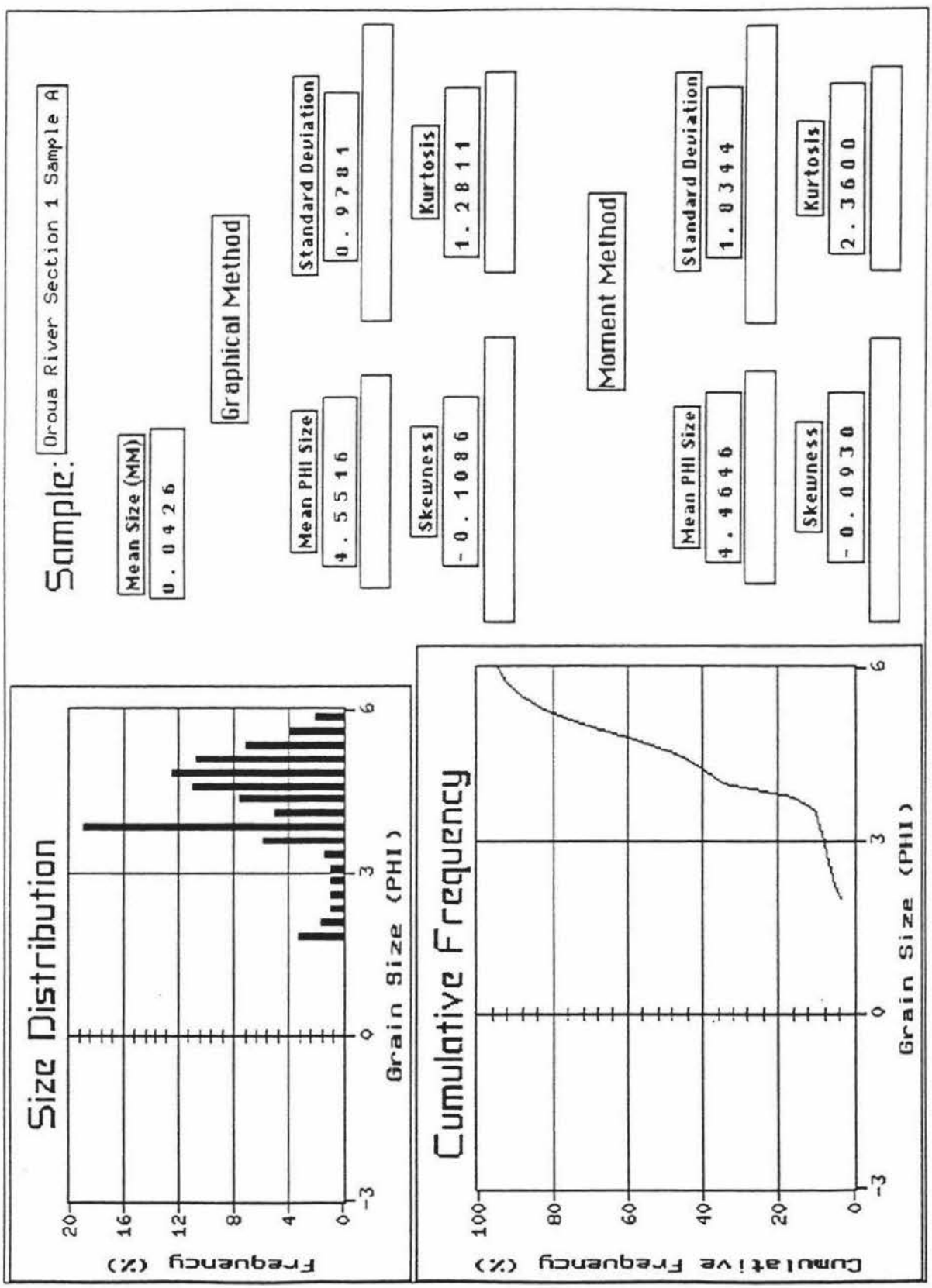

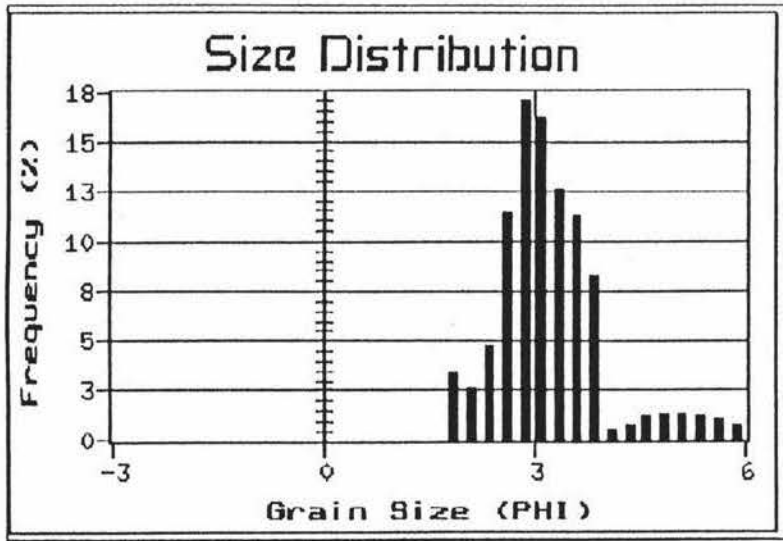

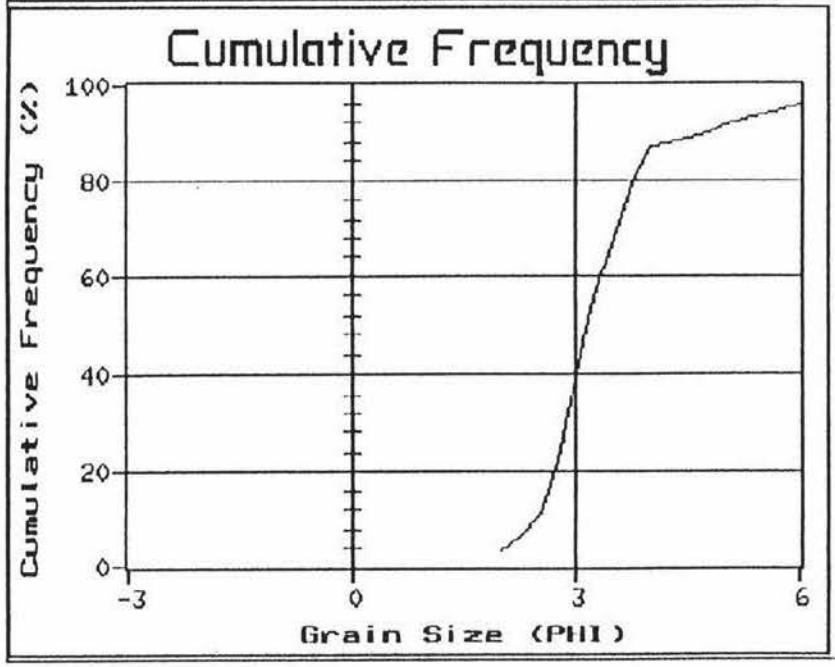

Sample: Oroua River Section 1 Sample B

Mean Size (MM)
0.1072

Graphical Method

Mean PHI Size
3.2210

Standard Deviation
0.8514

Skewness
0.2796

Kurtosis
1.6807

Moment Method

Mean PHI Size
3.3267

Standard Deviation
1.4973

Skewness
0.6293

Kurtosis
4.0098

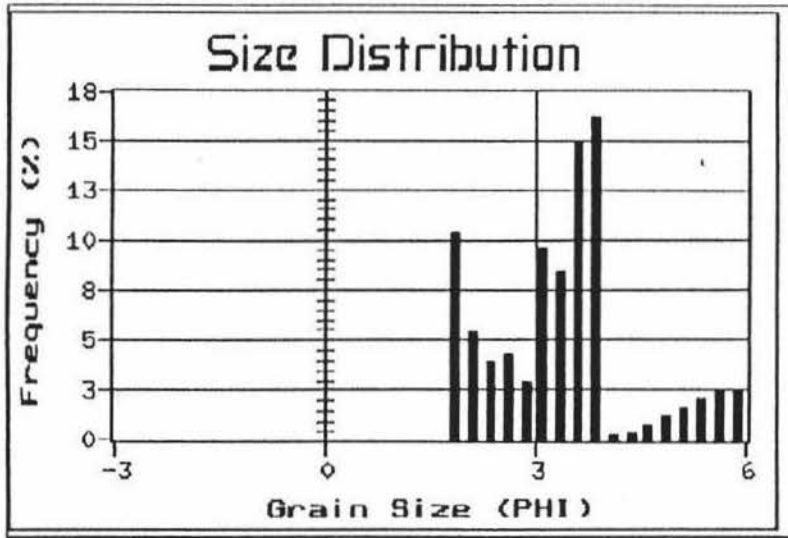

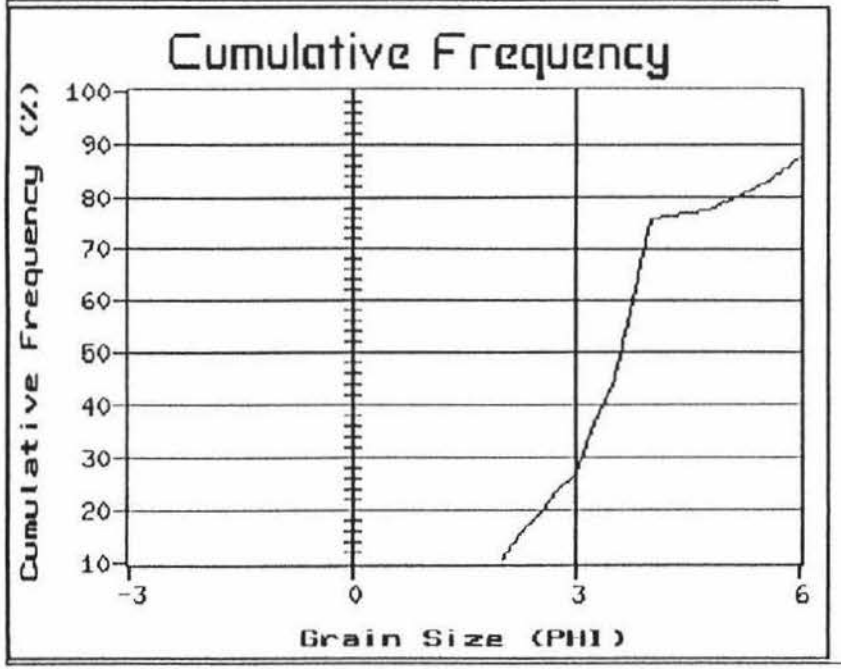

Sample: Oroua River Section 1 Sample D

Mean Size (MM)
0.0701

Graphical Method

Mean PHI Size	Standard Deviation
3.8347	1.7970

Skewness	Kurtosis
0.1927	2.2576

Moment Method

Mean PHI Size	Standard Deviation
3.6816	3.0768

Skewness	Kurtosis
0.0554	0.2682

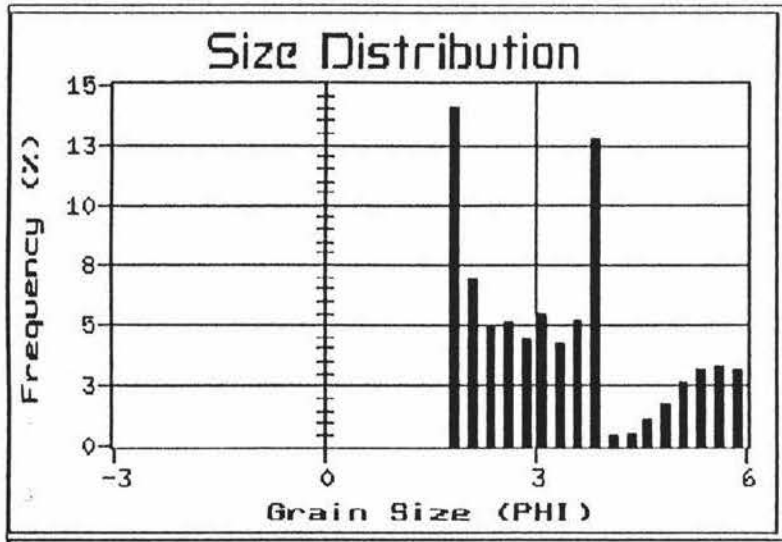

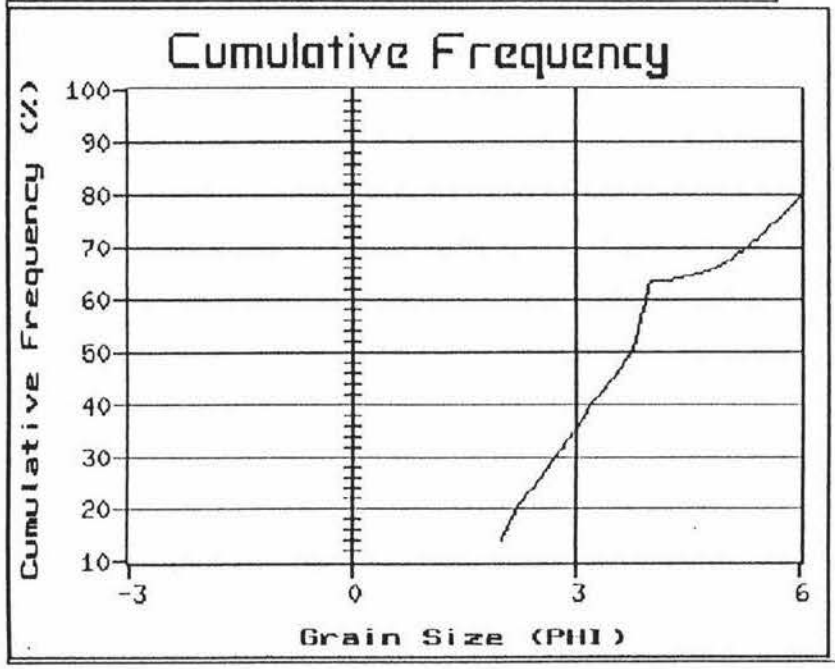

Sample: Beehive Creek Sample 2

Mean Size (MM)
0.0596

Graphical Method

Mean PHI Size
4.0692

Standard Deviation
2.2054

Skewness
0.2100

Kurtosis
0.9428

Moment Method

Mean PHI Size
3.9085

Standard Deviation
5.8319

Skewness
0.0181

Kurtosis
0.0805

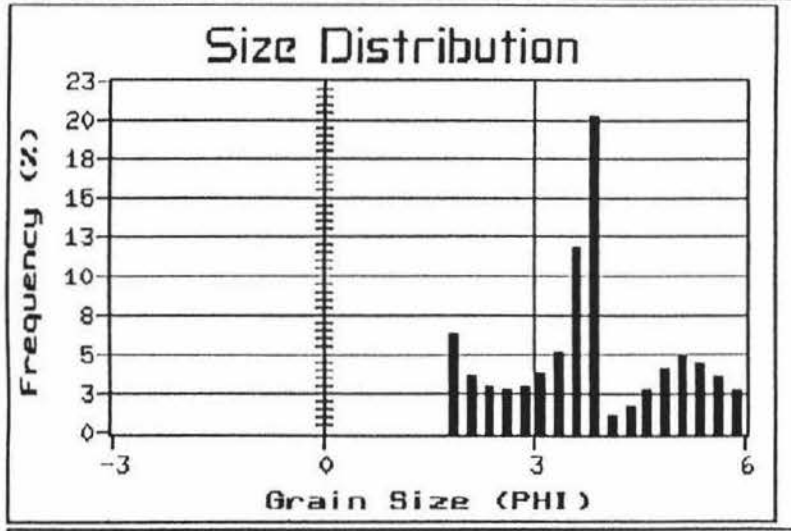

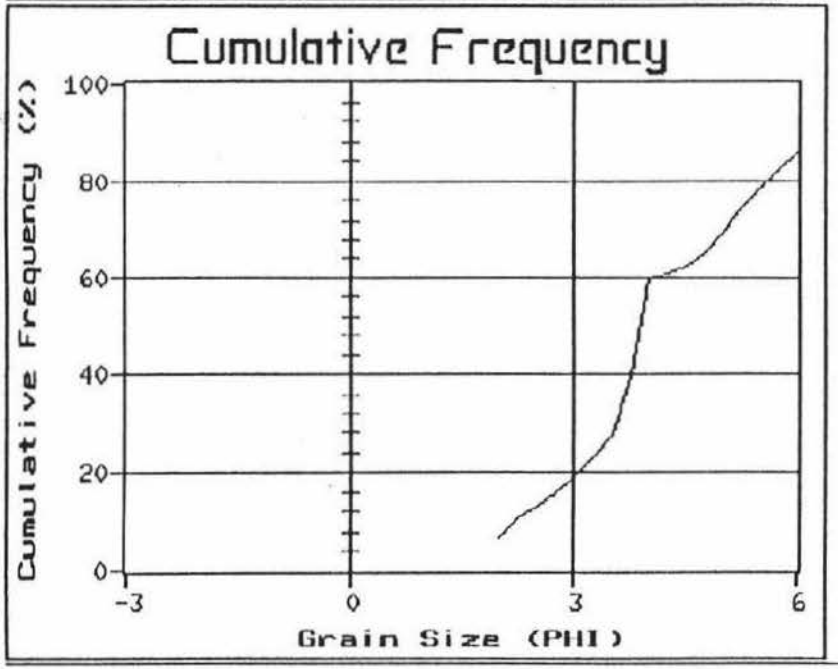

Sample: Beehive Creek Sample 4

Mean Size (MM)
0.0558

Graphical Method

Mean PHI Size
4.1643

Standard Deviation
1.7040

Skewness
0.2634

Kurtosis
1.3181

Moment Method

Mean PHI Size
4.2100

Standard Deviation
3.6773

Skewness
0.0429

Kurtosis
0.3067

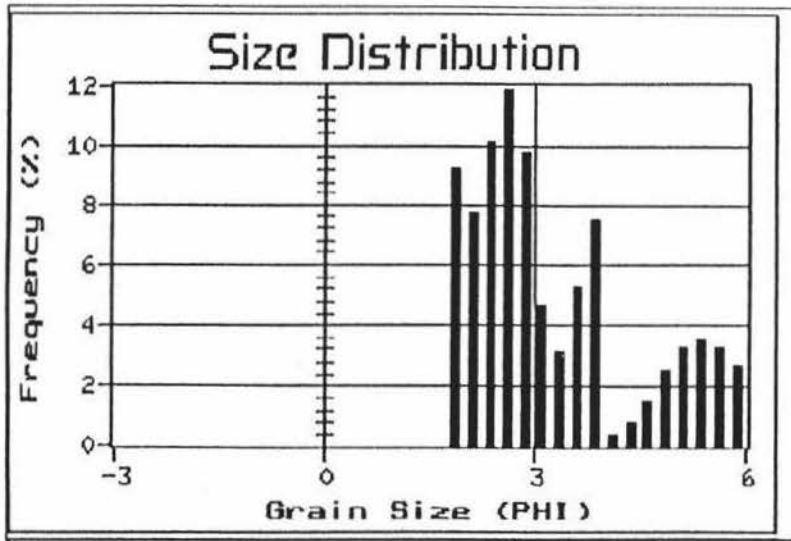

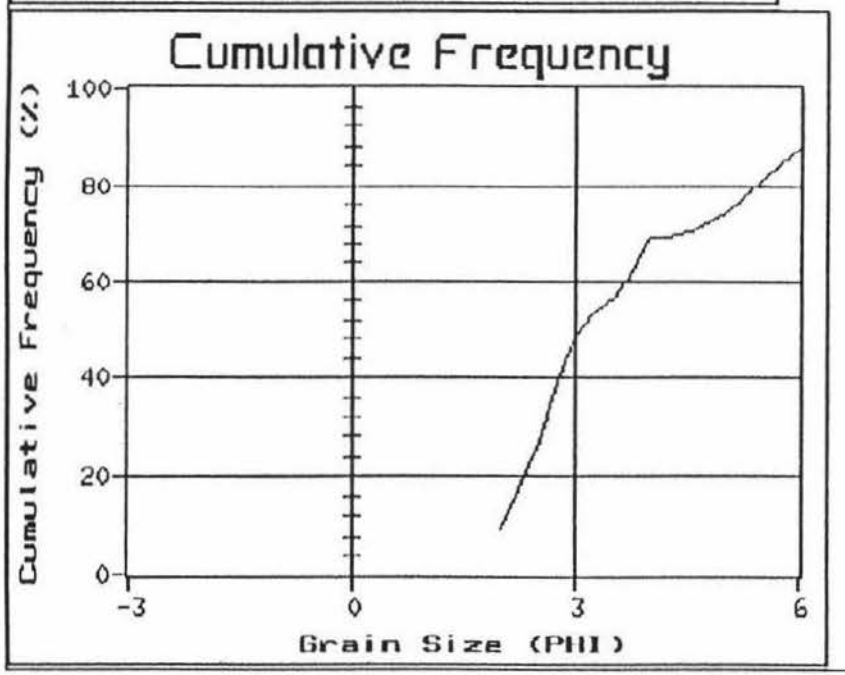

Sample: Beehive Creek Sample 5

Mean Size (MM)
0.0796

Graphical Method

Mean PHI Size
3.6507

Standard Deviation
1.8345

Skewness
0.4463

Kurtosis
1.0194

Moment Method

Mean PHI Size
3.6154

Standard Deviation
4.3633

Skewness
0.0747

Kurtosis
0.2007

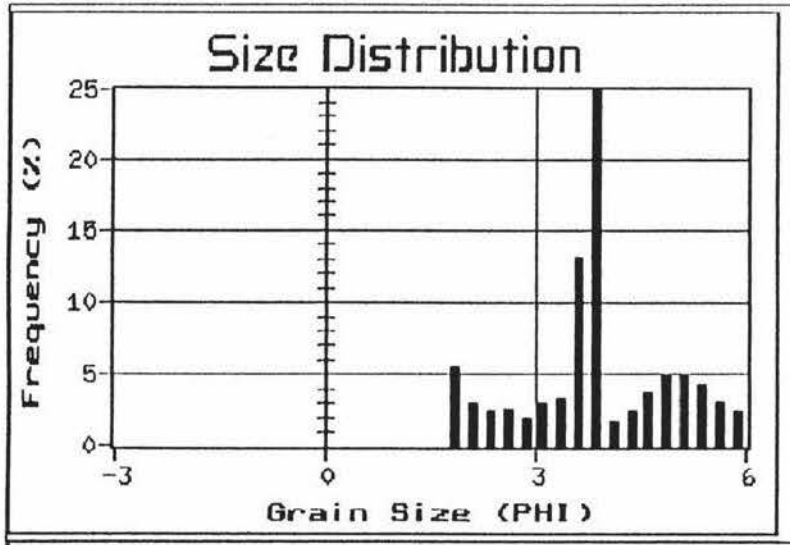

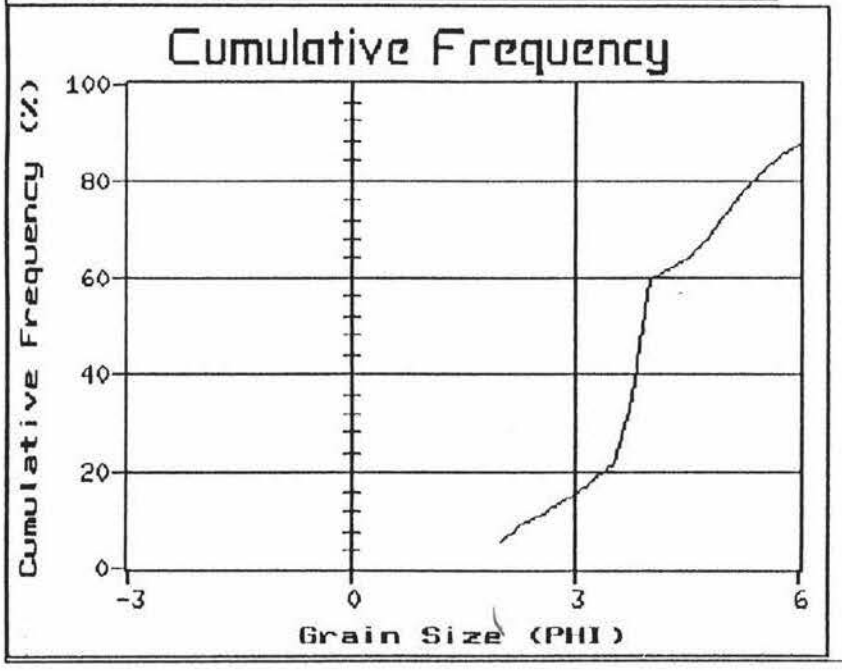

Sample: Beehive Creek Sample 7

Mean Size (MM)
0.0542

Graphical Method

Mean PHI Size	Standard Deviation
4.2047	1.5091

Skewness	Kurtosis
0.3061	1.4942

Moment Method

Mean PHI Size	Standard Deviation
4.2101	3.1786

Skewness	Kurtosis
0.0539	0.4670

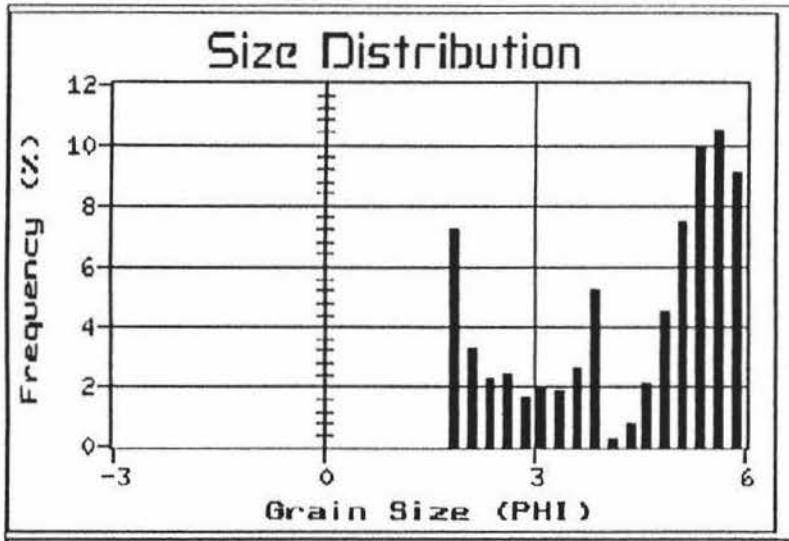

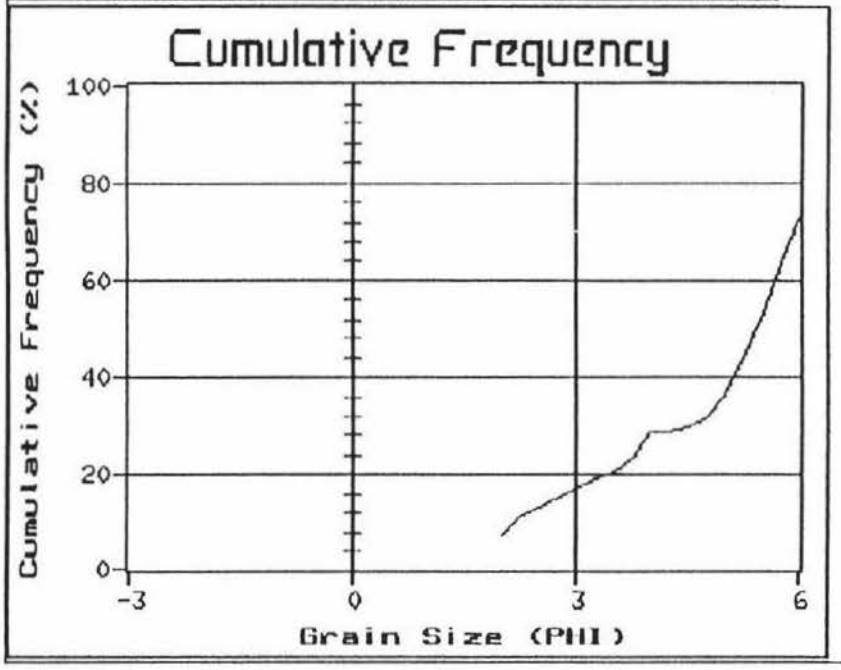

Sample: Beehive Creek Sample 8

Mean Size (MM)
0.0332

Graphical Method

Mean PHI Size
4.9113

Standard Deviation
1.9110

Skewness
-0.3117

Kurtosis
1.2260

Moment Method

Mean PHI Size
4.9661

Standard Deviation
4.3912

Skewness
-0.0598

Kurtosis
0.1945